Development of Multiplex Mass Spectrometry Methods for Probing the Response to Copper Toxicity in the Blue Crab

By
Christopher Sauer

A dissertation submitted in partial fulfillment of
the requirements for the degree of

Doctorate of Philosophy
(Chemistry)

at the
UNIVERSITY OF WISCONSIN-MADISON
2022

Date of final oral examination: December 17, 2021
The dissertation is approved by the following members of the Final Oral Committee:
Lingjun Li, Professor, Chemistry and Pharmaceutical Science
Ying Ge, Professor, Chemistry and Cell and Regenerative Biology
Regina Murphy, Professor, Chemical and Biological Engineering
Lloyd Smith, Professor, Chemistry

Acknowledgements

I owe a great deal of gratitude to many people who have supported me throughout my schooling and research. First and foremost, I would like to acknowledge my advisor, Professor Lingjun Li. Her mentorship, guidance, and unwavering support have been the root of my successes in graduate school at the University of Wisconsin-Madison. She has taught me to be a better scientist by providing discussion on experimental design, data interpretation, and alternative strategies. Professor Li continuously demonstrates what it means to be diplomatic, collaborative, and hardworking, serving as a role model for me outside of research too. Graduate school is a difficult time for everyone but having Lingjun Li as an advisor has made it a great experience and provided me with ample career opportunities. I will always be grateful for her support and mentorship.

I would also like to thank my other committee members, Professor Regina Murphy, Professor Lloyd Smith, and Professor Ying Ge for their feedback and support. They have lent their time and expertise to improve my research and help me reach my goals. Their input during my thesis background oral exam, original research proposal, committee meetings, and the defense of this dissertation have held me to a higher standard and improved the quality of my work, helping me to become a better student and scientist.

Early in my life, I had excellent teachers that inspired me to pursue a career in science. Had it not been for Shelley Dorner and my other science teachers in high school, I likely would never have majored in chemistry and would not be where I am

today. This interest in science was furthered by Dr. Kurt Hecox at the Medical College of Wisconsin and professors at the University of Minnesota, especially Professor Michael Bowser. As an undergraduate advisor, Dr. Bowser, along with my graduate student mentor, Rachel Harstadt, helped instill in me an interest in bioanalytical research and gave me preparation for success in graduate school. I would also like to thank Professor Edgar Arriaga, Professor Michael Bowser, and Dr. Kurt Hecox for their generous letters of recommendation for graduate school and fellowship applications.

When I joined the Li Lab in 2016, I felt immediately welcomed by the friendly and helpful students in the lab. They have all been amazing colleagues, offering their diverse scientific backgrounds to advance my own research. Specifically, I would like to acknowledge the mentorship of Drs. Amanda Buchberger and Kellen DeLaney for taking me under their wings. Not only did they show me how to perform many of the experiments in this work, but they also helped me with navigating graduate school in general. I also want to thank other graduate students who supported me throughout graduate school, including Dr. Jillian Johnson, Dr. Dustin Frost, Dr. Xiaofang Zhang, Dr. Zhengwei Chen, Dr. Yatao Shi, Dr. Qinjingwen Cao, Dr. Yang Liu, Dr. Zihui Li, Dr. Qinying Yu, and Dr. Yusi Cui. I would also like to thank my current coworkers and co-authors, Nhu Vu, Ashley Phetsanthad, Olga Riusech, Dylan Tabang, Hannah Miles, Graham Delafield, Wenxin Wu, and many others. Their help and support have improved this research and my time in lab.

Throughout my time in graduate school, I have had the privilege of mentoring three undergraduate researchers, Makaila Wallin, Mason Job, and Jamie Covaleski.

Makaila was always eager to learn and contribute to projects, while also being patient with me as I was still a novice graduate student trying to figure things out. Mason worked with me for over a year on the metallothionein projects, providing valuable input and not giving up when things became frustrating. Jamie is an incredibly smart, and excited scientist, and I am happy she is continuing in the lab after I graduate. These three have been amazing to work with and I'm fortunate to have them be a part of my graduate school experience.

I also acknowledge the funding sources that have made my dissertation work possible. I have been funded as a teaching assistant through the Department of Chemistry as well as a trainee on a NIH-funded T32 training grant through the Biotechnology Training Program (T32 GM008349). As a dissertator I have been fortunate enough to receive funding through a Ruth L. Kirschstein National Research Service Award F31 predoctoral fellowship (F31ES031859).

Lastly, I would like to thank my family and friends for their support throughout my life, but especially these last five years. My family, Diane and Tim Luft, Scott Sauer, and Rob and Alissa Sauer, have always been there to listen to me vent about troubles at work, offer ideas, and provide encouragement when things became difficult. Along with my friends and extended family, they have helped me to enjoy my time in graduate school and come out better for it. This dissertation would not have been possible without all of them.

Development of Multiplex Mass Spectrometry Methods for Probing the Response to Copper Toxicity in the Blue Crab

Christopher Sauer
Under the supervision of Professor Lingjun Li
University of Wisconsin – Madison

Abstract

Neuropeptides are diverse neuromodulators that originate in the neuroendocrine system and play important roles in many biochemical pathways. Copper toxicity is of particular interest as copper effluxes are increasing from pollution and copper is becoming more bioavailable due to ocean acidification. Characterizing neuropeptidomic changes can improve understanding of the neurochemical signaling pathways and biochemical processes involved in responding to environmental stress like copper toxicity. This dissertation explores different mass spectrometry (MS) strategies to characterize neuropeptides and related biomolecules in response to elevated copper levels with an emphasis on quantitative methods. This is performed in a crustacean model organism using custom *N,N*-dimethyl leucine isobaric tags (DiLeu). These tags have had extensive applications for bottom-up proteomics but have been much less explored for their application to neuropeptide quantitation due to inherent challenges in measuring these low-abundance analytes. Optimization of the MS acquisition parameters is performed to translate proteomic methods and facilitate neuropeptidomic experiments with higher throughput and broader coverage. Additionally, methods to quantify related copper-binding proteins (e.g., metallothioneins) were also developed to provide a more comprehensive understanding and multi-omic view of the underlying biochemical processes involved in copper toxicity. Overall, the work presented in this dissertation

provides an improved framework for studying the functional roles of neuropeptides and proteins involved in the copper stress response.

Chapter 1

Introduction and Research Summary

Introduction

Neuropeptides are important signaling peptides with a range of functions within the neuroendocrine system. They are encoded as part of larger precursor proteins, or preprohormones, that are cleaved and modified to yield the mature, bioactive peptide.[1] These peptides can then exert their modulating effects both locally and as long-range circulating hormones.[2] Prior research has shown neuropeptides to be involved in a variety of biological processes, including environmental stress,[3,4] behavior,[5] and neurological disorders.[6] Discerning the exact roles of neuropeptides in these processes is difficult, however, as neuropeptide function is dependent upon many factors, such as location, concentration, and the presence of other co-modulating neuropeptides.[2] It is therefore important to profile the entire suite of neuropeptides expressed to gain insights into their specific functions. This is challenging due to the structural diversity of neuropeptides, as well as their low *in vivo* abundance, and has resulted in ample opportunities for advances in the field of neuropeptidomics.

Crustacean model organisms have proven useful to improve our understanding of neuropeptides and the larger neuroendocrine system. The simple, well-characterized nervous system found in crustaceans has been the subject of many electrophysiology experiments and provides a relevant model for studying neuropeptide function as many crustacean neuropeptides have mammalian homologs.[7] Although these models have enabled the study of neuropeptidomics for a variety of applications, advances in the analytical techniques to characterize neuropeptides have proven to be highly important and can be broadly transferred to the study of other model organisms. Through the

development of mass spectrometry (MS), neuropeptides are able to be identified by their sequence, characterized by post-translational modification (PTM) content, and quantified between samples.[2] The employment of MS has facilitated thorough profiling of neuropeptides to help discern their roles in physiological processes. Additionally, MS has been extensively utilized to study other biomolecules of interest, such as proteins, lipids, and metabolites. This allows multi-omic workflows to be developed to provide a detailed picture of the biochemical changes that occur between experimental samples.

The overall aim of this research is to further develop quantitative MS techniques to study relative changes in neuropeptides and related biomolecules. The effectiveness of different labeling methods (both isobaric and isotopic) and MS acquisition settings are demonstrated in this work. The developed methods are then used to profile changes in a blue crab model organism, *Callinectes sapidus*, in response to environmental stress, specifically hypoxia and copper toxicity.

Research Summary

As neuropeptide function is dependent upon location, structure, concentration, and the presence of other neuropeptides, thorough profiling of the neuropeptidome is needed to discern the role of neuropeptides in different biological processes. **Chapter 2** provides information on the background literature relevant to the study of neuropeptides.[8] The importance of studying neuropeptides is presented along with the challenges currently facing the field. Analytical method development is discussed with an emphasis on quantitative mass spectrometric approaches. These include label-free quantitation

methods, isobaric labeling, and isotopic labeling. There have also been considerable advances in quantitative mass spectrometry imaging (MSI) that have led to enhanced localization of neuropeptides. Additionally, the multi-omic workflows are discussed in which proteomics and metabolomics can be used to inform neuropeptidomic research and help corroborate findings or generate new hypotheses. The chapter is concluded with an overview of the limitations still facing the field of neuropeptidomics and an outlook for future research in the field.

Profiling neuropeptides in a sample can be accomplished using different MS strategies, the simplest being a label-free strategy. Samples are analyzed separately, and quantitation of specific analytes is achieved by comparing signal intensities, spectral counts, or area under the curve of the chromatogram.[9] These methods require fewer sample processing steps due to the omission of labeling but require more instrument time as samples cannot be analyzed together. This not only increases analysis time but also increases the potential for instrumental drift and run-to-run variability, necessitating more controls and normalization consideration. Conversely, a simple reductive dimethylation reaction can be used to quickly label neuropeptides at a modest cost. In **Chapter 3**, this labeling strategy is used to analyze four samples simultaneously.[10] Isotopic formaldehyde and a reducing agent (borane pyridine) are used to incorporate different mass additions to the primary amines of neuropeptides from different samples. The labeled samples are then pooled together and able to be analyzed in a single liquid chromatography (LC)-MS. This enabled the relative quantitation of neuropeptide expression after exposure to three durations of hypoxia

compared to a control (unexposed to hypoxia). As the reductive dimethylation labeling creates a mass difference at the precursor mass level (MS^1), matrix-assisted laser desorption and ionization (MALDI)-MS can be used in conjunction with electrospray ionization (ESI)-MS to provide complementary identifications and deeper coverage of the crustacean neuropeptidome. Using reductive dimethylation, significant changes were observed in many neuropeptides, with majority of peptides downregulated in response to hypoxia. This labeling strategy is effective; however, it is limited in its multiplexing abilities as each channel increases spectral complexity multiplicatively, resulting in fewer identifiable neuropeptides.

To address the limitations of an isotopic labeling strategy, such as reductive dimethylation, an isobaric labeling strategy can be used. By adding the same nominal mass regardless of channel, isobaric tags create no distinction at the precursor mass level. Upon fragmentation and tandem MS (MS/MS or MS^2) analysis, however, unique reporter ions can be produced from each channel. This allows the spectral complexity at the MS^1 level to be maintained and only adds complexity to the low mass region of the MS^2 spectra which is indicative of relative abundance of each sample, and thereby enables higher orders of multiplexing.[11] Isobaric tagging has had many applications with proteomics, but the low concentrations of neuropeptides present challenges. Isobaric tagging workflows rely on data-dependent acquisitions, in which a preset number of MS^2 spectra are collected per MS^1 spectrum. The low abundance of neuropeptides often results in them not being selected for MS^2 analysis and therefore not identified or quantified. In **Chapter 4**, a systematic optimization strategy is used to

enable an isobaric tagging workflow while still maintaining high neuropeptidome coverage.[12] Neuropeptides were labeled with custom tags developed in the Li Lab, *N,N*-dimethyl leucine (DiLeu). The multiplexed samples were analyzed by LC-MS, and by modifying select data-dependent acquisition settings, the number of unique neuropeptides able to be identified and quantified in a single LC-MS run was increased by three-fold. This improvement enabled application of the 4-plex DiLeu labeling scheme to a biological study.

Copper plays important roles in protein structure and signal modulation but can quickly cause oxidative stress at elevated concentrations. Furthermore, copper toxicity is an increasing ecological concern as copper levels are increasing due to agricultural runoff, industrial pollution, and poorly managed wastewater.[13] In aquatic ecosystems, copper poses higher toxicity as its bioavailability increases with the acidification of oceans. To better understand the response to copper toxicity in an organism, the methods developed in **Chapter 4** were used to characterize the neuropeptidomic changes after 1, 2, and 4 hours of exposure in a blue crab model. Several significant changes were found throughout the brain, sinus glands (SGs), pericardial organs (POs), and thoracic ganglia (TG). In general, there was an increase in inhibitory peptides (e.g., allatostatin A- and B-type) in the pericardial organs. Additionally, an interesting pigment dispersing hormone (PDH) showed possible transport from the sinus glands to the brain. This exact same PDH displayed the same pattern in response to hypoxia (**Chapter 3**) as well, potentially indicating a general stress response factor.

The initial 4-plex DiLeu labeling strategy used in **Chapter 4** did prove effective but increasing the multiplexing capabilities is often advantageous as it improves throughput and can reduce run-to-run variability. The 4-plex DiLeu tags have been expanded to a 12-plex by taking advantages of the mDa mass differences that arise from the incorporation of ^{2}H, ^{13}C, and ^{15}N (mass defects). These mass defects allow the initial 4 reporter ions to be "split" into a total of 12 with only a few mDa between some reporter ions.[11] While this increases the total number of channels that can be analyzed simultaneously, it also requires a greater resolving power. This in turn increases the scan time, reducing the total number of spectra that can be collected in a single LC-MS run. To minimize trade-offs between throughput and the number of identifiable neuropeptides, the mass spectrometry acquisition parameters were further optimized. Unlike **Chapter 4**, however, a less systematic but faster design of experiments was used in **Chapter 5** to optimize six parameters simultaneously. A single sample was analyzed by different combinations of parameters, dictated by an orthogonal array optimization strategy.[14] This allowed for the evaluation of six parameters at three levels each in only 18 runs. The orthogonal array optimization resulted in an approximately 2.5-fold increase in identifiable neuropeptides when comparing optimum vs unoptimized parameters. This demonstrates not only the effectiveness, but also the importance of method optimization for LC-MS analyses. The optimization of the 12-plex analyses will allow the methods to be used in future studies to study environmental stress (e.g., copper toxicity), but with a greater number of evaluable experimental conditions. A

detailed protocol and the overview of the methods described in **Chapters 4 and 5** is provided in **Chapter 6**.[15]

Neuropeptidomics has the potential to provide much information on the signaling pathways involved in responding to stressors like copper toxicity. It is also important, however, to examine other biomolecules that may be involved in mediating environmental copper exposure. Metallothionein proteins are of particular interest as they are responsible for binding a variety of heavy metals, including copper, to maintain metal homeostasis.[16] This small family of proteins helps chelate and transport metals so they can be metabolized or excreted, and their dysregulation has been implicated in many disease states, such as genetic disorders, neurological degeneration, and of course metal toxicity. Studying these proteins can be challenging as they are highly unique; they are low molecular weight (6-7 kDa), highly cysteine-rich (>30%), and have acetylated N-termini.[17] Additionally, proteins within this family are structurally similar, but play roles in different biological processes. Analysis of these proteins has been achieved using bottom-up proteomics, but much information about conformation, PTMs, and metal-binding is lost during this process.[18] Alternatively, in **Chapter 7**, methods are developed to not only analyze the intact metallothionein proteins (top-down MS), but also quantify them using DiLeu isobaric tags. This is challenging due to the many cysteine residues (~20) that need to be alkylated to prevent side reactions with the amine-reactive DiLeu tags. Additionally, the blocked N-terminus (acetylated) inhibits labeling, leaving only the lysine residues able to be labeled. Modifying conventional reduction and alkylation protocols to use greater reagent concentrations

and longer incubation times have resulted in high alkylation efficiency.[18] Differential labeling of alkylated products has shown reliable quantitation when comparing observed ratios to the known ratio in which the samples were pooled. Isolating the metallothionein proteins from tissue extracts has proven challenging as there is a complex matrix of both large proteins and small molecule metabolites that need to be removed. Work is being done to improve affinity-based extraction methods, such as immobilized metal affinity chromatography (IMAC), and size-based methods like molecular weight cutoff (MWCO) filtration.[19] These challenges are discussed in more detail in the future directions section of this thesis (**Chapter 9**). Combining the extraction protocols with the developed labeling methods will allow for efficient quantitation of different metallothionein proteins, thereby providing insights into the roles of these proteins in responding to heavy metal toxicity.

An overview of this research is provided in **Chapter 8** as part of a collaboration with the Wisconsin Institute for Scientific Literacy (WISL) and is intended to provide a description of the thesis to a broader audience without formal scientific training. The conclusions and findings from this thesis work are provided in **Chapter 9**, along with a description of the possible future directions of the projects presented here.

References

1. Hook V, Lietz CB, Podvin S, Cajka T, Fiehn O. Diversity of Neuropeptide Cell-Cell Signaling Molecules Generated by Proteolytic Processing Revealed by Neuropeptidomics Mass Spectrometry. *J Am Soc Mass Spectrom*. 2018;29(5):807-

816. doi:10.1007/s13361-018-1914-1

2. Li L, Sweedler J V. Peptides in the Brain: Mass Spectrometry–Based Measurement Approaches and Challenges. *Annu Rev Anal Chem*. 2008;1(1):451-483. doi:10.1146/annurev.anchem.1.031207.113053
3. Chen R, Xiao M, Buchberger A, Li L. Quantitative Neuropeptidomics Study of the Effects of Temperature Change in the Crab Cancer borealis. *J Proteome Res*. 2014;13:5767-5776.
4. Liu Y, Buchberger AR, Delaney K, Li Z, Li L. Multifaceted Mass Spectrometric Investigation of Neuropeptide Changes in Atlantic Blue Crab, Callinectes sapidus, in Response to Low pH Stress. *J Proteome Res*. 2019;18(7):2759-2770. doi:10.1021/acs.jproteome.9b00026
5. DeLaney K, Hu M, Hellenbrand T, Dickinson PS, Nusbaum MP, Li L. Mass spectrometry quantification, localization, and discovery of feeding-related neuropeptides in cancer borealis. *ACS Chem Neurosci*. 2021. doi:10.1021/acschemneuro.1c00007
6. Gelman JS, Wardman J, Bhat VB, Gozzo FC, Fricker LD. Chapter 31 Quantitative Peptidomics to Measure Neuropeptide Levels in Animal Models Relevant to Psychiatric Disorders. In: *Psychiatric Disorders: Methods and Protocols, Methods in Molecular Biology*. Vol 829. ; 2012:487-503. doi:10.1007/978-1-61779-458-2
7. Christie AE, Stemmler EA, Dickinson PS. Crustacean neuropeptides. *Cell Mol Life Sci*. 2010;67(24):4135-4169. doi:10.1007/s00018-010-0482-8
8. Sauer CS, Phetsanthad A, Riusech OL, Li L. Developing Mass Spectrometry for the

Quantitative Analysis of Neuropeptides. *Expert Rev Proteomics*. 2021. doi:10.1080/14789450.2021.1967146

9. Fricker L. Chapter 8 Quantitative Peptidomics : General Considerations. In: *Peptidomics: Methods and Strategies, Methods in Molecular Biology*. Vol 1719. ; 2018:121-140.
10. Buchberger AR, Sauer CS, Vu NQ, DeLaney K, Li L. A Temporal Study of the Perturbation of Crustacean Neuropeptides Due to Severe Hypoxia Using 4-Plex Reductive Dimethylation. *J Proteome Res*. 2020;19:1548-1555. doi:10.1021/acs.jproteome.9b00787
11. Frost DC, Greer T, Li L. High-resolution enabled 12-plex DiLeu isobaric tags for quantitative proteomics. *Anal Chem*. 2015;87(3):1646-1654. doi:10.1021/ac503276z
12. Sauer CS, Li L. Mass Spectrometric Profiling of Neuropeptides in Response to Copper Toxicity via Isobaric Tagging. *Chem Res Toxicol*. 2021. doi:10.1021/acs.chemrestox.0c00521
13. Gaetke LM, Chow-Johnson HS, Chow CK. Copper: toxicological relevance and mechanisms. *Arch Toxicol*. 2014;88(11):1929-1938. doi:10.1007/s00204-014-1355-y
14. Cao J, Gonzalez-Covarrubias V, Covarrubias VM, et al. A rapid, reproducible, on-the-fly orthogonal array optimization method for targeted protein quantification by LC/MS and its application for accurate and sensitive quantification of carbonyl reductases in human liver. *Anal Chem*. 2010;82(7):2680-2689.

doi:10.1021/ac902314m

15. Sauer CS, Li L. Multiplexed Quantitative Neuropeptidomics via DiLeu Isobaric Tagging. In: *Methods in Enzymology 663: Antimicrobial Peptides*. ; 2022.
16. Engel DW. Metal regulation and molting in the blue crab, Callinectes sapidus: copper, zinc, and metallothionein. *Biol Bull*. 1987;172(November 1986):69-82.
17. Irvine GW, Stillman MJ. Residue modification and mass spectrometry for the investigation of structural and metalation properties of metallothionein and cysteine-rich proteins. *Int J Mol Sci*. 2017;18(5). doi:10.3390/ijms18050913
18. Mehus AA, Muhonen WW, Garrett SH, Somji S, Sens DA, Shabb JB. Quantitation of Human Metallothionein Isoforms: A Family of Small, Highly Conserved, Cysteine-rich Proteins. *Mol Cell Proteomics*. 2014;13(4):1020-1033. doi:10.1074/mcp.m113.033373
19. Nischwitz V, Michalke B, Kettrup A. Optimisation of extraction procedures for metallothionein-isoforms and superoxide dismutase from liver samples using spiking experiments. *Analyst*. 2003;128(1):109-115. doi:10.1039/b209497e

Chapter 2

Developing Mass Spectrometry for the Quantitative Analysis of Neuropeptides

Adapted from:

Sauer, C.S., Phetsanthad, A., Riusech, O.L., Li, L. Developing Mass Spectrometry for the Quantitative Analysis of Neuropeptides. *Expert Review of Proteomics.* 2021. https://doi.org/10.1080/14789450.2021.1967146

Structured Abstract:

Introduction:

Neuropeptides are signaling molecules originating in the neuroendocrine system that can act as neurotransmitters and hormones in many biochemical processes. Their exact function is difficult to characterize, however, due to dependence on concentration, post-translational modifications, and the presence of other comodulating neuropeptides. Mass spectrometry enables sensitive, accurate, and global peptidomic analyses that can profile neuropeptide expression changes to understand their roles in many biological problems, such as neurodegenerative disorders and metabolic function.

Areas Covered:

We provide a brief overview of the fundamentals of neuropeptidomic research, limitations of existing methods, and recent progress in the field. This review is focused on developments in mass spectrometry and encompasses labeling strategies, post-translational modification analysis, mass spectrometry imaging, and integrated multi-omic workflows, with discussion emphasizing quantitative advancements.

Expert Opinion:

Neuropeptidomics is critical for future clinical research with impacts in biomarker discovery, receptor identification, and drug design. While advancements are being made to improve sensitivity and accuracy, there is still room for improvement. Better quantitative strategies are required for clinical analyses, and these methods also need to be amenable to mass spectrometry imaging, post-translational modification analysis, and multi-omics to facilitate understanding and future treatment of many diseases.

Keywords: Imaging, Label-free, Mass Spectrometry, Multiplexing, Multi-omics, Neuropeptides, Peptidomics, PTMs, Quantitation, Stable Isotope Labeling

Article Highlights:

- Developments in quantitative mass spectrometry have enabled greater sensitivity, higher throughput, and more comprehensive analyses of neuropeptidomics, improving understanding of the signaling pathways involved in many diseases.
- Both isotopic and isobaric labeling strategies have seen increased usage, especially as instrument advancements enable greater multiplexing, and label-free neuropeptidomics remains common due to reduced sample loss and spectral complexity. Recent incorporation of data-independent acquisition strategy has benefits for both labeling and label-free methods.
- Post-translational modification analysis remains challenging, but is in greater demand, especially with the discovery of glycosylated neuropeptides. These analyses have benefited from adapting glycoproteomics methods and improvements in instrumentation, such as the availability of ETD and EThcD for fragmentation.
- Recent advances in normalization methods, matrix development, data analysis, etc., have enabled mass spectrometry imaging to not only be useful for localization, but also for quantitation of neuropeptides.

- Neuropeptides play roles in diverse signaling pathways that involved a suite of co-modulating neuropeptides, proteins, neurotransmitters, and metabolites, highlighting the need for multi-omic workflows. These methods have seen increased use in recent years, facilitated by developments in analyte extraction and separations, differential labeling, and instrumentation.

1. Introduction:

Regulation of the nervous system is a strictly controlled process influenced by a plethora of signaling peptides, neurotransmitters, hormones, and other modulating molecules.[1,2] These neuromodulators are critical to behavior,[3–5] stress responses,[6–11] maintaining homeostasis,[12,13] and many other biological processes.[14–16] Neuropeptides, signaling peptides originating in the neuroendocrine system, are of particular interest as they have highly diverse function and structure, dynamic expression, and many sites of action.[1] Dysregulation of neuropeptides has been implicated in many diseases and biological states, including heavy metal toxicity,[8] hypoxia,[7] Alzheimer's disease,[17] depression,[18] and others. As a result, comprehensive characterization of neuropeptides could have many benefits such as discovering biomarkers or elucidating important biological pathways involved. However, such global analysis is challenging not only due to many neuropeptides having low in vivo abundance and high structural diversity, but also because neuropeptide function is influenced by many factors, such as location, post-translational modifications, and the presence of other co-modulating neuropeptides.[1]

This complexity inherent to all neuropeptidomic studies is exacerbated by the difficulties in determining possible neuropeptide sequences. Neuropeptides are produced by the select processing of precursor proteins (i.e., preprohormone) encoded within the genome.[19] These preprohormones contain a signaling sequence and the remaining prohormone. After cleavage of the signaling sequence, the prohormone is selectively and specifically cleaved by endopeptidases, such as various prohormone convertases, to produce several peptide sequences from a single precursor protein.[20] The peptides are then processed further and post-translationally modified to produce the bioactive neuropeptides.[20] The intricate pathways from genome to active neuropeptide, splice variants, and diversity of post-translational modifications lead to many possible peptide forms that are difficult to predict from genomics or even transcriptomics alone. This compounded with the fact that many model organisms do not have a fully sequenced genome to use as a reliable starting point for predicting a full neuropeptide database makes neuropeptide studies even more challenging.

Mass spectrometry (MS)-based approaches have led to enhanced workflows for detecting, characterizing, and quantifying neuropeptides in various samples. MS can provide detailed, high-accuracy information about the intact mass, sequence, modifications, and expression levels of a detected neuropeptide.[1] Furthermore, MS analyses can profile many analytes (neuropeptides) from a sample in a single experiment without requiring extensive *a priori* knowledge. This unbiased, untargeted

method facilitates discovery-based neuropeptidomics. As neuropeptide function is influenced by the other neuropeptides present, methods to detect the suite of neuropeptides expressed in a sample are critical to understanding the underlying signaling mechanisms of neuropeptides.

Using various labeling and label-free strategies, MS can further provide useful quantitative information that can be used to determine neuropeptide expression differences between samples.[21] Alternative MS analysis methods, such as data-independent acquisition (DIA) can enable greater depth of coverage for the neuropeptidome.[22] These quantitative strategies can be applied not only to the detection and identification of neuropeptides, but also to identifying different forms of neuropeptides with post-translational modifications.[23] Additionally, there have been many developments in the field of MS imaging (MSI) to enable the detection of neuropeptides in specific locations of a tissue or tissue section.[13,24,25] This spatial distribution provides an additional level of information for quantitative neuropeptidomics. Furthermore, MS has applications in numerous -omics (e.g., proteomics, metabolomics), that can offer complementary information to the quantitative neuropeptidomic workflows. By combining the structure elucidation, quantitative information, spatial distribution, and analysis of correlated biomolecules, analysis by MS has greatly improved our understanding of neuropeptides and their roles in many biological processes. This review aims to highlight recent developments in the broader field of neuropeptidomics with an emphasis on quantitative strategies.

2. Quantitative Strategies:

As neuropeptide function has some dependence on concentration,[26] being able to reliably identify and quantify neuropeptides is necessary for understanding their function, especially as it relates to different biological states. A recent review has been published detailing mass spectrometry strategies applied to functional neuropeptidomics.[27] These functional studies are challenging, however, due to the low concentrations (as low as femtomolar) *in vivo*[26] of neuropeptides, highlighting the continual need for improved quantitative methods. Although MS is not inherently quantitative, its widespread application and growth in the -omic fields has led to the development of various strategies for accurate and sensitive quantitation. The quantification of neuropeptides has been achieved with label-free methods that allow analysis of the neuropeptides without modification and minimal sample loss;[28] a variety of labeling strategies that facilitate more reliable quantitation and greater throughput analyses;[29] and more recently, DIA workflows to increase reproducibility and enable detection of more low abundance analytes and thus deeper profiling of the neuropeptidome.[22] These methods are of course not the only quantitative methods for neuropeptidomics and others have been reported and summarized in other reviews.[30,31]

2.1 Label-free Quantitation:

In MS workflows, certain steps, such as desalting, are crucial, but researchers will often forgo extraneous steps to reduce sample loss for low abundance species like many

neuropeptides. Label-free quantitation (LFQ) strategies may suffer from reduced throughput, but they often provide the least amount of sample processing (and fewer losses from it). In LFQ methods, samples are analyzed independently of each other, commonly using LC-MS or LC-MS/MS approaches.[21,32] Quantitation is typically performed by comparing signal intensities (e.g., chromatographic peak area). By examining the extracted ion chromatogram (XIC) of analytes, quantitation is achieved by comparing peak areas between sample runs. Controlling for run-to-run variability is critical for reliable quantitation as samples are run separately.[28] Software is typically used to align the XICs by retention time and filter data, such as ensuring the precursor/fragment ions and the charge states match between aligned peaks.[33,34] Additionally, normalization between analyses needs to be considered to facilitate more accurate comparisons between samples, as variations can arise from instrument calibration, sample preparation, and ambient temperature during analysis. Various methods and software packages for normalization exist and are systematically evaluated in a recent article by Välikangas et al.[35] Ye et al. demonstrated the efficacy of LFQ to quantify neuropeptide expression changes as a result of feeding in a rat model.[36] Anapindi, et al. similarly used XIC analysis to examine neuropeptide expression, but on a much larger scale; over 200 LC-MS runs were performed to identify and quantify over 1500 neuropeptides to examine their effect on chronic migraine and opioid-induced hyperalgesia.[4] Targeted approaches have also proven useful; Salem et al. performed relative quantitation of surrogate neuropeptides and their fragments to characterize the processing of pro-neuropeptides to mature

neuropeptides.[37] Frequently, targeted approaches will employ parallel reaction monitoring (PRM) in which a targeted precursor ion and subsequent fragment ion are analyzed. Similarly, multiple reaction monitoring (MRM) analyses a single precursor ion and multiple fragment ions from that precursor ion. As these approaches minimize interference from other matrix components, sensitivity and throughput are greatly enhanced.[38] Although often used for measuring surrogate peptides from a targeted protein, MRM and PRM have seen use in peptidomics workflows, such as the analysis of orexin in mice cerebrospinal fluid[39] and the identification of endogenous signaling peptides in insects.[40] While MRM and PRM have high sensitivity, the simplicity of using XICs for quantitation allows it to be easily applied to novel and/or less developed MS workflows. Bianco et al., for example, used XICs to characterize differences between arginine and lysine vasopressin after analysis by Fourier transform ion cyclotron resonance (FTICR) MS with multiphoton dissociation.[41]

LFQ workflows can also employ spectral counting for quantitation. Spectral counting assesses protein abundance by correlating concentration to the number of times a constituent peptide is identified, with the idea being that more abundant proteins will be identified more frequently in a single run.[33] The protein abundance index (PAI) is calculated from the normalized level of observed peptides per protein and its exponential modification (emPAI) is used to estimate protein concentrations.[42] In neuropeptidomic experiments, however, identifications are not made based on constituent peptides, as done in bottom-up proteomics, because the endogenous

neuropeptide is generally not digested prior to LC-MS analysis. This greatly reduces the applicability of spectral counting in neuropeptidomic experiments, but it still has gained some use, typically with XIC information used for improved confidence. Southey et al. has shown that spectral counting and spectral indexing (based upon the cumulative intensity of product ions) provide more informative characterization of neuropeptides in the rat suprachiasmatic nucleus over XIC.[28] Other groups have published quantitative methods that utilize both XIC and spectral counting for characterizing endogenous peptides outside of the central nervous system. By comparing the peptidomes of patients with systemic juvenile idiopathic arthritis (SJIA) to healthy patients, LFQ methods enabled the detection of 17 potential biomarkers for SJIA in urine.[43] Similarly, Labas et al. used LFQ methods to characterize peptides in chicken semen to identify key peptides for phenotyping.[44] Although these applications do not address neuropeptides specifically, the peptidomics workflow is translatable and provides future directions for neuropeptide analyses. Even as other quantitative methods are developed, the scalability and ease of using LFQ will likely ensure its continued use in the future.

2.2 Label-based Strategies*:*

Although label-free quantitation is adaptable, requires fewer sample processing steps, and is amenable to many samples, it often requires a greater number of LC-MS runs and can suffer from run-to-run variability. Conversely, many labeling strategies exist that allow samples to be run simultaneously, enabling accurate multiplex quantitation with fewer control samples required, reduced instrument time, and decreased effects

due to instrument variation.[21] For neuropeptide applications, most labeling reactions occur post-extraction and create a mass difference between channels via stable isotope incorporation to differentially label samples. Reductive dimethylation is frequently used to label neuropeptides as it targets primary amines (N-termini and lysine residues), common to most neuropeptides. Additionally, this reaction is low cost and easily accessible, requiring only isotopic formaldehyde and a reducing agent such as borane pyridine or cyanoborohydride.[45] Isotopic dimethylation has been used extensively in the Li lab to study neuropeptidomic changes in crustacean models.[7,10,11,46,47] Moreover, the group has shown the method is compatible with both electrospray ionization (ESI) and matrix-assisted laser desorption/ionization (MALDI) methods to provide complementary coverage of neuropeptides in a single sample.[7] Wilson et al. has developed an online dimethyl labeling system in which neuropeptides are derivatized on-column with either light or heavy reagents.[48] The Fricker lab has also published several articles using isotopic labeling for quantitative peptidomics. They have expanded the reductive dimethyl labeling scheme to an impressive five channels while improving accuracy with isotopic correction calculations.[45] Similarly, the lab has expanded the use of trimethylammoniumbutyryl (TMAB) chemical tags to a 4-plex.[49,50] TMAB tags add a permanent positive charge via a quaternary amine to N-termini and lysine residues of peptides using an amine-reactive NHS ester. These tags have been widely used in peptidomics to study numerous biological processes, including peptide degradation,[51] prohormone processing,[52] narcotic effects,[53] and can be transferred to neuropeptidomic applications. These tags are effective, easily synthesized, and increase signal intensity

by incorporating a permanent positive charge. This permanent charge, coming from a charged quaternary amine, does make the peptide more prone to dissociation, thus increasing instability and limiting application.

One of the major limitations with isotopic labeling, as evidenced by Buchberger et al.[7] and others,[45] is the added spectral complexity with higher multiplexing. This can lead to difficulties in accurately calculating relative abundances, even with isotopic corrections. Additionally, given the wide dynamic range of neuropeptides, it is possible (and perhaps likely) that peaks corresponding to downregulated neuropeptides could be too low in intensity to be quantified or even be detected. Even analytes of high enough intensity might still not be selected for fragmentation and tandem MS analysis by commonly used data-dependent acquisition (DDA) settings, simply due to the greater number of precursor peaks that come with an isotopic labeling workflow. Isobaric tagging–where neuropeptides are labeled with isotopically encoded tags that add the same mass but produce unique reporter ions upon tandem MS analysis–can offer advantages over conventional isotopic labeling. **Figure 1** depicts the differences between isotopic (**1A**) and isobaric tagging (**1B**). These methods are capable of significantly higher order multiplexing, such as 8-plex with iTRAQ,[54] 16-plex with TMTpro,[55] or 21-plex with DiLeu,[56] because only the MS^2 spectra have added complexity due to the unique reporter ions. Moreover, the tags are strategically designed to create reporter ions in regions of the spectrum that do not contain other useful peaks. Isobaric tags have been used often for proteomics applications, but have had fewer applications with peptides,

especially neuropeptides. Dimethylated leucine (DiLeu), for example, has been used to quantify neuropeptides in lobster brains as a function of growth cycle,[15] and also as part of a multi-omic profiling of the mouse hypothalamus,[57] but the low abundance of many neuropeptides still presents challenges. As quantitation occurs at the MS^2 level, isobaric tagging requires analytes be selected for fragmentation and subsequent tandem MS analysis. Low abundance analytes, like many neuropeptides, are often omitted from tandem MS analysis using conventional DDA strategies. Recently, Sauer and Li have shown that optimization of the DDA parameters can facilitate a greater depth of coverage in the crustacean neuropeptidome. This enabled the characterization of many neuropeptides dysregulated in response to copper toxicity.[8] Similar optimization strategies have been used to improve proteomic coverage,[58,59] highlighting a problem not unique to the field of neuropeptidomics. As instrumentation and analytical capabilities improve, it is likely that we will see an increased prevalence of isobaric and isotopic labeling methods reported for neuropeptides and other low abundance analytes.

2.3 Data-Independent Acquisition:

Conventional identification and quantitation of peptides and proteins by mass spectrometry typically involves DDA to trigger and obtain MS^2 fragmentation spectra. Prioritizing fragmentation of the higher signal intensity ions, this acquisition method is biased towards higher abundance and more easily ionizable species. Fragmentation spectra are crucial to obtain confident identification of biomolecules. Neuropeptides are

often of low abundance compared to other biological and neurological matrix components;[60] their analysis can benefit greatly by using a less biased fragmentation scheme. DIA methods were developed to overcome the limitations of DDA, by fragmenting all molecules within a desired m/z window, not only the highest signal intensity ions,[61] demonstrated in **Figure 2**. During DIA MS, all molecules within a *m/z* isolation window of user-defined width are fragmented, without a precursor selection to trigger fragmentation. Fragmentation ion spectra are collected from different isolation windows in a cyclic manner, from the beginning of the defined *m/z* survey range to the end before repeating. MS^1 spectra are collected every cycle, or however often is desired. The use of DIA enables the identification, and therefore potential quantitation, of more molecules compared to DDA,[61–64] including lower abundance molecules such as neuropeptides.[22] As a newer method, DIA MS does not have the breadth of application that DDA does and is not yet commonly applied to neuropeptide analyses. However, the field of neurobiology has seen great benefit from the adoption of quantitative DIA MS, as discussed in a recent review on its application to quantitatively analyze the brain proteome.[65]

Although not all quantitative, a few MS analyses using DIA have recently been performed to better improve the characterization of neuropeptides. DIA MS was used in the untargeted quantification study of neuropeptide expression changes in response to feeding activity in crustacea.[66] The authors were able to detect and quantify 137 peptides directly from microdialysate with minimal sample preparation; no extraction or

precipitation steps were required, demonstrating the utility of DIA for the quantification of limited samples.[66] While DIA MS is a powerful technique for untargeted quantification of neuropeptides, Saidi et al. demonstrated its limitations and higher variances during targeted quantification studies of neuropeptides found in animal spinal cord tissues.[38] Delaney and Li also evaluated the utility of DIA MS for the quantification of neuropeptides from crustacean neural tissue. While improving the technical and biological reproducibility of analysis and number of overall neuropeptides identified compared to DDA, the DIA method showed poor quantitative accuracy using a label free approach.[22] To improve LFQ of peptide hormones using DIA MS, a method was developed using an internal standard peptide, enabling accurate quantitation.[67] As the field of DIA MS quantification further develops, new strategies to improve its abilities to characterize neuropeptides will need to be developed.

The utility of DIA searches using a spectral library-free approach and database searches generated from FASTA sequences has been demonstrated for analysis and quantitation. Model spectra generated from these methods are not always as reliable for neuropeptides as the algorithms are often developed for tryptic peptides. PTMs and structural diversity of endogenous peptides complicate these matters, making it difficult to obtain good results without high-quality spectral libraries. Although identification through spectral library searches have been shown to increase identification and quantitation reproducibility,[68] spectral library generation, requiring high amounts of starting material, may not always be feasible due to the limited sample concentration of

neuropeptides. Database searching and spectral-free methods[69–73] will likely be more beneficial to the future study of neuropeptides by DIA MS.

Overall, DIA has been shown to improve sensitivity of analysis for both identification and LFQ,[74] enabling consistent detection with up to a 10-fold increase in sensitivity compared to DDA, and improving the quantitative dynamic range of analysis.[61,75] Notably, the reproducibility and quantitative performance of DIA MS methods was evaluated by 11 sites worldwide, and reproducible quantitation of proteins was observed.[75] Reproducibility is very important for the quantitation of samples; the same analytes must consistently be identified across all conditions for comparison. A large limitation to DIA analysis is the duty cycle for each scan and total time it takes to cycle through the entire desired *m/z* range. Careful consideration is required when choosing parameters such as maximum ion injection time, automatic gain control target, isolation window width, and full *m/z* range, among others, as this may cause analytes to not be fragmented during the appropriate window before fully eluting during the LC gradient.[76] This issue is further exacerbated during DIA MS for quantitation as accurate quantitation requires data to be collected at multiple points across a peak profile. Further complicating quantitation by DIA MS, multiplexed label-based methods increase spectral complexity, although such methods have recently been utilized in a few proteomics experiments.[77–80] Additional information about the utility and considerations of DIA MS for neuropeptide analysis and quantitation, including software resources can be found in a recent comprehensive review detailing advances in the MS analysis of

neuropeptides [manuscript under review]. More general reviews for proteomics also exist.[63,71,81–83]

DIA can also be beneficial for the analysis of heavily modified analytes where MS signal intensity is distributed across multiple proteoforms, as this increases the number of precursors needed to be selected for fragmentation using DDA. A limitation to this method is the deconvolution of data; multiple precursor ions are co-fragmented in MS^2 spectra and PTMs can further complicate fragmentation spectra. Although it has been shown to benefit the analysis of glycosylated proteins,[84–86] this analysis has not yet been applied to the field of neuropeptidomics. Even with the limitations of DIA, it has been shown to successfully identify more peptides and neuropeptides, with improved reproducibly. With a limit of detection (LOD) in the amol range[61] and improved quantitation capabilities,[75] the field of neuropeptidomics would benefit greatly from the adoption of quantitative DIA MS workflows.

3. Post-Translational Modifications:

Neuropeptides and other bioactive peptides are formed after enzymatic cleavage of larger precursors by peptidases. Additional enzymes can alter these peptides with PTMs, altering their structure, function, and stability, among other effects, contributing to the vast diversity of neuropeptides. Neuropeptide modifications can include amidation, phosphorylation, acetylation, glycosylation, and sulfation, to name a few.[87] Identifying and differentiating between these forms is crucial to understand molecular mechanisms

in neurobiology, and thus these modified neuropeptides are investigated using MS by a variety of labs,[10,88–90] thoroughly summarized in a few recent reviews.[91] The quantification of post-translationally modified neuropeptides faces additional challenges. Labeling approaches often target specific residues and moieties, so post-translational modification of these residues often inhibits quantitation via labeling. For example, many tags target primary amines and are therefore ineffective or less effective for peptides with acetylated N-termini. Further challenging analysis of modified peptides is the decreased ion signal intensity from distribution of already low abundance neuropeptides across the differentially modified forms. This leads to the need for targeted analyses and enrichment strategies to detect and quantify peptides with PTMs,[92–94] especially for those modified by highly dynamic glycosylation.[94–97] As MS considerations are more prominent for peptides modified by glycosylation,[93,98,99] we will focus on the discussion of glycosylated peptides.

Estimated to modify potentially 33% of all known human peptide hormones, changes in glycosylation have a large impact on the role and efficacy of neuropeptides and other bioactive peptides.[100–103] It is therefore of interest to improve quantification abilities for these lower abundance peptides with decreased ionization efficiency compared to their non-modified counterpart.[96] During a targeted analysis to characterize insulin and other signaling peptides in pancreatic islets, Yu et al. discovered insulin to be glycosylated and found this form to be differentially regulated in mouse models of diabetes.[104] This demonstrates the need for more attention to be given to the analysis and quantification

of modified signaling molecules. To this goal, Hansen et al. investigated the potential presence of glycans on atrial natriuretic peptide (ANP), a peptide hormone with its proteolytic degradation and potency being regulated by glycosylation. They characterized and quantified glycosylated ANPs using a targeted MS approach and demonstrated glycosylation on ANP to impact its stability, circulation time, and receptor activation in rats.[105]

To improve the characterization of glycosylated neuropeptides, sensitive and accurate MS methods must be developed. Several dissociation methods have been investigated to better identify glycopeptides, namely collision-based[106–109] and electron-based[106,108,109] dissociation methods. Hybrid methods have also been developed to improve glycopeptide analysis such as electron-transfer/higher-energy collision dissociation (EThcD),[109] higher energy collision dissociation (HCD) product ion-triggered electron transfer dissociation,[110] and HCD product ion-triggered EThcD.[104] EThcD has also been shown to be valuable for quantitative proteomics of phosphorylated biomolecules as well.[111] The type of fragmentation scheme used is important to consider during glycopeptide analysis. Riley et al. demonstrated the need for optimizing dissociation methods, finding peptides modified by N-glycans and O-glycans require different dissociation methods for optimal fragmentation.[112] The information-rich fragment ion spectra generated from EThcD, shown in **Figure 3**, is vital for the confident localization of O-glycans. To characterize glycosylated neuropeptides in crustaceans, Cao et al. utilized HCD triggered EThcD.[23] This study demonstrates the

method's utility for sensitive glyconeuropeptide analysis. Though not applied to endogenous peptides, Zhu et al. describe a three-part workflow for the in-depth investigation of proteins and glycoproteins in the central nervous system.[113] More broad strategies for the quantification of glycosylated proteins and digested peptides have been discussed thoroughly in a recent review.[114] Although glycoproteomics and its quantification is of great interest to the scientific community, we can see that there has been a disproportional amount of investigation into glycosylated neuropeptides, and even less with quantitative approaches applied. This is an underdeveloped field but as glycoproteomic strategies improve in the future, we expect to see them applied to the field of neurobiology towards quantifying endogenous peptides more readily.

4. Mass Spectrometry Imaging:

As various modes of MS are being applied to neuropeptide discovery, there has been an increased emphasis in determining the biological relevance through localizing neuropeptides. MSI has been preferentially implemented in these studies due to the unique advantage of permitting targeted and untargeted detection of analytes within a tissue or cell while still providing spatial information.[115,116] To achieve this, many researchers often use MALDI, where the surface area of a tissue is portioned into data-attainable units (pixels) and imaged through several laser ablations. Quantitative MSI of neuropeptides can be achieved in different ways including absolute quantification using labels to create a calibration curve and semiquantitative spiking with an internal

standard.[115] Here we discuss recent advances in MSI that enable quantitative and semiquantitative analysis of neuropeptides.

Within the field of neuropeptidomics, relative quantitation is widely practiced due to easier sample preparation and reduced costs. Information obtained by these relative quantitation methods can be increased through biological means such as immunohistology assays and Nissl staining.[117,118] These techniques are applied to tissue after MSI to normalize neuropeptide quantities with respect to number of nerves and free amines present. The relative abundance and spatial information from MSI is valuable, but still comes with challenges such as localized ion suppression, availability of software, duration of data collection, and having a sufficient MSI analyzer.[119–122] These issues are exacerbated by the low concentration of neuropeptides in tissue. There have, however, been advances in desorption electrospray ionization (DESI) and liquid extraction surface analysis (LESA) MSI in lipidomics that may help mitigate these issues.[123–125] Zemaitis et al. demonstrates an increased signal intensity in DESI-MSI compared to MALDI-MSI, leading to higher resolving power for lipids.[123] This can likely be attributed to a lack of matrix clusters, which in MALDI, contribute to a pattern of low ionization efficiency.[123,124] Some imaging techniques seek to circumnavigate these issues by performing DESI and MALDI on the same tissue, permitting both proteomic/peptidomic and metabolomic analyses.[125] The use of LESA shows increased signal intensity due to larger sampling size, making this method faster and more sensitive at the sacrifice of spatial resolution.[125] Both LESA and DESI come at the

expense of spatial resolution; where MALDI can often distinguish sub-micron distances, DESI is limited to 50-100 micron and LESA images often have pixel sizes of 1000 microns. These techniques can be coupled with subsequent LC-MS/MS to verify trends of relative abundances seen in imaging experiments or XIC for LFQ.[116,126]

Practices are being explored in drug MSI for better absolute quantitation using more sensitive mass analyzers, such as FTICR, coupled with an increased number of internal standards as well as adjusting calibration curves to pixel deviation.[122,127] Techniques under development work to decrease the LOD such as those discussed in metabolomics works implementing surface-assisted laser desorption/ionization (SALDI)[128] and other matrix-free MSI methods where nanoparticles are used to coat the tissue to enhance ionization efficiency as well as spatial resolutions (**Figure 4**).[129,130] These methods incorporate metals and have been found to retain spatial resolution of MALDI (~2-5 microns) while increasing ionization efficiency for small molecules. They are, however, presently limited to small molecules like drugs and metabolites. Such relative abundance techniques, combined with LFQ via LC-MS/MS back-correlation and software development, could greatly improve the accuracy and performance of quantitative MSI studies. The many forms of MSI complement the diversity of biological problems being studied, and advancements in MSI of neuropeptides will provide insights into the anatomy and physiology of neurological function and regulation. This in turn will help clinicians and other researchers identify and treat various health conditions.

5. Multi-omics:

The exact roles of neuropeptides are often difficult to discern when strictly observing only neuropeptides. Their receptors are typically proteins, such as G protein-coupled receptors (GPCRs);[131] they regulate biochemical pathways with downstream metabolite products;[132] and are often co-expressed and co-released with small molecule neurotransmitters.[133] Multi-omic workflows have emerged in which elements of proteomic, peptidomic, metabolomic, etc. experiments are integrated to provide more comprehensive information.[134–136] As a result, multi-omic experiments have seen increased popularity in neuropeptide experiments in recent years.

5.1 Small Molecule Studies:

Characterizing neuropeptides and relevant small molecules in a single experiment is difficult due to stark differences in extraction efficiencies, solubilities, ionization efficiencies, fragmentation patterns, and subsequent data analysis. Specific applications have further constraints, such as matrix compatibilities for MSI. Nevertheless, researchers have made recent advances in combining neuropeptidomics with small molecule analyses (e.g., lipidomics and metabolomics), typically by processing the two separately, then co-analyzing the data. Keller et al. addressed the extraction issues using both acidified methanol and methanol/water/chloroform extractions to efficiently recover proteins, peptides, and metabolites. Two molecular weight cut-off (MWCO) filters were used to separate metabolites (<3 kDa), peptides (3-30 kDa), and proteins (>30 kDa).[136] Although not specifically studying neuropeptides, the reported extraction

methods (i.e., acidified methanol), have been used previously for neuropeptides.[7,8,22,46] Gutierrez et al. reported a similar strategy in which an acetone/chloroform precipitation was used to separate proteins and metabolites.[135] This method, dubbed SPOT (sample preparation for multi-omic technologies), is not described for the study of endogenous peptides, but could be adapted by adding a MWCO step similar to Keller et al. For some approaches, neuropeptides do not necessarily need to be isolated from metabolites prior to LC-MS analysis. Chen et al. used atmospheric pressure (AP) MALDI to study neuropeptides, lipids, and other biomolecules from the same tissue section, but incorporated different ionization methods.[137] This niche strategy eliminates issues with extraction and ionization efficiency differences by collecting data directly from the tissue section. The lack of tandem MS data, however, does require researchers to rely on accurate mass matching, possibly losing confidence in data interpretation

Often co-expressed and released with neuropeptides, neurotransmitters are another target for multi-omics. Wojnicz et al. report a method that combines short neuropeptides (4 residues) and metabolite analyses to study bovine cells without the need for separate extractions. Using synthetic standards, they created a calibration curve that allowed absolute quantitation of both neuropeptides and neurotransmitters.[132] These methods would likely have limited applicability to larger neuropeptides but are important in establishing multi-omic strategies. Similarly, zwitterion exchange has been used for online separation prior to LC-MS to quantify neurotransmitters and select neuropeptides (oxytocin and vasopressin) simultaneously

from blood.[138] Alternative separation and sampling methods, like microdialysis coupled to LC-MS, have offered sensitive assays for quantifying both neuropeptides and neurotransmitters, summarized in a review by Zestos and Kennedy.[139]

5.2 Proteomics:

Although similar in structure to proteins, neuropeptides require different analytical workflow than proteins largely due to size differences. Most multi-omic workflows that combine proteomics with the study of endogenous peptides like neuropeptides analyze the two separately and interpret the combined data. For example, Liu et al. describes the use of label-free neuropeptidomics with multiplex DiLeu-labeled neuroproteomics, workflow highlighted in **Figure 5**, to profile changes in the mouse hypothalamus resulting from the gut microbiome.[57] This study demonstrated the impact of the gut microbiome on neurochemical processes.[57] Similarly, Chen et al. combined label-free and labeled data to interrogate proteomic, metabolomic, and peptidomic (translatable to neuropeptides) dysregulation in metabolic diseases.[134] Neuroproteomics has also revealed dysregulation of neuropeptide and neurotransmitter release with impacts in neuropsychiatric diseases, such as addiction, using LFQ MS.[140] Conversely, Hook et al. characterizes neuropeptide variants to inform neuroproteomics and precursor protein analysis to better understand proteolytic processing and how it relates to cell-cell signaling.[87] The study of endogenous peptides outside of the neuroendocrine system can also provide translatable methods for multi-omic neuropeptide studies. For example, Labas et al. do not specifically study neuropeptides, but report a LFQ assay to

combine proteomic and peptidomic data to phenotype chicken semen in a multi-omic experiment using spectral counting and XICs from LC-MS data.[44] By omitting the digestion step typically used to study proteins (bottom-up proteomics), Li et al., describe the use of top-down MS methods to study microproteins and endogenous peptides in mouse brain tissue extracts.[141] Top-down MS methods like these are crucial for studying different protein and peptide forms but need adaptation to studying larger proteins and neuropeptides simultaneously.

While several advances have been made to address MS concerns when studying classes of molecules with distinct chemical properties, such as sequential extractions, methods employing simultaneous co-analysis are far from being common. To fully understand the interplay between different types of biomolecules, improvements into interpreting large amounts of data is also required. As investigations into complicated multi-interaction diseases and biological functions are increasingly being pursued by the scientific community, we expect to see more extensive multi-omics experiments adopted into future workflows.

6. Conclusion:

The field of neuropeptidomics is constantly evolving and recent improvements have led to enhanced detection and quantitation of neuropeptides. Their low *in vivo* abundance, complex functions, and structural diversity make their analysis challenging, but MS analyses have mitigated many of these difficulties.[142] Isotopic labeling strategies, such

as dimethyl labeling[45] and TMAB labeling,[49] differentiate neuropeptides at the precursor ion level but are only used to compare a few experimental conditions. Enhanced multiplexing can be achieved with the incorporation of isobaric tagging because it does not significantly increase spectral complexity.[8] Labeling strategies do enable higher throughput and typically more reliable quantitation, but additional sample processing steps often cause sample loss which is detrimental for low abundance analytes like many neuropeptides. As a result LFQ methods are still common.[140] These methods are also more compatible with DIA methods, facilitating greater sensitivity and neuropeptidome coverage.[22] Quantitative strategies are also employed in imaging workflows to provide spatial distribution, utilizing a variety of normalization methods to ensure quantitation is accurate, summarized nicely in a review by Tobias and Hummon.[115] Analysis of PTMs, especially glycosylation, has greatly benefited from improvements in hybrid MS fragmentation method, such as the use of HCD-triggered EThcD to improve fragmentation of glycopeptides (and glyconeuropeptides).[23] As neuropeptidomic workflows become more common and accessible, their findings can be incorporated into larger multi-omic workflows.[57] There is still much room for improvement in terms of technology and method development, but recent advances in neuropeptidomics have provided much insight into the complex signaling pathways involving neuropeptides, with impacts in the fields of biomarker discovery and drug development.

7. Expert Opinion:

The field of neuropeptidomics is instrumental to our understanding of neuromodulation and signaling. This in turn has applications in clinical settings in the areas of biomarker discovery, drug discovery, and drug action.[131,133,143] Neuropeptide dysregulation has been linked to many biological problems and diseases, such as Alzheimer's disease,[144] obesity,[145] cancer,[146] and depression.[147] The advances in neuropeptidomics have enabled researchers to better understand many of these conditions and the related signaling pathways. This can facilitate the discovery of new, more reliable biomarkers. Additionally, knowledge gained from these signaling pathways may provide new drug action sites or possibly even modifying neuropeptides to act as drugs themselves.

Adoption of neuropeptidomics in a clinical setting does still present challenges, however. As neurochemistry is incredibly complex, most studies are performed in organisms with simpler neuroendocrine systems, including some mammals like mice and rats,[148] and many invertebrates, such as crustaceans[149] and nematodes.[150] Translation from these models to humans is difficult and, at the very least, will require more sophisticated, less invasive sampling methods (e.g., microdialysis). Clinical research involving humans also has the added complexity of genetic diversity. Biomarker discovery and genetic risk score assessments have historically been biased, and more and more research is demonstrating the importance of clinical research that accounts for sex, age, and racial diversity.[151–158] Additionally, MS analyses of neuropeptides, while sensitive, accurate, and quantitative, may not offer high enough throughput for clinical applications. Multiplexing techniques, such as the

aforementioned DiLeu tags,[8,56,159] can greatly improve throughput, but are not commercially available. Conversely, the tags that are commercially available (e.g., TMT)[55] are expensive and do not offer as high a degree of multiplexing. Furthermore, clinical applications could necessitate absolute quantitation, often requiring expensive isotopic peptide standards. The Li Lab has developed chemical tags that enable low cost, absolute quantitation. These isotopic DiLeu (iDiLeu) tags are used to create a calibration curve from a synthesized peptide and compare the target peptide to the calibration curve.[160] Methods like this still require synthetic peptides, albeit much cheaper as the isotopes are incorporated via chemical labeling, not during the synthesis of peptides. When the iDiLeu tags are combined with multiplex isobaric tagging reagents, the throughput of absolute quantification can be greatly enhanced, which could be highly beneficial for absolute quantification and biomarker validation with large cohort of clinical specimens.

Advances in quantitation are often aided by chemical labeling methods, but improvements in sample analysis are other avenues to consider. As mass spectrometers become more sophisticated, neuropeptidomic analyses are greatly enhanced. For example, increased scan times enable greater depth of coverage, especially for low level analytes like neuropeptides. Increased resolving power can help differentiate between neuropeptides with similar masses, and can facilitate greater multiplexing, as seen by the incorporation of mass defects in DiLeu 12- and 21-plex tags.[56,159] Newer instruments are also capable of performing alternative fragmentation methods, such as

ETD and EThcD, to provide more detailed MS^2 data. This is especially beneficial for analysis of PTMs like glycosylation.[23] DIA experiments have also offered many improvements, especially for low concentration analytes that normally are missed by DDA settings (e.g., neuropeptides)[22], despite being a relatively new method. These benefits are certain to increase as DIA sees more popularity and data analysis/deconvolution software improves. Advances in MALDI-MS have given rise to instruments with high acquisition rates and decreased laser size to generate MSI data with high spatial resolution without requiring extra time.[161] Further improvements in instrumentation will undoubtedly enable more robust neuropeptidomic experiments.

We speculate the field of neuropeptidomics to continue thrive on its current trajectory, but with increased prevalence, informing many biological studies. This is largely due to recent advances in quantitation and the many possibilities of its application for quantitative neuropeptidomics. As instrumentation enables faster analyses, either through increased scan times, or faster separation modes like capillary electrophoresis,[162] LFQ could see increased use as throughput improves. Conversely, these advances could also lead to an increase in the use of labeling techniques as instruments are able to resolve miniscule mass differences to enable more accurate and sensitive analyses of neuropeptides. Ultimately these methods will both see continued use depending on application, but it will be interesting to see how they are incorporated into larger experiments. As neuropeptides have profound impacts on many biochemical and physiological processes, their study will undoubtedly be important in larger

proteomic and metabolomic experiments, and we predict an increase in multi-omic studies, even at the single-cell level with continued improvements in instrumentation and microscale sample preparation. Advances in neuropeptide analyses are also not limited to quantitation. Spatial distribution information gained from MSI can be used to characterize neuropeptide function, receptors, etc.[117] Additionally, ion mobility MS (IM-MS) is routinely used to provide structural information that can be used to distinguish isobaric neuropeptides and better understand neuropeptide conformation and possibly functional roles dependent on its tertiary/quaternary structure.[95,163] As IM-MS and MSI methods are further developed, our understanding of neuropeptides will greatly improve. Combining the structural and quantitative aspects of mass spectrometry will provide richer characterization of neuropeptides, and thus has the power to lead to better biomarkers and drug design to help combat neurological disorders, obesity, and other common health concerns.

Author Contributions:

All authors have substantially contributed to the writing and design of the review article. The original draft was written by C.S.S., A.P., and O.L.R., with revising and rewriting performed by L.L.

Declaration of Interests:

The authors have no relevant affiliations or financial involvement with any organization or entity with a financial interest in or financial conflict with the subject matter or materials discussed in the manuscript. This includes employment, consultancies,

honoraria, stock ownership or options, expert testimony, grants or patents received or pending, or royalties.

Funding:

This manuscript was funded by the National Science Foundation (CHE-1710140) and National Institutes of Health through grants (R01DK071801, U01CA231081, RF1 AG052324, and P41GM108538). C.S.S. acknowledges a National Institute of Environmental Health Sciences fellowship as part of the National Ruth L. Kirschstein Research Service Award fellowship program (F31ES031859). A.P. was supported in part by the NIH Chemistry–Biology Interface Training Grant (T32 GM008505). O.L.R was supported by the UW-Madison/ACS Bridge to the Chemistry Doctorate Program. The UW/ACS Bridge Program is supported in part by the National Science Foundation Award NSF-1834545 to the American Chemical Society, supplemented by funds from the UW-Madison Graduate School, Office of Vice Chancellor for Research and Graduate Education and the Department of Chemistry. L.L. acknowledges a Vilas Distinguished Achievement Professorship and Charles Melbourne Johnson Professorship with funding provided by the Wisconsin Alumni Research Foundation and University of Wisconsin-Madison School of Pharmacy.

References:

1. Li L, Sweedler J V. Peptides in the Brain: Mass Spectrometry–Based Measurement Approaches and Challenges. *Annu Rev Anal Chem*. 2008;1(1):451-483. doi:10.1146/annurev.anchem.1.031207.113053

2. Gäde G, Šimek P, Marco HG. Biochemically identified neuropeptides in a caddisfly (Trichoptera) and a pygmy mole cricket (Orthoptera: Caelifera: Tridactyloidea). *Arch Insect Biochem Physiol*. 2021;106(4):1-11. doi:10.1002/arch.21778

3. Habenstein J, Schmitt F, Liessem S, et al. Transcriptomic, peptidomic and mass spectrometry imaging analysis of the brain in the ant Cataglyphis nodus . *J Neurochem*. 2021;(March):1-22. doi:10.1111/jnc.15346

4. Anapindi KDB, Yang N, Romanova E V., et al. PACAP and other neuropeptide targets link chronic migraine and opioid-induced hyperalgesia in mouse models. *Mol Cell Proteomics*. 2019;18(12):2447-2458. doi:10.1074/mcp.RA119.001767

5. Ueda D, Yonemochi N, Kamata T, Kamei J, Waddington JL, Ikeda H. Increase in neuropeptide Y activity impairs social behaviour in association with glutamatergic dysregulation in diabetic mice. *Br Pharmacol Soc*. 2021;178:726-740. doi:10.1111/bph.15326

6. Chen R, Xiao M, Buchberger A, Li L. Quantitative neuropeptidomics study of the effects of temperature change in the crab cancer borealis. *J Proteome Res*. 2014;13(12):5767-5776. doi:10.1021/pr500742q

7. Buchberger AR, Sauer CS, Vu NQ, DeLaney K, Li L. A Temporal Study of the Perturbation of Crustacean Neuropeptides Due to Severe Hypoxia Using 4-Plex Reductive Dimethylation. *J Proteome Res*. 2020;19:1548-1555. doi:10.1021/acs.jproteome.9b00787

8. Sauer CS, Li L. Mass Spectrometric Profiling of Neuropeptides in Response to Copper Toxicity via Isobaric Tagging. *Chem Res Toxicol*. 2021.

doi:10.1021/acs.chemrestox.0c00521

9. Buchberger AR, Vu NQ, Johnson J, Delaney K, Li L. A Simple and E ff ective Sample Preparation Strategy for MALDI-MS Imaging of Neuropeptide Changes in the Crustacean Brain Due to Hypoxia and Hypercapnia Stress. *J Am Soc Mass Spectrom*. 2020;31:1058-1065. doi:10.1021/jasms.9b00107
10. Liu Y, Buchberger AR, Delaney K, Li Z, Li L. Multifaceted Mass Spectrometric Investigation of Neuropeptide Changes in Atlantic Blue Crab, Callinectes sapidus , in Response to Low pH Stress. *J Proteome Res*. 2019;18:2759-2770. doi:10.1021/acs.jproteome.9b00026
11. Zhang Y, Buchberger A, Muthuvel G, Li L. Expression and distribution of neuropeptides in the nervous system of the crab Carcinus maenas and their roles in environmental stress. *Proteomics*. 2015;15(23-24):3969-3979. doi:10.1002/pmic.201500256
12. Chen R, Ma M, Hui L, Zhang J, Li L. Measurement of Neuropeptides in Crustacean Hemolymph via MALDI Mass Spectrometry. *J Am Soc Mass Spectrom*. 2009;20(4):708-718. doi:10.1016/j.jasms.2008.12.007
13. DeLaney K, Hu M, Hellenbrand T, Dickinson PS, Nusbaum MP, Li L. Mass spectrometry quantification, localization, and discovery of feeding-related neuropeptides in cancer borealis. *ACS Chem Neurosci*. 2021. doi:10.1021/acschemneuro.1c00007
14. Hu M, Helfenbein K, Buchberger AR, Delaney K, Liu Y, Li L. Exploring the Sexual Dimorphism of Crustacean Neuropeptide Expression Using Callinectes sapidus as

a Model Organism. *J Proteome Res*. 2021;20:2739-2750. doi:10.1021/acs.jproteome.1c00023

15. Jiang X, Xiang F, Jia C, Buchberger AR, Li L. Relative Quantitation of Neuropeptides at Multiple Developmental Stages of the American Lobster Using *N* , *N* -Dimethyl Leucine Isobaric Tandem Mass Tags. *ACS Chem Neurosci*. 2018:acschemneuro.7b00521. doi:10.1021/acschemneuro.7b00521
16. Mikołajczyk A, Złotkowska D. Subclinical lipopolysaccharide from Salmonella Enteritidis induces neuropeptide dysregulation in the spinal cord and the dorsal root ganglia. *BMC Neurosci*. 2019:1-13. doi:10.1186/s12868-019-0502-z
17. Ishii XM, Hiller AJ, Pham L, Mcguire MJ, Iadecola C, Wang G. Amyloid-Beta Modulates Low-Threshold Activated Voltage- Gated L-Type Calcium Channels of Arcuate Neuropeptide Y Neurons Leading to Calcium Dysregulation and Hypothalamic Dysfunction. *J Neurosci*. 2019;39(44):8816-8825.
18. Khairuddin S, Aquili L, Chin B, et al. Neuroscience and Biobehavioral Reviews Dysregulation of the orexinergic system : A potential neuropeptide target in depression. *Neurosci Biobehav Rev*. 2020;118(March):384-396. doi:10.1016/j.neubiorev.2020.07.040
19. Ye H, Wang J, Zhang Z, et al. Defining the neuropeptidome of the spiny lobster Panulirus interruptus brain using a multidimensional mass spectrometry-based platform. *J Proteome Res*. 2015;14(11):4776-4791. doi:10.1021/acs.jproteome.5b00627
20. Fricker LD. Proteolytic processing of Neuropepties. *Neuromethods*. 2016;114:209-

220.

21. Protein LS, Anand S, Samuel M, Ang C, Keerthikumar S, Mathivanan S. Chapter 4 Label-Based and Label-Free Strategies for Protein Quantitation. In: *Proteome Bioinformatics, Methods in Molecular Biology*. Vol 1549. ; 2017:31-43. doi:10.1007/978-1-4939-6740-7
22. Delaney K, Li L. Data Independent Acquisition Mass Spectrometry Method for Improved Neuropeptidomic Coverage in Crustacean Neural Tissue Extracts. *Anal Chem*. 2019;(91):5150-5158. doi:10.1021/acs.analchem.8b05734
23. Cao Q, Yu Q, Liu Y, Chen Z, Li L. Signature-Ion-Triggered Mass Spectrometry Approach Enabled Discovery of N- And O-Linked Glycosylated Neuropeptides in the Crustacean Nervous System. *J Proteome Res*. 2020;19(2):634-643. doi:10.1021/acs.jproteome.9b00525
24. Jiang S, Liang Z, Hao L, Li L. Investigation of signaling molecules and metabolites found in crustacean hemolymph via in vivo microdialysis using a multifaceted mass spectrometric platform. *Electrophoresis*. 2016;37(7-8):1031-1038. doi:10.1002/elps.201500497
25. Vu NQ, Buchberger AR, Johnson J, Li L. Complementary neuropeptide detection in crustacean brain by mass spectrometry imaging using formalin and alternative aqueous tissue washes. *Anal Bioanal Chem*. 2021;413(10):2665-2673. doi:10.1007/s00216-020-03073-x
26. Maes K, Van Liefferinge J, Viaene J, et al. Improved sensitivity of the nano ultra-high performance liquid chromatography-tandem mass spectrometric analysis of

low-concentrated neuropeptides by reducing aspecific adsorption and optimizing the injection solvent. *J Chromatogr A*. 2014;1360:217-228. doi:10.1016/j.chroma.2014.07.086

27. Haes W De, Sinay E Van, Detienne G, Temmerman L, Schoofs L, Boonen K. Functional neuropeptidomics in invertebrates. *BBA - Proteins Proteomics*. 2015;1854(7):812-826. doi:10.1016/j.bbapap.2014.12.011
28. Southey BR, Lee JE, Zamdborg L, et al. Comparing Label-Free Quantitative Peptidomics Approaches to Characterize Diurnal Variation of Peptides in the Rat Suprachiasmatic Nucleus. *Anal Chem*. 2014;86:443-452.
29. Boonen K, Haes W De, Houtven J Van, et al. Chapter 9 Quantitative Peptidomics with Isotopic and Isobaric Tags. In: *Peptidomics: Methods and Strategies, Methods in Molecular Biology*. Vol 1719. ; 2018:141-159.
30. Lee JE. Neuropeptidomics: Mass Spectrometry-Based Identification and Quantitation of Neuropeptides. *Genomics and Informatics*. 2016;14(1):12-19.
31. Buchberger A, Yu Q, Li L. Advances in Mass Spectrometric Tools for Probing Neuropeptides. *Annu Rev Anal Chem*. 2015;8(1):485-509. doi:10.1146/annurev-anchem-071114-040210
32. Wang M, You J, Bemis KG, Fitzpatrick DPG. Chapter 10 Label-Free Mass Spectrometry-Based Protein Quantification Technologies in Protein Biomarker Discovery. In: *Methods in Pharmacology and Toxicology: Biomarker Methods in Drug Discovery and Development*. ; 2008:211-230.
33. Fricker L. Chapter 8 Quantitative Peptidomics : General Considerations. In:

Peptidomics: Methods and Strategies, Methods in Molecular Biology. Vol 1719. ; 2018:121-140.

34. Wu C, Monroe ME, Xu Z, et al. An Optimized Informatics Pipeline for Mass Spectrometry-Based Peptidomics. *J Am Soc Mass Spectrom*. 2015;26:2002-2008. doi:10.1007/s13361-015-1169-z
35. Välikangas T, Suomi T, Elo LL. A systematic evaluation of normalization methods in quantitative label-free proteomics. *Brief Bioinform*. 2018;19(1):1-11. doi:10.1093/bib/bbw095
36. Ye H, Wang J, Tian Z, et al. Quantitative Mass Spectrometry Reveals Food Intake-Induced Neuropeptide Level Changes in Rat Brain : Functional Assessment of Selected Neuropeptides as Feeding Regulators * □. *Mol Cell Proteomics*. 2017;16(11):1922-1937. doi:10.1074/mcp.RA117.000057
37. Salem J Ben, Nkambeu B, Arvanitis DN, Beaudry F. Deciphering the Role of EGL-3 for Neuropeptides Processing in Caenorhabditis elegans Using High-Resolution Quadrupole–Orbitrap Mass Spectrometry. *Neurochem Res*. 2018;43(11):2121-2131. doi:10.1007/s11064-018-2636-2
38. Saidi M, Kamali S, Beaudry F. Neuropeptidomics: Comparison of parallel reaction monitoring and data-independent acquisition for the analysis of neuropeptides using high-resolution mass spectrometry. *Biomed Chromatogr*. 2019;33(7):1-11. doi:10.1002/bmc.4523
39. Hopkins K, Mukherjee S, Ponce D, Mangum J, Jacobson LH, Hoyer D. Development of a LC-ESI-MRM method for the absolute quantification of orexin A

in the CSF of individual mice. *Med Drug Discov*. 2021;11(February):100102. doi:10.1016/j.medidd.2021.100102

40. Fleites LA, Johnson R, Kruse AR, et al. Peptidomics Approaches for the Identification of Bioactive Molecules from Diaphorina citri. *J Proteome Res*. 2020;19(4):1392-1408. doi:10.1021/acs.jproteome.9b00509
41. Bianco G, Battista FG, Buchicchio A, Amarena CG, Schmitt-Kopplin P, Guerrieri A. Structural characterization of arginine vasopressin and lysine vasopressin by fourier-transform ion cyclotron resonance mass spectrometry and infrared multiphoton dissociation. *Eur J Mass Spectrom*. 2015;21(3):211-219. doi:10.1255/ejms.1339
42. Shinoda K, Tomita M, Ishihama Y. emPAI Calc — for the estimation of protein abundance from large-scale identification data by liquid chromatography-tandem mass spectrometry. *Bioinformatics*. 2010;26(4):576-577. doi:10.1093/bioinformatics/btp700
43. Ling XB, Lau K, Deshpande C, et al. Urine Peptidomic and Targeted Plasma Protein Analyses in the Diagnosis and Monitoring of Systemic Juvenile Idiopathic Arthritis. *Clin Proteomics*. 2010;6:175-193. doi:10.1007/s12014-010-9058-8
44. Labas V, Grasseau I, Cahier K, Gargaros A. Qualitative and quantitative peptidomic and proteomic approaches to phenotyping chicken semen. *J Proteomics*. 2014;112:313-335. doi:10.1016/j.jprot.2014.07.024
45. Tashima AK, Fricker LD. Quantitative Peptidomics with Five-plex Reductive Methylation labels. *J Am Soc Mass Spectrom*. 2018;29(5):866-878.

doi:10.1007/s13361-017-1852-3

46. Hu M, Helfenbein K, Buchberger AR, DeLaney K, Liu Y, Li L. Exploring the Sexual Dimorphism of Crustacean Neuropeptide Expression Using Callinectes sapidus as a Model Organism . *J Proteome Res*. 2021. doi:10.1021/acs.jproteome.1c00023
47. Chen R, Xiao M, Buchberger A, Li L. Quantitative neuropeptidomics study of the effects of temperature change in the crab cancer borealis. *J Proteome Res*. 2014;13(12):5767-5776. doi:10.1021/pr500742q
48. Wilson RE, Jaquins-Gerstl A, Weber SG. On-Column Dimethylation with Capillary Liquid Chromatography-Tandem Mass Spectrometry for Online Determination of Neuropeptides in Rat Brain Microdialysate. *Anal Chem*. 2018;90(7):4561-4568. doi:10.1021/acs.analchem.7b04965
49. Berezniuk I, Sironi JJ, Wardman J, et al. Quantitative Peptidomics of Purkinje Cell Degeneration Mice. *PLoS One*. 2013;8(4):1-12. doi:10.1371/journal.pone.0060981
50. Gelman JS, Wardman J, Bhat VB, Gozzo FC, Fricker LD. Chapter 31 Quantitative Peptidomics to Measure Neuropeptide Levels in Animal Models Relevant to Psychiatric Disorders. In: *Psychiatric Disorders: Methods and Protocols, Methods in Molecular Biology*. Vol 829. ; 2012:487-503. doi:10.1007/978-1-61779-458-2
51. Wardman J, Fricker LD. Chapter 17 Quantitative Peptidomics of Mice Lacking Peptide-Processing Enzymes. In: *Proprotein Covertases, Methods in Molecular Biology*. ; 2011:307-323. doi:10.1007/978-1-61779-204-5
52. Zhang, Xin, Hui, Pan, Peng, Bonnie, Steiner, Donald F., Pintar, John E., Fricker

LD. Neuropeptidomic analysis establishes a major role for prohormone covertase-2 in neuropeptide biosynthesis. *J Neurochem*. 2010;112:1168-1179. doi:10.1111/j.1471-4159.2009.06530.x

53. Berezniuk, Iryna, Rodriguiz, Ramona M., Zee, Michael L., Marcus, David J., Pintar, John, Morgan, Daniel J., Wetsel, William C., Fricker LD. ProSAAS-derived peptides are regulated by cocaine and are required for sensitization to the locomotor effects of cocaine. *J Neurochem*. 2017;143:268-281. doi:10.1111/jnc.14209
54. Moulder R, Bhosale SD, Goodlett DR, Lahesmaa R. Analysis of the plasma proteome using iTRAQ and TMT-based Isobaric labeling. *Mass Spectrom Rev*. 2018;37:583-606. doi:10.1002/mas.21550
55. Li J, Vranken JG Van, Vaites LP, et al. TMTpro reagents: a set of isobaric labeling mass tags enables simultaneous proteome-wide measurements across 16 samples. *Nat Methods*. 2020;17(April). doi:10.1038/s41592-020-0781-4
56. Frost DC, Feng Y, Li L. 21-plex DiLeu Isobaric Tags for High-Throughput Quantitative Proteomics. *Anal Chem*. 2020;92(12):8228-8234. doi:10.1021/acs.analchem.0c00473
57. Liu R, Wei P, Keller C, et al. Integrated Label-Free and 10-Plex DiLeu Isobaric Tag Quantitative Methods for Pro fi ling Changes in the Mouse Hypothalamic Neuropeptidome and Proteome: Assessment of the Impact of the Gut Microbiome. *Anal Chem*. 2020;92:14021-14030. doi:10.1021/acs.analchem.0c02939
58. Andrews GL, Dean RA, Hawkridge AM, Muddiman DC. Improving proteome

coverage on a LTQ-orbitrap using design of experiments. *J Am Soc Mass Spectrom*. 2011;22(4):773-783. doi:10.1007/s13361-011-0075-2

59. Hecht ES, McCord JP, Muddiman DC. Definitive Screening Design Optimization of Mass Spectrometry Parameters for Sensitive Comparison of Filter and Solid Phase Extraction Purified, INLIGHT Plasma N-Glycans. *Anal Chem*. 2015;87(14):7305-7312. doi:10.1021/acs.analchem.5b01609
60. Svensson M, Skold K, Nilsson A, Falth M, Nydahl, Katarina Svenningsson P, Andren PE. Neuropeptidomics : MS Applied to the Discovery of Novel Peptides from the Brain. *Anal Chem*. 2007:15-21.
61. Gillet LC, Navarro P, Tate S, et al. Targeted Data Extraction of the MS/MS Spectra Generated by Data-independent Acquisition: A New Concept for Consistent and Accurate Proteome Analysis. *Mol Cell Proteomics*. 2012;11(6):1-17. doi:10.1074/mcp.O111.016717
62. Panchaud A, Scherl A, Shaffer SA, et al. Precursor Acquisition Independent From Ion Count: How to Dive Deeper into the Proteomics Ocean. *Anal Chem*. 2009;81(15):6481-6488.
63. Krasny L, Huang PH. Data-independent acquisition mass spectrometry (DIA-MS) for proteomic applications in oncology. *Mol Omi*. 2021;17:29-42. doi:10.1039/d0mo00072h
64. Panchaud A, Jung S, Sha SA, Aitchison JD, Goodlett DR. Faster, Quantitative, and Accurate Precursor Acquisition Independent From Ion Count. *Anal Chem*. 2011;83:2250-2257.

65. Li KW, Gonzalez-lozano MA, Koopmans F, Smit AB. Recent Developments in Data Independent Acquisition (DIA) Mass Spectrometry: Application of Quantitative Analysis of the Brain Proteome. *Front Mol Neurosci*. 2020;13:1-8. doi:10.3389/fnmol.2020.564446

66. Schmerberg CM, Liang Z, Li L. Data-Independent MS/MS Quantification of Neuropeptides for Determination of Putative Feeding-Related Neurohormones in Microdialysate. *ACS Chem Neurosci*. 2015;6:174-180. doi:10.1021/cn500253u

67. Xiao P, Zhang F, Wang X, Song D, Li H. Analysis of B-type natriuretic peptide impurities using label-free data-independent acquisition mass spectrometry technology. *Clin Chem Labratory Med*. 2021;59(1):217-226. doi:10.1515/cclm-2020-0012

68. Fernandez-Costa C, Martinez-Bartolome S, McClatchy DB, Saviola AJ, Yu N-K, Yates JR. Impact of the Identification Strategy on the Reproducibility of the DDA and DIA Results. *J Proteome Res*. 2020;19:3153-3161. doi:10.1021/acs.jproteome.0c00153

69. Tsou C, Tsai C, Teo GC, Chen Y, Nesvizhskii AI. Untargeted , spectral library-free analysis of data-independent acquisition proteomics data generated using Orbitrap mass spectrometers. *Proteomics*. 2016;16:2257-2271. doi:10.1002/pmic.201500526

70. Chen C, Hou J, Tanner JJ. Bioinformatics Methods for Mass Spectrometry-Based Proteomics Data Analysis. *Int J Mol Sci*. 2020;21(2873):1-25.

71. Zhang F, Ge W, Ruan G, Cai X, Guo T. Data-Independent Acquisition Mass

Spectrometry-Based Proteomics and Software Tools : A Glimpse in 2020. *Proteomics*. 2020;20:1-12. doi:10.1002/pmic.201900276

72. Pino LK, Just SC, Maccoss MJ, et al. Acquiring and Analyzing Data Independent Acquisition Proteomics Experiments without Authors Acquiring and Analyzing Data Independent Acquisition Proteomics Experiments without. *Mol Cell Proteomics*. 2020;19(7):1088-1103. doi:10.1074/mcp.P119.001913
73. Searle BC, Pino LK, Egertson JD, et al. Chromatogram libraries improve peptide detection and quantification by data independent acquisition mass spectrometry. *Nat Commun*. 2018;9(5128):1-12. doi:10.1038/s41467-018-07454-w
74. He B, Shi J, Wang X, Jiang H, Zhu H. Label-free absolute protein quantification with data-independent acquisition. *J Proteomics*. 2019;200:51-59. doi:10.1016/j.jprot.2019.03.005
75. Collins BC, Hunter CL, Liu Y, et al. Multi-laboratory assessment of reproducibility, qualitative and quantitative performance of SWATH-mass spectrometry. *Nat Commun*. 2017;8(291):1-11. doi:10.1038/s41467-017-00249-5
76. Venable JD, Dong M, Wohlschlegel J, Dillin A, Iii JRY. Automated approach for quantitative analysis of complex peptide mixtures from tandem mass spectra. *Nat Methods*. 2004;1(1):1-7. doi:10.1038/NMETH705
77. Zhong X, Frost DC, Yu Q, Li M, Gu TJ, Li L. Mass Defect-Based DiLeu Tagging for Multiplexed Data-Independent Acquisition. *Anal Chem*. 2020;92:11119-11126. doi:10.1021/acs.analchem.0c01136
78. Di Y, Zhang Y, Zhang L, Tao T, Lu H. MdFDIA: A Mass Defect Based Four-Plex

Data-Independent Acquisition Strategy for Proteome Quantification. *Anal Chem*. 2017;89(19):10248-10255. doi:10.1021/acs.analchem.7b01635

79. Zhang S, Di Y, Yao J, et al. Mass defect-based carbonyl activated tags (mdCATs) for multiplex data-independent acquisition proteome quantification. *Chem Commun*. 2021;57(6):737-740. doi:10.1039/d0cc06493a
80. Tian X, De Vries MP, Permentier HP, Bischoff R. A Versatile Isobaric Tag Enables Proteome Quantification in Data-Dependent and Data-Independent Acquisition Modes. *Anal Chem*. 2020;92(24):16149-16157. doi:10.1021/acs.analchem.0c03858
81. Ludwig C, Aebersold R, Gillet L, Rosenberger G, Amon S, Collins BC. Data-independent acquisition-based SWATH-MS for quantitative proteomics: a tutorial. *Mol Syst Biol*. 2018;14:1-23. doi:10.15252/msb.20178126
82. Bilbao A, Varesio E, Luban J, Strambio-de-castillia C. Processing strategies and software solutions for data-independent acquisition in mass spectrometry. *Proteomics*. 2015;15:964-980. doi:10.1002/pmic.201400323
83. Huang X, Liu M, Nold MJ, et al. Software for quantitative proteomic analysis using stable isotope labeling and data independent acquisition. *Anal Chem*. 2011;83(18):6971-6979. doi:10.1021/ac201555m
84. Ye Z, Mao Y, Clausen H, Vakhrushev SY. Glyco-DIA: a method for quantitative O-glycoproteomics with in silico-boosted glycopeptide libraries. *Nat Methods*. 2019;16:902-910. doi:10.1038/s41592-019-0504-x
85. Madsen JA, Farutin V, Lin YY, Smith S. Data-independent oxonium ion profiling of

multi-glycosylated biotherapeutics. *MAbs*. 2018;10(7):968-978. doi:10.1080/19420862.2018.1494106

86. Lin C, Krisp C, Packer NH, Molloy MP. Development of a data independent acquisition mass spectrometry workflow to enable glycopeptide analysis without predefined glycan compositional knowledge. *J Proteomics*. 2018;172:68-75.
87. Hook V, Lietz CB, Podvin S, Cajka T, Fiehn O. Diversity of Neuropeptide Cell-Cell Signaling Molecules Generated by Proteolytic Processing Revealed by Neuropeptidomics Mass Spectrometry. *J Am Soc Mass Spectrom*. 2018;29(5):807-816. doi:10.1007/s13361-018-1914-1
88. Mast DH, Checco JW, Sweedler J V. Differential post-translational amino acid isomerization found among neuropeptides in aplysia californica. *ACS Chem Biol*. 2020;15(1):272-281. doi:10.1021/acschembio.9b00910
89. Cao L, Qu Y, Zhang Z, Wang Z, Prykova I, Wu S. Intact Glycopeptide Characterizatoin Using Mass Spectrometry. *Physiol Behav*. 2017;176(3):139-148. doi:10.1586/14789450.2016.1172965.Intact
90. Han B, Fang Y, Feng M, et al. Quantitative Neuropeptidome Analysis Reveals Neuropeptides Are Correlated with Social Behavior Regulation of the Honeybee Workers. *J Proteome Res*. 2015;14(10):4382-4393. doi:10.1021/acs.jproteome.5b00632
91. DeLaney K, Phetsanthad A, Li L. Advances in High-Resolution Maldi Mass Spectrometry for Neurobiology. *Mass Spectrom Rev*. 2020. doi:10.1002/mas.21661

92. Fricker LD, Lim J, Pan H, Che FY. Peptidomics: Identification and quantification of endogenous peptides in neuroendocrine tissues. *Mass Spectrom Rev*. 2006;25(2):327-344. doi:10.1002/mas.20079

93. Hsu JL, Chen SH. Stable isotope dimethyl labelling for quantitative proteomics and beyond. *Philos Trans R Soc A Math Phys Eng Sci*. 2016;374(2079). doi:10.1098/rsta.2015.0364

94. Ren RJ, Dammer EB, Wang G, Seyfried NT, Levey AI. Proteomics of protein post-translational modifications implicated in neurodegeneration. *Transl Neurodegener*. 2014;3(1):1-13. doi:10.1186/2047-9158-3-23

95. Li G, Delafield DG, Li L. Improved structural elucidation of peptide isomers and their receptors using advanced ion mobility-mass spectrometry. *TrAC - Trends Anal Chem*. 2020;124. doi:10.1016/j.trac.2019.05.048

96. Wohlgemuth J, Karas M, Eichhorn T, Hendriks R, Andrecht S. Quantitative site-specific analysis of protein glycosylation by LC-MS using different glycopeptide-enrichment strategies. *Anal Biochem*. 2009;395(2):178-188. doi:10.1016/j.ab.2009.08.023

97. Chen CC, Su WC, Huang BY, Chen YJ, Tai HC, Obena RP. Interaction modes and approaches to glycopeptide and glycoprotein enrichment. *Analyst*. 2014;139(4):688-704. doi:10.1039/c3an01813j

98. Zhang H, Li X jun, Martin DB, Aebersold R. Identification and quantification of N-linked glycoproteins using hydrazide chemistry, stable isotope labeling and mass spectrometry. *Nat Biotechnol*. 2003;21(6):660-666. doi:10.1038/nbt827

99. Dalpathado DS, Desaire H. Glycopeptide analysis by mass spectrometry. *Analyst*. 2008;133(6):731-738. doi:10.1039/b713816d

100. Madsen TD, Hansen LH, Hintze J, et al. An atlas of O-linked glycosylation on peptide hormones reveals diverse biological roles. *Nat Commun*. 2020;11(1). doi:10.1038/s41467-020-17473-1

101. Flintegaard T V., Thygesen P, Rahbek-Nielsen H, et al. N-glycosylation increases the circulatory half-life of human growth hormone. *Endocrinology*. 2010;151(11):5326-5336. doi:10.1210/en.2010-0574

102. Polt R, Dhanasekaran M, Keyari CM. Glycosylated neuropeptides: A new vista for neuropsychopharmacology? *Med Res Rev*. 2005;25(5):557-585. doi:10.1002/med.20039

103. Moradi SV, Hussein WM, Varamini P, Simerska P, Toth I. Glycosylation, an effective synthetic strategy to improve the bioavailability of therapeutic peptides. *Chem Sci*. 2016;7(4):2492-2500. doi:10.1039/c5sc04392a

104. Yu Q, Canales A, Glover MS, et al. Targeted Mass Spectrometry Approach Enabled Discovery of O-Glycosylated Insulin and Related Signaling Peptides in Mouse and Human Pancreatic Islets. *Anal Chem*. 2017;89(17):9184-9191. doi:10.1021/acs.analchem.7b01926

105. Hansen LH, Madsen TD, Goth CK, et al. Discovery of O-glycans on atrial natriuretic peptide (ANP) that affect both its proteolytic degradation and potency at its cognate receptor. *J Biol Chem*. 2019;294(34):12567-12578. doi:10.1074/jbc.RA119.008102

106. Mechref Y. Use of CID/ETD mass spectrometry to analyze glycopeptides. *Curr Protoc Protein Sci*. 2012;1(SUPPL.68). doi:10.1002/0471140864.ps1211s68

107. Hart-Smith G, Raftery MJ. Detection and characterization of low abundance glycopeptides via higher-energy c-trap dissociation and orbitrap mass analysis. *J Am Soc Mass Spectrom*. 2012;23(1):124-140. doi:10.1007/s13361-011-0273-y

108. Khatri K, Pu Y, Klein JA, et al. Comparison of Collisional and Electron-Based Dissociation Modes for Middle-Down Analysis of Multiply Glycosylated Peptides. *J Am Soc Mass Spectrom*. 2018;29(6):1075-1085. doi:10.1007/s13361-018-1909-y

109. Yu Q, Wang B, Chen Z, et al. Electron-Transfer/Higher-Energy Collision Dissociation (EThcD)- enabled Intact Glycopeptide/Glycoproteome Characterization. *Physiol Behav*. 2018;176(5):139-148. doi:10.1007/s13361-017-1701-4.Electron-Transfer/Higher-Energy

110. Singh C, Zampronio CG, Creese AJ, Cooper HJ. Higher energy collision dissociation (HCD) product ion-triggered electron transfer dissociation (ETD) mass spectrometry for the analysis of N-linked glycoproteins. *J Proteome Res*. 2012;11(9):4517-4525. doi:10.1021/pr300257c

111. Yu Q, Shi X, Feng Y, Kent KC, Li L. Improving Data Quality and Preserving HCD-Generated Reporter Ions with EThcD for Isobaric Tag-based Quantitative Proteomics and Proteome-wide PTM Studies. *Physiol Behav*. 2016;176(1):100–106. doi:10.1016/j.aca.2017.03.003.Improving

112. Riley NM, Malaker SA, Driessen MD, Bertozzi CR. Optimal Dissociation Methods Differ for N- A nd O-Glycopeptides. *J Proteome Res*. 2020;19(8):3286-3301.

doi:10.1021/acs.jproteome.0c00218

113. Zhu R, Song E, Hussein A, Kobeissy FH. Chapter 9: Glycoproteins Enrichment and LC-MS/MS Glycoproteomics in Central Nervous System Applications. In: *Neuroproteomics: Methods and Protocols*. Vol 1598. ; 2017:213-227. doi:10.1007/978-1-4939-6952-4
114. Delafield DG, Li L. Recent advances in analytical approaches for glycan and glycopeptide quantitation. *Mol Cell Proteomics*. 2021;20:0-21. doi:10.1074/MCP.R120.002095
115. Tobias F, Hummon AB. Considerations for MALDI-Based Quantitative Mass Spectrometry Imaging Studies. *J Proteome Res*. 2020;19:3620-3630. doi:10.1021/acs.jproteome.0c00443
116. Delaney K, Hu M, Hellenbrand T, Dickinson PS, Nusbaum MP. Mass Spectrometry Quantification, Localization, and Discovery of Feeding-Related Neuropeptides in Cancer borealis. *ACS Chem Neurosci*. 2021;12:782-798. doi:10.1021/acschemneuro.1c00007
117. Hulme H, Fridjonsdottir E, Gunnarsdottir H, et al. Simultaneous mass spectrometry imaging of multiple neuropeptides in the brain and alterations induced by experimental parkinsonism and L-DOPA therapy. *Neurobiol Dis*. 2020;137(December 2019):104738. doi:10.1016/j.nbd.2020.104738
118. Pratavieira M, Ribeiro A, Esteves FG, Sato KU, Malaspina O, Palma MS. MALDI Imaging Analysis of Neuropeptides in Africanized Honeybee (Apis mellifera) Brain: Effect of Aggressiveness. *J Proteome Res*. 2018;17:2358-2369.

doi:10.1021/acs.jproteome.8b00098

119. Taylor AJ, Dexter A, Bunch J. Exploring Ion Suppression in Mass Spectrometry Imaging of a Heterogeneous Tissue. *Anal Chem*. 2018;90:5637-5645. doi:10.1021/acs.analchem.7b05005

120. Cobice DF, Livingstone DEW, Mackay CL, et al. Spatial Localization and Quantitation of Androgens in Mouse Testis by Mass Spectrometry Imaging. *Anal Chem*. 2016;88:10362-10367. doi:10.1021/acs.analchem.6b02242

121. Källback P, Shariatgorji M, Nilsson A, Andrén PE. Novel mass spectrometry imaging software assisting labeled normalization and quantitation of drugs and neuropeptides directly in tissue sections. *J Proteomics*. 2012;75:4941-4951. doi:10.1016/j.jprot.2012.07.034

122. Kallback P, Vallianatou T, Nilsson A, et al. Cross-validated Matrix-Assisted Laser Desorption/Ionization Mass Spectrometry Imaging Quantitation Protocol for a Pharmaceutical Drug and Its Drug-Target Effects in the Brain Using Time-of-Flight and Fourier Transform Ion Cyclotron Resonance Analyzers. *Anal Chem*. 2020;92:14676-14684. doi:10.1021/acs.analchem.0c03203

123. Swales JG, Strittmatter N, Tucker JW, Clench MR, Webborn PJH, Goodwin RJA. Spatial Quantitation of Drugs in tissues using Liquid Extraction Surface Analysis Mass Spectrometry Imaging. *Sci Rep*. 2016;6:1-9. doi:10.1038/srep37648

124. Zhao C, Cai Z. Three-dimensional quantitative mass spectrometry imaging in complex system: From subcellular to whole organism. *Mass Spectrom Rev*. 2020:1-19. doi:10.1002/mas.21674

125. Zemaitis KJ, Izydorczak AM, Thompson AC, Wood TD. Streamlined Multimodal DESI and MALDI Mass Spectrometry Imaging on a Singular Dual-Source FT-ICR Mass Spectrometer. *Metabolites*. 2021;11(253):1-15.

126. Theron L, Centeno D, Coudy-Gandilhon C, et al. A Proof of Concept to Bridge the Gap between Mass Spectrometry Imaging, Protein Identification and Relative Quantitation: MSI~LC-MS/MS-LF. *Proteomes*. 2016;4(32):1-16. doi:10.3390/proteomes4040032

127. Dewez F, Pauw E De, Heeren RMA, Balluff B. Multilabel Per-Pixel Quantitation in Mass Spectrometry Imaging. *Anal Chem*. 2021;93:1393-1400. doi:10.1021/acs.analchem.0c03186

128. Shrivas K, Hayasaka T, Sugiura Y, Setou M. Method for simultaneous imaging of endogenous low molecular weight metabolites in mouse brain using TiO2 nanoparticles in nanoparticle-assisted laser desorption/ionization-imaging mass spectrometry. *Anal Chem*. 2011;83(19):7283-7289. doi:10.1021/ac201602s

129. Chu H, Unnikrishnan B, Anand A, Mao J. Nanoparticle-based laser desorption/ionization mass spectrometric analysis of drugs and metabolites. *J Food Drug Anal*. 2018;26:1215-1228. doi:10.1016/j.jfda.2018.07.001

130. Mclaughlin N, Bielinski TM, Tressler CM, Barton E, Glunde K, Stumpo KA. Pneumatically Sprayed Gold Nanoparticles for Mass Spectrometry Imaging of Neurotransmitters. *J Am Soc Mass Spectrom*. 2020;31:2452-2461. doi:10.1021/jasms.0c00156

131. Lolait SJ, Roper JA, Hazell GGJ, Li Y, Thomson FJ, Carroll AMO. Chapter 10:

Neuropeptide Receptors. In: *Molecular Neuroendocrinology: From Genome to Physiology*. ; 2016:195-215.

132. Wojnicz A, Avendaño-Ortiz J, de Pascual R, Ruiz-Pascual L, García AG, Ruiz-Nuño A. Simultaneous monitoring of monoamines, amino acids, nucleotides and neuropeptides by liquid chromatography-tandem mass spectrometry and its application to neurosecretion in bovine chromaffin cells. *J Mass Spectrom*. 2016;51(8):651-664. doi:10.1002/jms.3794
133. Gantait AM, Bataineh YA, Surchi HS, et al. Chapter 16: Neuropeptides and Neurotransmission. In: *Frontiers in Pharmacology of Neurotransmitters*. ; 2020:553-577.
134. Chen D, Zhao X, Sui Z, et al. A multi-omics investigation of the molecular characteristics and classification of six metabolic syndrome relevant diseases. *Theranostics*. 2020;10(5):2029-2046. doi:10.7150/thno.41106
135. Gutierrez DB, Gant-Branum RL, Romer CE, et al. An Integrated, High-Throughput Strategy for Multiomic Systems Level Analysis. *J Proteome Res*. 2018;17(10):3396-3408. doi:10.1021/acs.jproteome.8b00302
136. Keller C, Wei P, Wancewicz B, Cross TWL, Rey FE, Li L. Extraction optimization for combined metabolomics, peptidomics, and proteomics analysis of gut microbiota samples. *J Mass Spectrom*. 2021;56(4). doi:10.1002/jms.4625
137. Chen B, OuYang C, Tian Z, Xu M, Li L. A high resolution atmospheric pressure matrix-assisted laser desorption/ionization-quadrupole-orbitrap MS platform enables in situ analysis of biomolecules by multi-mode ionization and acquisition.

Anal Chim Acta. 2018;1007:16-25. doi:10.1016/j.aca.2017.12.045

138. Johnsen E, Leknes S, Wilson SR, Lundanes E. Liquid chromatography-mass spectrometry platform for both small neurotransmitters and neuropeptides in blood, with automatic and robust solid phase extraction. *Sci Rep*. 2015;5:1-8. doi:10.1038/srep09308
139. Zestos AG, Kennedy RT. Microdialysis Coupled with LC-MS/MS for In Vivo Neurochemical Monitoring. *AAPS J*. 2017;19(5):1284-1293. doi:10.1208/s12248-017-0114-4
140. Oliveros A, Starski P, Lindberg D, Choi S, Heppelmann CJ, Dasari S. Label-Free Neuroproteomics of the Hippocampal-Accumbal Circuit Reveals Deficits in Neurotransmitter and Neuropeptide Signaling in Mice Lacking Ethanol-Sensitive Adenosine Transporter. *J Proteome Res*. 2017;16:1445-1459. doi:10.1021/acs.jproteome.6b00830
141. Li W, Petruzziello F, Zhao N, et al. Separation and identification of mouse brain tissue microproteins using top-down method with high resolution nanocapillary liquid chromatography mass spectrometry. *Proteomics*. 2017;17(12):1-5. doi:10.1002/pmic.201600419
142. Li L, Sweedler J V. Peptides in the Brain: Mass Spectrometry–Based Measurement Approaches and Challenges. *Annu Rev Anal Chem*. 2008;1(1):451-483. doi:10.1146/annurev.anchem.1.031207.113053
143. Shetgaonkar GG, Kumar L. Chemistry of Neurochemicals : Psychopharmaceuticals and Neuropeptides. In: *Principles of Neurochemistry*. ; 2020:41-70.

144. Li C, Wu X, Liu S, et al. Roles of Neuropeptide Y in Neurodegenerative and Neuroimmune Diseases. *Front Neurosci*. 2019;13:1-11. doi:10.3389/fnins.2019.00869

145. Nillni EA. Chapter 2: Neuropeptides Controlling Our Behavior. In: *Energy Balance, Neuropeptide Hormones, and Neuroendocrine Function*. ; 2018:29-54. doi:10.1007/978-3-319-89506-2

146. Cheng Y, Tang X, Li Y, Zhao D, Cao Q. Depression-Induced Neuropeptide Y Secretion Promotes Prostate Cancer Growth by Recruiting Myeloid Cells. *Clin Cancer Res*. 2019;25(8):2621-2632. doi:10.1158/1078-0432.CCR-18-2912

147. Urban JH. *Chapter 7: Neuropeptide Y and Amygdala Circuitry : Modulation of Stress-Related Behavior*. Vol 26. 1st ed. Elsevier B.V.; 2020. doi:10.1016/B978-0-12-815134-1.00007-6

148. Salem J Ben, Nkambeu B, Beaudry F. Characterization of neuropeptide K processing in rat spinal cord S9 fractions using high-resolution quadrupole–Orbitrap mass spectrometry. *Biomed Chromatogr*. 2018;32(6):1-9. doi:10.1002/bmc.4204

149. DeLaney K, Buchberger AR, Li L. Chapter 17: Identification, Quantitation, and Imaging of the Crustacean Peptidome. In: *Methods in Molecular Biology*. Vol 1719. ; 2018:247-269. doi:10.1007/978-1-4939-7537-2_18

150. Husson SJ, Mertens I, Janssen T, Lindemans M, Schoofs L. Neuropeptidergic signaling in the nematode Caenorhabditis elegans. *Prog Neurobiol*. 2007;82(1):33-55. doi:10.1016/j.pneurobio.2007.01.006

151. Perry DJ, Wasserfall CH, Oram RA, et al. Application of a Genetic Risk Score to Racially Diverse Type 1 Diabetes Populations Demonstrates the Need for Diversity in Risk-Modeling. *Sci Rep*. 2018;8:1-13. doi:10.1038/s41598-018-22574-5

152. Guo W, Zhou M, Qiu J, et al. Association of LAG3 genetic variation with an increased risk of PD in Chinese female population. *J Neuroinflammation*. 2019;16(270):1-8.

153. Philibert R, Glatt SJ. Optimizing the chances of success in the search for epigenetic biomarkers: Embracing genetic variation. *Am J Med Genet Part B*. 2017;174B:589-594. doi:10.1002/ajmg.b.32569

154. Devi R, Jie L, Yan T, et al. Human tuberculosis and Mycobacterium tuberculosis complex: A review on genetic diversity, pathogenesis and omics approaches in host biomarkers discovery. *Microbiol Res*. 2021;246. doi:10.1016/j.micres.2020.126674

155. Zhang F, Finkelstein J. Inconsistency in race and ethnic classification in pharmacogenetics studies and its potential clinical implications. *Pharmgenomics Pers Med*. 2019;12:107-123.

156. Brown AF, Liang L, Vassar SD, et al. Trends in Racial/Ethnic and Nativity Disparities in Cardiovascular Health Among Adults Without Prevalent Cardiovascular Disease in the United States, 1988 to 2014. *Ann Intern Med*. 2018;168:541-549. doi:10.7326/M17-0996

157. Babulal GM, Quiroz YT, Albensi BC, et al. Perspectives on ethnic and racial disparities in Alzheimer's disease and related dementias: Update and areas of

immediate need. *Alzheimer's Dement*. 2019;15:292-312.

158. Landry BLG, Ali N, Williams DR, Rehm HL, Bonham VL. Lack Of Diversity In Genomic Databases Is A Barrier To Translating Precision Medicine Research Into Practice. *Health Aff*. 2018;37(5):780-785.
159. Frost DC, Greer T, Li L. High-resolution enabled 12-plex DiLeu isobaric tags for quantitative proteomics. *Anal Chem*. 2015;87(3):1646-1654. doi:10.1021/ac503276z
160. Greer T, Lietz CB, Xiang F, Li L. Novel isotopic N,N-Dimethyl Leucine (iDiLeu) reagents enable absolute quantification of peptides and proteins using a standard curve approach. *J Am Soc Mass Spectrom*. 2014;26(1):107-119. doi:10.1007/s13361-014-1012-y
161. Genangeli M, Heijens AMM, Rustichelli A, et al. MALDI-Mass Spectrometry Imaging to Investigate Lipid and Bile Acid Modifications Caused by Lentil Extract Used as a Potential Hypocholesterolemic Treatment. *J Am Soc Mass Spectrom*. 2019;30:2041-2050. doi:10.1007/s13361-019-02265-9
162. Lombard-banek C, Yu Z, Swiercz AP, Marvar PJ, Nemes P. A microanalytical capillary electrophoresis mass spectrometry assay for quantifying angiotensin peptides in the brain. *Anal Bioanal Chem*. 2019;411:4661-4671.
163. Mast DH, Liao H-W, Romanova E V., Sweedler J V. Analysis of Peptide Stereochemistry in Single Cells by Capillary Electrophoresis–Trapped Ion Mobility Spectrometry Mass Spectrometry. *Anal Chem*. 2021. doi:10.1021/acs.analchem.1c00445

Figures:

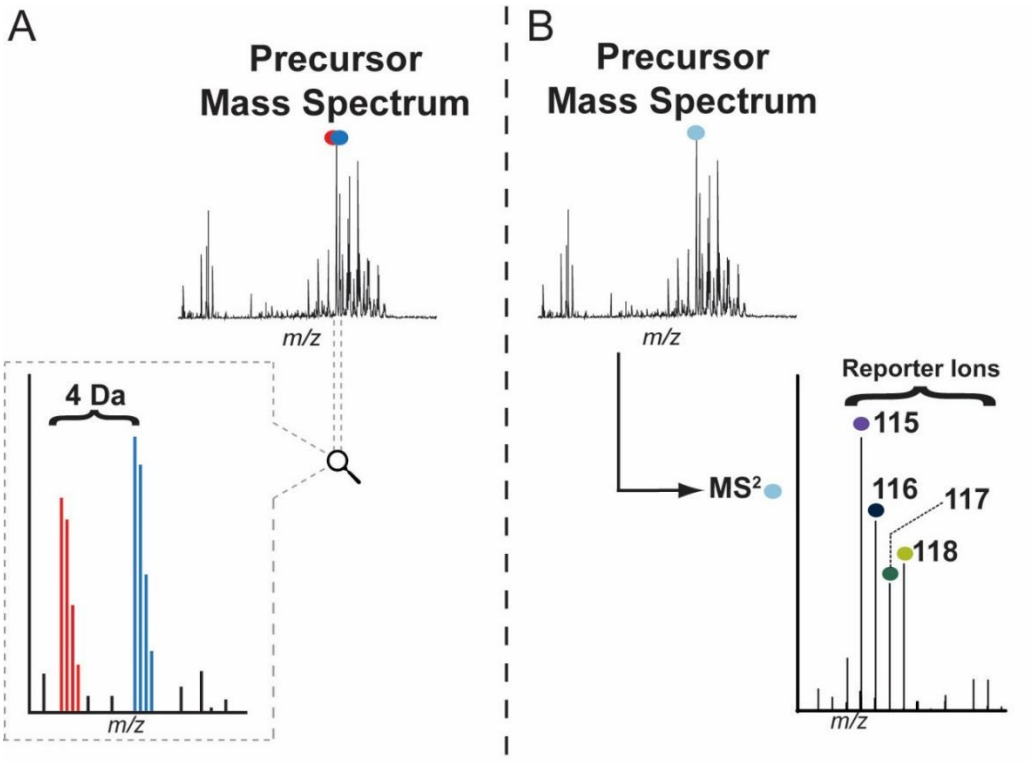

Figure 1: Comparison between isotopic (A) and isobaric (B) labeling. In isotopic labeling strategies, analytes are differentiated at the precursor mass level due to the incorporation of light and heavy tags. Isobaric workflows result in no differentiation at the precursor mass level, but upon fragmentation, unique reporter ions for each channel form, giving rise to quantitation based on relative intensities of reporter ions.

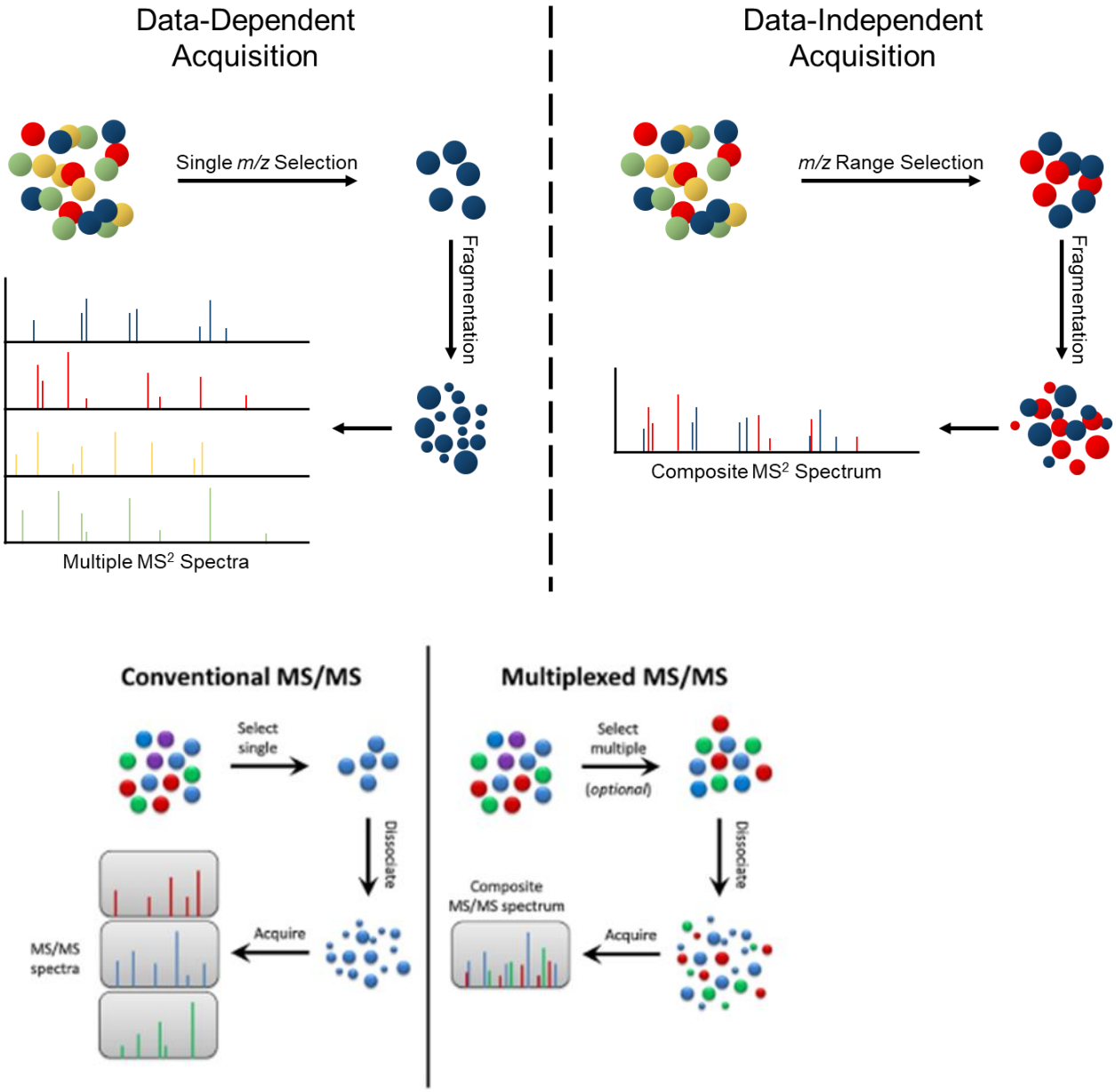

Figure 2: Depiction of differences between DDA and DIA. In DDA, a single m/z is selected at a time for MS/MS. In DIA, several analytes are selected for simultaneous MS/MS across a wide m/z window and the composite mass spectrum is deconvoluted during data analysis to discern constituent analytes.

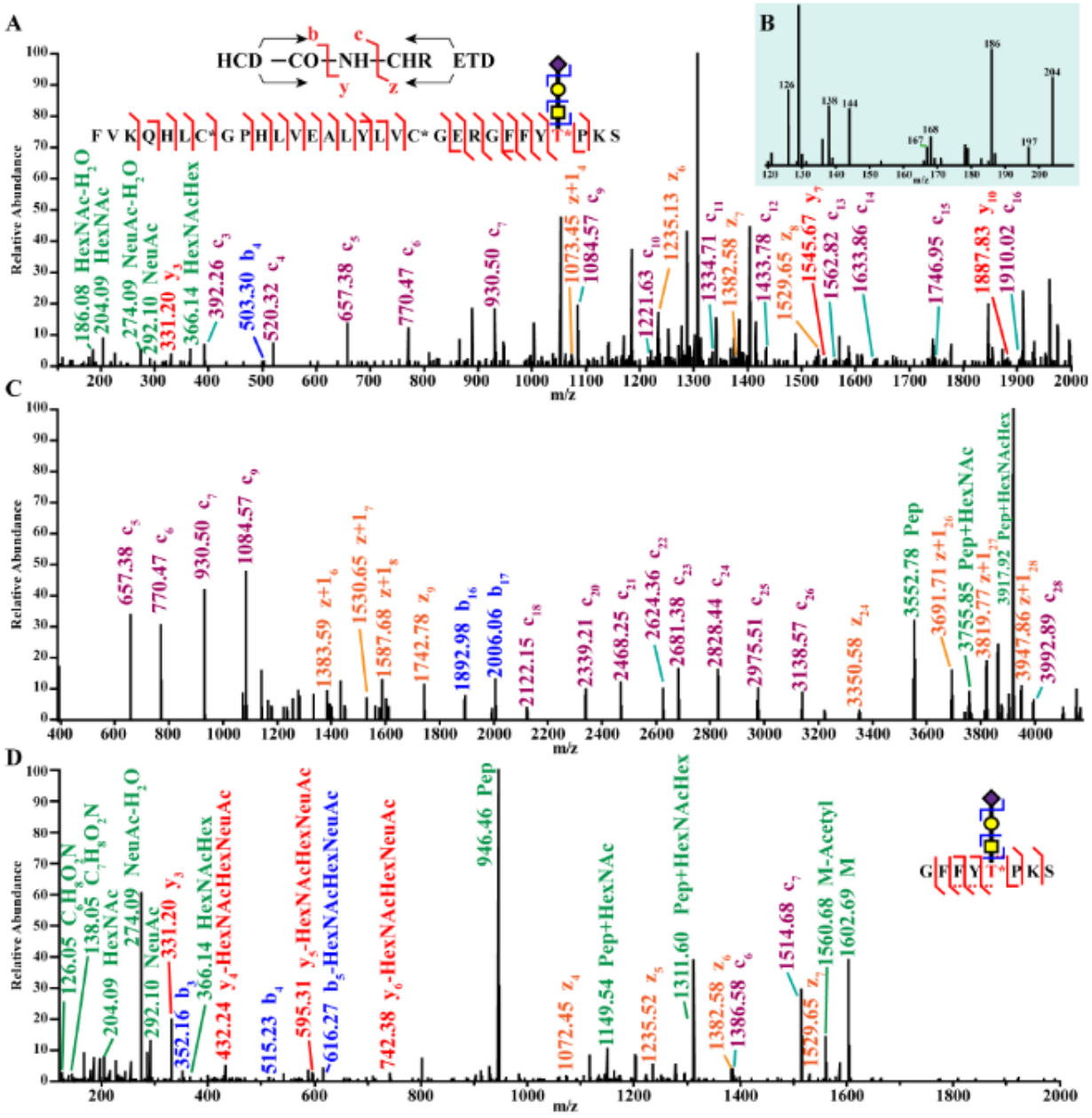

Figure 3: Sample spectra from mouse insulin. Using EThcD (A) and charge deconvolution (C) resulted in high sequence coverage due to production of both b/y- and c/z-ions. The spectrum in D highlights the glycan localization, and the low mass region is shown enlarged in (B). Figure reprinted with permission from Yu, et al. [104].

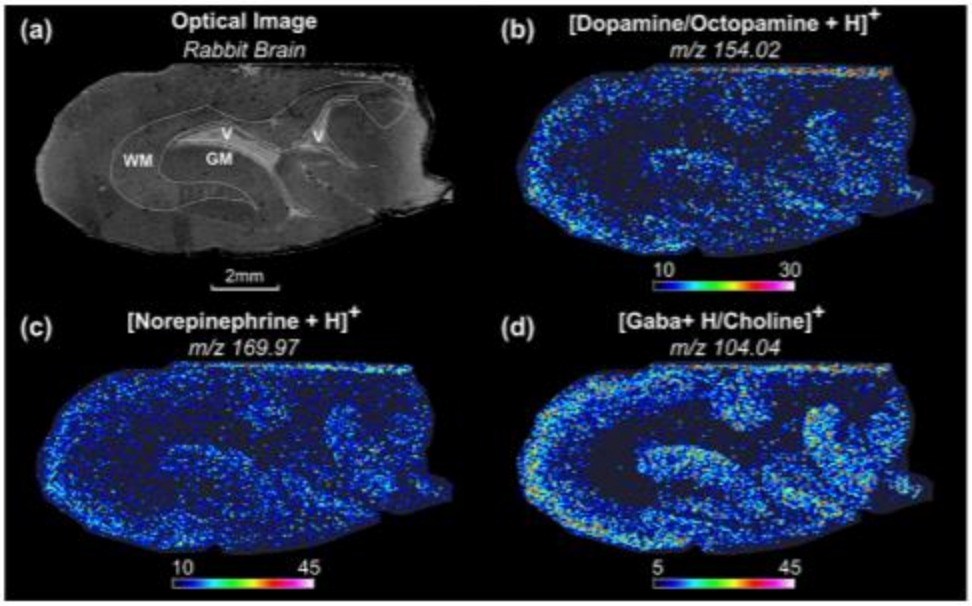

Figure 4: MSI enhancements from application of gold nanoparticles. Comparison of images from extracted neurotransmitters (b-d) to the optical image (a) shows differential expression based on grey/white matter regions of the brain. Image reprinted with permission from McLaughlin et al. [130]

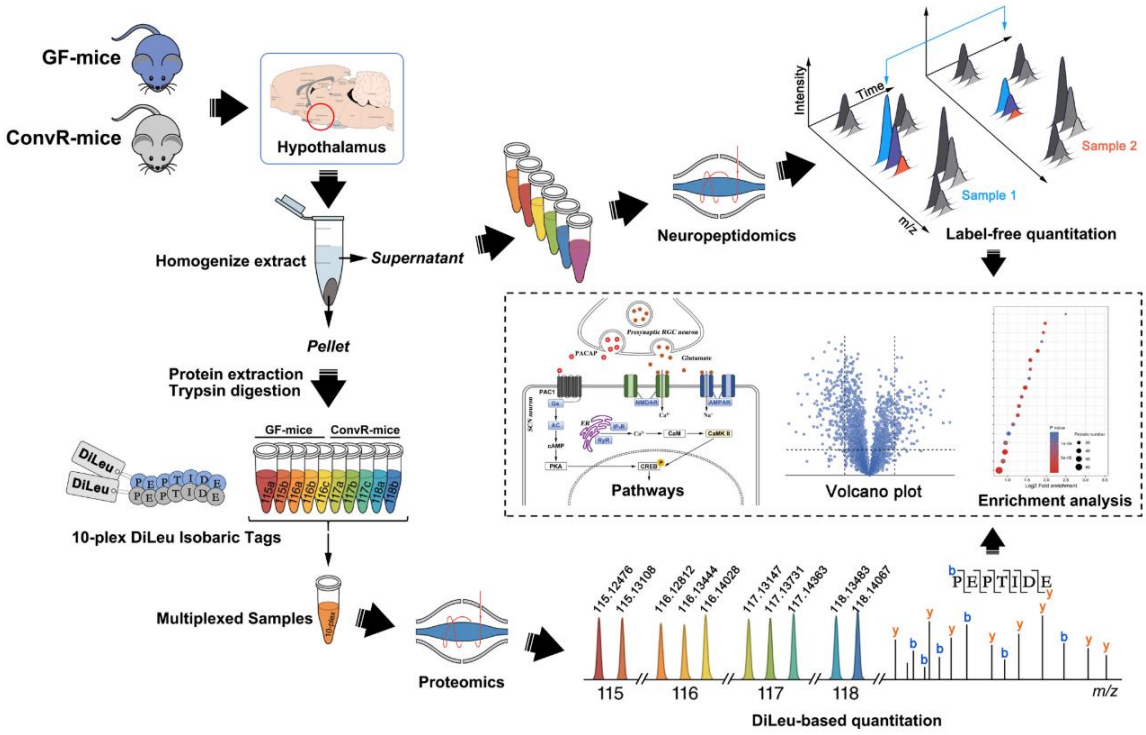

Figure 5: Multi-omic workflow for studying neuropeptides and proteins. Neuropeptides were extracted from the hypothalamus of germ-free (GF) and conventionally raised (ConvR) mice and analyzed using LFQ. Proteins were pelleted, digested, and differentially labeled with 10-plex DiLeu isobaric tags. The differentially labeled samples were pooled together and analyzed simultaneously to perform relative quantitation based on reporter ion intensities. Adapted from Liu et al. [53] with permission.

Chapter 3

Temporal Study of the Perturbation of Crustacean Neuropeptides Due to Severe Hypoxia Using 4-Plex Reductive Dimethylation

Adapted from:

Sauer, C.S.*, Buchberger, A.R.*, Vu, N.Q., DeLaney, K., Li, L. A Temporal Study of the Perturbation of Crustacean Neuropeptides Due to Severe Hypoxia Stress Using 4-Plex Reductive Dimethylation. *J. Proteome Res.* 2020, 19, 1548-1555. ***Co-First Authors**

Abstract

Hypoxia (*i.e.,* low oxygen (O_2) levels) is a common environmental challenge for several aquatic species, including fish and invertebrates. To survive or escape these conditions, these animals have developed novel biological mechanisms, some regulated by neuropeptides. By utilizing mass spectrometry, this study aims to provide a global perspective of neuropeptides in the blue crab, *Callinectes sapidus*, and their changes over time (0, 1, 4, and 8 hours) due to acute, severe hypoxia (~10% O_2 water saturation) stress using a 4-plex reductive dimethylation strategy to increase throughput. Using both electrospray ionization and matrix-assisted laser desorption/ionization provided complementary coverage– 88 neuropeptides were identified. Interesting trends include (1) an overall decrease in neuropeptide expression due to hypoxia exposure, (2) a return to basal levels after 4 or 8 hours of exposure following an initial response, (3) changes only after 4+ hours exposure, and (4) an oscillating pattern. Overall, this study boosts the power of multiplexed quantitation to understand the large-scale changes due to severe hypoxia stress over time.

Keywords: *Callinectes sapidus*, Quantitative peptidomics, Neuropeptide, Hypoxia, Reductive dimethylation, isotopic labeling

Introduction

Estuaries and coastal ecosystems are increasingly threatened by climate change, poorly managed wastewater, and agricultural and industrial runoff.[1] These factors often lead to eutrophication of coastal waters, causing large algal blooms and subsequent hypoxic (*i.e.,* low oxygen (O_2)) episodes that can last for hours to days.[2] Aquatic hypoxia also occurs naturally from a multitude of hydrodynamic and meteorological effects.[3] During hypoxic episodes, the dissolved O_2 in the water greatly decreases, causing massive dead zones and a reduction in biodiversity as organisms are deprived of oxygen. Environmental hypoxia occurs most frequently in the spring and summer and can last for months.[3] As commercially-fished species rapidly perish during these times, the repercussions of hypoxia become economic as well as environmental.[4]

Although many aquatic organisms are affected by hypoxia, the blue crab, *Callinectes sapidus*, is of particular interest. The blue crab possesses both environmental and economic relevance as it is frequently fished from estuaries plagued by eutrophication and hypoxia.[2] In the literature, hypoxia has been shown to cause decreased rates of reproduction, growth, and feeding, and increased mortality rates in aquatic species.[5] Due to the adverse effects of hypoxia, the blue crab has developed interesting ways of surviving the low levels of dissolved O_2. Prior studies have observed hypoxia-initiated defensive behaviors, including inactivity, self-burying, and migration towards shallower, more O_2-rich waters.[5] Additionally, the composition of hemocyanin (*i.e.*, O_2 transport protein analogous to hemoglobin) has been shown to change in response to hypoxia,[6, 7] demonstrating physiological defensive mechanisms as well.

The variable behavioral and physiological changes in *C. sapidus* suggest the presence of complex signaling pathways involved in survival. Neuropeptides are short amino acid chains that act as signaling molecules within the nervous and neuroendocrine system. Previously, neuropeptides have been implicated in a range of environmental stress responses, including temperature[8] and salinity fluctuations.[9] They can have highly diverse effects within the body while also maintaining low *in vivo* concentrations.[10] Prior research has shown that the crustacean hyperglycemic hormone (CHH) is a neuropeptide involved in regulating the response to hypoxia in the blue crab,[11] while global dynamic changes of neuropeptides during acute hypoxia have not been systematically evaluated. By examining the neuropeptide expression changes in the blue crab, their role in survival can be better understood.

Unfortunately, the high chemical diversity, low *in vivo* concentrations, and rapid degradation of neuropeptides makes their study challenging. Mass spectrometry (MS)–using both matrix-assisted laser desorption/ionization (MALDI) and electrospray ionization (ESI)–has proven to be an effective method of analyzing neuropeptides as it offers high sensitivity, high specificity, and can provide both quantitative and sequence information. Additionally, because it requires no prior knowledge of the analyte, MS is ideal for discovering novel neuropeptides involved in response to hypoxia. Relative quantitation of neuropeptides by MS is typically achieved by employing either MS^1-based labeling strategies (*e.g.*, reductive dimethylation (also known as dimethyl labeling), iDiLeu, and mTRAQ),[12-14] or tandem MS (MS/MS or MS^2-based) labels (*e.g.,* iTRAQ, TMT, and DiLeu).[15-17] MS/MS reporters require the neuropeptide be selected for

fragmentation to be quantified. The low abundance of many neuropeptides, however, makes their selection for MS/MS less likely. For this reason, MS^1-based labeling strategies are often selected for neuropeptide quantitative analyses.

Previously, experiments have utilized duplex reductive dimethylation to analyze neuropeptidomic changes in crustaceans.[8, 9] Stable isotopes, supplied by isotopic formaldehyde, are added to the N-termini and lysine side chains of peptides by reductive dimethylation, adding two methyl groups, which add either 28.03130 or 32.05641 Daltons (Da) to each primary amine, depending on the stable isotopes being incorporated. The heavy- and light-labeled samples are analyzed simultaneously to provide relative quantitation information between experimental and control conditions. Though effective, duplex labeling requires an individual control sample for each experimental sample. Expanding the multiplexing capabilities of reductive dimethylation strategies greatly reduces the number of samples needed as multiple samples can be compared to a single control. Simultaneous analysis of the differentially labeled samples also reduces the instrument time required and the run-to-run variability. A 4-plex reductive dimethylation method is achieved by selecting formaldehyde with different combinations of $^{12}C/^{13}C$ and H/D, providing four distinct mass additions (+28.03130, +30.03801, +32.05641, and +34.06312 Da) that can be incorporated at the N-termini and lysine residues via reductive dimethylation.[18-20] This is a cost-effective approach to increase both throughput and quantitative abilities.

In this study, 4-plex reductive dimethylation was used to quantify the relative changes in expression of neuropeptides in *Callinectes sapidus* after 1, 4, and 8 hours of hypoxia

exposure. These exposure durations are reflective of hypoxia exposure before blue crabs manage to escape hypoxic episodes and have been studied previously.[5] The multiplexed samples were analyzed by both MALDI- and ESI-MS to provide enhanced, complementary coverage of the crustacean neuropeptidome.[21] In fact, 88 identified neuropeptides were found using both ESI- and MALDI-MS analyses. Several trends were revealed in this time course study, including an oscillating expression pattern. A qualitative approach was also taken to investigate neuropeptides that only expressed themselves after hypoxia stress.

Materials and Methods

Methanol (MeOH), acetonitrile (ACN), glacial acetic acid (GAA), ammonium bicarbonate, and all crab saline components (see below) were purchased from Fisher Scientific (Pittsburgh, PA). Formaldehyde (CH_2O), ^{13}C-formaldehyde ($^{13}CH_2O$), D_2-formaldehyde (CD_2O), $^{13}CD_2$-formaldehyde ($^{13}CD_2O$), and borane pyridine complex (~8M BH_3) were acquired from Sigma-Aldrich (St. Louis, MO). 2,5-dihydroxybenzoic acid (DHB) was obtained from Acros Organics (Morris, New Jersey), and formic acid (FA) was purchased from Fluka (Mexico City, Mexico). All water (H_2O) used in this study was either HPLC grade or doubly distilled on a Millipore filtration system (Burlington, MA), and C18 Ziptips were purchased from Millipore (Burlington, MA). All LC solvents were Fisher Optima Grade.

Animals and Stress Experiment

All female blue crabs, *Callinectes sapidus*, were purchased from LA Crawfish Company (Natchitoches, LA). After transport, crabs were allowed to recover in artificial seawater made to be 35 parts per thousand (ppt) salinity, 17-18 °C, and 8-10 parts per million (ppm) (~80-100%) O_2 for several days (>5) prior to being exposed. To mimic severe hypoxia (1 ppm, ~10% O_2), a tank was sparged with N_2 gas for 30-40 minutes to reduce the dissolved O_2 to 1 ppm as measured by a Pinpoint II Oxygen Monitor. A plastic tarp was placed on top of the water's surface to minimize water-air oxygen exchange during sparging. A crab was then placed in the tank for the desired amount of time (*i.e.,* 1 hour, 4 hours, or 8 hours), anesthetized on ice for 20 minutes, and sacrificed for its organs of interest as previously described.[22] All dissections were performed in chilled (~ 10 ^{o}C) physiological saline (composition: 440 mM NaCl; 11 mM KCl; 13 mM $CaCl_2$; 26 mM $MgCl_2$; 10 mM Trizma acid; pH 7.4 (adjusted with NaOH)).

Sample Preparation

For each bioreplicate, one set of each tissue of interest (*i.e.,* sinus gland (SG) (2), brain, pericardial organ (PO) (2), commissarial ganglion (CoG) (2), and thoracic ganglion (TG)) was extracted with a Fisherbrand Model 120 probe sonicator/sonic dismembrator with chilled acidified MeOH (90:9:1 MeOH:H_2O:GAA; volume (v):v:v). Each sample was sonicated three times for 8 seconds at 50% amplitude with a 15 second break in between each sonication. After centrifugation at 20,000 rpm for 20 minutes at 4 °C, the supernatant was collected and dried down in a Savant SCV100 Speedvac. All crude extracts were purified using C18 ZipTips following the manufacturer's protocol. All samples were centrifuged at high speed (>10,000 rpm) briefly prior to purification.

Control and hypoxia-exposed samples were differentially labeled via reductive dimethylation using a previously published protocol[18-20] with slight modifications. The samples were all differentially labeled as follows: (a) control (*i.e,* 0 hours) with formaldehyde (CH_2O, +28.03130 Da), (b) 1 hr exposure with ^{13}C-formaldehyde ($^{13}CH_2O$, +30.04391 Da), (c) 4 hr exposure with D_2-formaldehyde (CD_2O, +32.05641 Da), and (d) 8 hr exposure with ^{13}C, D_2-formaldehyde ($13CD_2O$, +34.06902 Da). Borane pyridine was the reducing agent. All samples were mixed 1:1:1:1 after being quenched with ammonium bicarbonate. The multiplexed samples were then processed two different ways: (a) spotted with 150 mg/mL DHB (in 50:50 MeOH:H_2O with 0.1% FA) on a stainless-steel plate to be analyzed by a Thermo MALDI-LTQ-Orbitrap XL or (b) purified again with C18 ZipTips and analyzed by a Thermo Q Exactive (QE) coupled to a Waters nanoAquity system.

MS Data Collection

MALDI samples were spotted in triplicate and analyzed in the mass-to-charge ratio (*m/z*) 500-2000 range at a resolution of 60,000 on the MALDI-LTQ-Orbitrap XL. ESI samples were injected in triplicate onto a homemade C18 column (14-16 cm), from which the analytes were eluted using a 90-minute gradient (10% B to 35% B) with H_2O (0.1% FA) (A) and ACN (0.1% FA) (B) and analyzed by the QE in a mass range of *m/z* 200-2000 with a top 15 data-dependent acquisition method with high-energy collision dissociation. MS^1 and MS/MS spectra were collected at a 70,000 and 17,500 mass resolution, respectively. All data collection parameters for MALDI- and ESI-MS are included in Tables **S1** and **S2**, respectively.

Data Analysis

Data collected by MALDI-MS was analyzed by exporting all the *m/z* values from Xcalibur and processed using a custom program written in Java by accurate mass matching (±5 ppm) with an intensity threshold of 100. Neuropeptides were identified by matching their masses to an in-house database, accounting for the addition of +28.03130, +30.03801, +32.05641, and +34.06312 Da on the N-terminus from isotopic reductive dimethylation. Isotopic correction was performed manually post-extraction of the *m/z* intensities using previously published correction factors.[19] ESI-MS raw data were imported into PEAKS 8.5 software for *de novo* sequencing and database matching. Database search results initially were filtered using a 1% false discovery rate. Isotopic corrections were performed automatically within the software prior to the database search. Peak areas were then extracted for corresponding tandem MS-identified neuropeptide peak sets if they were detected in at least 1 technical replicate (n=3), 3 biological replicates (n=8 for brain, CoG, PO, and TG; n=7 for SG), were unique to that neuropeptide, and eluted within ± 2 minutes from each other. Dimethylation of both the N-terminus and lysine ε-aminos were considered for ESI data which has MS/MS data for validation; conversely, only labeling of one location (*i.e.,* N-terminus or lysine ε-aminos) was considered for MALDI data (*e.g.,* mass increase of one dimethyl group). Peptides known to be amidated (*e.g.,* RFamide, RYamide, allatostatin) were only considered in this data if they were identified in their amidated form. All fragments of a neuropeptides identified by ESI-MS were equally weighted for the calculation ratios. For both MALDI- and ESI-MS analyses, all channels were normalized by taking individual

intensity or peak areas divided by the total intensity or peak area. Ratios were then calculated by dividing the normalized intensity of either the +30.03801, +32.05641, or +34.06312 channel by the +28.03130 channel's normalized intensity. Statistical significance between experimental and control samples was determined by a Dunnett's test, which is utilized for comparing multiple experimental conditions to a single control.[23, 24] If only the control and one other time point were detected, a t-test was used to determine significance. All parameters used for data processing are included for MALDI- and ESI-MS in **Table S1** and **S3**, respectively.

Results and Discussion

Method Development

Hypoxia is rampant in coastal estuaries, and profiling the molecules (*e.g.,* neuropeptides) that are implicated in the stress response, especially in crustaceans that tend to reside in these areas, is a priority.[4, 25] In particular, a temporal component is important to consider more than just the immediate response to a stress. Short-term changes could be due to hyperarousal, and long-term exposure could reveal an alternative, possibly novel mechanism for surviving these stressful conditions until the hypoxic episode ends, which could be a few hours to days.[26] In order to examine four time points (*i.e.,* 0, 1, 4, and 8 hours), a multiplexing strategy was implemented using reductive dimethylation. In the literature, this technique has been utilized in a 2-plex, 3-plex, and 5-plex form, but a 4-plex version has not been investigated further.[9, 12, 18, 27-30] To utilize a 4-plex version of reductive dimethylation, deuterium is not required to be

present in the reducing agent, unlike the 3- and 5-plex. Thus, a borane pyridine complex is used as a reducing agent, which has already been proven to be successful for the 2-plex reductive dimethylation model (**Figure 1**).[8, 9, 20, 30] One concern for multiplexing beyond 2-plex is isotopic overlap, and formulas have been derived to handle this issue specifically for 5-plex reductive methylation.[19] These published corrections values were used for the processing of the MALDI data but was unnecessary for ESI data as the pre-processing performed in PEAKS automatically includes correcting the raw data for isotopic interferences.

Figure 2a shows an example spectrum of allatostatin B-type VPNDWAHRFGSWamide (*m/z* 1470.703) found in the PO from the 4-plex labeled experimental data set. As expected, four distinct peaks in the spectra that were separated by ~2 Da are seen. In this spectrum, a dynamic, overall increase in neuropeptide expression due to increased time exposure of hypoxia stress is also observed. To test the quantitative accuracy of this system a 1:1:1:1 labeling experiment was performed, and the average abundance ratios were all within 15% of the expected ratio (+30/+28: 0.89; +32/+28: 0.93; +34/+28: 0.99). Compared to 2-plex reductive dimethylation, which traditionally has been used for crustacean neuropeptidomic studies,[8, 9, 30] one particular challenge is identifying all channels due to spectral complexity, as seen in **Tables S4-7**. It is important to note that detecting the control channel is imperative for quantitative analysis, but there is value in also investigating those neuropeptides that are not expressed in the control channel (see *Qualitative Analysis*) (**Table S8**).

Overall, in this study, 88 neuropeptides across five different tissues (*i.e.,* SG, brain, PO, CoG, and TG) were identified using both MALDI- and ESI-MS, with a majority of the identifications coming from ESI-MS only (~60%) (**Figure 3**). This small overlap is likely due to 3 factors: (1) Different neuropeptide masses that can be identified between ESI- and MALDI-MS. MALDI-MS is known to primarily produce singly-charged ions, which limits the instrument's ability to analyze neuropeptides with *m/z* 2000 or lower (i.e., due to our mass range being *m/z* 500-2000). Compared to MALDI-MS, ESI-MS has the inherent advantage of producing multiply charged ions, allowing for the identification of larger neuropeptides. (2) MALDI- and ESI-MS have different identification strategies. No MS/MS is performed during MALDI-MS analysis; only accurate mass matching (±5 ppm) is done to identified neuropeptides. On the other hand, ESI-MS relies upon MS/MS fragmentation to *de novo* sequence the MS/MS spectra and then match to a provided database. This translates to point (3). Accurate mass matching limits the identifications to only full-length neuropeptides. Since ESI-MS relies upon *de novo* sequencing, truncated fragments of the neuropeptides can be identified as well. Taking all this into consideration, it is not surprising that only 5 neuropeptides were found in common. The five neuropeptides that overlapped included (1) RFamide SMPTLRLRFamide (*m/z* 1119.646), (2) orcomyotropin FDAFTTGRGHS (*m/z* 1186.516), (3) orcokinin NFDEIDRSGFA (*m/z* 1198.549), (4) orcokinin NFDEIDRSGFA (*m/z* 1270.570), and (5) allatostatin B-type VPNDWAHFRGSWamide (*m/z* 1470.703). Although they may overlap, in some cases they were identified in different tissues (*i.e.,* orcomyotropin FDAFTTGRGHS (*m/z* 1186.516)) or were identified in different channels (*i.e.,* RFamide

SMPTLRLRFamide (*m/z* 1119.646)), boasting the power of using complementary methodology to improve the understanding of the temporal effects of hypoxia stress.

Quantitative Analysis

Neuropeptides identified in the ESI- and MALDI-MS datasets in at least three biological replicates are shown in **Tables S4 -S7**. All neuropeptides that had a statistically significant change at in multiple time points during the hypoxia exposure time course are highlighted in **Figures 4** and **5**. From these results, several trends were revealed: (1) Of the neuropeptides quantified, the bulk majority are decreased in expression in response to hypoxia. This could be interpreted as a decrease in overall activity to conserve energy to try to outlive the hypoxic episode. This is substantiated by prior publications demonstrating decreased gene expression in response to hypoxia.[31] (2) Although an initial response was observed at 1 hour of exposure, after 4 or 8 hours of exposure the neuropeptide expression was no longer significantly different than the control (*i.e.,* basal levels). This suggests a hyperarousal response and is seen in the allatostatin A-type SKSPYSFGLamide, RFamide SENRNFLRFamide, and the RYamide GFVSNRYamide. The dysregulation of these neuropeptides could provide an initial survival mechanism for short bouts of hypoxia. For example, in crustaceans, allatostatin A-type neuropeptides are well documented for being inhibitory neuro/myomodulators,[32] so their expression changes could serve to protect the crab from hypoxia by decreasing heart rate. (3) Some neuropeptides were only increased or decreased after a certain duration of hypoxia exposure (*i.e.,* after 4 or 8 hours). This trend was observed across different tissue types but most notably in the PO. Four allatostatin A-type neuropeptides

(*i.e.,* SNPYSFGLamide, AGPYSFGLamide, SDMYSFGLamide, and SGNYNFGLamide) and two orcokinins (*i.e.,* NFDEIDRSSFGFV and NFDEIDRSGFGFV) showed significant decreases after 8 hours of hypoxia exposure. The down regulation of these neuropeptides could suggest a survival mechanism better suited to longer hypoxia exposure (as opposed to those in trend 2). Alternatively, the hypoxia-exposed crab could be approaching death after 8 hours of severe hypoxia, so the downregulation of these neuropeptides could be a result of that process. (4) An oscillating expression pattern was observed. After 1 hour of exposure, there was a significant change in the neuropeptide content, followed by a return to the basal level at the 4-hour time point. Finally, after eight hours of exposure, the expression levels are similar to what was observed at the 1-hour time point. This trend is most prevalent in the SG, with both up and downregulation observed. Moreover, the change is not limited to specific neuropeptide families and was seen in the allatostatin A-type TPHTYSFGLamide, allatostatin B-type neuropeptides AWSNLGQAWamide and STNWSSLRSAWamide, CHH-precursor related peptide SLKSDTVTPLLG, orcokinin NFDEIDRSGFG, and orcomyotropin FDAFTTGFGHS. The variety of neuropeptides and families suggests that, in general, the crab may be going in and out of either escape or coma-like activities in order to survive the harsh, hypoxic environment.

Of interest are also neuropeptides that do not have statistically significant change, especially those that do not change across the entire time course. When looking through both the ESI- and MALDI-MS data, the bulk of neuropeptides identified did not have any significant change at any point in the time course (20/35 and 31/58

neuropeptides for MALDI- and ESI-MS data, respectively). This overall trend is not unique to any tissue, but many neuropeptide families, including calcitonin-like hormone, cryptocyanin, others, proctolin, pyrokinin, SIFamide, and RYamides, showed no significant change throughout the entire study, indicating that these families may contain neuropeptides whose expression levels were resistant to hypoxia stress-induced biochemical changes. These neuropeptide families have diverse or unknown functions; for example, protcolin has widespread modulatory function throughout the entire nervous system, while pyrokinin's, SIFamides, and RYamide's function has not been studied in the same detail, meaning little is known about their bioactivity.[32]

Qualitative Analysis

For relative quantitation of a neuropeptide, the neuropeptide must be identified in at least the control and one other channel. Unfortunately, this does not allow quantification of neuropeptides that were expressed only after hypoxia exposure or ceased to be expressed after hypoxia exposure. **Table S8** provides a representative sample of those neuropeptides that were unable to be quantified. All tissues except the TG had neuropeptides that were only measurable in the control condition, such as allatostatin A-type GPYSFGLamide (*m/z* 739.377) in the brain, CoG, and PO. This could indicate these neuropeptides were released from the tissue into the hemolymph or degraded after hypoxia exposure. Similar to trend 3 (see *Quantitative Analysis*), there were several examples of neuropeptides only appearing after hypoxia exposure. Some neuropeptides were detected over the entire time course (*e.g.,* allatostatin A-type TPHTYSFGLamide (*m/z* 1021.510) in the PO and crypotocyanin KIFEPLRDKN (*m/z*

1259.711) in the SG), while others may only appeared at specific time points. For example, allatostatin A-type AGPYAFGLamide (*m/z* 794.420) in the PO and RFamide LAPQRNFLRFamide (*m/z* 1260.732) in the SG were only detected after 1 hour of severe hypoxia exposure but were not detected in the other channels. Overall, due to the variable neuropeptide families, their functions, and various tissues, it is difficult to discern the true physiological implications of each of these trends. It is clear, however, that they all play distinct roles in how the crustacean survives both short- and long-term hypoxia stress.[32]

Of particular interest to hypoxia stress are RFamides, RYamides, and tachykinins, because their mammalian homologs, neuropeptide Y (NPY) and substance P (SP), have been implicated in hypoxia stress.[33-39] All three families are known for their dynamic functional roles in the nervous system, and it is expected that they will have a diverse response due to stress, including hypoxia stress.[32] In the brain, PO, and SG, several RFamide and RYamide isoforms consistently appeared only after hypoxia stress. Many of these were highlighted in the trends above, including RFamide AYNRSFLRFamide (*m/z* 1172.632) in the brain, RFamide DPSFLRFamide (*m/z* 853.409) in the PO, RFamide SGRNFLRFamide (*m/z* 995.553) in the SG, RYamide LGRVSNRYamide (*m/z* 954.516) in the PO, and RYamide LSSRFVGGSRYamide (*m/z* 1227.659) in the PO. The range of changes observed in RFamides and RYamides, which are homologs to NPY,[37, 38] emphasizes the importance of analyzing isoforms due to their possible different functions within the body, especially in understanding stress. It should also be noted that two tachykinin family neuropeptides (*i.e.,* APSGFLGMRG (*m/z* 992.498) in the brain

and SGFLGMRamide (*m/z* 766.403) in the CoG), which are homologous to SP,[40] were identified only after exposure to severe hypoxia. Either way, validation studies with hemolymph analysis are of interest to truly characterize if these neuropeptides were being released after hypoxia exposure (in cases where the neuropeptides were only detected in the control condition) or were already present in the hemolymph to target these tissues after exposure to hypoxia stress (in cases where they appear only after hypoxia stress).

Conclusions and Future Directions

Neuropeptidomic studies offer new possibilities in untangling complex signaling pathways involved in a wide range of biological processes, such as environmental stress response. Characterization of neuropeptides, however, presents many challenges as these signaling molecules are highly diverse and the analysis is often sample-limited. By utilizing isotopic reductive dimethylation, the efficacy of using multiplex labeling to quantify neuropeptidomic changes in the blue crab, *Callinectes sapidus* after exposure to different durations of severe hypoxia is demonstrated. Several statistically significant changes were observed in both the MALDI- and ESI-MS data sets. Complementing the data presented here and offering further validation of the results, analyzing the spatial distribution of neuropeptides using MS imaging would allow observation of changes that would otherwise be missed by analyzing only abundance changes. Furthermore, analysis of the crustacean circulating fluid (*i.e.,* hemolymph) could demonstrate the secretion and transport of specific signaling molecules.

Supporting Information

The following supporting information is available free of charge at ACS website http://pubs.acs.org.

Supporting Tables S1-8.

Table S1. MALDI-MS instrument acquisition and data analysis settings.

Table S2. Chromatography and ESI-MS instrument acquisition.

Table S3. ESI-MS data analysis settings.

Table S4. Ratios (stressed/control) of neuropeptides that were detected in at least three biological replicates in the MALDI-MS results.

Table S5. Ratios (stressed/control) of neuropeptides that were detected in at least three biological replicates for the brain, CoG, and TG in the ESI-MS results.

Table S6. Ratios (stressed/control) of neuropeptides that were detected in at least three biological replicates for the PO in the ESI-MS results.

Table S7. Ratios (stressed/control) of neuropeptides that were detected in at least three biological replicates for the SG in the ESI-MS results.

Table S8. Select neuropeptides that were unquantifiable due to no detection in either the control tissue or the hypoxia-stressed tissue.

Data deposition

The mass spectrometry proteomics data have been deposited to the ProteomeXchange Consortium via the PRIDE [1] partner repository with the dataset identifier PXD014688.

Acknowledgements

This work was supported by a National Science Foundation grant (CHE- 1710140) and the National Institutes of Health (NIH) through grant 1R01DK071801. A.R.B. would like to thank NIH for a General Medical Sciences National Ruth L. Kirschstein Research Service Award (NRSA) Fellowship 1F31GM119365. C.S.S. and N.Q.V. would like to thank the National Institute of General Medical Sciences of the NIH under Award Number T32GM008349 for the Biotechnology Training Program Predoctoral Traineeship support. K.D. acknowledges a predoctoral fellowship supported by the NIH under NRSA T32 HL 007936 from the National Heart Lung and Blood Institute to the University of Wisconsin-Madison Cardiovascular Research Center and the National Institutes of Health-General Medical Sciences F31 National Research Service Award (1F31GM126870-01A1) for funding. The Orbitrap instruments were purchased through the support of an NIH shared instrument grant (S10RR029531) and Office of the Vice Chancellor for Research and Graduate Education at the University of Wisconsin-Madison. L.L. acknowledges a Vilas Distinguished Achievement Professorship and Charles Melbourne Johnson Distinguished Chair Professorship with funding provided by the Wisconsin Alumni Research Foundation and University of Wisconsin-Madison School of Pharmacy.

Conflicts of Interest

The authors declare no competing financial interest.

References

1. Barbier, E. B.; Hacker, S. D.; Kennedy, C.; Koch, E. W.; Stier, A. C.; Silliman, B. R., The value of estuarine and coastal ecosystem services. *Ecological Monographs* **2011,** *81* (2), 169-193.

2. Rabalais, N. N.; Diaz, R. J.; Levin, L. A.; Turner, R. E.; Gilbert, D.; Zhang, J., Dynamics and distribution of natural and human-caused hypoxia. *Biogeosciences* **2010,** *7* (2), 585-619.

3. Diaz, R. J.; Rosenberg, R., Marine Benthic hypoxia: a review of its ecological effects and the behavioural responses of benthic macrofauna. *Oceanography and Marine Biology - an Annual Review, Vol 33* **1995,** *33*, 245-303.

4. Santana, R.; Lessa, G. C.; Haskins, J.; Wasson, K., Continuous Monitoring Reveals Drivers of D Oxygen Variability in a Small California Estuary. *Estuaries and Coasts* **2018,** *41* (1), 99-113.

5. Stover, K. K.; Burnett, K. G.; McElroy, E. J.; Burnett, L. E., Locomotory fatigue and size in the Atlantic blue crab, Callinectes sapidus. *Biological Bulletin* **2013,** *224* (2), 68-78.

6. Bell, G. W.; Eggleston, D. B.; Noga, E. J., Environmental and physiological controls of blue crab avoidance behavior during exposure to hypoxia. *Biological Bulletin* **2009,** *217* (2), 161-172.

7. Bell, G. W.; Eggleston, D. B.; Noga, E. J., Molecular keys unlock the mysteries of variable survival responses of blue crabs to hypoxia. *Oecologia* **2010,** *163* (1), 57-68.

8. Zhang, Y.; Buchberger, A.; Muthuvel, G.; Li, L., Expression and distribution of neuropeptides in the nervous system of the crab Carcinus maenas and their roles in environmental stress. *Proteomics* **2015***15* (23–24), 3969–3979.

9. Chen, R. B.; Xiao, M. M.; Buchberger, A.; Li, L. J., Quantitative neuropeptidomics study of the effects of temperature change in the crab cancer borealis. *Journal of Proteome Research* **2014,** *13* (12), 5767-5776.

10. Li, L. J.; Sweedler, J. V., Peptides in the Brain: Mass Spectrometry-Based Measurement Approaches and Challenges. In *Annual Review of Analytical Chemistry*, Annual Reviews: Palo Alto, 2008; Vol. 1, pp 451-483.

11. Chung, J. S.; Zmora, N., Functional studies of crustacean hyperglycemic hormones (CHHs) of the blue crab, Callinectes sapidus - The expression and release of CHH in eyestalk and pericardial organ in response to environmental stress. *Febs Journal* **2008,** *275* (4), 693-704.

12. Kovanich, D.; Cappadona, S.; Raijmakers, R.; Mohammed, S.; Scholten, A.; Heck, A. J. R., Applications of stable isotope dimethyl labeling in quantitative proteomics. *Analytical and Bioanalytical Chemistry* **2012,** *404* (4), 991-1009.

13. Greer, T.; Lietz, C. B.; Xiang, F.; Li, L. J., Enable Absolute Quantification of Peptides and Proteins Using a Standard Curve Approach. *Journal of the American Society for Mass Spectrometry* **2015,** *26* (1), 107-119.

14. Hwang, C. Y.; Kim, K.; Choi, J. Y.; Bahn, Y. J.; Lee, S. M.; Kim, Y. K.; Lee, C.; Kwon, K. S., Quantitative proteome analysis of age-related changes in mouse gastrocnemius muscle using mTRAQ. *Proteomics* **2014,** *14* (1), 121-132.

15. Wiese, S.; Reidegeld, K. A.; Meyer, H. E.; Warscheid, B., Protein labeling by iTRAQ: A new tool for quantitative mass spectrometry in proteome research. *Proteomics* **2007,** *7* (3), 340-350.

16. Werner, T.; Becher, I.; Sweetman, G.; Doce, C.; Savitski, M. M.; Bantscheff, M., High-resolution enabled TMT 8-plexing. *Analytical Chemistry* **2012,** *84* (16), 7188-7194.

17. Xiang, F.; Ye, H.; Chen, R. B.; Fu, Q.; Li, L. J., N,N-Dimethyl leucines as novel Isobaric tandem mass tags for quantitative proteomics and peptidomics. *Analytical Chemistry* **2010,** *82* (7), 2817-2825.

18. Wu, Y.; Wang, F. J.; Liu, Z. Y.; Qin, H. Q.; Song, C. X.; Huang, J. F.; Bian, Y. Y.; Wei, X. L.; Dong, J.; Zou, H. F., Five-plex isotope dimethyl labeling for quantitative proteomics. *Chemical Communications* **2014,** *50* (14), 1708-1710.

19. Tashima, A. K.; Fricker, L. D., Quantitative Peptidomics with Five-plex Reductive Methylation labels. *J Am Soc Mass Spectrom* **2018,** *29* (5), 866-878.

20. DeLaney, K.; Buchberger, A.; Li, L., Identification, Quantitation, and Imaging of the Crustacean Peptidome. *Methods Mol Biol* **2018,** *1719*, 247-269.

21. Stapels, M. D.; Barofsky, D. F., Complementary use of MALDI and ESI for the HPLC-MS/MS analysis of DNA-binding proteins. *Analytical Chemistry* **2004,** *76* (18), 5423-5430.

22. Gutierrez, G. J.; Grashow, R. G., Cancer borealis stomatogastric nervous system dissection. *J Vis Exp* **2009,** (25), e1207, doi:10.3791/1207.

23. McHugh, M. L., Multiple comparison analysis testing in ANOVA. *Biochemia Medica* **2011,** *21* (3), 203-209.

24. Jaki, T.; Hothorn, L. A., Statistical evaluation of toxicological assays: Dunnett or Williams test - Take both. *Archives of Toxicology* **2013,** *87* (11), 1901-1910.

25. Gray, J. S.; Wu, R. S. S.; Or, Y. Y., Effects of hypoxia and organic enrichment on the coastal marine environment. *Marine Ecology Progress Series* **2002,** *238*, 249-279.

26. Wasson, K.; Lyon, B. E., Flight or fight: Flexible antipredatory strategies in porcelain crabs. *Behavioral Ecology* **2005,** *16* (6), 1037-1041.

27. Hsu, J. L.; Huang, S. Y.; Chen, S. H., Dimethyl multiplexed labeling combined with microcolumn separation and MS analysis for time course study in proteomics. *Electrophoresis* **2006,** *27* (18), 3652-3660.

28. Boersema, P. J.; Raijmakers, R.; Lemeer, S.; Mohammed, S.; Heck, A. J. R., Multiplex peptide stable isotope dimethyl labeling for quantitative proteomics. *Nature Protocols* **2009,** *4* (4), 484-494.

29. Boersema, P. J.; Aye, T. T.; van Veen, T. A. B.; Heck, A. J. R.; Mohammed, S., Triplex protein quantification based on stable isotope labeling by peptide dimethylation applied to cell and tissue lysates. *Proteomics* **2008,** *8* (22), 4624-4632.

30. Zhang, Y.; DeLaney, K.; Hui, L.; Wang, J.; Sturm, R. M.; Li, L., A Multifaceted Mass Spectrometric Method to Probe Feeding Related Neuropeptide Changes in Callinectes sapidus and Carcinus maenas. *J Am Soc Mass Spectrom* **2018**, *29* (5), 948-960.

31. Brown-Peterson, N. J.; Larkin, P.; Denslow, N.; King, C.; Manning, S.; Brouwer, M., Molecular Indicators of Hypoxia in the Blue Crab *Callinectes sapidus*. Marine Ecology-Progress Series, 2005; Vol. 286, pp 203-215.

32. Christie, A. E.; Stemmler, E. A.; Dickinson, P. S., Crustacean neuropeptides. *Cell Mol Life Sci* **2010,** *67* (24), 4135-69.

33. Poncet, L.; Denoroy, L.; Dalmaz, Y.; Pequignot, J. M.; Jouvet, M., Alteration in central and peripheral substance P- and neuropeptide Y-like immunoreactivity after chronic hypoxia in the rat. *Brain Research* **1996,** *733* (1), 64-72.

34. Wang, Z. Z.; Dinger, B.; Fidone, S. J.; Stensaas, L. J., Changes in tyrosine hydroxylase and substance P immunoreactivity in the cat carotid body following chronic hypoxia and denervation. *Neuroscience* **1998,** *83* (4), 1273-1281.

35. Lee, E. W.; Michalkiewicz, M.; Kitlinska, J.; Kalezic, I.; Switalska, H.; Yoo, P.; Sangkharat, A.; Ji, H.; Li, L. J.; Michalkiewicz, T.; Ljubisavljevic, M.; Johansson, H.; Grant, D. S.; Zukowska, Z., Neuropeptide Y induces ischemic angiogenesis and restores function of ischemic skeletal muscles. *Journal of Clinical Investigation* **2003,** *111* (12), 1853-1862.

36. Moss, I. R.; Laferriere, A., Central neuropeptide systems and respiratory control during development. *Respiratory Physiology & Neurobiology* **2002,** *131* (1-2), 15-27.

37. Husson, S. J.; Mertens, I.; Janssen, T.; Lindemans, M.; Schoofs, L., Neuropeptidergic signaling in the nematode Caenorhabditis elegans. *Prog Neurobiol* **2007,** *82* (1), 33-55.

38. Dockray, G. J., The expanding family of -RFamide peptides and their effects on feeding behaviour. *Exp Physiol* **2004,** *89* (3), 229-35.

39. Coast, G. M.; Schooley, D. A., Toward a consensus nomenclature for insect neuropeptides and peptide hormones. *Peptides* **2011,** *32* (3), 620-31.

40. Satake, H.; Kawada, T.; Nomoto, K.; Minakata, H., Insight into Tachykinin-Related Peptides, Their Receptors, and Invertebrate Tachykinins: A review. *Zoolog Sci* **2003,** *20* (5), 533-49.

Figures

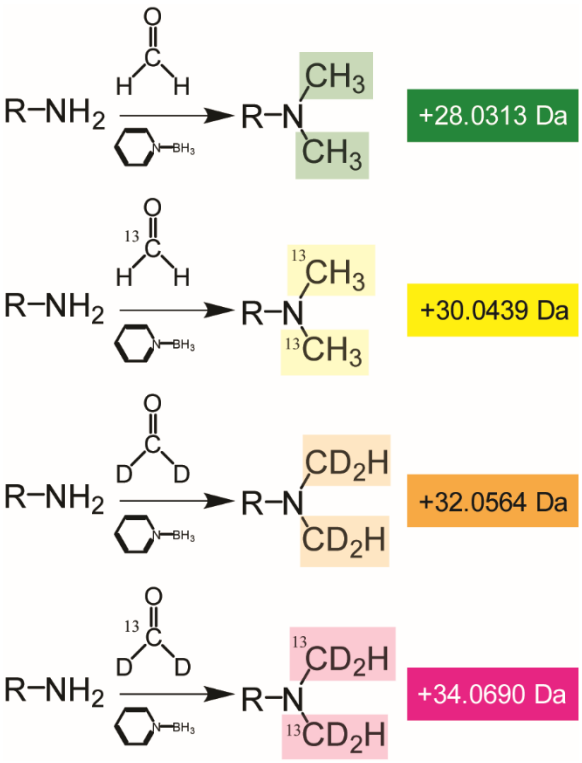

Figure 1. Reaction scheme for each channel of the 4-plex reductive dimethylation utilized in this study. ^{13}C and D were the only isotopes utilized.

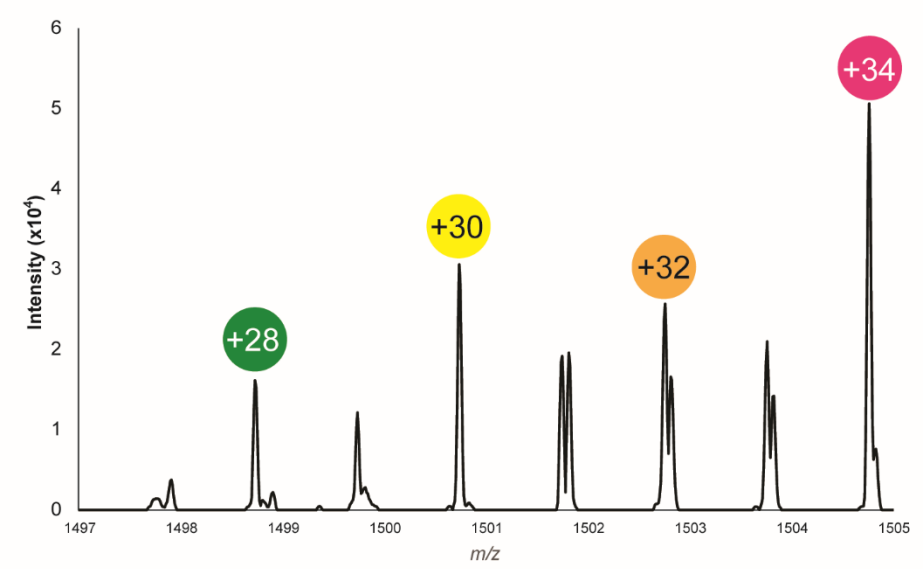

Figure 2. Sample spectrum of 4-plex reductive dimethylation. Each label is spaced by ~2 (2.0126 Da to be exact). The representative neuropeptide is allatostatin B-type VPNDWAHRFGSWamide (*m/z* 1470.703) found in the PO. The accurate mass increases are described in Figure 1 and as follows: +28=+28.0313 Da, +30=+30.0439 Da; +32 =+32.0564 Da; +34=34.0690 Da.

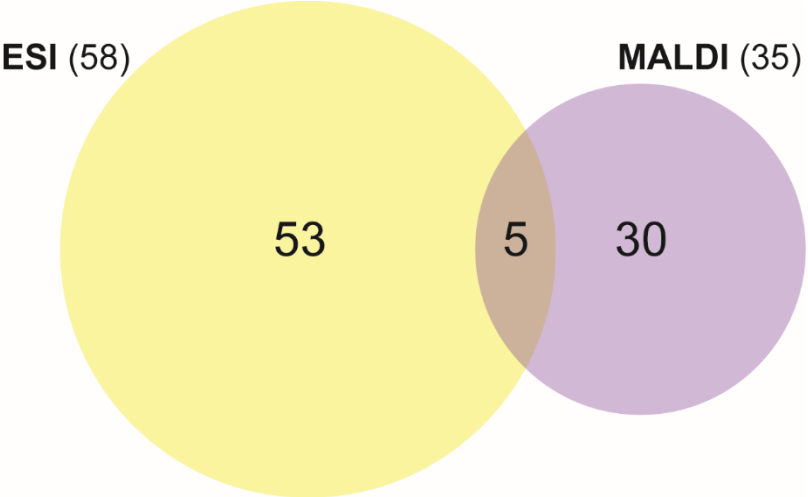

Figure 3. A Venn diagram depicting the neuropeptide overlap (regardless of expression changes) between ESI- and MALDI-MS. Only neuropeptides that were found in at least 3 biological replicates in both the control and at least one other channel in the SG, brain, PO, CoG, or TG were included. The five neuropeptides that overlapped included (1) RFamide SMPTLRLRFamide (*m/z* 1119.646), (2) orcomyotropin FDAFTTGRGHS (*m/z* 1186.516), (3) orcokinin NFDEIDRSGFA (*m/z* 1198.549), (4) orcokinin NFDEIDRSGFA (*m/z* 1270.570), and (5) allatostatin B-type VPNDWAHFRGSWamide (*m/z* 1470.703).

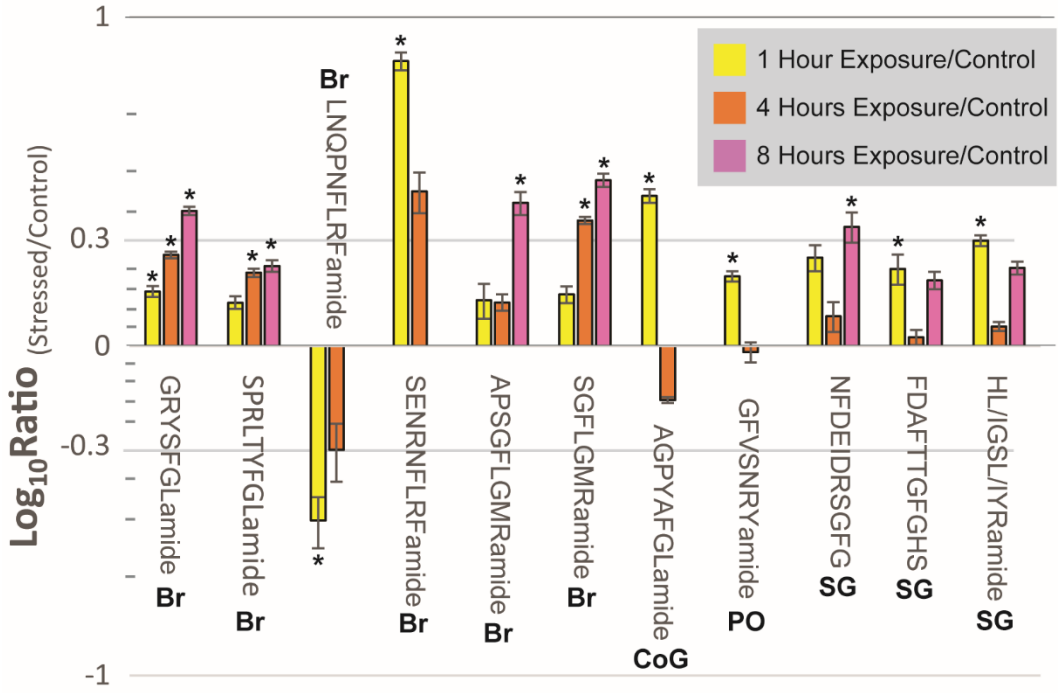

Figure 4. A bar graph of the ratios of all neuropeptides found to have significant differences between a control and at least two of the three time points (*i.e.,* 1 hour (yellow), 4 hour (orange), and 8 hour (pink)) for severe (*i.e.,* 1 ppm O_2) hypoxia exposure identified by MALDI-MS. Neuropeptides were found in the brain (Br), CoG, PO, and SG. The x-axis shows the neuropeptides' sequences, and the y-axis represents the $\log_{10}$ ratio of hypoxia-stressed to a control. The asterisk (*) represents statistical significance determined by a Dunnett's test. The error bars reflect the standard error of the mean (SEM).

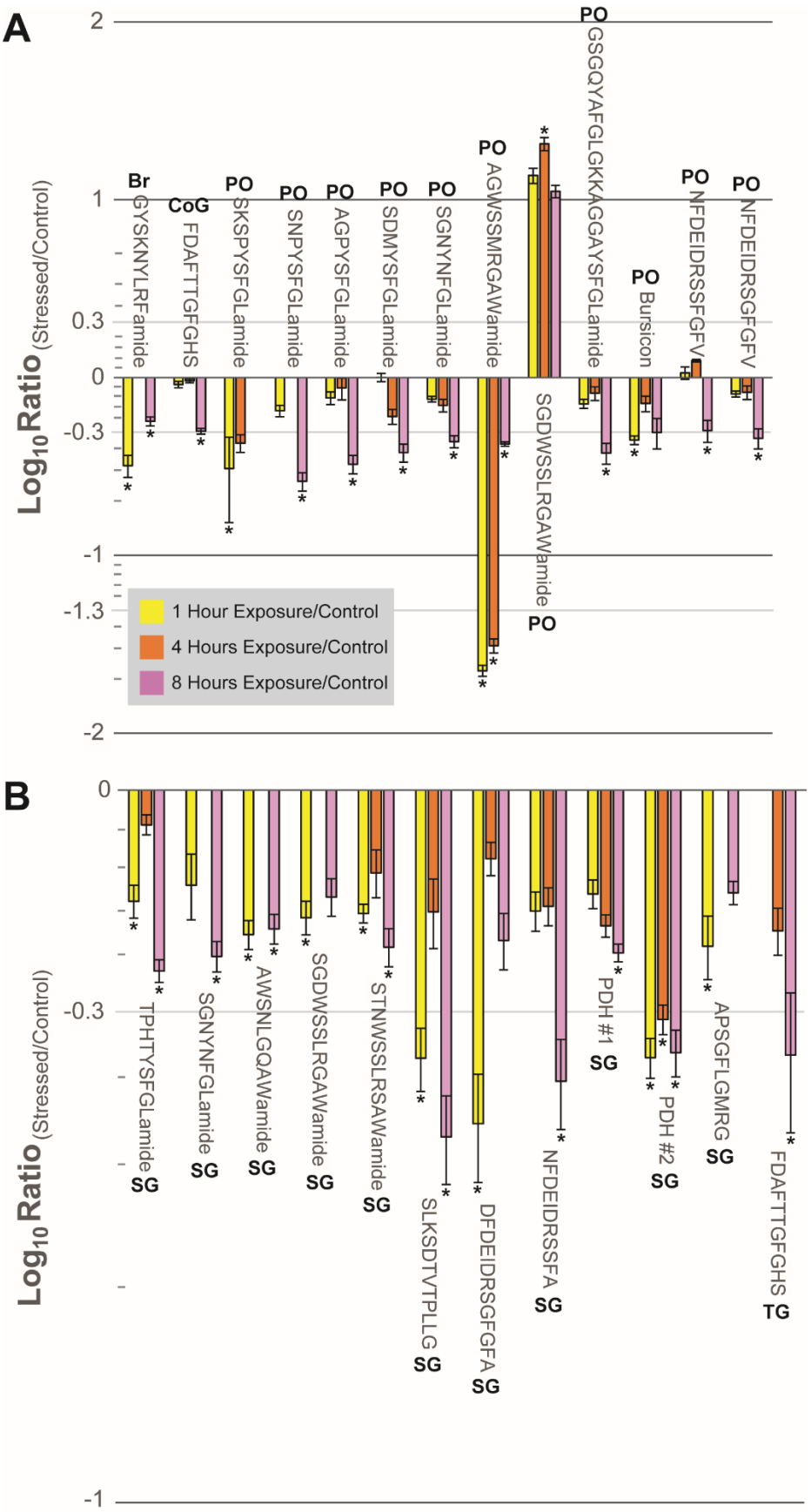
A
Log10 Ratio (Stressed/Control)
2
1
0.3
0
-0.3
-1
-1.3
-2
1 Hour Exposure/Control
4 Hours Exposure/Control
8 Hours Exposure/Control
Br GYSKNYLRFamide
CoG FDAFTTGFGHS
PO SKSPYSFGLamide
PO SNPYSFGLamide
PO AGPYSFGLamide
PO SDMYSFGLamide
PO SGNYNFGLamide
PO AGWSSMRGAWamide
PO SGDWSSLRGAWamide
PO GSGQYAFGLGKKAGGAYSFGLamide
PO Bursicon
PO NFDEIDRSSFGFV
PO NFDEIDRSGFGFV
B
Log10 Ratio (Stressed/Control)
0
-0.3
-1
TPHTYSFGLamide SG
SGNYNFGLamide SG
AWSNLGQAWamide SG
SGDWSSLRGAWamide SG
STNWSSLRSAWamide SG
SLKSDTVTPLLG SG
DFDEIDRSGFGFA SG
NFDEIDRSSFA SG
PDH #1 SG
PDH #2 SG
APSGFLGMRG SG
FDAFTTGFGHS TG

Figure 5. Bar graphs of the ratios of all neuropeptides found to have significant differences between a control and at least two of the three time points (*i.e.,* 1 hour (yellow), 4 hour (orange), and 8 hour (pink)) for severe (*i.e.,* 1 ppm O_2) hypoxia exposure identified by ESI-MS. (A) Neuropeptides found in the brain (Br), CoG, and PO. (B) Neuropeptides found in the SG and TG. The x-axis shows the neuropeptides' sequences, while the y-axis represents the log (to the power of 10) ratio of hypoxia-stressed to a control. The asterisk (*) represents statistical significance determined by a Dunnett's test. The error bars represent standard error of the mean (SEM). Bursicon (PO) refers to the sequence DECSLRPVIHILSYPGCTSKPIPSFACQGRCTSYVQVSGSKLWQTERSMCCQESGEREAAITLNCP KPRPGEPKEKKVLTRAPIDCMCRPCTDVEEGTVLAQKIANFIQDSMPDSVPFLK. PDH #1 (SG) and PDH # 2 (SG) refer to neuropeptides QELKYQEREMVAELAQQIYRVAQAPWAAAVGPHKRNSELINSILGLPKVMNDAamide and QEDLKYFEREVVSELAAQILRVAQGPSAFVAGPHKRNSELINSLLGIPKVMNDAamide found in the pigment dispersing hormone family.

For TOC Only

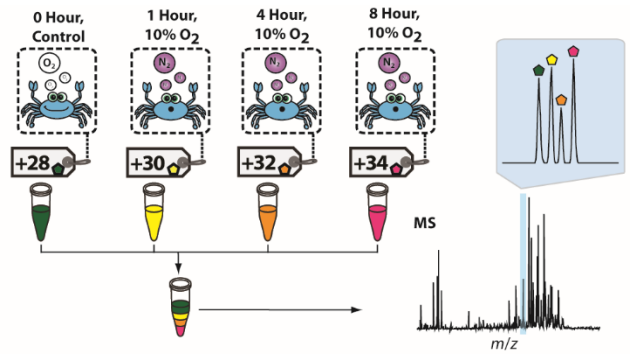
0 Hour, Control
1 Hour, 10% O_2
4 Hour, 10% O_2
8 Hour, 10% O_2
+28
+30
+32
+34
MS
m/z

Table S1. MALDI-MS instrument acquisition and data analysis settings.

MALDI-MS Instrument Acquisition and Data Analysis Settings			
Mass Spectrometer	Thermo MALDI-LTQ-Orbitrap XL	***Resolution***	60,000 @ *m/z* 400
Laser	60 Hz 337 nm N_2	***Spectrum Processing***	Xcalibur 2.2 (Thermo)
Laser Energy	15.00 µJ	***Spectral Analysis***	Custom Java Program (written by K. DeLaney)
Number of Laser Pulses	200	***Peptide Identification***	Accurate Mass Matching
Microscans	50	***Mass Accuracy***	5 ppm
Ion Trap AGC Target	3.0e4	***Minimum Intensity Threshold***	100
FTMS AGC Target	1.0e6	***Isotopic Correction***	Manual; *JASMS* 29(5):866-878.
Mass Range	*m/z* 500-2000	***Hypothesis Test***	ANOVA/Dunnet's Test/t-test

Table S2. Chromatography and ESI-MS instrument acquisition.

Chromatography and ESI-MS Instrument Acquisition			
Sample Volume	2 uL	***Isolation Window***	2.0 m/z
Stationary Phase	Hand-Packed C_{18} column 75µm ID x 360 µm OD ~15 cm 3.0 µm cap; 1.7 µm particles	***MS^2 AGC Target***	2e5
LC Solvent A	100% H_2O 0.1% formic acid	***MS^2 Maximum IT***	120 ms
LC Solvent B	100% acetonitrile, 0.1% formic acid	***Normalized Collision Energy***	30
Gradient Ramp and Duration ***Flow Rate***	10-35% B in 90 minutes 3.0 µL/min	***Minimum Intensity Req.***	1.7e3
Mass Spectrometer	Thermo Q Exactive	***Dynamic Exclusion***	30 s
Spray Voltage	1.9 kV	***MS^2 acquisition***	Data dependent, profile
In-Source CID	None	***MS^2 Fragmentation***	HCD
MS^1 scan range	*m/z* 200-2000	***MS^2 Detection***	Orbitrap
MS^1 resolution	70,000 @ *m/z* 400	***MS^2 fixed first mass***	*m/z* 100
MS^1 AGC Target	1e6	***MS^2 resolution***	17,500 @ *m/z* 400
MS^1 Maximum IT	250 ms	***Advanced Precursor Determination***	N/A

Table S3. ESI-MS data analysis settings.

ESI-MS Data Analysis Settings			
Platform	PEAKS 8.5	***Precursor Options***	Corrected
Validation	Decoy-fusion	***Charge Options***	No correction
Database	In-house crustacean neuropeptide database	***Filter Options***	No filter
Digest	None	***Process***	True
Precursor Mass Tolerance	20 ppm	***Quantitation***	Peak Area
Fragment Mass Tolerance	0.2 Da	***Normalization***	Peak area of individual neuropeptides divided by total peak area
Precursor Mass Search Type	Monoisotopic	***Scaling***	None
Max Missed Cleavages	100	***Ratio Calculation***	Heavy/Light
Non-specific Cleavage	Both	***Hypothesis Test***	ANOVA/Dunnet's Test
Static Modifications	None	***FDR Estimation***	Enabled
Max Variable PTM Per Peptide	3	***Target FDR***	0.01
Dynamic Modifications	Amidation, Oxidation (M), Dehydration, Pyro-glu from E, Pyro-glu from Q, Dimethylation (N-term+K): 28.03, Dimethylation-$^{13}CH_2$ (N-term+K): 30.04, Dimethylation-C^2H_2 (N-term+K):32.06, DiMethylation-$^{13}C^2H_2$ (N-term+K): 34.06	***Export Settings***	Project View → Project Name → PEAKS (database search results) → FDR → 1% → Apply → Export → Text Formats → DB search peptides (peptides.csv)

Table S4. Ratios (stressed/control) of neuropeptides that were detected in at least three biological replicates in the MALDI-MS results. In column "Sig?", the highlighted cells (yellow, orange, or pink) are those with significant changes based upon the Dunnett's test. If only the control and one other time point were detected, a t-test was used to determine significance. Blacked-out cells are those that were identified in fewer than three biological replicates. AST-A: allatostatin type-A; AST-B: allatostatin type-B; CPRP: crustacean hyperglycemic hormone (CHH) precursor-related peptide; SEM: standard error of the mean; Y: yes; N: no.

				1 ppm O2, 1 Hour			1 ppm O2, 4 Hour			1 ppm O2, 8 Hour		
Tissue	Family	Sequence	*m/z*	Ratio	SEM	Sig?	Ratio	SEM	Sig?	Ratio	SEM	Sig?
Brain	AST-A	GRYSFGLamide	798.426	1.465	0.055	Y	1.892	0.045	Y	2.574	0.074	Y
		PRNYAFGLamide	936.505				1.544	0.092	N			
		SGHYIFGLamide	892.468				1.963	0.080	Y			
		SPRLTYFGLamide	1052.589	1.355	0.059	N	1.669	0.051	Y	1.751	0.070	Y
	Pyrokinin	TNFAFSPRLamide	1051.568				1.460	0.023	N			
	RFamide	AYPSLRLRFamide	1121.658	0.941	0.008	N	0.792	0.042	N			
		EFLRFamide	710.398				0.684	0.036	N	0.950	0.049	N
		GNRNFLRFamide	1022.565				1.066	0.042	N	0.651	0.105	N
		LNQPNFLRFamide	1147.637	0.295	0.052	Y	0.484	0.096	N			
		LTNRNFLRFamide	1179.675	1.615	0.083	N				1.066	0.078	N
		SENRNFLRFamide	1181.617	7.340	0.459	Y	2.949	0.418	N			
		SMPTLRLRFamide	1119.646	1.107	0.048	N	1.033	0.015	N	0.880	0.054	N
	Tachykinin	APSGFLGMRamide	934.493	1.377	0.168	N	1.357	0.077	N	2.719	0.219	Y
		SGFLGMRamide	766.403	1.434	0.084	N	2.405	0.059	Y	3.189	0.146	Y
CoG	AST-A	AGPYAFGLamide	794.420	2.858	0.138	Y	0.685	0.014	N			
PO	AST-A	NPYSFGLamide	796.399	2.943	0.588	N	0.950	0.177	N	1.297	0.351	N
	AST-B	VPNDWAHFRGSWamide	1470.703				1.240	0.076	N	1.641	0.219	N
	CPRP	KLLSSSNSPSSTP	1304.669				1.489	0.016	Y			
		RSVEGASRMEKLL	1475.800	0.794	0.045	N						
		TPLGFLSQDHSV	1300.653	0.693	0.080	N						
	Cryptocyanin	KIFEPLREDNL	1373.742	1.076	0.025	N						
	Proctolin	RYLPT	649.367	0.875	0.156	N	1.113	0.105	N	1.608	0.231	N
	RFamide	GYGDRNFLRFamide	1243.633	0.285	0.035	Y						
	RYamide	GFVSNRYamide	841.432	1.630	0.059	Y	0.960	0.067	N			
		SGFYANRYamide	976.464	1.442	0.073	N				0.828	0.182	N
	Tachykinin	APSGFLGM	779.376	2.154	0.424	N	0.515	0.120	N	0.975	0.324	N
SG	AST-A	PRNYAFGLamide	936.505				1.174	0.075	N			
	CPRP	ASLKSDTVTPLR	1287.727				1.517	0.048	Y			
		RSAEGLGRMamide	975.515	1.847	0.144	N	1.045	0.128	N	1.702	0.063	N
	Orcokinin	NFDEIDRSGFA	1270.570	1.659	0.092	N	1.080	0.062	N	1.754	0.339	N
		NFDEIDRSGFG	1256.554	1.857	0.168	N	1.232	0.128	N	2.303	0.242	Y
		NFDEIDRSSFGFV	1532.702				0.730	0.079	N	1.141	0.039	N
	Orcomyotropin	FDAFTTGFGHS	1186.516	1.717	0.182	Y	1.064	0.056	N	1.584	0.098	N
	Others	HL/IGSL/IYRamide	844.479	2.090	0.079	Y	1.148	0.036	N	1.729	0.079	N
	RFamide	NQPNFLRFamide	1034.553	1.033	0.089	N	1.027	0.029	N			
	Tachykinin	APSGFLGMRamide	934.493	1.187	0.192	N	0.520	0.083	N	1.285	0.056	N
TG	CPRP	KLLSSSNSPSSTP	1304.669				1.640	0.162	N			
		TPLGFLSQDHSV	1300.653				0.980	0.027	N			
	RFamide	DENRNFLRFamide	1209.612	1.108	0.053	N	0.657	0.089	N	0.932	0.022	N

Table S5. Ratios (stressed/control) of neuropeptides that were detected in at least three biological replicates for the brain, CoG, and TG in the ESI-MS results. In column "Sig?", the highlighted cells (yellow, orange, or pink) are those were significant changes based upon the Dunnett's test. If only the control and one other time point were detected, a t-test was used to determine significance. Blacked-out cells are those that were identified in fewer than three biological replicates. AST-A: allatostatin type-A; AST-B: allatostatin type-B; PDH: pigment dispersing hormone; SEM: standard error of the mean; Y: yes, N: no.

				1 ppm O2, 1 Hour			1 ppm O2, 4 Hour			1 ppm O2, 8 Hour		
Tissue	Family	Sequence	*m/z*	Ratio	SEM	Sig?	Ratio	SEM	Sig?	Ratio	SEM	Sig?
Brain	AST-A	TPHTYSFGLamide	1021.510							1.062	0.018	N
	AST-B	AWSNLGQAWamide	1031.506	0.888	0.062	N	0.956	0.082	N	0.922	0.040	N
		NNNWTKFQGSWamide	1380.644	0.634	0.028	N	0.713	0.026	N			
		SGDWSSLRGAWamide	1220.581	0.908	0.055	N	0.886	0.018	N	1.078	0.056	N
		TGWNKFQGSWamide	1209.580	0.931	0.041	N	1.491	0.049	N	1.264	0.048	N
		VPNDWAHFRGSWamide	1470.703	0.991	0.049	N	0.777	0.049	N	1.050	0.066	N
		TSWGKFQGSWamide	1182.569	0.932	0.058	N	1.391	0.047	N	0.982	0.038	N
		STNWSSLRSAWamide	1293.633	0.782	0.046	N	0.829	0.016	N	0.818	0.061	N
	Orcokinin	NFDEIDRSGFA	1270.570				1.010	0.050	N	1.032	0.120	N
		NFDEIDRSSFGF	1433.633	1.580	0.271	N				1.630	0.232	N
		NFDEIDRSGFGFA	1474.660							0.963	0.029	N
		NFDEIDRSSFGFN	1547.676	0.824	0.030	N				0.799	0.084	N
		NFDEIDRSSFGFV	1532.702	0.971	0.031	N				0.991	0.020	N
		NFDEIDRSGFGFV	1502.691	1.130	0.077	N				1.818	0.131	N
		NFDEIDRSSFA	1300.580	0.627	0.046	N	0.890	0.030	N	0.829	0.161	N
	Orcomyotropin	FDAFTTGFGHS	1186.516	0.553	0.057	N	0.503	0.048	N	0.836	0.102	N
	Others	HL/IGSL/IYRamide	844.479	0.767	0.068	N	0.574	0.037	N	0.897	0.054	N
	PDH	QELKYQEREMVAELAQQIYRVAQAPWAAAVG PHKRNSELINSILGLPKVMNDAamide	5973.138	0.877	0.064	N	1.346	0.085	N	1.211	0.067	N
		QREPTASKCQAATELAIQILQAVKGAHTGVAAG PHKRNSELINSLLGLPKFMIDAamide	5792.122	0.902	0.060	N	0.742	0.039	N	0.565	0.053	N
	RFamide	GYSKNYLRFamide	1146.605	0.320	0.045	Y				0.567	0.034	Y
		SMPTLRLRFamide	1119.646							0.888	0.037	N
		QDLDHVFLRFamide	1288.680	0.878	0.018	N				0.829	0.057	N
		KPDPSQLANMAEALKYLEQELDKYYSQVSRPRF amide	3913.991	0.735	0.055	N	0.823	0.053	N	0.699	0.040	N
	SIFamide	GYRKPPFNGSIFamide	1381.738	0.770	0.026	N	0.850	0.051	N	0.901	0.053	N
CoG	AST-A	TPHTYSFGLamide	1021.510	0.989	0.085	N	1.070	0.048	N	0.621	0.056	N
	Orcokinin	DFDEIDRSSFGFN	1548.660				1.078	0.053	N			
		NFDEIDRSGFA	1270.570	1.557	0.053	N	1.047	0.132	N	0.749	0.067	N
		NFDEIDRSGFGFA	1474.660	0.972	0.089	N				0.785	0.061	N
		NFDEIDRSSFGFN	1547.676	1.174	0.064	N	0.692	0.118	N	1.094	0.093	N
	Orcomyotropin	FDAFTTGFGHS	1186.516	0.913	0.038	N	0.959	0.024	N	0.499	0.019	Y
	PDH	QEDLKYFEREVVSELAAQILRVAQGPSAFVAGPH KRNSELINSLLGIPKVMNDAamide	5947.165	0.983	0.079	N	1.138	0.145	N	0.815	0.067	N
	RFamide	QDLDHVFLRFamide	1288.680	1.273	0.040	Y						
TG	Orcomyotropin	FDAFTTGFGHS	1186.516				0.634	0.048	N	0.423	0.095	Y

Table S6. Ratios (stressed/control) of neuropeptides that were detected in at least three biological replicates for the PO in the ESI-MS results. The highlighted cells (*e.g.,* yellow, orange, or pink) are those were significant changes based upon the Dunnett's test. If only the control and one other time point were detected, a t-test was used to determine significance. Blacked-out cells are those that were identified in fewer than three biological replicates. AST-A: allatostatin type-A; AST-B: allatostatin type-B; AST: allatostatin; CPRP: CHH precursor-related peptide; SEM: standard error of the mean; Y: yes; N: no.

				1 ppm O2, 1 Hour			1 ppm O2, 4 Hour			1 ppm O2, 8 Hour		
Tissue	Family	Sequence	*m/z*	Ratio	SEM	Sig?	Ratio	SEM	Sig?	Ratio	SEM	Sig?
PO	AST-A	DGPYSFGLamide	854.404	1.241	0.103	N	1.100	0.201	N			
		DPYAFGLRHTSFVLYAFGLamide	2173.210	1.014	0.067	N	0.946	0.080	N	0.666	0.057	N
		SKSPYSFGLamide	984.515	0.308	0.155	Y	0.428	0.048	N			
		SNPYSFGLamide	883.431	0.650	0.048	N				0.261	0.031	Y
		AGPYSFGLamide	810.415	0.767	0.063	N	0.872	0.122	N	0.326	0.039	Y
		SDMYSFGLamide	918.403	1.002	0.054	N	0.603	0.057	N	0.378	0.043	Y
		SGNYNFGLamide	870.410	0.756	0.028	N	0.696	0.057	N	0.436	0.034	Y
	AST-B	AGWSSMRGAWamide	1107.533	0.022	0.002	Y	0.031	0.003	Y	0.422	0.012	Y
		AWSNLGQAWamide	1031.506				1.400	0.047	N	0.618	0.068	N
		LNNNWSKFQGSWamide	1479.713	0.947	0.060	N	1.345	0.084	N	0.707	0.061	N
		NDWSKFGQSWamide	1253.570	1.019	0.063	N	1.006	0.070	N	0.728	0.067	N
		NNNWTKFQGSWamide	1380.644	0.936	0.043	N	1.007	0.064	N	0.643	0.032	N
		SGDWSSLRGAWamide	1220.581	13.672	1.335	N	20.610	1.747	Y	11.147	0.875	N
		STDWSSLRSAWamide	1294.618	0.804	0.068	N	1.358	0.079	N			
		TGWNKFQGSWamide	1209.580	0.992	0.078	N	1.526	0.097	N	0.699	0.051	N
		VPNDWAHFRGSWamide	1470.703	0.634	0.042	N	0.799	0.082	N	0.449	0.048	N
		TSWGKFQGSWamide	1182.569	0.149	0.016	N	1.780	0.090	N	0.806	0.056	N
		STNWSSLRSAWamide	1293.633	0.468	0.060	N	1.115	0.099	N	0.322	0.025	N
	AST Combos	GSGQYAFGLGKKAGGAYSFGLamide	2035.040	0.711	0.041	N	0.815	0.073	N	0.376	0.051	Y
	Bursicon	DECSLRPVIHILSYPGCTSKPIPSFACQGRCTSYVQVSGSKLWQTERSMCCQESGEREAAITLNCPKPRPGEPKEKKVLTRAPIDCMCRPCTDVEEGTVLAQKIANFIQDSMPDSVPFLK	13257.451	0.445	0.025	Y	0.715	0.072	N	0.491	0.095	N
	CPRP	RSAEGLGRMGRLLASLKSDTVTPLRGFEGETGHPLE	3838.003	1.888	0.145	N	1.559	0.093	N	0.420	0.039	N
	Orcokinin	DFDEIDRSGFA	1271.554				1.128	0.061	N	0.483	0.057	N
		DFDEIDRSSFA	1301.564	0.579	0.040	N	0.572	0.041	N			
		DFDEIDRSSFGFN	1548.660				2.960	0.161	Y			
		NFDEIDRSGFA	1270.570	0.933	0.075	N	0.736	0.038	N	0.655	0.053	N
		NFDEIDRSSFGF	1433.633	0.377	0.163	N	1.283	0.150	N	0.967	0.356	N
		NFDEIDRSGFGFA	1474.660				2.015	0.131	N	0.954	0.225	N
		NFDEIDRSSFGFN	1547.676	0.742	0.130	N	1.797	0.149	N	0.899	0.112	N
		NFDEIDRSSFGFV	1532.702	1.063	0.084	N	1.245	0.020	N	0.503	0.071	Y
		NFDEIDRSGFGFV	1502.691	0.808	0.032	N	0.825	0.073	N	0.456	0.059	Y
		NFDEIDRSSFA	1300.580	0.992	0.095	N	0.912	0.056	N	0.621	0.081	N
	Orcomyotropin	FDAFTTGFGHS	1186.516	1.367	0.107	N	1.096	0.108	N	1.048	0.136	N
	Others	HL/IGSL/IYRamide	844.479	1.052	0.052	N	0.985	0.052	N	0.704	0.060	N
	RFamide	GYSKNYLRFamide	1146.605	Y	0.060	N						
		GYNRSFLRFamide	1158.617	Y	0.055	N						
		QDLDHVFLRFamide	1288.680	0.979	0.054	N	0.753	0.065	N	0.700	0.200	N
		DGGRNFLRFamide	1080.570	0.732	0.077	N						
	RYamide	LSGFYANRYamide	1089.548	0.803	0.043	N	0.354	0.075	N	0.476	0.024	N
		QGFYSQRYamide	1030.474	1.152	0.166	N						
		SGFYADRYamide	977.448	0.781	0.040	N				0.436	0.056	N

Table S7. Ratios (stressed/control) of neuropeptides that were detected in at least three biological replicates for the SG in the ESI-MS results. The highlighted cells (*e.g.,* yellow, orange, or pink) are those were significant changes based upon the Dunnett's test. If only the control and one other time point were detected, a t-test was used to determine significance. Blacked out cells are those that were identified in fewer than three biological replicates. AST-A: allatostatin type-A; AST-B: allatostatin type-B; CLH: calcitonin-like hormone; CPRP: CHH precursor-related peptide; PDH: pigment dispersing hormone; SEM: standard error of the mean, Y: yes; N: no.

				1 ppm O2, 1 Hour			1 ppm O2, 4 Hour			1 ppm O2, 8 Hour		
Tissue	Family	Sequence	*m/z*	Ratio	SEM	Sig?	Ratio	SEM	Sig?	Ratio	SEM	Sig?
SG	AST-A	DGPYSFGLamide	854.404							0.696	0.038	Y
		SKSPYSFGLamide	984.515				1.029	0.042	N			
		TPHTYSFGLamide	1021.510	0.697	0.037	Y	0.894	0.029	N	0.556	0.020	Y
		SGNYNFGLamide	870.410	0.734	0.078	N				0.583	0.029	Y
	AST-B	AGWSSMRGAWamide	1107.533	0.659	0.036	N				0.739	0.040	N
		AWSNLGQAWamide	1031.506	0.626	0.029	Y				0.638	0.031	Y
		NNNWTKFQGSWamide	1380.644	0.714	0.044	N	0.714	0.030	N	0.722	0.025	N
		SGDWSSLRGAWamide	1220.581	0.661	0.036	Y				0.707	0.043	N
		TGWNKFQGSWamide	1209.580	1.552	0.191	N	3.125	0.233	N	2.772	0.281	N
		VPNDWAHFRGSWamide	1470.703							0.561	0.022	Y
		TSWGKFQGSWamide	1182.569	0.629	0.045	N	1.083	0.169	N	1.189	0.070	N
		STNWSSLRSAWamide	1293.633	0.670	0.020	Y	0.764	0.059	N	0.601	0.037	Y
	CLH	GLDLGLGRGFSGSQAAKHLMGLAAANFANFAG GPamide	3272.675	1.763	0.169	N				0.607	0.058	N
	CPRP	RSAEGLGRMGRLLASLKSDTVTPLRGFEGETGH PLE	3838.003	1.568	0.046	N	1.465	0.094	N	1.450	0.052	N
		SLKSDTVTPLLG	1230.694	0.419	0.043	Y	0.674	0.076	N	0.325	0.046	Y
	Orcokinin	DFDEIDRSGFA	1271.554	0.786	0.106	N	1.206	0.079	N	0.367	0.054	N
		DFDEIDRSGFGFA	1475.644	0.339	0.059	Y	0.801	0.043	N	0.614	0.056	N
		DFDEIDRSGFGFV	1503.675	1.021	0.030	N	1.445	0.177	N	0.791	0.093	N
		DFDEIDRSSFGFA	1505.654				0.689	0.048	N	0.975	0.048	N
		DFDEIDRSSFGFN	1548.660	0.827	0.237	N	1.622	0.065	N	0.490	0.023	N
		NFDEIDRSGFA	1270.570	0.745	0.038	N	0.963	0.043	N	0.546	0.065	N
		NFDEIDRSGFGFA	1474.660				1.088	0.032	N			
		NFDEIDRSSFGFN	1547.676	0.858	0.108	N	1.158	0.101	N	0.720	0.042	N
		NFDEIDRSGFGFV	1502.691	0.396	0.070	N	1.205	0.052	N	1.163	0.079	N
		NFDEIDRSSFA	1300.580	0.675	0.043	N	0.686	0.042	N	0.389	0.056	Y
	Orcomyotropin	FDAFTTGFGHS	1186.516	0.890	0.079	N	0.854	0.050	N	0.778	0.044	N
	Others	HL/IGSL/IYRamide	844.479	0.831	0.039	N	0.926	0.048	N	1.496	0.078	N
	PDH	NSGMINSILGIPRVMTEAamide	1901.994	0.807	0.044	N	0.703	0.059	N			
		QELKYQEREMVAELAQQIYRVAQAPWAAAVG PHKRNSELINSILGLPKVMNDAamide	5973.138	0.714	0.033	N	0.644	0.023	N	0.590	0.017	Y
		QELHVPEREAVANLAARILKIVHAPHDAAGVPH KRNSELINSLLGISALMNEAamide	5712.103	1.177	0.074	N	1.116	0.062	N	0.851	0.082	N
		QDLKYQEREMVAELAQQIYRVAQAPWAGAVG PHKRNSELINSILGLPKVMNDAamide	5945.107	0.608	0.104	N						
		QREPTASKCQAATELAIQILQAVKGAHTGVAAG PHKRNSELINSLLGLPKFMIDAamide	5792.122	1.725	0.102	N	0.762	0.314	N	0.405	0.037	N
		QEDLKYFEREVVSELAAQILRVAQGPSAFVAGPH KRNSELINSLLGIPKVMNDAamide	5947.165	0.420	0.027	Y	0.475	0.023	Y	0.427	0.032	Y
	RFamide	DARTAPLRLRFamide	1314.775	0.641	0.045	N				0.721	0.063	N
		GAHKNYLRFamide	1104.606							1.381	0.055	N
		GYNRSFLRFamide	1158.617	0.582	0.154	N	0.585	0.032	N	0.922	0.077	N
		GYSKNYLRFamide	1146.605	0.659	0.086	N	0.668	0.062	N	0.762	0.064	N
		QDLDHVFLRFamide	1288.680	0.822	0.055	N				0.675	0.047	N
		DGGRNFLRFamide	1080.570	0.438	0.052	N				0.885	0.076	N
	SIFamide	GYRKPPFNGSIFamide	1381.738	0.703	0.043	N	0.646	0.072	N	0.691	0.049	N
	Tachykinin	APSGFLGMRG	992.498	0.603	0.062	Y				0.717	0.027	N

Table S8. Select neuropeptides that were unquantifiable due to no detection in either the control tissue or the hypoxia-stressed tissue. Only neuropeptides that appeared in over three biological replicates (light color) or 6 biological replicates (dark color) were selected. AST-A: allatostatin A-type; AST-B: allatostatin B-type; PDH: pigment dispersing hormone; CPRP: CHH precursor-related peptide; E: electrospray ionization (ESI); M: matrix-assisted laser desorption/ionization (MALDI).

Tissue	Family	Sequence	*m/z*	E or M?	Control	1 hour	4 hour	8 hour
Brain	AST-A	GPYSFGLamide	739.377	M	X			
	AST-B	AGWSSMRGAWamide	1107.533	E		X	X	X
	PDH	QEDLKYFEREVVSELAAQILRVAQG PSAFVAGPHKRNSELINSLLGIPKVM NDAamide	5947.165	E		X	X	X
	RFamide	AYNRSFLRFamide	1172.632	M				X
	Tachykinin	APSGFLGMRG	992.498	E		X		X
CoG	AST-A	GPYSFGLamide	739.377	M	X			
	AST-B	TGWNKFQGSWamide	1209.580	E		X	X	X
	Tachykinin	SGFLGMRamide	766.403	M		X	X	X
PO	AST-A	AGPYAFGLamide	794.420	M		X		
		EPYEFGLamide	853.409	M	X			
		GPYSFGLamide	739.377	M	X			
		LKAYDFGLamide	925.514	M	X			
		TPHTYSFGLamide	1021.510	E		X	X	X
	AST-B	AGWSSTSRAWamide	1107.533	E			X	X
	RFamide	DPSFLRFamide	853.409	M	X			
		QDNDHVFLRFamide	1272.612	E		X	X	
	RYamide	FYSQRYamide	862.421	M		X	X	
	RYamide	LSSRFVGGSRYamide	1227.659	E		X	X	X
SG	CPRP	RGFEGETGHPN	1200.539	M	X			
	Cryptocyanin	KIFEPLRDKN	1259.711	M		X	X	X
	Orcokinin	DFDEIDRSSFA	1301.564	E		X	X	X
		NFDEIDRSSFGF	1433.633	E		X		X
		NFDEIDRSGFGFA	1474.660	M		X	X	X
		NFDEIDRSSFGFV	1532.702	E		X	X	X
	RFamide	SGRNFLRFamide	995.553	E		X	X	X
		SMPTLRLRFamide	1119.646	E		X		X
		YAIAGRPRFamide	1049.600	E		X	X	X
		HDLVQVFLRFamide/ HPLSFVSALRFamide	1272.721	M		X	X	X
		LAPQRNFLRFamide	1260.732	M		X		
		LAYNRSFLRFamide	1285.716	M		X		X

Chapter 4

Mass Spectrometric Profiling of Neuropeptides in Response to Copper Toxicity via Isobaric Tagging

Adapted from:

Sauer, C.S., Li, L. Mass Spectrometric Profiling of Neuropeptides in Response to Copper Toxicity via Isobaric Tagging. *Chem. Res. Toxicol.* 2021, 34, 1329-1336.

Abstract:

Copper is a necessary nutrient but quickly becomes toxic at elevated levels. To properly handle environmental copper influxes and maintain metal homeostasis, organisms utilize various methods to chelate, excrete, and metabolize heavy metals. These mechanisms are believed to involve complex signaling pathways mediated by neuropeptides. This study incorporates custom N,N-dimethyl leucine isobaric tags to characterize the neuropeptidomic changes after different time points (1, 2, and 4 hours) of copper exposure in a model organism, blue crab, *Callinectes sapidus*. Using a modified simplex optimization strategy, the number of identifiable and quantifiable neuropeptides was increased three-fold to facilitate a deeper understanding of the signaling pathways involved in responding to heavy metal exposure. The time course exposure showed many interesting findings, including upregulation of inhibitory allatostatin peptides in the pericardial organs. Additionally, there was evidence of transport of a pigment dispersing hormone from the sinus glands to the brain. Overall, this study improves the multiplexing capabilities of neuropeptidomic studies to understand the temporal changes associated with copper toxicity.

Keywords: *Callinectes sapidus*, Mass Spectrometry, Copper Toxicity, Neuropeptide, Quantitation, Isobaric Tags

Introduction:

Neuropeptides represent a large, highly diverse class of signaling molecules within the nervous system. These signaling peptides have been shown to play physiological roles in many biochemical processes and can potentially serve as biomarkers for a variety of disease states, such as Alzheimer's disease, cancers,[1] and environmental stress.[2–5] The exact function of a particular neuropeptide is difficult to study due to their function being dependent on location, concentration, and the presence of other co-modulating neurotransmitters or neuropeptides.[6] As a result, thorough approaches to profile all neuropeptides in a sample is critical to characterize neuropeptidomic changes in a meaningful way. Global profiling of neuropeptides is challenging, however, due to their diverse structures and low in vivo concentrations. Mass spectrometry (MS) offers fast, highly sensitive analyses for probing many biomolecules at once, without needing to know the exact make-up of the sample.

Quantitative analysis of neuropeptides has been achieved using several different quantitative strategies. Label-free methods have been reported but suffer from low throughput and instrumental variability (i.e., signal drift).[7] Reductive dimethylation and other isotopic labeling strategies, resulting in a differential mass shift at the MS^1 level, have been used to provide relative expression changes in neuropeptidomic studies.[3] These methods enable multiple samples to be analyzed simultaneously, but they can also result in complex spectra that make data interpretation difficult. This limits the multiplexing potential of MS^1-based labeling strategies. Alternatively, isobaric tags facilitate relative quantitation at the MS^2 level by incorporating isotopically encoded tags

with the same nominal mass addition, but different reporter ions formed upon fragmentation. These tags do not increase spectral complexity, offering higher multiplexing capabilities. Additionally, they require less sample from a single channel. Commercially available isobaric tags, such as iTRAQ[8] and TMT,[9] can be expensive for academic lab settings. Instead, the Li Lab has developed N,N-dimethyl leucine (DiLeu) isobaric tags that label primary amines.[10,11] These tags are readily synthesized and offer up to a 21-plex experiment,[12] enabling a cost-effective experiment with reduced sample needs, required instrument time, and run-to-run variability.

Despite these advantages, the application of isobaric tags in neuropeptidomic analyses has been scarce.[13] The low in vivo abundance of neuropeptides often results in a lack of selection for fragmentation through tandem MS analysis using typical data-dependent acquisition settings. While this is a challenge for neuropeptidomics in general, it is especially problematic when using isobaric tags as quantitation is performed exclusively at the MS^2 level. Optimization of various data acquisition parameters (e.g., resolution, number of MS^2 scans events, and dynamic exclusion window) have been shown to facilitate deeper profiling in -omic studies by reducing redundant analyses and increasing the number of spectra corresponding to low-abundance analytes, as well as reducing scan time to increase the total number of spectra acquired in a single LC-MS run.[14,15] As there are numerous parameters affecting the data-dependent acquisition of spectra, it can be laborious to optimize all of them. This is exacerbated by the fact that many of the parameters are interconnected and need to be optimized simultaneously. Design of experiments (DoE) have been used to

discern and evaluate the influence of specific parameters on peptide identifications.[16–18] A multitude of designs exist, the simplest of which is the factorial DoE.[19] In a factorial DoE a number of factors, x, are evaluated at a number of levels, y, leading to x^y combinations to be tested. As the number of factors and levels increases, the number of tests required for optimization rapidly increases. As a result, factorial DoE are less useful when trying to determine a precise optimum. Advanced modeling and statistical analyses can be used to ascertain optimum conditions, but still require many tests for confident interpretation.

In this work, the MS^1 resolution, MS^2 resolution, dynamic exclusion window, and number of MS^2 scan events were selected for optimization due to their direct effect on instrument scan time, redundant analyses, and analysis of lower abundance analytes. These factors were evaluated at two levels with a simple factorial DoE to provide a rough evaluation of their effect on neuropeptide identifications. The dynamic exclusion window and MS^2 scan events were then systematically optimized using a modified simplex algorithm.[20] Using this approach, a set of conditions (i.e., a simplex) is evaluated. The conditions are then ranked, and the next set of conditions are in the geometrically opposed region from the point of worst performance. This simplex algorithm has been modified to include not only the geometric reflection, but also a contracted reflection, elongated reflection, and a reflection contracted in the direction of the low performance points. This modification allows the optimum (determined when additional simplexes provide no improvement) to be reached faster and with fewer points tested overall. Because the resolving power of the orbitrap instrument used in

this experiment is fixed at preset values, optimization is constrained and incompatible with the geometric reflections used in the simplex method. Using this modified simplex optimization strategy for the dynamic exclusion window and number of MS^2 scan events resulted in a three-fold increase in the number of neuropeptides identified from the crustacean model organism, *Callinectes sapidus*. This performance improvement could further benefit from optimization of additional parameters (e.g., automatic gain control target, maximum injection time, and isolation window width) and is the subject of ongoing research.

These optimized parameters can be used to study neuropeptidomic changes under various experimental conditions. Herein, we use DiLeu isobaric tags to examine neuropeptide expression after exposure to environmental copper. Concerns over copper in the environment are growing due to increased prevalence of copper in agricultural runoff, industrial pollution, and poorly managed wastewater.[21] Moreover, as atmospheric carbon dioxide increases, causing ocean acidification, copper becomes more bioavailable and therefore more toxic.[22] Interestingly, although toxic at high levels, copper is also a necessary nutrient and plays roles in neuromodulation, protein structure, and enzymatic activity.[23] This dichotomy of being a potent toxin and required nutrient suggests that interesting pathways are involved in handling large effluxes of copper in the environment. In this study, the blue crab is used as a model organism due to its relatively simple nervous system and relevance as it frequently inhabits coastal estuaries plagued by large copper effluxes. To better understand how copper affects neuropeptide expression, a 4-plex experiment was performed using DiLeu tags

to characterize expression changes after 1, 2, and 4 hours of exposure to 10 μM copper (Cu^{2+}) relative to a control. Statistically significant changes were observed at all time points in four neuroendocrine tissues (brain, sinus glands, pericardial organs, and thoracic ganglia), demonstrating the feasibility and usefulness of DiLeu multiplex tags for quantifying endogenous expression of neuropeptides.

Methods:

Materials:

Methanol (MeOH), acetonitrile (ACN), glacial acetic acid, crab saline components (described below) and LC-MS solvents were purchased from Fisher Scientific (Pittsburgh, PA). Isotopic leucines and formaldehyde, triethylammonium bicarbonate (TEAB), N,N-dimethylformamide (DMF), 4-(4,6-dimethoxy- 1,3,5-triazin-2-yl)-4-methylmorpholinium tetrafluoroborate (DMTMM), ammonium formate, and copper (II) chloride were purchased from Sigma Aldrich (St. Louis, MO). N-methylmorpholine (NMM) was purchased from TCI America, (Tokyo, Japan). C18 ZipTips were purchased from Millipore (Burlington, MA). Strong cation exchange (SCX) spin tips were purchased from PolyLC (Columbia, MD).

Animals and Copper Exposure Experiment:

Female blue crabs, *Callinectes sapidus*, were purchased from a local grocery store (Midway Asian Markets, Madison, WI) and maintained in tanks with recirculating

artificial seawater (30 ppt salinity) and a 12 h:12 h light:dark cycle. Crabs exposed to copper were placed in a tank of 10 μM Cu^{2+} (from $CuCl_2$) for 0 (control), 1, 2, or 4 h prior to sacrifice. All crabs, regardless of experimental conditions, were anesthetized on ice for 20 min before sacrificing for its organs as previously described.[24] Neuropeptide-rich tissues–brains, paired sinus glands (SG), paired pericardial organs (PO), and thoracic ganglia (TG)–were dissected in chilled saline (440 mM NaCl, 11 mM KCl, 13 mM $CaCl_2$, 26 mM $MgCl_2$, 11 mM trizma base, 5 mM maleic acid, adjusted to pH 7.45 with NaOH) and stored in acidified methanol (90:9:1 MeOH:H_2O:glacial acetic acid). Tissues were stored at -80 °C until future processing.

Neuropeptide Extraction:

Neuropeptides were extracted via ultrasonication using a Fisherbrand 120 probe sonicator/sonic dismembrator. Tissues submerged in acidified methanol were sonicated at 50% amplitude for 8 s three times with 15 s rest between pulses. Samples were then centrifuged at 20,000 x *g* for 20 min at 4°C before collecting the supernatant. The supernatant was then dried down using a Savant SCV100 SpeedVac. Crude extracts were then purified using C18 ZipTips per the manufacturer's protocol.

Labeling:

For the optimization experiments, neuropeptide extracts from several tissues were pooled together to create enough sample for multiple LC-MS injections. Four equal aliquots of this sample were then differentially labeled using DiLeu tags. For the copper

toxicity experiments, extracts were differentially labeled by exposure duration (control, 1 h, 2 h, and 4 h). Each bioreplicate for the copper toxicity experiments had one crab at each time point with four crabs total for each multiplexed sample. A total of four biological replicates (n=4) were analyzed with three technical replicates (repeated LC-MS injections). The labeling procedure has been described previously along with the synthesis of the tags.[11] Briefly, purified neuropeptide extracts were resuspended in a 50:50 mixture of ACN:0.5 M triethylammonium bicarbonate. The isotopic dimethyl leucine tags were activated to a triazine ester form by the addition of 50 µL activation solution (15.5 mg DMTMM, 495 µL dry DMF, 5 µL NMM) per 1 mg dimethyl leucine. After being vortexed at room temperature for 30 min, the activated tag was added to the neuropeptide extracts at a 20:1 label-to-peptide ratio. The labeling reaction was quenched after 30 min by the addition of NH_2OH for a final concentration of 0.25% NH_2OH. The labeled neuropeptide extracts were then pooled together before drying down. Excess labeling reagents were removed using SCX spin tips. Multiplexed samples were loaded to the columns in 0.1% formic acid, 20% ACN, 80% water and excess label was washed away using the same buffer. The sample was eluted using 0.4 M ammonium formate, 20% ACN, 80% water. Multiplexed samples were then desalted once again using C18 ZipTips before being analyzed by LC-MS.

MS Data Collection:

Samples were analyzed in triplicate on a Thermo Q Exactive HF mass spectrometer coupled to a Dionex UltiMate3000 nanoLC system using a homemade C18 column (15

cm). Neuropeptides were eluted over a 90 min gradient from 10% B to 35% B (solvent A = 0.1% formic acid in water; solvent B = 0.1% formic acid in ACN). Spectra were collected at a m/z range of 200-2000 using HCD (high-energy collision dissociation) for fragmentation. The MS^1 resolution, MS^2 resolution, dynamic exclusion window, and number of MS^2 scan events varied from run-to-run and are detailed below. More detailed information about the instrument parameters can be found in **Table S1**.

Data Analysis:

Raw files were processed using Proteome Discoverer 2.1 to identify neuropeptides from an in-house crustacean neuropeptide database. Static modifications included DiLeu labeling at the N-terminus and lysine residues, along with C-terminal amidation of known amidated neuropeptides (*e.g.,* RFamide and RYamide peptides). Dynamic modifications included oxidation of Met, deamidation of Asn and Gln, methylation of Asp, Glu, His, Lys, Arg, Ser, and Thr, and dehydration of Ala, Asp, Glu, Ser, Thr, Tyr residues. Quantitation and normalization of reporter ions was also performed in Proteome Discoverer 2.1 and exported to Excel. Additional information for the data analysis is provided in **Table S2**. Neuropeptides described below as "identified" were present in at least two of three technical replicates, identified and quantified across all four channels, and for the copper toxicity experiments, present in at least three bioreplicates. The quantitative ratios were then tested using Dunnett's test[25,26] to determine statistical significance between experimental conditions and the control.

Results and Discussion:

Factorial Design of Experiments

An initial factorial DoE was performed to roughly evaluate the influence of the MS^1 and MS^2 resolution, dynamic exclusion window, and number of MS^2 scan events. These factors were selected as they have a direct influence on the scan time, the total number of acquired spectra, and the ability to reduce redundant analyses. This DoE assessed combinations of high and low values for each of the four parameters for a total of 16 unique sets of conditions. The combinatorial testing parameters and results are given in **Figure 1**. Overall, more identifications were achieved with reduced MS^1 and MS^2 resolution and an increased number of MS^2 scans events. As the resolution (both MS^1 and MS^2) is decreased, the scan time with an orbitrap mass analyzer also decreases, allowing more spectra to be acquired. This in turn enables more MS^2 scans per precursor scan to be collected to identify and quantify more unique neuropeptides. Analysis of the isolation interference between the experiments in which the resolving power was high compared to low showed the lower resolution not only resulted in more total peptide spectral matches (PSMs), but also that more of those PSMs were high enough quality for identification and quantitation of neuropeptides. More details can be found in the Supplemental Information (**Figure S1**). This observance could be attributed to the fact that there are simply more spectra to have peptides matched to, and that the spectral purity is more so affected by isolation window width, not resolution. The influence of the dynamic exclusion window was more variable, highlighting the need for a more systematic approach to optimization. As the dynamic

exclusion window widens, neuropeptides with high signal are less likely to dominate the acquired MS^2 spectra. If the window is too wide, however, there is risk of losing identifications due to collecting MS^2 spectra too early in the elution profile (where signal is often too low for meaningful results) and prohibiting future analyses across the peak width. It is also important to note that peptides have variable peak widths, so a reliable dynamic exclusion window cannot be easily predicted.

Modified Simplex Optimization

Many parameters show some degree of interplay and optimization needs to consider this. For example, the number of MS^2 scan events affects the optimum dynamic exclusion window (and vice versa), compounding the challenges with efficiently optimizing these parameters. An approach that optimizes these parameters simultaneously is therefore required and can be accomplished via a modified simplex strategy. A comprehensive overview of the simplex optimization strategy has been published by Bezerra, M.A., et al.[20] Initially, three sets of conditions (vertices of the graphical representation in **Figure 2**) were examined (V_1, V_2, and V_3). The second simplex was geometrically reflected away from V_2 (the worst performing condition) and additional points (e.g., R_1, CR_1, etc.) were evaluated. After four iterations, optimum parameters were reached, demonstrated by the fifth simplex showing no improvement over previous simplexes. In total 17 conditions were evaluated. Some conditions were omitted from later simplexes if there was already a set of conditions at or very close to that point. **Figure 2** shows the results from these 17 conditions with the relative

number of neuropeptides identified as a heat map overlaid on the simplex optimization plot. The table in **Figure 2** shows the neuropeptides identified for each vertex of the simplex optimization. A more sequential view of the data in **Figure 2** is shown in **Figure S2**. The conditions near the optimum region (shown in red) offer over a three-fold increase in the number of neuropeptides able to be identified, compared to the initial, unoptimized conditions (Simplex 1 from **Figure 2**). Although this performance increase is great, it could be further improved in the future by more systematically optimizing the resolving power and other MS parameters.

As data-dependent acquisition is known to have limited reproducibility, three conditions (R2, CR3, and CW4) were tested again to determine the ideal parameters to use for later analyses. Vertices R2, CR3, and CW4 were selected based on neuropeptides identified and proximity to the optimum region shown in **Figure 2**. A separate neuropeptide-rich sample was then analyzed by the three conditions with five technical replicates each. There were 59, 60, and 51 neuropeptides identified across all 4 channels in at least 2 technical replicates for R2, CR3, and CW4, respectively. Condition CR3 was selected for future analyses due to its greater number of neuropeptide identifications and higher reproducibility among technical replicates. It should be noted that R2 would likely be sufficient for most analyses, but CR3 had a slight advantage. The optimum dynamic exclusion window of 35 s appears to match with the chromatographic peak widths for neuropeptides. For the C18 RPLC separations used in this experiment, it was observed that most neuropeptides elute over 30-60 s, but some

elute in as little as 15 s and some over 90 s. The dynamic exclusion window seems skewed towards the low range of peak widths, but this could be due to some neuropeptides having similar masses and retention times. A lower dynamic exclusion might enable more of these similar neuropeptides to be differentiated at the MS^2 level. The simplex data also showed that higher MS2 scan events facilitated deeper profiling. This is rather intuitive as it allows more low abundance ions to be selected for tandem MS, but 39 MS^2 scan events is surprisingly higher than typical LC-MS experiments (often using a Top 5, Top 10, or Top 15 method).

The optimized methods also showed high quantitative accuracy of reporter ion ratios. The differentially labeled samples used for optimization were pooled at a 1:1:1:1 ratio (DiLeu reporter ions 115:116:117:118) and the observed ratio (averaged for all identified neuropeptides) was 1:0.94:0.93:0.89, demonstrating suitable quantitative accuracy. The distribution of neuropeptides by family for the neuropeptides identified under the optimum conditions are shown in **Figure 3**. The diversity of neuropeptide families demonstrate that the methods are not biased towards a particular sequence motif. The quantitative accuracy and lack of bias will enable the methods to be used to collect meaningful neuropeptidomic data to study crustaceans under environmental stress.

Copper Toxicity

Using a DiLeu labeling strategy and the optimized acquisition settings, CR3 (low MS1 and MS2 resolving power, 39 MS2 scan events, and a 35 s dynamic exclusion window),

this study demonstrates the feasibility of using isobaric tagging to study neuropeptidomic changes in response to acute copper toxicity. Neuropeptides have been shown to be involved in the stress response to many environmental stressors, such as salinity,[4] pH,[5] and hypoxia.[3] Heavy metals can also act as potent environmental stressors by causing oxidative stress and dysregulating metal homeostasis within an organism. Copper is of particular interest as it is an important component of many proteins, such as hemocyanin (analogous to hemoglobin in humans),[27,28] and dysregulation of copper homeostasis has been implicated in several diseases, including Alzheimer's disease, anemia, and liver disease.[23,29]

In this experiment, crabs were exposed to 10 μM copper ($CuCl_2$) for 0 (control), 1, 2, and 4 hr. The extracted neuropeptides were differentially labeled with 4-plex DiLeu tags to provide relative quantitation of neuropeptides compared to a control sample. **Figures 4 and 5** depict the significant neuropeptide expression changes in the TG and POs (**Figure 4**) and SGs and brain (**Figure 5**) as a ratio to the control after each exposure duration. These ratios are expressed as a log_2 ratio for easier viewing (positive results show upregulation, negative show downregulation). Statistical significance was determined using Dunnett's test (n = 4) and is denoted by a star in the bar graphs. More precise relative quantitative information for the neuropeptides shown in **Figures 4 and 5** are given in **Tables S3 and S4** along with the neuropeptides that did not show significant changes.

There are interesting dysregulation patterns in neuropeptides with significant changes observed resulting from copper toxicity. Within the POs, which act upon the cardiac system, upregulation of many allatostatin A-type and B-type (AST-A and AST-B, respectively) was observed. AST-A have been well-documented as being inhibitory neuromodulators that slow down a number of processes, including feeding/digestion and cardiac contractions.[30,31] The initial burst in AST-A output seen after 1 hour in the POs suggests a hyperarousal signal to decrease cardiac output. Similarly, B-type allatostatin neuropeptides have been shown to act as myoinhibitors.[31,32] There is a significant upregulation of AST-B neuropeptides after 2 hr exposure, suggesting the activation of signaling pathways to decrease muscle contractions in the cardiac system. These neuropeptides could also be secreted into the hemolymph (circulating fluid in crustaceans) to act as hormones (rather than locally in the cardiac system). Future experiments to analyze allatostatin neuropeptides in the hemolymph could demonstrate interesting hormonal signaling pathways but are not included in this study due to the challenges of analyzing trace-level neuropeptides in the complex matrix of hemolymph. Although similar in modulation behaviors, the AST-A and AST-B type families have unique structures and signaling pathways.[30] The temporal shift in upregulation between these families further supports that distinct pathways are involved in their regulation.

In the brain and SGs, there is an interesting pigment dispersing hormone (PDH) with sequence QELKYQEREMVAELAQQIYRVAQAPWAAAVGPHKRNSELINSILGLPKVMNDAamide that is significantly downregulated in the SGs and upregulated in the brain. This

sequence is highlighted in blue shade in **Figure 5**. As PDH is synthesized in the SGs,[31] this pattern is likely indicative of hormonal signaling from the SGs to the brain. Historically, pigment dispersing hormones were shown to primarily regulate the light-adapting pigments in the eyestalks and were named accordingly.[33,34] Though typically seen as a result of light-receptor activity, the PDH activity reported here is not believed to be the result of circadian rhythm. Exposures and dissections were not carried out at set times during the day and as a result, are independent of biological changes due to circadian rhythm. Moreover, the exact same neuropeptide has previously been shown by our lab to display the same temporal dysregulation in response to hypoxia (low levels of dissolved oxygen).[3] The expression changes of this PDH could therefore be indicative of a general stress response, or perhaps more specifically related to respiratory distress as copper can also impair gill function by disrupting ion channels.[27] The insect ortholog for PDH, known as pigment dispersing factor (PDF),[35] has been shown to play roles in many processes outside of circadian rhythm, including locomotor activity, courtship, and hormone biosynthesis.[31] The findings here support the growing evidence for PDH also acting as a neurotransmitter and neuromodulator in the nervous system and having diverse functional behavior.

There were also interesting general trends observed across the four tissue types. In the TG, there is significant upregulation of two orcokinin neuropeptides (NFDEIDRSGFA and NFDEIDRSSFA), but only after 4 hours of exposure. Conversely, a third orcokinin, NFDEIDRSGFGFA, shows upregulation after only 1 hour of exposure. The differences in

dysregulation of neuropeptides within the same family is seen in other tissue types as well (e.g., RFamide neuropeptides in the brain) and highlight the fact that even though they are structurally very similar, neuropeptides of the same family can have different functions, target receptors, degradation pathways, etc. Additionally, while some neuropeptides, like the RYamides in the pericardial organs, show a consistent pattern of up/downregulation over 4 hours, many others show a hyperarousal pattern. In these cases, the neuropeptide is increased or decreased at one time point and returns to baseline. These findings demonstrate the efficacy of multiplexed analyses as the increased throughput and reduced sample needs enables time course studies. Transient shifts in neuropeptide expression that would have gone unnoticed previously are now able to be observed with minimal added effort and cost.

Conclusions and Future Directions:

Quantitative neuropeptidomics can provide many insights into the complex signaling pathways involved in the response to environmental stress like heavy metal toxicity. The deployment of a custom isobaric tag, DiLeu, and systematic optimization of data-dependent acquisition settings has enabled thorough, multiplexed analyses of neuropeptides. In this study, four parameters were examined with two selected for extensive optimization. Omission of MS^1 and MS^2 resolving power from further optimization reduced experimentation needs but is nonetheless a limitation of this study. Similarly, other optimizable parameters related to MS data acquisition have been shown to improve analyses and are the subject of future work within our lab. Despite

these limitations in optimization, a three-fold increase in quantifiable neuropeptides was still observed. The optimized parameters were used to study neuropeptides in response to acute copper toxicity. Several statistically significant trends were observed in key neuroendocrine tissues across different exposure durations. These findings represent the critical first steps in understanding the physiological effects of copper toxicity and the signaling pathways that may be involved in an organism surviving polluted ecosystems. Future work to characterize the neuropeptides in the hemolymph would offer more robust interpretation of the hormonal/paracrine signaling involved. Additionally, by incorporating isobaric tags with mDa mass differences resulting from mass defects, the Li Lab has expanded the DiLeu tagging protocol up to a 21-plex.[12] Using these tags in the future will allow more experimental conditions (e.g., different exposure durations or severities of exposure) to be evaluated, facilitating a more in-depth understanding of copper toxicity in aquatic environments.

Acknowledgements:

This work was supported by a National Science Foundation grant (CHE-1710140) and National Institutes of Health grants (R01DK071801, S10RR029531). The instruments used in this project were generously provided by Thermo Fisher Scientific. C.S.S. acknowledges the help and support of the Biotechnology Training Program (T32GM008349) under the National Institutes of General Medical Sciences as well as a National Institute of Environmental Health Sciences fellowship as part of the National Ruth L. Kirschstein Research Service Award fellowship program (F31ES031859)). L.L.

acknowledges a Vilas Distinguished Achievement Professorship and Charles Melbourne Johnson Distinguished Chair Professorship with funding provided by the Wisconsin Alumni Research Foundation and University of Wisconsin–Madison School of Pharmacy.

Supporting Information:

The Supporting Information is available free of charge at https://pubs.acs.org/

Supporting Tables S1-S4 and Supporting Figure S1 and S2 (.docx)

Table S1: LC-MS instrument settings

Table S2: Proteome Discoverer data analysis settings

Table S3: All neuropeptides identified in the thoracic ganglia (TG) and pericardial organs (PO)

Table S4: All neuropeptides identified in the sinus glands (SG) and brain

Figure S1: Comparison of isolation interference between high and low resolving powers

Figure S2: Sequential results from simplex algorithm

References:

(1) Sweedler, Jonathan V.,Xie, Fang, Bora, A. *Protein and Peptide Mass Spectrometry in Drug Discovery.* Chapter 1.4. **2012**, 221–227.

(2) Chen, R.; Xiao, M.; Buchberger, A.; Li, L. Quantitative Neuropeptidomics Study of the Effects of Temperature Change in the Crab *Cancer borealis*. *J. Proteome Res.* **2014**, *13* (12), 5767–5776.

(3) Buchberger, A. R.; Sauer, C. S.; Vu, N. Q.; DeLaney, K.; Li, L. A Temporal Study of the Perturbation of Crustacean Neuropeptides Due to Severe Hypoxia Using 4-Plex Reductive Dimethylation. *J. Proteome Res. 2020, 19, 4, 1548-1555*

(4) Zhang, Y.; Buchberger, A.; Muthuvel, G.; Li, L. Expression and Distribution of Neuropeptides in the Nervous System of the Crab *Carcinus maenas* and Their Roles in Environmental Stress. *Proteomics* **2015**, *15* (23–24), 3969–3979.

(5) Liu, Y.; Buchberger, A. R.; Delaney, K.; Li, Z.; Li, L. Multifaceted Mass Spectrometric Investigation of Neuropeptide Changes in Atlantic Blue Crab, *Callinectes sapidus*, in Response to Low PH Stress. *J. Proteome Res.* **2019**, *18*, 2759–2770.

(6) Li, L.; Sweedler, J. V. Peptides in the Brain: Mass Spectrometry–Based Measurement Approaches and Challenges. *Annu. Rev. Anal. Chem.* **2008**, *1* (1), 451–483.

(7) Romanova, E. V; Dowd, S. E.; Sweedler, J. V. Quantitation of Endogenous Peptides Using Mass Spectrometry Based Methods. *Curr Opin Chem Biol* **2013**, *17* (5), 801–808.

(8) Wiese, S.; Reidegeld, K. A.; Meyer, H. E.; Warscheid, B. Protein Labeling by ITRAQ: A New Tool for Quantitative Mass Spectrometry in Proteome Research. *Proteomics* **2007**, *7* (3), 340–350.

(9) Werner, T.; Becher, I.; Sweetman, G.; Doce, C.; Savitski, M. M.; Bantscheff, M. High-Resolution Enabled TMT 8-Plexing. *Anal. Chem.* **2012**, *84* (16), 7188–7194.

(10) Xiang, F.; Ye, H.; Chen, R.; Fu, Q.; Li, N. N,N-Dimethyl Leucines as Novel Isobaric Tandem Mass Tags for Quantitative Proteomics and Peptidomics. *Anal. Chem.* **2010**, *82* (7), 2817–2825.

(11) Frost, D. C.; Greer, T.; Li, L. High-Resolution Enabled 12-Plex DiLeu Isobaric Tags for Quantitative Proteomics. *Anal. Chem.* **2015**, *87* (3), 1646–1654.

(12) Frost, D. C.; Feng, Y.; Li, L. 21-Plex DiLeu Isobaric Tags for High-Throughput Quantitative Proteomics. *Anal. Chem.* **2020**, *92* (12), 8228–8234.

(13) Jiang, X.; Xiang, F.; Jia, C.; Buchberger, A. R.; Li, L. Relative Quantitation of Neuropeptides at Multiple Developmental Stages of the American Lobster Using *N*, *N*-Dimethyl Leucine Isobaric Tandem Mass Tags. *ACS Chem. Neurosci.* **2018**, acschemneuro.7b00521.

(14) Zhang, Y.; Wen, Z.; Washburn, M. P.; Florens, L. Effect of Dynamic Exclusion Duration on Spectral Count Based Quantitative Proteomics. *Anal. Chem.* **2009**, *81* (15), 6317–6326.

(15) Kalli, A.; Smith, G. T.; Sweredoski, M. J.; Hess, S. Evaluation and Optimization of Mass Spectrometric Settings during Data-Dependent Acquisition Mode: Focus on LTQ-Orbitrap Mass Analyzers. *J Proteome Res* **2014**, *12* (7), 3071–3086.

(16) Randall, S. M.; Cardasis, H. L.; Muddiman, D. C. Factorial Experimental Designs Elucidate Significant Variables Affecting Data Acquisition on a Quadrupole Orbitrap Mass Spectrometer. *J. Am. Soc. Mass Spectrom.* **2013**, *24* (10), 1501–1512.

(17) Andrews, G. L.; Dean, R. A.; Hawkridge, A. M.; Muddiman, D. C. Improving Proteome Coverage on a LTQ-Orbitrap Using Design of Experiments. *J. Am. Soc. Mass Spectrom.* **2011**, *22* (4), 773–783.

(18) Hecht, E. S.; McCord, J. P.; Muddiman, D. C. Definitive Screening Design Optimization of Mass Spectrometry Parameters for Sensitive Comparison of Filter and Solid Phase Extraction Purified, INLIGHT Plasma N-Glycans. *Anal. Chem.* **2015**, *87* (14), 7305–7312.

(19) Lundstedt, T.; Seifert, E.; Abramo, L.; Thelin, B.; Nyström, Å.; Pettersen, J.; Bergman, R. Experimental Design and Optimization. *Chemom. Intell. Lab. Syst.* **1998**, *42* (1–2), 3–40.

(20) Bezerra, M. A.; dos Santos, Q. O.; Santos, A. G.; Novaes, C. G.; Ferreira, S. L. C.; de Souza, V. S. Simplex Optimization: A Tutorial Approach and Recent Applications in Analytical Chemistry. *Microchem. J.* **2016**, *124*, 45–54.

(21) Keller, A. A.; Adeleye, A. S.; Conway, J. R.; Garner, K. L.; Zhao, L.; Cherr, G. N.; Hong, J.; Gardea-Torresdey, J. L.; Godwin, H. A.; Hanna, S.; et al. Comparative Environmental Fate and Toxicity of Copper Nanomaterials. *NanoImpact* **2017**, *7* (May), 28–40.

(22) Dietrich, A. M.; Postlethwait, N.; Gallagher, D. L. Quantifying Bioavailability and Toxicity of Copper to Americamysis Bahia - Mysid Shrimp. *Int. J. Environ. Sci. Dev.* **2013**, *4* (1), 37–43.

(23) Kardos, J.; Héja, L.; Simon, Á.; Jablonkai, I.; Kovács, R.; Jemnitz, K. Copper Signalling : Causes and Consequences. **2018**, *3*, 1–22.

(24) Gutierrez, G. J.; Grashow, R. G. Cancer Borealis Stomatogastric Nervous System Dissection. *J. Vis. Exp.* **2009**, No. 25, 1–5.

(25) McHugh, M. L. Multiple Comparison Analysis Testing in ANOVA. *Biochem. Medica* **2011**, *21* (2), 203–209.

(26) Jaki, T.; Hothorn, L. A. Statistical Evaluation of Toxicological Assays: Dunnett or Williams Test - Take Both. *Arch. Toxicol.* **2013**, *87* (11), 1901–1910.

(27) Martins, C. D. M. G.; Barcarolli, I. F.; de Menezes, E. J.; Giacomin, M. M.; Wood, C. M.; Bianchini, A. Acute Toxicity, Accumulation and Tissue Distribution of Copper in the Blue Crab Callinectes Sapidus Acclimated to Different Salinities: In Vivo and in Vitro Studies. *Aquat. Toxicol.* **2011**, *101* (1), 88–99.

(28) Paganini, C. L.; Bianchini, A. Copper Accumulation and Toxicity in Isolated Cells from Gills and Hepatopancreas of the Blue Crab (*Callinectes sapidus*). *Environ. Toxicol. Chem.* **2009**, *28* (6), 1200–1205.

(29) Rossbach, L. M.; Shaw, B. J.; Piegza, D.; Vevers, W. F.; Atfield, A. J.; Handy, R. D. Sub-Lethal Effects of Waterborne Exposure to Copper Nanoparticles Compared to Copper Sulphate on the Shore Crab (*Carcinus maenas*). *Aquat. Toxicol.* **2017**, *191* (April), 245–255.

(30) Christie, A. E.; Stemmler, E. A.; Dickinson, P. S. Crustacean Neuropeptides. *Cell. Mol. Life Sci.* **2010**, *67* (24), 4135–4169.

(31) Takei, Y.; Ando, H.; Tsutsui, K. *Handbook of Hormones*; 2015.

(32) Szabo, T. M.; Chen, R.; Goeritz, M. L.; Maloney, R. T.; Tang, L. S.; Li, L.; Marder, E. Distribution and Physiological Effects of B-Type Allatostatins (Myoinhibitory Peptides,

MIPs) in the Stomatogastric Nervous System of the Crab, *Cancer borealis*. *J. Comp. Neurol.* **2011**, *519* (13), 2658–2676.

(33) Klein, J. M.; Mohrherr, C. J.; Sleutels, F.; Riehm, J. P.; Ranga Rao, K. Molecular Cloning of Two Pigment-Dispersing Hormone (PDH) Precursors in the Blue Crab *Callinectes sapidus* Reveals a Novel Member of the PDH Neuropeptide Family. *Biochem. Biophys. Res. Commun.* **1994**, *205* (1), 410–416.

(34) Sousa, G. L.; Lenz, P. H.; Hartline, D. K.; Christie, A. E. General and Comparative Endocrinology Distribution of Pigment Dispersing Hormone- and Tachykinin-Related Peptides in the Central Nervous System of the Copepod Crustacean *Calanus finmarchicus*. **2008**, *156*, 454–459.

(35) Nässel, D. R.; Winther, Å. M. E. Drosophila Neuropeptides in Regulation of Physiology and Behavior. *Prog. Neurobiol.* **2010**, *92* (1), 42–104.

Figures

Table of Content (TOC) Entry

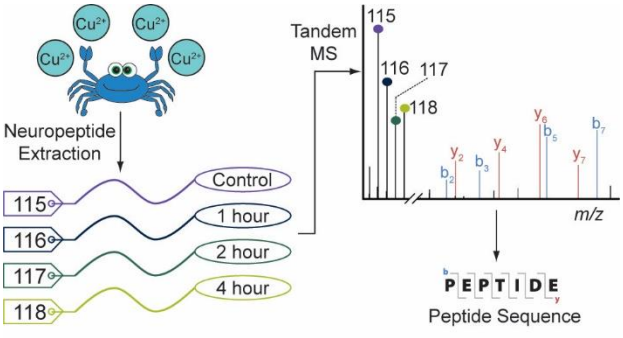

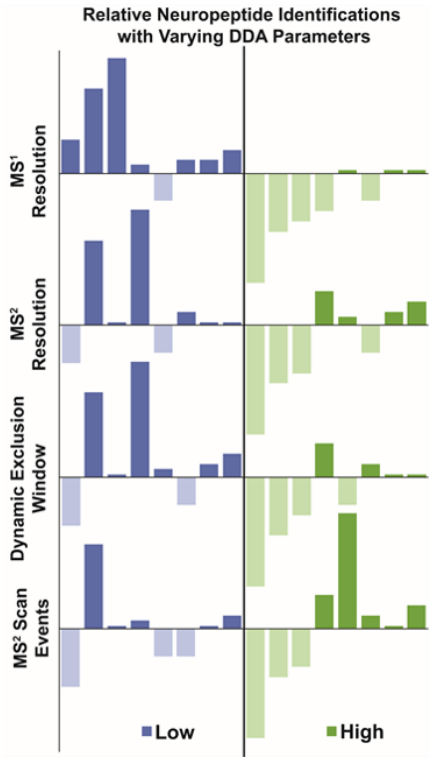

MS¹ Resolution	MS² Resolution	Dynamic Exclusion	MS² Scan Events	Total IDs	Relative IDs
240k	240k	180 s	25	18	-10.7
240k	240k	180 s	5	23	-5.7
240k	240k	15 s	25	24	-4.7
240k	15k	180 s	25	25	-3.7
15k	240k	180 s	25	32	3.3
15k	15k	15 s	5	37	8.3
240k	15k	15 s	5	29	0.3
15k	15k	15 s	25	40	11.3
15k	240k	15 s	5	30	1.3
15k	15k	180 s	5	26	-2.7
240k	240k	15 s	5	26	-2.7
15k	15k	180 s	25	30	1.3
240k	15k	180 s	5	29	0.3
240k	15k	15 s	25	29	0.3
15k	240k	180 s	5	30	1.3
15k	240k	15 s	25	31	2.3

Figure 1: Results from factorial DoE. The data is shown as bar graphs on the left with each of the y-axes representing the deviation from the average number of neuropeptides identified across all 16 conditions. The 16 conditions are represented in each plot; the different plots are merely arranged by low/high (blue/green) values for the selected parameter to more quickly visualize how the number of neuropeptides identified changes when a selected parameter is low/high, regardless of the other parameters. The numeric values are provided in the table shown at right. The Total IDs column represents the total neuropeptides identified and the Relative IDs are the deviations from the average across the 16 conditions.

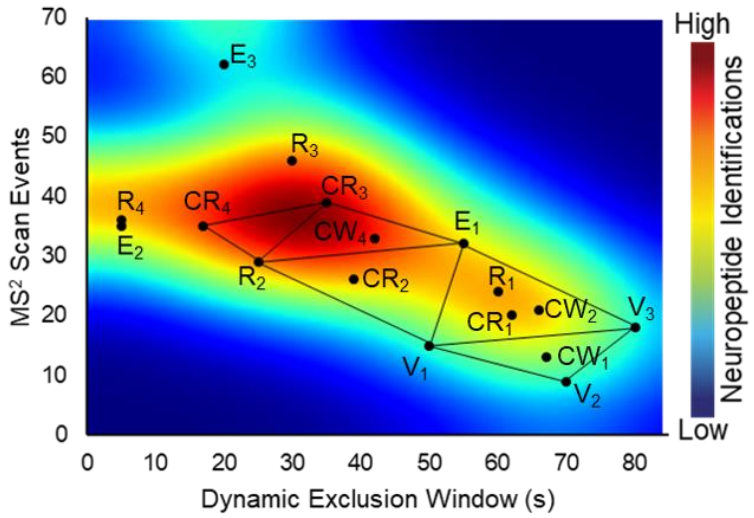

Simplex	Vertex	Dynamic Exclusion Window (s)	MS^2 Scan Events	Neuropeptides Identified
1	V1	50	15	29
	V2	70	9	25
	V3	80	18	27
2	R1	60	24	29
	E1	55	32	41
	CR1	62	20	35
	CW1	67	13	24
3	R2	25	29	88
	E2	5	35	81
	CR2	39	26	63
	CW2	66	21	54
4	R3	30	46	54
	E3	20	62	53
	CR3	35	39	72
5	R4	5	36	64
	CR4	42	33	55
	CW4	17	35	66

Figure 2: Modified simplex optimization. The optimization of the dynamic exclusion window and number of MS^2 scan events is represented graphically with an overlaid heatmap to depict the relative number of identified neuropeptides under each condition. The initial vertices are denoted by V_1, V_2, and V_3; the subsequent simplexes contain points reflected away from the point of worst performance (R), an elongated reflection (E), a contracted reflection (CR), and the contracted reflection closer to the direction of the worst point (CW).

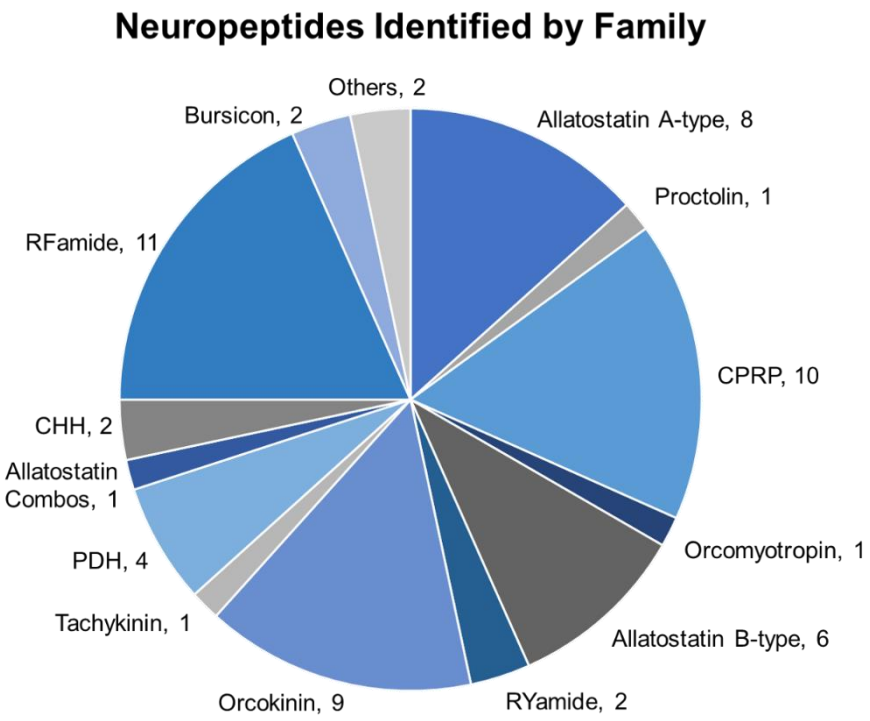

Figure 3: Neuropeptide family distribution. The pie chart shows the distribution of neuropeptides belonging to select families. CHH = crustacean hyperglycemic hormone, CPRP = CHH precursor related peptide, PDH = pigment dispersing hormone.

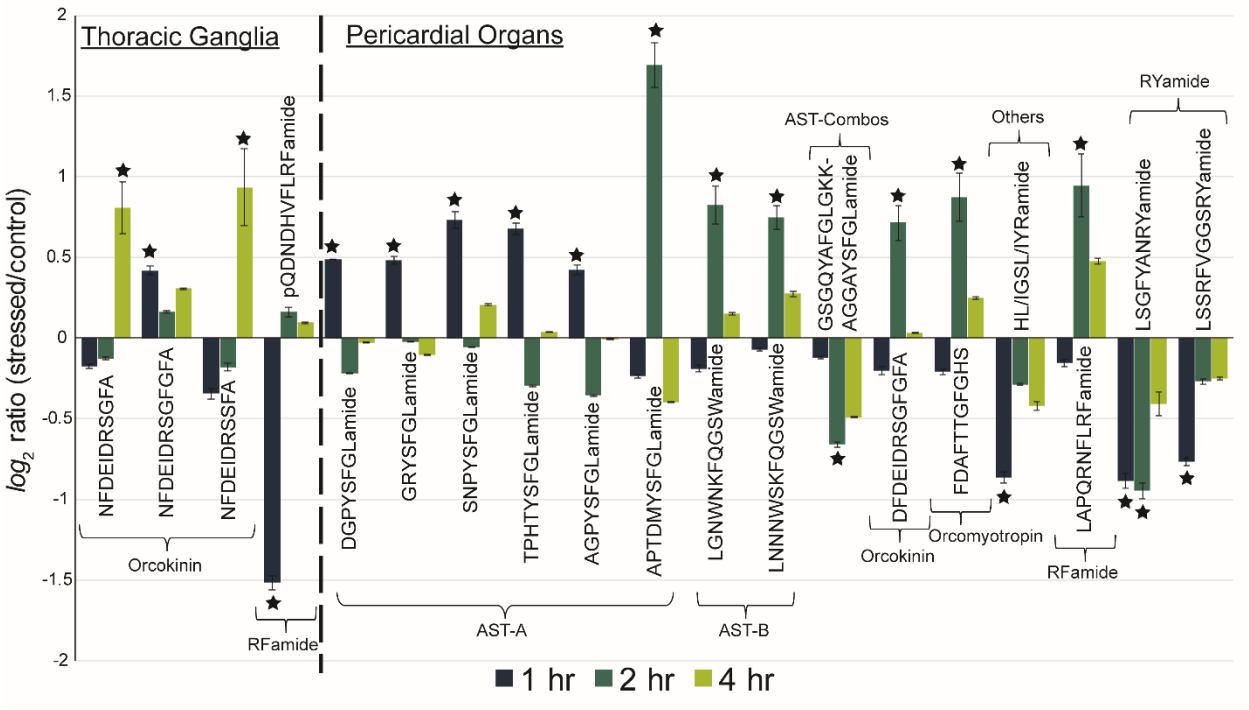

Figure 4: Neuropeptidomic changes in the thoracic ganglia and pericardial organs. Neuropeptide sequences with at least one significant (denoted by star) change are listed across the x-axis and grouped by family. AST-A = allatostatin A-type, AST-B = allatostatin B-type, and AST-Combos = allatostatin combos. The ratio for the intensity of reporter ions for a stress condition (1, 2, or 4 hr copper exposure) relative to the control are depicted on the y-axis as a log_2 ratio to clearly see up/downregulation of neuropeptides relative to the x-axis. The error bars denote the standard error of the mean (n=4).

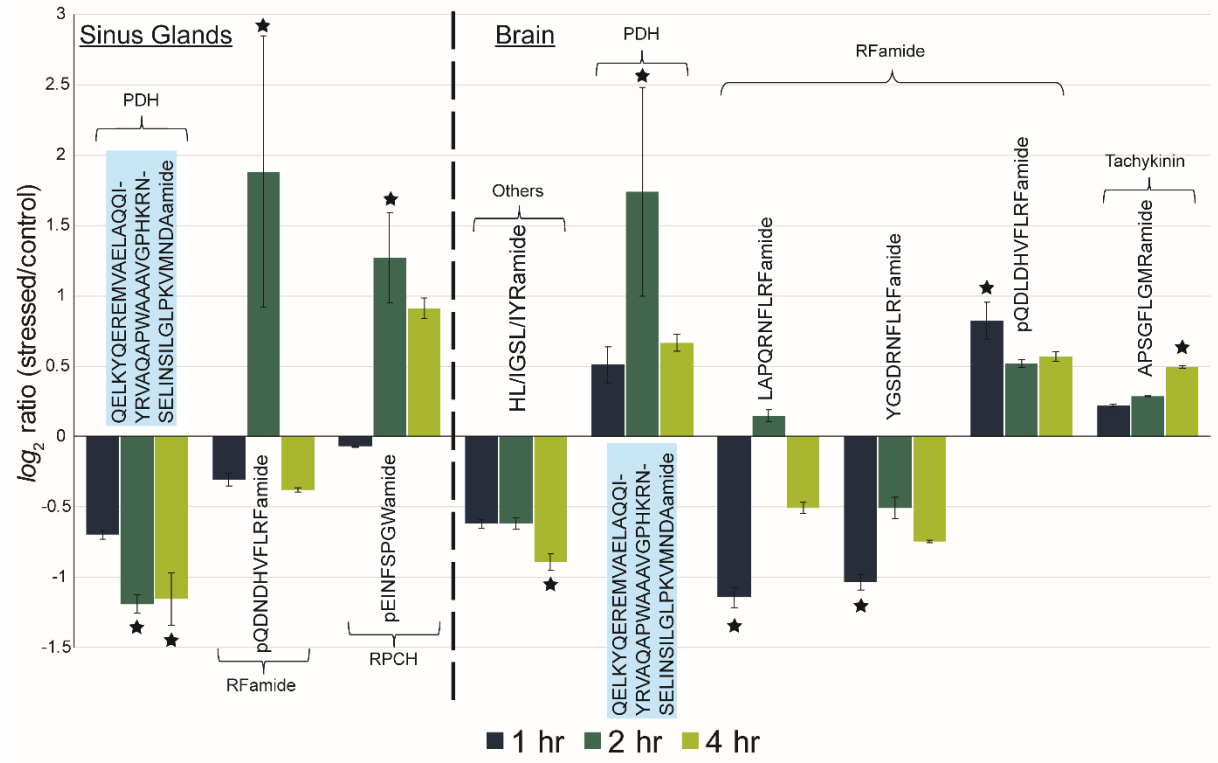

Figure 5: Neuropeptidomic changes in the sinus glands and brain. Neuropeptide sequences with at least one significant (denoted by star) change are listed across the x-axis and grouped by family. PDH = pigment dispersing hormone, RPCH = red pigment concentrating hormone. The PDH highlighted in blue is identical in sequence in both the sinus glands and brain. The ratio for the intensity of reporter ions for a stress condition (1, 2, or 4 hr copper exposure) relative to the control are depicted on the y-axis as a log_2 ratio to clearly see up/downregulation of neuropeptides relative to the x-axis. The error bars denote the standard error of the mean (n=4).

Table S1: LC-MS instrument settings

Chromatography and ESI-MS Instrument Acquisition			
Sample Volume	1.5 µL	***Isolation Window***	2.0 m/z
Stationary Phase	Hand-Packed C_{18} column 75µm ID x 360 µm OD ~15 cm 3.0 µm cap; 1.7 µm particles	***MS^2 AGC Target***	1e5
LC Solvent A	100% H_2O 0.1% formic acid	***MS^2 Maximum IT***	250 ms
LC Solvent B	100% acetonitrile, 0.1% formic acid	***Normalized Collision Energy***	27
Gradient Ramp and Duration ***Flow Rate***	10-35% B in 120 minutes 3.0 µL/min	***Minimum Intensity Req.***	3.2e4
Mass Spectrometer	Thermo Q Exactive HF	***MS^2 acquisition***	Data dependent, centroid
Spray Voltage	2 kV	***MS^2 Fragmentation***	HCD
In-Source CID	None	***MS^2 Detection***	Orbitrap
MS^1 scan range	*m/z* 200-2000	***MS^2 fixed first mass***	*m/z* 100
MS^1 AGC Target	5e5	***Advanced Precursor Determination***	N/A
MS^1 Maximum IT	150 ms		

Table S2: Proteome Discoverer 2.1 data analysis settings

Data Analysis Settings			
Min. Precursor Mass	350 Da	***Max. Modifications***	3
Max. Precursor Mass	5000 Da	***Static Modifications***	DiLeu @ N-term and K Amidated C-term*
Precursor Mass Tolerance	25 ppm	***Dynamic Modifications***	Deamidation @ N, Q Dehydration @ A, D, E, S, T, Y Methylation @ D, E, H, R, S, T
Fragment Mass Tolerance	0.02 Da		
Target FDR	1%		
Min. Peptide Length	5		
Quantitation Integration Tolerance	20 ppm	***Co-isolation Threshold***	50%

*C-term amidation was selected as a static modification only for peptides known to be amidated, including, but not limited to, RFamide and RYamide neuropeptides.

Table S3: All neuropeptides identified in the thoracic ganglia (TG) and pericardial organs (PO) in at least 3 biological replicates. Ratios are expressed as *log_2* ratios for consistency with the figures in the manuscript. The standard error of the mean (SEM) is reported as well. The "Sig?" column represents statistical significance determined by Dunnett's test with N = no and Y = yes. CPRP: CHH precursor-related peptide (CHH: crustacean hyperglycemic hormone).

				1 hr Exposure			2 hr Exposure			4 hr Exposure		
Tissue	Family	Sequence	m/z	Ratio	SEM	Sig?	Ratio	SEM	Sig?	Ratio	SEM	Sig?
TG	Allatostatin B-type	VPNDWAHFRGSWamide	1470.7	-0.5	0.036	N	-0.57	0.057	N	-0.23	0.03	N
	Calcitonin	GLDLGLGRGFSGSQAAKHLMGLAAANFANFAGGPamide	3272.67	-1.89	0.06	N	0.592	0.553	N	0.171	0.027	N
	Orcokinin	NFDEIDRSGFA	1270.57	-0.17	0.016	N	-0.13	0.007	N	0.806	0.161	Y
		NFDEIDRSSFGFA	1504.67	0.095	0.003	N	0.011	8E-04	N	0.337	0.016	N
		NFDEIDRSGFGFA	1474.66	0.419	0.025	Y	0.16	0.009	N	0.307	0.006	N
		NFDEIDRSSFGFN	1547.68	0.118	0.013	N	-0.26	0.022	N	0.612	0.107	N
		NFDEIDRSSFA	1300.58	-0.34	0.033	N	-0.18	0.024	N	0.933	0.238	Y
	Orcomyotropin	FDAFTTGFGHS	1186.52	0.06	0.002	N	-0.42	0.015	N	-0.16	0.009	N
	RFamide	pQDNDHVFLRFamide	1272.71	-1.51	0.043	Y	0.161	0.028	N	0.094	0.007	N
		pQDLDHVFLRFamide	1271.68	-0.55	0.076	N	-0.2	0.027	N	0.227	0.047	N
	Tachykinin	APSGFLGMRamide	917.462	-0.04	0.002	N	-0.37	0.026	N	-0.21	0.016	N
		YPSGFLGMRamide	1026.52	-0.39	0.021	N	-0.54	0.019	N	-0.63	0.082	N
PO	Allatostatin A-type	DGPYSFGLamide	854.404	0.486	0.004	Y	-0.22	0.004	N	-0.03	9E-04	N
		GRYSFGLamide	798.426	0.479	0.025	Y	-0.02	7E-04	N	-0.11	0.002	N
		SNPYSFGLamide	883.431	0.731	0.05	Y	-0.06	0.001	N	0.206	0.005	N
		TPHTYSFGLamide	1021.56	0.677	0.035	Y	-0.3	0.007	N	0.039	0.002	N
		GGSLYSFGLamide	899.462	-0.04	0.001	N	-0.01	6E-04	N	-0.17	0.007	N
		AGPYSFGLamide	810.414	0.421	0.029	Y	-0.36	0.004	N	-0.01	4E-04	N
		GGPYSYGLamide	812.43	-0.41	0.024	N	-0.47	0.031	N	-0.54	0.017	N
		SGQYSFGLamide	857.415	-0.13	0.005	N	0.044	0.004	N	-0.13	0.012	N
		SDMYSFGLamide	918.403	0.121	0.002	N	-0.26	0.009	N	-0.17	0.007	N
		APTDMYSFGLamide	1100.51	-0.24	0.009	N	1.693	0.138	Y	-0.4	0.003	N
		NEVPDPETERNSYDFGLamide	1980.89	-0.7	0.04	N	1.071	0.735	N	-0.33	0.023	N
		DARGALDLDQSPAYASDLGKRIGSAYSFGLamide	3113.57	-0.29	0.034	N	-0.83	0.016	N	-0.49	0.022	N
		AGQYSFGLamide	841.42	-0.08	0.005	N	-0.48	0.025	N	-0.43	0.047	N
		SGNYNFGLamide	870.41	0.274	0.005	N	-0.1	0.002	N	-0.06	0.002	N
	Allatostatin B-type	AWSNLGQAWamide	1031.51	-0.45	0.025	N	0.303	0.031	N	-0.17	0.008	N
		LGNWNKFQGSWamide	1504.8	-0.19	0.021	N	0.823	0.115	Y	0.152	0.007	N
		LNNNWSKFQGSWamide	1648.8	-0.07	0.008	N	0.748	0.074	Y	0.273	0.015	N
		SGDWSSLRGAWamide	1220.58	-0.2	0.02	N	0.484	0.049	N	0.2	0.014	N
		TGWNKFQGSWamide	1209.58	0.177	0.026	N	0.746	0.111	N	0.241	0.016	N
		STNWSSLRSAWamide	1293.63	0.036	0.004	N	0.661	0.077	N	0.401	0.032	N
	Allatostatin Combos	DPYAFGLGKRPDMYAFGLamide	2017	0.103	0.003	N	-0.32	0.008	N	-0.21	0.015	N
		GSGQYAFGLGKKAGGAYSFGLamide	2035.04	-0.12	0.009	N	-0.66	0.018	Y	-0.49	0.004	N
	CPRP	RSAEGLGRMGRLLASLKSDTVTPLRGFEGETGHPLE	3838	-0.39	0.048	N	0.201	0.036	N	0.303	0.031	N
	Orcokinin	DFDEIDRSGFGFA	1475.64	-0.2	0.024	N	0.712	0.11	Y	0.032	0.002	N
		NFDEIDRSGFA	1270.57	-0.4	0.062	N	0.281	0.043	N	-0.12	0.016	N
		NFDEIDRSGFamide	1198.55	-0.18	0.024	N	0.051	0.005	N	-0.62	0.061	N
		NFDEIDRSSFGFA	1504.67	-0.26	0.03	N	0.443	0.055	N	0.087	0.008	N
		NFDEIDRSGFGFA	1474.66	-0.02	0.002	N	0.674	0.053	N	0.022	9E-04	N
		NFDEIDRSSFGFN	1547.68	-0.25	0.029	N	0.539	0.072	N	0.243	0.026	N
		NFDEIDRTGFGFH	1554.7	-0.65	0.091	N	-0.13	0.021	N	-0.93	0.039	N
		NFDEIDRSSFA	1300.58	-0.39	0.061	N	0.199	0.03	N	0.236	0.043	N
	Orcomyotropin	FDAFTTGFGHS	1186.52	-0.21	0.016	N	0.874	0.15	Y	0.247	0.008	N
	Others	HLNGSLNYRamide	844.479	-0.86	0.035	Y	-0.29	0.004	N	-0.42	0.027	N
	RFamide	LAPQRNFLRFamide	1288.81	-0.16	0.024	N	0.944	0.195	Y	0.476	0.019	N
		pQDNDHVFLRFamide	1272.71	-0.07	0.003	N	0.122	0.005	N	-0.23	0.007	N
	RYamide	LEWYSQRYamide	1171.56	-0.03	9E-04	N	-0.51	0.054	N	0.297	0.048	N
		LSGFYANRYamide	1117.58	-0.89	0.046	Y	-0.95	0.05	Y	-0.41	0.072	N
		LSSRFVGGSRYamide	1257.7	-0.77	0.024	Y	-0.27	0.016	N	-0.25	0.008	N

Table S4: All neuropeptides identified in the sinus glands (SG) and brain in at least 3 biological replicates. Ratios are expressed as *log_2* ratios for consistency with the figures in the manuscript. The standard error of the mean (SEM) is reported as well. The "Sig?" column represents statistical significance determined by Dunnett's test with N = no and Y = yes. CPRP: CHH precursor-related peptide (CHH: crustacean hyperglycemic hormone); PDH: pigment dispersing hormone; RPCH: red pigment concentrating hormone.

				1 hr Exposure			2 hr Exposure			4 hr Exposure		
Tissue	Family	Sequence	m/z	Ratio	SEM	Sig?	Ratio	SEM	Sig?	Ratio	SEM	Sig?
SG	Allatostatin A-type	DGPYSFGLamide	854.404	-0.34	0.025	N	0.251	0.058	N	0.258	0.036	N
		GRYSFGLamide	798.426	-0.26	0.029	N	0.924	0.274	N	0.204	0.018	N
		SNPYSFGLamide	883.431	0.127	0.022	N	0.275	0.05	N	0.341	0.028	N
		TPHTYSFGLamide	1021.56	-0.05	0.011	N	-0.26	0.038	N	-0.06	0.009	N
		AGPYSFGLamide	810.414	0.156	0.034	N	0.365	0.032	N	0.485	0.093	N
		SDMYSFGLamide	918.403	-0.33	0.039	N	0.301	0.053	N	-0.04	0.004	N
		SGAYSFGLamide	800.394	0.208	0.03	N	-0.03	4E-04	N	0.557	0.061	N
		SGNYNFGLamide	870.41	-0.6	0.039	N	-0.16	0.017	N	-0.29	0.015	N
	Allatostatin Combos	GSGQYAFGLGKKAGGAYSFGLamide	2035.04	-0.83	0.083	N	-0.21	0.017	N	-0.81	0.05	N
	CPRP	RSTQGYGRMDRILAALKTSPMEPSAALAVENGTTHPLE	4069.06	-0.14	0.013	N	-0.29	0.015	N	-0.2	0.004	N
		RSTQGYGRMDRILAALKTSPMEPSAALAVQHGTTHPLE	4091.09	0.298	0.038	N	-0.83	0.04	N	-0.24	0.03	N
		RSAQGMGKMERLLASYRAAVEPNTPLGDLPGGLVHPVE	4017.08	-0.34	0.009	N	0.02	5E-04	N	-0.12	0.006	N
		RSAEGLGRMGRLLASLKSDTVTPLRGFEGETGHPLE	3838	-0.1	0.006	N	-0.16	0.003	N	-0.1	0.004	N
		RSAQGLGKMERLLVSYRGAVEPNTPLGDLSGSLGHPVE	3991.08	-0.33	0.021	N	0.392	0.064	N	0.434	0.038	N
		RSAEGLGRMamide	975.515	-0.31	0.02	N	0.801	0.227	N	0.456	0.028	N
	Orcokinin	DFDEIDRSGFA	1271.55	0.085	0.02	N	0.245	0.015	N	0.309	0.02	N
		DFDEIDRSGFGFA	1475.64	-0.05	0.006	N	0.247	0.012	N	0.553	0.031	N
		DFDEIDRSSFGFA	1505.65	0.43	0.064	N	0.026	0.001	N	0.082	0.006	N
		DFDEIDRSSFGFN	1548.66	0.003	5E-04	N	-0.16	0.006	N	-0.02	0.001	N
		NFDEIDRSGFA	1270.57	0.125	0.018	N	-0.28	0.016	N	-0.22	0.022	N
		NFDEIDRSGFamide	1198.55	-0.35	0.05	N	-0.27	0.027	N	-0.09	0.013	N
		NFDEIDRSSFGFA	1504.67	7E-04	1E-04	N	-0.21	0.003	N	0.022	0.003	N
		NFDEIDRSGFGFA	1474.66	0.086	0.011	N	0.073	0.003	N	0.486	0.055	N
		NFDEIDRSSFGFN	1547.68	0.085	0.012	N	-0.25	0.004	N	-0.05	0.006	N
		NFDEIDRSSFGFV	1532.7	0.029	0.004	N	-0.31	0.007	N	-0.1	0.014	N
		NFDEIDRTGFGFH	1554.7	-0.16	0.011	N	-0.23	0.007	N	-0.49	0.031	N
		NFDEIDRSGFGFV	1502.69	-0.46	0.06	N	-0.26	0.008	N	0.339	0.076	N
		NFDEIDRSSFA	1300.58	-0.05	0.005	N	-0.25	0.011	N	-0.2	0.01	N
	Orcomyotropin	FDAFTTGFGHS	1186.52	0.223	0.025	N	0.608	0.053	N	0.839	0.079	N
	Others	HL/IGSL/IYRamide	844.479	-0.53	0.022	N	-0.44	0.054	N	-0.22	0.024	N
	PDH	QELKYQERE MVAELAQQIYRVAQAPWAAAVGPHKRNSE LIN SILGLPKVMND Aamide	5973.14	-0.69	0.034	N	-1.19	0.063	Y	-1.15	0.186	Y
	RFamide	pQDNDHVFLRFamide	1272.71	-0.31	0.044	N	1.882	0.965	Y	-0.38	0.014	N
		pQDLDHVFLRFamide	1271.68	-0.2	0.039	N	-0.11	0.016	N	-0.17	0.007	N
	RPCH	pEINFSPGWamide	930.447	-0.07	0.001	N	1.268	0.321	Y	0.912	0.072	N
	Tachykinin	APSGFLGMRamide	917.462	-0.2	0.036	N	-0.03	0.003	N	0.176	0.015	N
		YPSGFLGMRamide	1026.52	-0.13	0.038	N	-0.3	0.053	N	0.183	0.026	N
Brain	Allatostatin A-type	SNPYSFGLamide	883.431	-0.41	0.033	N	-0.47	0.049	N	-0.76	0.033	N
	Allatostatin B-type	SGDWSSLRGAWamide	1220.58	-0.33	0.013	N	-0.32	0.021	N	0.05	0.006	N
		STNWSSLRSAWamide	1293.63	-0.69	0.033	N	0.056	0.013	N	-0.45	0.004	N
	Orcokinin	DFDEIDRSGFA	1271.55	-0.41	0.02	N	-0.41	0.031	N	-0.28	0.059	N
		NFDEIDRSGFA	1270.57	0.358	0.01	N	0.357	0.035	N	0.109	0.011	N
		NFDEIDRSGFamide	1198.55	0.376	0.013	N	0.231	0.022	N	0.134	0.013	N
		NFDEIDRSSFGFA	1504.67	0.257	0.013	N	0.127	0.006	N	0.229	0.031	N
		NFDEIDRSGFGFA	1474.66	-0.14	0.003	N	-0.2	0.008	N	0.029	0.002	N
		NFDEIDRSSFGFN	1547.68	-0.03	6E-04	N	-0.07	0.004	N	0.018	0.002	N
		NFDEIDRTGFGFH	1554.7	0.164	0.009	N	0.372	0.026	N	-0.06	0.002	N
		NFDEIDRSSFA	1300.58	0.347	0.013	N	0.272	0.026	N	0.059	0.006	N
	Orcomyotropin	FDAFTTGFGHS	1186.52	-0.32	0.017	N	-0.67	0.089	N	-0.23	0.025	N
	Others	HL/IGSL/IYRamide	844.479	-0.62	0.029	N	-0.62	0.042	N	-0.89	0.056	Y
	PDH	QELKYQERE MVAELAQQIYRVAQAPWAAAVGPHKRNSE LIN SILGLPKVMND Aamide	5973.14	0.509	0.129	N	1.738	0.742	Y	0.668	0.062	N
	RFamide	LAPQRNFLRFamide	1288.81	-1.14	0.071	Y	0.148	0.042	N	-0.5	0.04	N
		pQDNDHVFLRFamide	1272.71	0.041	0.014	N	0.746	0.214	N	-1.42	0.029	N
		YGSDRNFLRFamide	1273.64	-1.03	0.055	Y	-0.51	0.078	N	-0.74	0.009	N
		pQDLDHVFLRFamide	1271.68	0.824	0.131	Y	0.52	0.029	N	0.566	0.032	N
	Tachykinin	APSGFLGMRamide	917.462	0.219	0.008	N	0.287	0.005	N	0.492	0.009	Y

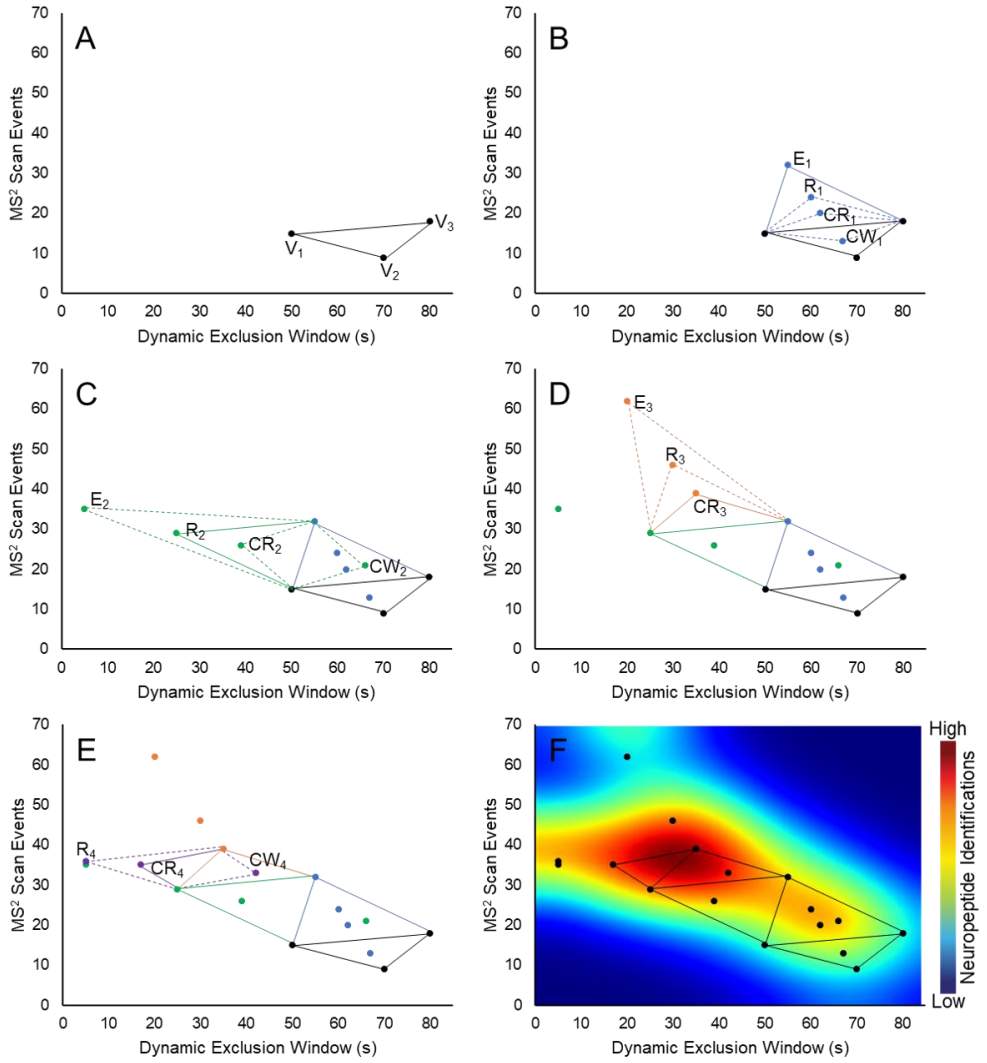

Simplex	Vertex	Dynamic Exclusion Window (s)	MS^2 Scan Events	Neuropeptides Identified
1	V_1	50	15	29
	V_2	70	9	25
	V_3	80	18	27
2	R_1	60	24	29
	E_1	55	32	41
	CR_1	62	20	35
	CW_1	67	13	24
3	R_2	25	29	88
	E_2	5	35	81
	CR_2	39	26	63
	CW_2	66	21	54
4	R_3	30	46	54
	E_3	20	62	53
	CR_3	35	39	72
5	R_4	5	36	64
	CR_4	42	33	55
	CW_4	17	35	66

Figure S1: Sequential results from modified simplex algorithm. Solid lines show the original and subsequent simplexes. Dashed lines connect the simplexes to all evaluated points to show the progression during optimization. A. Initial vertices selected. B. Geometric reflection away from V2 across the midpoint of V1 and V3. C. Geometric reflection away from V3 across the midpoint of V1 and E1. D. Geometric Reflection away from V1 across the midpoint of R2 and E1. E. Geometric reflection away from E1 across the midpoint of CR3 and R2. F. All points overlaid on a heatmap depicting the relative identifications of neuropeptides from different regions of the graph. In the graphs, points from Simplex 1 are given in black, Simplex 2 in blue, Simplex 3 in green, Simplex 4 in orange, and Simplex 5 in purple. The table below numerically depicts the same information given in the graphs.

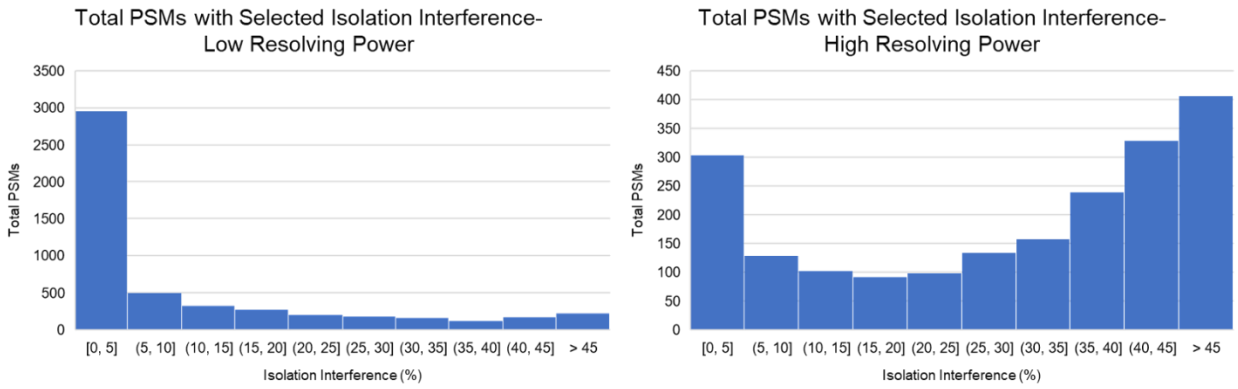

Figure S2: Comparison of isolation interference between high and low resolving powers. The two histograms show the total number of PSMs that were used for quantitation that have a given isolation interference (determined by Proteome Discoverer). Experimental data is shown from the factorial design of experiments, with 4 conditions having high MS^1 and MS^2 resolving power and 4 conditions having low resolving power. The final bin was set to ">45" as no PSMs with isolation interference above 50% were used for quantitation (controlled by the co-isolation threshold given in **Table S2**). When using the low MS^1 and MS^2 resolving power, not only were there more PSMs, but the isolation interference was lower. This resulted in a greater percentage of PSMs being used for identification and quantitation. For the low resolving power, there were 10,999 PSMs across the 4 experimental conditions where both MS^1 and MS^2 resolving power were low, with 5,125 being used for quantification (46.6%). Conversely, for the high resolving power, there were only 5,512 PSMs across the 4 experimental conditions where both MS^1 and MS^2 resolving power were high, with 1,991 being used for quantification (36.1%).

Chapter 5

Enhancing Neuropeptidomics Throughput via 12-plex DiLeu Isobaric Tags

Abstract

The study of neuropeptides presents many opportunities for improving the understanding of neuroendocrine signaling, and recently, isobaric tagging has enabled greater throughput analyses of neuropeptides. To further reduce analysis times, sampling needs, and run-to-run variation, an expanded 12-plex isobaric workflow is developed here for the application of neuropeptidomic analyses. To ensure low abundance neuropeptides are still identified, several mass spectrometry acquisition parameters were optimized. An orthogonal array optimization strategy reduced the total number of LC-MS injections required for optimization and allowed the impact of specific parameters to be estimated to inform future parameter selection. Top performing conditions were compared in a secondary experiment before deciding on optimal parameters. This work led to a 2.75-fold increase in identifiable neuropeptides compared to unoptimized parameters. Overall, this study demonstrates the importance of mass spectrometry method optimization and provides a workflow for future higher throughput quantitative neuropeptidomic studies.

Introduction

Neuropeptides are a large, highly diverse group of signaling peptides that originate in the neuroendocrine system. They are potent signal modulators that act both locally and hormonally to influence many biological processes.[1] As a result, neuropeptides have been shown to play roles in many biological problems of interest, including stress response,[2–5] behavior,[6] and diseases like Alzheimer's disease and

cancers.[7] They are the subject of ongoing research and have the potential to serve as biomarkers or even therapeutics.

Neuropeptidomics presents many challenges, however, due to the structural diversity of neuropeptides and their low *in vivo* abundance. Additionally, because neuropeptide function is dependent in part on the other co-expressed neuropeptides, analytical methods need to be capable of profiling all neuropeptides in a sample.[1] Fast, sensitive methods like liquid chromatography coupled to mass spectrometry (LC-MS) have been demonstrated to be highly effective in characterizing these elusive signaling molecules, without requiring knowledge of the exact chemical composition of the sample.

Quantitation of neuropeptides can be readily achieved using label-free quantitation (LFQ) methods, requiring minimal sample processing. These methods, however, require samples be analyzed separately, limiting throughput and requiring robust normalization methods to account for instrumental drift.[8] Isotopic labeling methods, like reductive dimethylation,[9–11] are simple, but lack multiplexing capabilities due to spectral complexity. Alternatively, isobaric tagging approaches can be used to perform relative quantitation of many samples simultaneously while maintaining spectral complexity. In isobaric labeling workflows, the same nominal mass is added to each channel, creating no distinction between samples at the precursor mass level (MS^1). Upon tandem MS (MS^2) analysis, unique reporter ions form, enabling relative quantitation between samples based on the intensity of the corresponding reporter ions.[12]

Numerous isobaric tags exist, including commercially available options like isobaric tags for relative and absolute quantitation (iTRAQ)[12] and tandem mass tags (TMT),[13] along with a tag developed in the Li Lab, N,N-dimethyl leucine (DiLeu).[14] These tags have been shown to be effective in bottom-up proteomics workflows[15–17] but have had limited application in the field of neuropeptidomics.[18,19] Neuropeptides can be challenging to study using isobaric tags as their low abundance can often inhibit their selection for MS^2 analyses, thereby preventing their identification and quantitation. Recently, the effectiveness of optimizing the data acquisition settings has been demonstrated in the analysis of DiLeu-labeled neuropeptides using 4-plex tags. By systematically optimizing the resolution, dynamic exclusion window, and number of MS^2 scan events, a threefold increase in neuropeptide identifications was achieved.[20]

To further improve throughput, the multiplexing capabilities of the DiLeu tags needed to be expanded. This was achieved through the incorporation of different stable isotopes in each tag. Despite ^{2}H, ^{13}C, and ^{15}N each adding one neutron, different mass additions arise from differences in nuclear binding energies. These mass defects are on the mDa scale and allow for more tags with unique, distinguishable reporter ions. The initial 4-plex DiLeu tags can be synthesized using different combinations of isotopic leucine and isotopic formaldehyde to create an expanded 12-plex labeling scheme with additional peaks arising from mass defects between isotopes.[21] This greatly improves throughput but requires a greater tandem mass spectrometry (MS^2) resolving power to accurately resolve the mDa mass differences between adjacent reporter ions (**Figure 1**).[21] In turn, this increases the scan times and the total number of spectra acquired.

To balance the trade-off between higher throughput 12-plex tags and the reduced identifications caused by higher resolutions, optimization of the DDA settings is once again performed. Systematic methods like a full factorial design of experiments (DoE)[22–24] or simplex optimization[19] are powerful, but require many experiments, limiting the number of parameters that can be analyzed and optimized. To optimize six parameters (MS^1 resolution, MS^2 resolution, MS^2 scan events, dynamic exclusion window, maximum injection time, and automatic gain control (AGC) target) simultaneously and efficiently, an orthogonal array optimization (OAO) strategy is used.[25] This design of experiments is similar to a factorial design in that combinations of parameters are evaluated based on desired performance (*e.g.,* number of identified neuropeptides). The OAO, however, does not test every possible condition, but rather uses an orthogonal array to test the same sample space with fewer experiments.[26,27] This on-the-fly optimization method may not be as robust as a full factorial strategy, but it allows far fewer conditions to be evaluated, greatly expediting the process. The overall workflow is depicted in **Figure 2**.

The orthogonal array used in this work (**Table 1**) is an $L_{18}(2^1 \times 3^5)$ in which one factor (MS^2 resolution) is evaluated at two levels and the other five factors are evaluated at three levels each, requiring 18 runs to evaluate the same sample space as a full factorial DoE requiring 486 runs. Increasing the MS^2 resolution past 60k yields no improvement in quantitative accuracy (see **Figure 1**),[21] so only low and medium values are evaluated. The OAO strategy also allows the impact of different factors to be estimated to inform further optimization and has led to an increase of 2.75-fold in the

number of identifiable and quantifiable neuropeptides in a single run. This work lays the foundation for studying neuropeptide expression changes in response to environmental stress with enhanced throughput.

Experimental Methods

Materials

LC-MS solvents, methanol, and glacial acetic acid were purchased from Fisher Scientific (Pittsburgh, PA). Triethylammonium bicarbonate (TEAB), N,N-dimethylformamide (DMF), ammonium formate, 4-(4,6-dimethoxy- 1,3,5-triazin-2-yl)-4-methylmorpholinium tetrafluoroborate (DMTMM), and isotopic leucine and formaldehyde were purchased from Sigma-Aldrich (St. Louis, MO). N-methylmorpholine (NMM) was purchased from TCI America, (Tokyo, Japan). Strong cation exchange (SCX) spin tips were purchased from PolyLC (Columbia, MD). C18 ZipTips were purchased from Millipore (Burlington, MA).

Neuropeptide Extraction

Neuroendocrine tissues including the brain, pericardial organs, sinus glands, and thoracic ganglia were dissected from blue crabs as previously described.[28] Briefly, sacrificed crabs were anesthetized on ice for 15 min prior to dissection. Tissues were placed into acidified methanol (90/9/1 methanol/water/acetic acid) and stored at -80 °C prior to extraction. To generate a consistent sample to be used for all optimization

experiments, tissues from eight crabs were pooled together and extracted by ultrasonication using a Fisherbrand 120 probe sonicator. The pooled tissues were submerged in acidified methanol and sonicated at an amplitude of 50% for 8 s three times with 15 s rest between pulses. The homogenized tissues were centrifuged at 20,000 x g for 20 min at 4 °C. The supernatant was collected and dried down by vacuum centrifugation. The crude extracts were then purified by manufacturer's protocol using C18 ZipTips.

DiLeu Labeling and Purification

The tag synthesis and labeling protocol has been described previously.[21] Briefly, 12 equal aliquots of the extracted neuropeptides were resuspended in 50:50 ACN:0.5 M TEAB. The DiLeu tags were activated to their triazine ester form by the addition of 50 µL activation solution (14.08 mg DMTMM in 495 µL dry DMF with 4.72 µL NMM) and vortexed for 30 min at room temperature. The activated DiLeu was added to the resuspended neuropeptides at a 20:1 label:peptide ratio by mass. After 1 hr the reaction was quenched by the adding 5% NH_2OH to a final concentration of 0.25%. The labeled neuropeptides were pooled together before drying down by vacuum centrifugation. SCX spin tips were used to remove excess tagging reagents from the neuropeptides. Labeled samples were loaded and washed in 0.1% formic acid, 20% ACN, and then eluted with 0.4 M ammonium formate in 20% ACN. The addition of salt required one last desalting step, so the multiplexed samples were purified again using C18 ZipTips.

LC-MS Analysis

Multiplexed samples were analyzed in duplicate with a Thermo Orbitrap Elite Mass Spectrometer coupled to a Waters nano Acquity using a homemade 15 cm C18 column. Neuropeptides were eluted over a 60 min gradient from 5-35% solvent B (solvent A = 0.1% formic acid in water; solvent B = 0.1% formic acid in ACN). Spectra were collected with an m/z range of 200-2000 using high-energy collision dissociation. The resolution, MS^2 scan events, dynamic exclusion window, maximum injection time, and AGC target were adjusted per the orthogonal array in Table 1.

Data Analysis

The raw files were processed using Proteome Discoverer 2.1. Neuropeptides were identified from an in-house crustacean database and quantified by reporter ion intensity. Files were searched with static DiLeu modification of N-termini and Lys and C-terminal amidation of neuropeptides known to be amidated endogenously. Dynamic modifications included oxidation (Met), deamidation (Asn, Gln), methylation (Asp, Glu, His, Lys, Arg, Ser, Thr), and dehydration (Ala, Asp, Glu, Ser, Thr, Tyr).

Results and Discussion

Previous work has shown that neuropeptide identifications can be significantly improved by altering the data-dependent acquisition (DDA) settings of a mass spectrometer.[19] In a DDA experiment, a precursor scan is performed followed by a

preset number of MS^2 scans of the most abundant species in the MS^1 spectrum. Certain parameters have direct and indirect influence on the number of relevant spectra that can be acquired in an LC-MS analysis. By adjusting these DDA parameters, more unique neuropeptides can be selected for fragmentation and redundant, uninformative analyses can be reduced.

In this work, six parameters are evaluated: the MS^1 resolution, MS^2 resolution, MS^2 scan events per precursor scan, the dynamic exclusion window (minimum amount of time between MS^2 analyses of the same precursor ion), the AGC target (signal threshold that must be reached before ions are injected into the mass spectrometer), and the maximum injection time (maximum time ions are able to accumulate before reaching the AGC target). These parameters exert some influence on each other–for example, if the maximum injection time is not high enough, the AGC target cannot be reached–and therefore require simultaneous optimization. This is accomplished in a fast, on-the-fly method using an orthogonal array optimization strategy. The 18 combinations of parameter values are given in **Table 1**, and the overall numbers of identified neuropeptides are shown in **Figure 3**. An average of 31.4 neuropeptides were identified across all 18 conditions, with the lowest performing point (Condition 18) yielding 17 identifications, and the highest performing point (Condition 17) yielding 47 identifications. This reflects a 2.75-fold increase in identifications between optimal and unoptimized conditions, demonstrating the benefits and importance of optimizing the DDA settings.

The OAO strategy also allows the influence of specific parameters to be estimated.[29] **Figure 4** shows the average number of identified neuropeptides when a given parameter is low, medium, and high, summarized by the K_1, K_2, and K_3 values respectively. Overall trends can be seen, such as there being minimal difference in the number of identifiable neuropeptides when either the MS^1 or MS^2 resolution is adjusted. This suggests that the increase in scan times with higher resolutions is less impactful than the effects of the other parameters. The other parameters did show more meaningful trends. For example, fewer identifications are observed with an increase in the number of MS^2 scan events. This is likely because the additional MS^2 scans are sampling species with too low abundance, thereby generating poor quality spectra from which to identify the neuropeptides. Simply decreasing the number of MS^2 scan events is not necessarily a viable solution as setting it too low can result in fewer identifications as the total number of MS^2 spectra decreases. Previous optimization work with DiLeu-labeled neuropeptides has shown benefits from a high number of MS^2 scan events[19] but used a more sensitive instrument (Thermo QExactive HF vs the Thermo Orbitrap Elite used here). The more sensitive instrument can more reliably identify the low abundance species, so the number of MS^2 scan events before uninformative precursor ions are selected is higher. This highlights the dependence of the instrumentation on optimization, and methods developed on one instrument may not be directly transferrable to another.

The dynamic exclusion window is often correlated to the peak width of the analytes. This helps to avoid excess sampling of an analyte across its elution profile but

allows analytes with similar m/z but different retention times to still be analyzed and detected. The structural diversity of neuropeptides often leads to variable elution profiles, however, making it difficult to reliably predict the optimum dynamic exclusion window. Here, a shorter dynamic exclusion windows is favorable, and again, could be related to the sensitivity of the instrument. Low abundance analytes may be getting sampled too early in the peak when the signal intensity is lower and need to be analyzed again a short time later when the intensity is greater in order to be reliably identified.

The maximum injection time and AGC target are directly related to each other; as the AGC target increases, the maximum injection time should also increase to give more time for ions to accumulate to reach the increased AGC target. It is, therefore, unsurprising that the two parameters would show similar trends. More impactful is that they show a clear trend towards greater identifications coming from a greater AGC target and maximum injection time. By increasing these parameters, the time for each scan is increased, but results in more reliable spectra from which to identify neuropeptides. This is especially beneficial for low abundance species that may have previously resulted in poor quality spectra, and increasing the AGC target and maximum injection time results in an overall increase in the number of neuropeptides identified in a single LC-MS run.

Selecting optimal parameters is not as simple as looking at the trends in individual parameters and selecting conditions from there. Using the example of AGC target and maximum injection time, one could be inclined to set both at a high value.

Looking at the two conditions where this was the case (Conditions 3 and 5 in **Table 1**), the performance was above average, but not as high as some of the other conditions where the AGC target and maximum injection time were either high/low (Condition 17) or low/high (Condition 7). This highlights the fact that optimization must consider the influence of all parameters, and that interplay between parameters is not readily discernable or predictable.

Further complicating matters is the fact that DDA workflows can often suffer from poor reproducibility due to variable ionization efficiency within a complex mixture. Methods like data-independent acquisition (DIA) have proven beneficial for expanding coverage of the neuropeptidome[30,31] but are incompatible with isobaric tagging as the total reporter ion signal cannot be deconvoluted from the constituent analytes. To address the reproducibility of DDA methods and determine optimal parameters from the many conditions evaluated, the top four conditions from the initial OAO were reevaluated with a secondary sample. Additionally, two new sets of conditions informed from the initial OAO were selected for evaluation. These six conditions are given in **Table 2**. Analyzing the secondary samples with these six conditions yielded an average of 33.8 neuropeptides identified with a range of 17-49 identifications. The relative performance of these conditions is shown in **Figure 5**.

From this secondary test, Conditions 2 and 5 showed the best performance and were comparable in terms of neuropeptides identified. Interestingly, there is minimal overlap in parameter values for these two conditions; only the number of MS^2 scan events is similar. Conversely, Conditions 5 and 6 are very similar, differing only in the

AGC target and maximum injection time, but result in a difference of 29 neuropeptide identifications. These findings once again highlight the importance of optimization methods being capable of simultaneously optimizing parameters. For future analyses, Condition 5 will be used as the increased MS^2 resolving power compared to Condition 2 can resolve the reporter ion peaks from interference from isotopic impurities. This facilitates more accurate quantitation for biological applications. The optimized methods here allow many samples to be analyzed at once, greatly increasing throughput for the study of neuropeptidomics. These optimized parameters are tailored to a specific system, but the experimental workflow using the OAO can be translated to other studies and/or for the optimization of additional parameters.

Conclusions

Advances in neuropeptide research have potential to improve understanding of many physiological processes, such as behavior,[6] stress,[2,5,19,32] and neurological disorders.[33] Quantifying neuropeptide expression changes can provide information in the underlying mechanisms and signaling pathways involved in these processes. Using 12-plex DiLeu isobaric tags allows for several experimental conditions to be compared to a control in a single LC-MS run. This greatly improves throughput and reduces sample requirements and run-to-run variability but requires optimization to ensure low abundance neuropeptides are still detected. Using an orthogonal array, six MS parameters were simultaneously optimized, with approximately 2.75 times as many identifications from optimized parameters compared to unoptimized. Some trends in

specific parameters were observed, but it was shown that the parameters need to be optimized simultaneously to consider interplay between parameters. The optimized methods developed in this work can be used to study many biological processes. Building on the 4-plex DiLeu-labeled neuropeptide work to study copper toxicity is of considerable interest as it would allow additional exposure durations and/or severities to be studied.

References

1. Li L, Sweedler J V. Peptides in the Brain: Mass Spectrometry–Based Measurement Approaches and Challenges. *Annu Rev Anal Chem*. 2008;1(1):451-483. doi:10.1146/annurev.anchem.1.031207.113053
2. Buchberger AR, Sauer CS, Vu NQ, DeLaney K, Li L. A Temporal Study of the Perturbation of Crustacean Neuropeptides Due to Severe Hypoxia Using 4-Plex Reductive Dimethylation. *J Proteome Res*. 2020;19:1548-1555. doi:10.1021/acs.jproteome.9b00787
3. Zhang Y, Buchberger A, Muthuvel G, Li L. Expression and distribution of neuropeptides in the nervous system of the crab Carcinus maenas and their roles in environmental stress. *Proteomics*. 2015;15(23-24):3969-3979. doi:10.1002/pmic.201500256
4. Chen R, Xiao M, Buchberger A, Li L. Quantitative neuropeptidomics study of the effects of temperature change in the crab cancer borealis. *J Proteome Res*. 2014;13(12):5767-5776. doi:10.1021/pr500742q

5. Liu Y, Buchberger AR, Delaney K, Li Z, Li L. Multifaceted Mass Spectrometric Investigation of Neuropeptide Changes in Atlantic Blue Crab, Callinectes sapidus, in Response to Low pH Stress. *J Proteome Res*. 2019;18(7):2759-2770. doi:10.1021/acs.jproteome.9b00026

6. Delaney K, Hu M, Hellenbrand T, Dickinson PS, Nusbaum MP, Li L. Mass Spectrometry Quantification, Localization, and Discovery of Feeding-Related Neuropeptides in Cancer borealis. *ACS Chem Neurosci*. 2021;12(4):782-798. doi:10.1021/acschemneuro.1c00007

7. Sweedler, Jonathan V.,Xie, Fang, Bora A. Chapter 1.4. 2012:221-227.

8. Romanova E V, Dowd SE, Sweedler J V. Quantitation of endogenous peptides using mass spectrometry based methods. *Curr Opin Chem Biol*. 2013;17(5):801-808. doi:S1367-5931(13)00102-6 [pii]\r10.1016/j.cbpa.2013.05.030 [doi]

9. Kovanich D, Cappadona S, Raijmakers R, Mohammed S, Scholten A, Heck AJR. Applications of stable isotope dimethyl labeling in quantitative proteomics. *Anal Bioanal Chem*. 2012;404(4):991-1009. doi:10.1007/s00216-012-6070-z

10. Fricker L. Chapter 8 Quantitative Peptidomics : General Considerations. In: *Peptidomics: Methods and Strategies, Methods in Molecular Biology*. Vol 1719. ; 2018:121-140.

11. Tashima AK, Fricker LD. Quantitative Peptidomics with Five-plex Reductive Methylation labels. *J Am Soc Mass Spectrom*. 2017;29:866-878. doi:10.1007/s13361-017-1852-3

12. Wiese S, Reidegeld KA, Meyer HE, Warscheid B. Protein labeling by iTRAQ: A new

tool for quantitative mass spectrometry in proteome research. *Proteomics*. 2007;7(3):340-350. doi:10.1002/pmic.200600422

13. Li J, Vranken JG Van, Vaites LP, et al. TMTpro reagents: a set of isobaric labeling mass tags enables simultaneous proteome-wide measurements across 16 samples. *Nat Methods*. 2020;17(April). doi:10.1038/s41592-020-0781-4
14. Xiang F, Ye H, Chen R, Fu Q, Li N. N,N-Dimethyl leucines as novel Isobaric tandem mass tags for quantitative proteomics and peptidomics. *Anal Chem*. 2010;82(7):2817-2825. doi:10.1021/ac902778d
15. Liu R, Wei P, Keller C, et al. Integrated Label-Free and 10-Plex DiLeu Isobaric Tag Quantitative Methods for Pro fi ling Changes in the Mouse Hypothalamic Neuropeptidome and Proteome: Assessment of the Impact of the Gut Microbiome. *Anal Chem*. 2020;92:14021-14030. doi:10.1021/acs.analchem.0c02939
16. Hao L, Thomas S, Greer T, et al. Quantitative proteomic analysis of a genetically induced prostate inflammation mouse model via custom 4-plex DiLeu isobaric labeling. *Am J Physiol - Ren Physiol*. 2019;316(6):F1236-F1243. doi:10.1152/ajprenal.00387.2018
17. Zhong X, Frost DC, Yu Q, Li M, Gu TJ, Li L. Mass Defect-Based DiLeu Tagging for Multiplexed Data-Independent Acquisition. *Anal Chem*. 2020;92:11119-11126. doi:10.1021/acs.analchem.0c01136
18. Jiang X, Xiang F, Jia C, Buchberger AR, Li L. Relative Quantitation of Neuropeptides at Multiple Developmental Stages of the American Lobster Using *N*

, *N*-Dimethyl Leucine Isobaric Tandem Mass Tags. *ACS Chem Neurosci*. 2018:acschemneuro.7b00521. doi:10.1021/acschemneuro.7b00521

19. Sauer, Christopher S., Li L. Multiplex Dimethylated Leucine (DiLeu) Isobaric Tags to Probe Neuropeptidomic Response to Copper Toxicity in the Blue Crab, Callinectes sapidus. In: Atlanta, GA: American Society for Mass Spectrometry; 2019.
20. Sauer CS, Li L. Multiplexed Quantitative Neuropeptidomics via DiLeu Isobaric Tagging. In: *Methods in Enzymology 663: Antimicrobial Peptides*. ; 2022.
21. Frost DC, Greer T, Li L. High-resolution enabled 12-plex DiLeu isobaric tags for quantitative proteomics. *Anal Chem*. 2015;87(3):1646-1654. doi:10.1021/ac503276z
22. Randall SM, Cardasis HL, Muddiman DC. Factorial experimental designs elucidate significant variables affecting data acquisition on a quadrupole orbitrap mass spectrometer. *J Am Soc Mass Spectrom*. 2013;24(10):1501-1512. doi:10.1007/s13361-013-0693-y
23. Andrews GL, Dean RA, Hawkridge AM, Muddiman DC. Improving proteome coverage on a LTQ-orbitrap using design of experiments. *J Am Soc Mass Spectrom*. 2011;22(4):773-783. doi:10.1007/s13361-011-0075-2
24. Hecht ES, McCord JP, Muddiman DC. Definitive Screening Design Optimization of Mass Spectrometry Parameters for Sensitive Comparison of Filter and Solid Phase Extraction Purified, INLIGHT Plasma N-Glycans. *Anal Chem*. 2015;87(14):7305-7312. doi:10.1021/acs.analchem.5b01609

25. Cao J, Gonzalez-Covarrubias V, Covarrubias VM, et al. A rapid, reproducible, on-the-fly orthogonal array optimization method for targeted protein quantification by LC/MS and its application for accurate and sensitive quantification of carbonyl reductases in human liver. *Anal Chem*. 2010;82(7):2680-2689. doi:10.1021/ac902314m

26. Rao RS, Kumar CG, Prakasham RS, Hobbs PJ. The Taguchi methodology as a statistical tool for biotechnological applications: A critical appraisal. *Biotechnol J*. 2008;3(4):510-523. doi:10.1002/biot.200700201

27. Bolboacă SD, Jäntschi L. Design of experiments: Useful orthogonal arrays for number of experiments from 4 to 16. *Entropy*. 2007;9(4):198-232. doi:10.3390/e9040198

28. Gutierrez GJ, Grashow RG. Cancer borealis stomatogastric nervous system dissection. *J Vis Exp*. 2009;(25):1-5. doi:10.3791/1207

29. Li B, Luo X, Deng B, et al. An Orthogonal Array Optimization of Lipid-like Nanoparticles for mRNA Delivery in Vivo. *Nano Lett*. 2015;15(12):8099-8107. doi:10.1021/acs.nanolett.5b03528

30. Saidi M, Kamali S, Beaudry F. Neuropeptidomics: Comparison of parallel reaction monitoring and data-independent acquisition for the analysis of neuropeptides using high-resolution mass spectrometry. *Biomed Chromatogr*. 2019;33(7):1-11. doi:10.1002/bmc.4523

31. Delaney K, Li L. Data Independent Acquisition Mass Spectrometry Method for Improved Neuropeptidomic Coverage in Crustacean Neural Tissue Extracts. *Anal*

Chem. 2019;(91):5150-5158. doi:10.1021/acs.analchem.8b05734

32. Chen R, Xiao M, Buchberger A, Li L. Quantitative Neuropeptidomics Study of the Effects of Temperature Change in the Crab Cancer borealis. *J Proteome Res*. 2014;13:5767-5776.

33. Li C, Wu X, Liu S, et al. Roles of Neuropeptide Y in Neurodegenerative and Neuroimmune Diseases. *Front Neurosci*. 2019;13:1-11. doi:10.3389/fnins.2019.00869

Figures

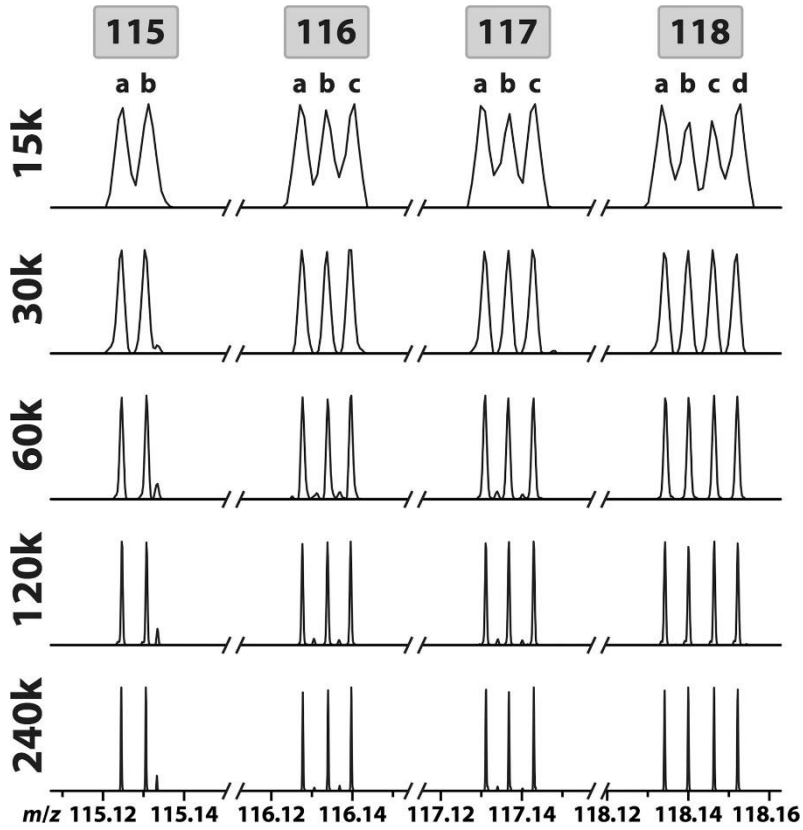

Figure 1: Reporter ion peaks with varying resolution. The reporter ions for the 4-plex DiLeu tags have spacings of ~1 Da and are easily resolvable. The mDa mass differences in the 12-plex labeling scheme require 30k resolving power to achieve baseline resolution. Isotopic interference from neighboring peaks can affect quantitation but is resolved from the reporter ions with resolutions of 60k or greater. Figure reprinted with permission from Frost, D.C. et al (https://pubs.acs.org/doi/pdf/10.1021/ac503276z).[21]

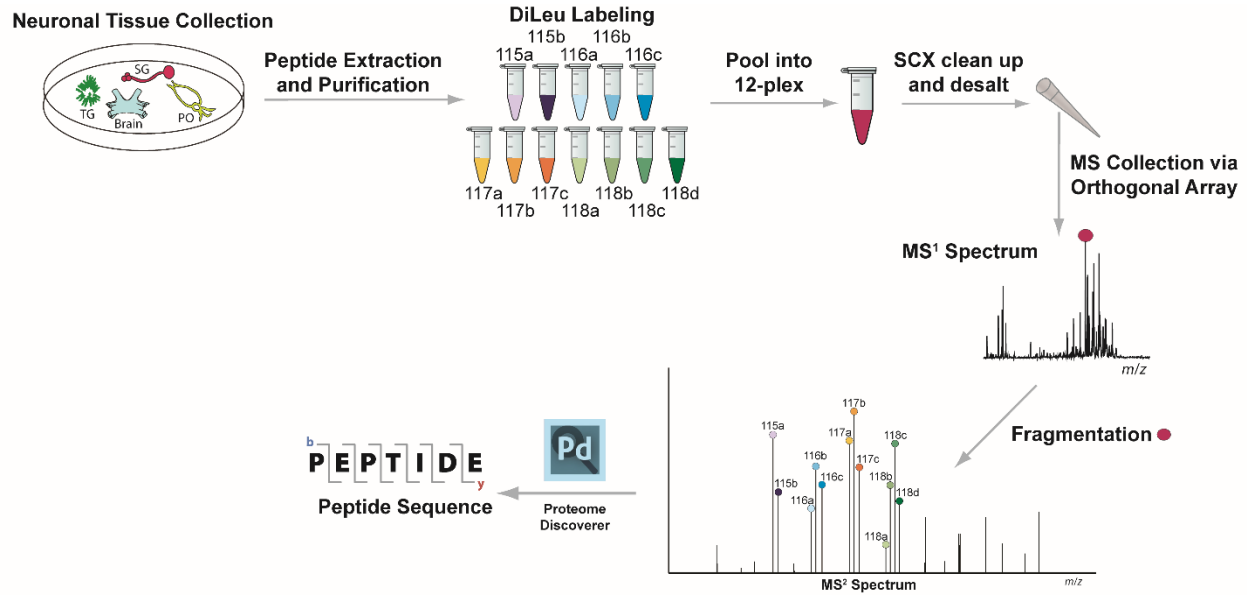

Figure 2: Method workflow for optimizing neuropeptide analyses. Neuroendocrine tissues (sinus glands (SG), pericardial organs (PO), thoracic ganglia (TG), and brain) were collected from blue crabs. Neuropeptides were extracted via ultrasonication and purified by C18 ZipTips prior to differential labeling with DiLeu. The samples were then pooled, cleaned up by SCX spin tips and desalted once more. The final sample was then analyzed by mass spectrometry with varied acquisition parameters. Neuropeptides were identified and quantified using Proteome Discoverer 2.1.

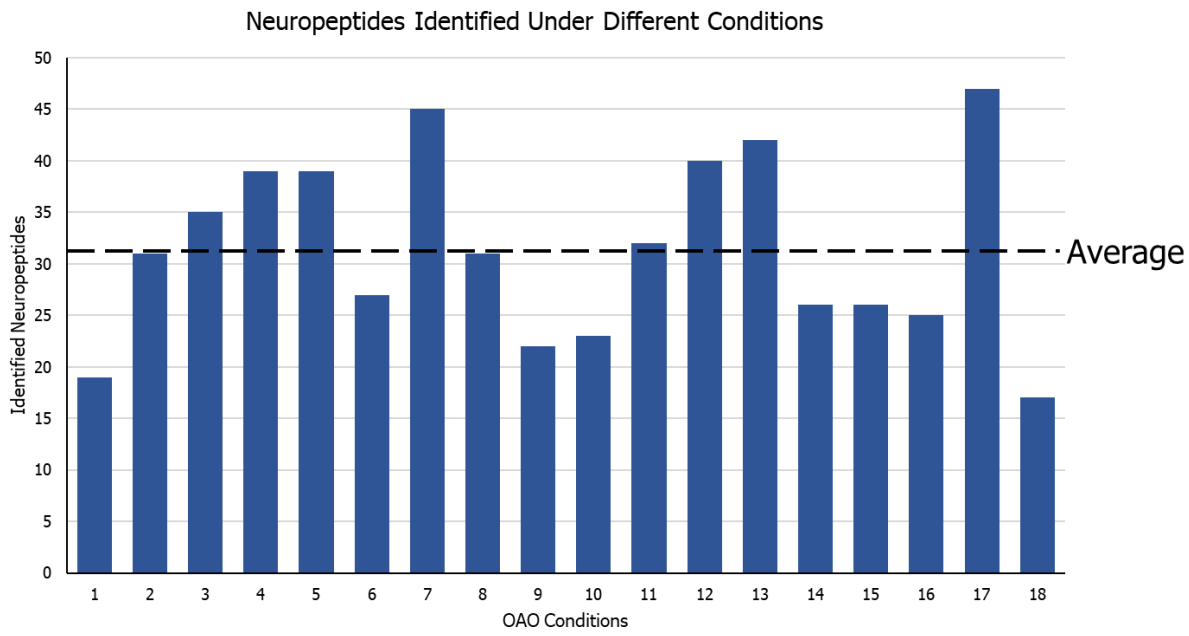

Figure 3: Number of neuropeptides identified from each OAO run. The average number of neuropeptides identified across all runs was 31.4 and is denoted with a dashed line. The overall minimum number of identifications from the 18 conditions was 17 and the maximum was 47.

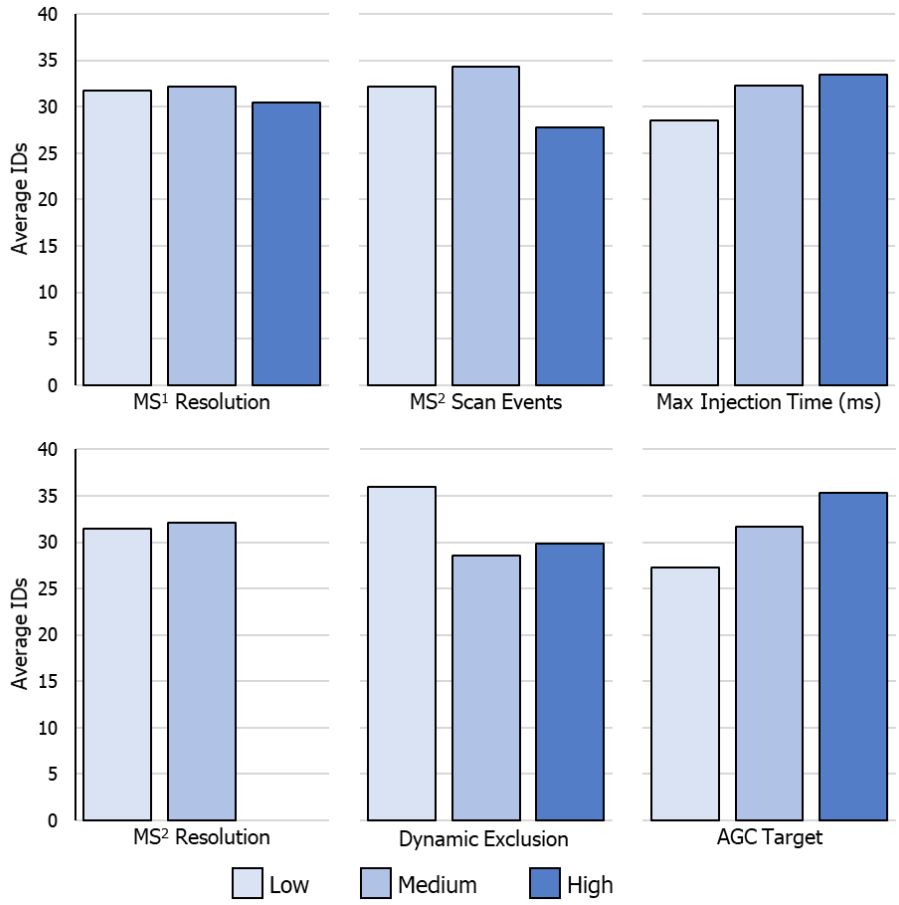

	MS¹ resolution	MS² resolution	MS² scan events	Dynamic exclusion window	Max injection time	AGC target
K_1	31.7	32.0	32.2	36.0	28.5	27.3
K_2	32.2	30.9	34.3	28.5	32.3	31.7
K_3	30.5	-	27.8	29.8	33.5	35.3
ΔK	1.7	1.1	6.5	7.5	5.0	8.0

Figure 4: Average neuropeptide identifications when a given parameter is low, medium, or high. The averages are given in the table below the graphs with K_1, K_2, and K_3 reflecting the averages when a parameter is low, medium, and high respectively. ΔK refers to the difference between K_{max} and K_{min}.

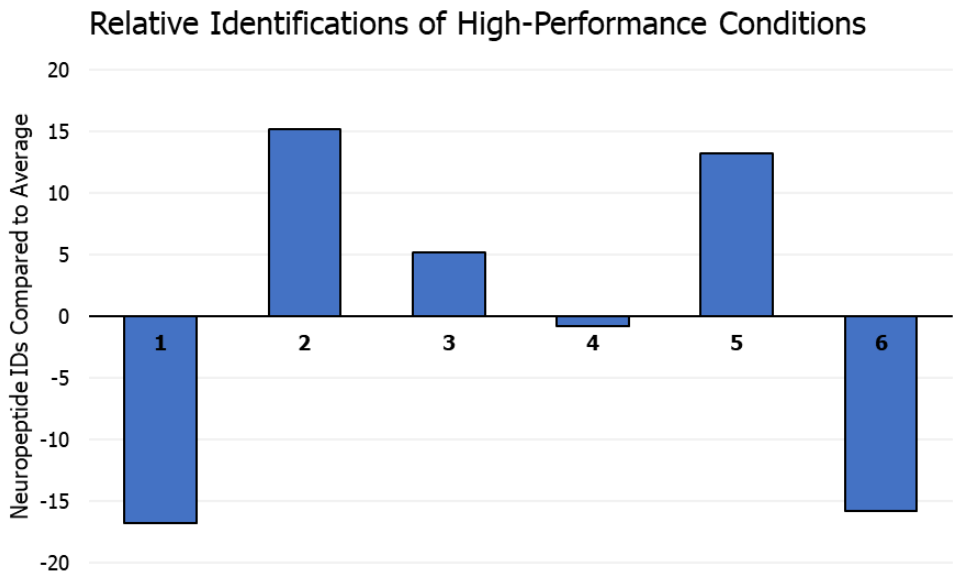

Figure 5: Relative number of neuropeptides identified using the top-performing conditions. An average of 33.8 neuropeptides were identified from the six conditions evaluated. The average is reflected in the x-axis and the deviation from this average is given on the y-axis for each condition.

Table 1: Orthogonal array optimization parameters. Low (L), medium (M), and high (H) values of each parameter are tested in different combinations. The parameter maintains orthogonality by ensuring each parameter couplet occurs the same number of times throughout the 18 total runs.

Run	MS^1 Resolution	MS^2 Resolution	MS^2 Scan Events	Dynamic Exclusion Window	Max Injection Time	AGC Target
1	L	L	L	L	L	L
2	L	L	M	M	M	M
3	L	L	H	H	H	H
4	M	L	L	L	M	M
5	M	L	M	M	H	H
6	M	L	H	H	L	L
7	H	L	L	M	L	H
8	H	L	M	H	M	L
9	H	L	H	L	H	M
10	L	M	L	H	H	M
11	L	M	M	L	L	H
12	L	M	H	M	M	L
13	M	M	L	M	H	L
14	M	M	M	H	L	M
15	M	M	H	L	M	H
16	H	M	L	H	M	H
17	H	M	M	L	H	L
18	H	M	H	M	L	M

Table 2: Evaluation of high-performance conditions. The top four conditions from the initial orthogonal array were evaluated with the parameters given in the table (Conditions 1-4). Conditions 5 and 6 were combinations of parameters informed from the initial orthogonal array results. The number of neuropeptides identified from a secondary sample is given in the final column.

Condition	MS^1 resolution	MS^2 resolution	MS^2 scan events	Dynamic exclusion window	Max injection time	AGC target	IDs
1	60k	60k	35	15 s	100 ms	1e6	17
2	120k	30k	10	30 s	50 ms	1e6	49
3	60k	30k	10	15 s	100 ms	5e5	39
4	120k	60k	25	15 s	200 ms	1e5	33
5	60k	60k	10	15 s	100 ms	5e5	47
6	60k	60k	10	15 s	50 ms	1e6	18

Chapter 6

Multiplexed Quantitative Neuropeptidomics via DiLeu Isobaric Tagging

Adapted from:

Sauer, C.S., Li, L. Multiplexed Quantitative Neuropeptidomics via DiLeu Isobaric Tagging. *Method in Enzymology*, Vol. 633. 2021. (In Print)

Contents:

Abstract

Neuropeptides are key signaling molecules in many pathways and can serve as potential biomarkers or therapeutics. Mass spectrometry has emerged as a powerful tool for studying neuropeptides with high sensitivity and accuracy. Isobaric tagging can further enhance this method by improving throughput and reducing sampling needs. In this chapter, we discuss the benefits and limitations of using isobaric tags to analyze neuropeptides. Methods for optimizing the data acquisition are also presented to enable a greater number of neuropeptides to be identified and quantified when using isobaric tags, specifically N,N-dimethyl leucine (DiLeu).

Keywords: Neuropeptides, Isobaric Labeling, DiLeu, Mass Spectrometry, Optimization, Data-Dependent Acquisition

1. Introduction

Neuropeptides are endogenous signaling peptides synthesized in the neuroendocrine system.[1] These important signal modulators are formed from the cleavage of precursor proteins (pre-prohormones) containing a signal peptide and the active neuropeptide(s). After cleavage, the neuropeptide is post-translationally modified to yield the mature, bioactive neuropeptide.[2] Mature neuropeptides can act in many ways, including local (paracrine) signaling, hormonal signaling, and in conjunction with other signaling molecules (e.g., neurotransmitters). They often target G protein coupled receptors (GPCRs) where they can have a wide range of functions.[3] These functions are also

dependent on many factors, including concentration, location in the organism, and the presence of other neuropeptides that could have co-modulating effects.[4]

As they can be potent, selective signaling molecules, neuropeptides play major roles in many biochemical and physiological processes, such as behavior,[5,6] feeding,[7] stress response,[8–10] and diseases states.[11–13] Neuropeptide function is not independent of its environment, so profiling the entire suite of neuropeptides is critical to our understanding of their functions and related signaling pathways. Developing methods to efficiently characterize and quantify all neuropeptides in a sample is therefore essential to improving our understanding of many diseases and could even provide avenues for biomarker discovery and therapeutics.

Analyzing neuropeptides, however, is easier said than done. These signaling peptides are often present at low abundance *in vivo*, with extracellular concentrations typically in the subfemtomolar range,[14] necessitating efficient extraction methods and highly sensitive instruments. The structural diversity of neuropeptides adds yet another layer of challenges to their analyses. As neuropeptides are transcribed as part of larger proteins, splice variants can arise to yield unique sequences.[2] Additionally, each of these sequences can be, and often are, post-translationally modified to induce structural (and subsequently, functional) changes. These PTMs include, but are not limited to, C-terminal amidation, N-terminal acetylation, methylation, phosphorylation, and the highly variable glycosylation.[15,16] Even though neuropeptides are relatively

small, typically fewer than 40 residues, multiple PTMs on a single neuropeptide can exist.[2] This diversity can result in even lower abundance of a neuropeptidoform (neuropeptide analog of proteoform) of interest.

Mass spectrometry (MS) continues to solidify its place in the field as the most effective method of analyzing neuropeptides. By measuring the mass-to-charge ratio (*m/z*) of analytes, MS can provide users with the mass of the intact neuropeptide. Tandem MS (MS/MS or MS^2), in which precursor ions are selected for fragmentation, results in characteristic backbone fragment ions (typically *b/y* or *c/z*) that can be used to discern more detailed structural information, including amino acid sequence and the residue location of PTMs.[17] Furthermore, MS can provide quantitative information in many ways, such as by evaluating the signal intensity of precursor ions, area under the curve from the chromatogram, or the intensity of diagnostic reporter ions at the MS^2 level.[18] Although other methods exist for characterizing and quantifying neuropeptides, MS is particularly useful as it provides this information with higher throughput and without a priori knowledge of the sample. By rapidly analyzing all analytes in the sample, neuropeptidomic data can be generated with high throughput and without the need for expensive antibodies or the time to develop targeted assays.[18] As neuropeptide function, and the signaling pathways they are involved in, are influenced by the many neuropeptides present in a sample, MS is a powerful tool for studying neuropeptides, their function, and their physiologic regulation.

2. Neuropeptide Multiplexing via Isobaric Tagging

The expression of neuropeptides is highly regulated by different synthesis and degradation pathways. These pathways can be perturbed by a multitude of different diseases,[11–13] stressors,[8–10] or even normal biological functions.[7] Quantifying the expression changes of neuropeptides over time, after a biological event of interest, in different tissue regions, etc. can provide many insights into the regulation, function, and interplay of neuropeptides.[19] Many methods of quantifying neuropeptides by MS exist, with the simplest being label-free quantification (LFQ). These workflows process each sample separately and compare signal intensity, area under the curve, etc. to quantify neuropeptide expression changes across different samples. A more detailed summary of LFQ methods is discussed in a recent review,[18] however, it is worth noting that the major limitations of these methods are low throughput and the requirement for large amounts of samples. Alternatively, using chemical tagging, neuropeptides can be differentially labeled and analyzed in a single MS experiment. These label-based approaches decrease run-to-run variability, the total amount of MS instrument time required, and the number of data files to be processed.[10]

2.1 Isobaric Tagging

With most chemical tagging strategies, stable isotopes (^{13}C, ^{2}H, ^{18}O, ^{15}N) are incorporated into different channels of the tag, thus incorporating different isotopes in the labeled product depending on the channel used. In an isotopic workflow, there exists light and heavy channels that are separated by a few Da due to the heavy

channel containing more/larger isotopes than the light channel. Labeled products (i.e., neuropeptides) are differentiated at the precursor mass level (MS^1) and quantitative information is gained from either area under the curve or peak intensity. Common examples include dimethyl labeling[8,20] and TMAB tags[21] and are summarized in a recent review.[18] As each channel increases the number of peaks in the spectra multiplicatively, spectra quickly become complicated, limiting the capacity for multiplexing.

Isobaric tagging alleviates this by incorporating the same nominal mass, regardless of channel, for a specific tag. Isotopes are strategically placed along the tag such that reporter ions of different masses form upon fragmentation and MS/MS analysis.[22] See **Figure 1**. At the precursor mass level, there is no additional spectral complexity, as all analytes of interest have the same mass addition, and there is only a modest increase in spectral complexity at the MS^2 level. Furthermore, the added peaks from the reporter ions are often in the low mass region (<200 Da) so they do not interfere with the peptide backbone ions (*b/y* or *c/z*). These advantages enable multiplexing capabilities of up to 21-plex using N,N-dimethyl leucine (DiLeu) tags developed in the Li Lab.[23] Additionally, there are commercially available options, such as tandem mass tags (TMT)[24] and isobaric tags for relative and absolute quantitation (iTRAQ).[25] These tags, however, are more expensive and lower throughput than DiLeu, thus we will be focusing on the use of DiLeu in this chapter.

[Figure 1 here]

The structure of the DiLeu tags is given in **Figure 2**. Like many isobaric tags, DiLeu consists of a reporter region that, upon fragmentation, yields unique reporter ions for quantitation, a balance group to ensure the same nominal mass is incorporated at the precursor mass level, and a functional group that enables the tag to be covalently linked to the peptide. In the case of DiLeu, the functional group is an amine-reactive triazine ester that causes DiLeu to label primary amines, such as N-termini and lysine residues.[22] The tags are synthesized readily by the reductive dimethylation of isotopic leucines, and the active triazine ester form is achieved by addition of N-methylmorpholine (NMM) and 4-(4,6-dimethoxy- 1,3,5-triazin-2- yl)-4-methylmorpholinium tetrafluoroborate (DMTMM BF_4). Originally, four tags were conceived with reporter ion masses at *m/z* 115, 116, 117, and 118.[26] With higher mass resolution, however, mDa mass differences arising from different mass additions from stable isotopes can be resolved. This has led to the expansion to a 12-plex labeling strategy (masses shown in **Figure 2**).[22] Very recently, the synthesis of the tags has been altered to allow for more isotopologues and up to 21-plex analyses.[23] This latest generation of DiLeu, however, has not yet been applied to neuropeptidomics, so we will be focusing our discussion on the 4- and 12-plex DiLeu tags.

[Figure 2 here]

2.2 Limitations for Neuropeptidomics

DiLeu has been shown to be effective in analyzing protein digests, resulting in high proteome coverage and quantitative accuracy.[27–29] The analysis of neuropeptides, however, presents some challenges when using isobaric tags, hence the limited publications featuring isobaric tagging of endogenous peptides. Although isobaric tagging offers numerous advantages, it does require that the analyte be selected for fragmentation and subsequent MS^2 analysis to form and measure the reporter ions. With proteins, not every constituent peptide needs to be identified to confidently quantify the starting protein from the sample, so long as there is sufficient sequence coverage. With endogenous peptides, however, the identification can come from only the single intact peptide.

Exacerbating this problem is the simple fact that neuropeptides are expressed with low *in vivo* abundance, and isobaric labeling workflows invariably use data-dependent acquisition (DDA) to collect mass spectra. In DDA analyses, a precursor scan is performed and the top ions (highest peak intensity) from that spectrum are selected for subsequent fragmentation and tandem MS analysis. After a preset number of MS^2 scans, another precursor scan is performed and the process repeats. DDA methods are widely used but are less useful for low level analytes. This is because it is often unlikely that conventional DDA methods will select low abundance analytes, like neuropeptides, for fragmentation and MS/MS analysis. As a result, the peptide backbone ions and reporter ions do not form, prohibiting accurate identification and quantitation of the analyte. Data-independent acquisition (DIA) methods (in which all ions are fragmented

together) are gaining traction in the field of peptidomics[30,31] but are incompatible with isobaric tagging as the reporter ion intensities cannot be deconvoluted from the source peptides. Inclusion lists and other targeted methods like parallel reaction monitoring (PRM)[32] can be useful too, but they lack application for discovery-based experiments or when PTMs are unknown. Comparatively, optimization of DDA parameters can improve the number of neuropeptides identified in an isobaric workflow by increasing the number of unique MS^2 scan events and reducing redundant analyses of higher abundance analytes.[10] In this chapter, we describe a protocol for the extraction, labeling, and LC-MS analysis of neuropeptides with discussion and details on how to optimize the analysis to greatly enhance neuropeptidomic coverage.

3. Protocol

An overview of the protocol is provided in **Figure 3**.

[Figure 3 here]

3.1 Extraction and Purification of Neuropeptides from Tissue

3.1.1 Materials and Equipment

1. Acidified methanol (90/9/1 methanol/water/acetic acid)
2. Resuspension solution: 0.1% formic acid (FA) in water
3. 10% FA in water
4. Elution solution 1: 0.1% FA in 25% acetonitrile (ACN) and 75% water

5. Elution solution 2: 0.1% FA in 50% acetonitrile (ACN) and 50% water

6. Elution solution 3: 0.1% FA in 75% acetonitrile (ACN) and 25% water

7. C_{18} resin-packed pipette tips (e.g., ZipTips or Omix Tips)

8. Ultrasonication probe dismembrator

9. Temperature controlled centrifuge (>20,000 x g)

10. Vacuum centrifuge drying system

3.1.2 Procedure

1. To the tissue sample, add enough acidified methanol to sufficiently cover the tissue. For crustacean brains, this is approximately 50-75 µL.

2. In a cold room (4 °C), use the ultrasonication probe dismembrator to homogenize the tissue and lyse cells. As the probe can generate heat, it is recommended to use a pulse setting with <10 s pulse and >15 s rest between pulses.

3. Centrifuge the homogenized samples at 20,000 x g, 4 °C for 20 min

4. Transfer the supernatant to a clean tube and discard the pellet.

5. Dry down the samples in the vacuum centrifuge.

6. Resuspend samples in 15 µL resuspension buffer and ensure pH <4. Use the 10% FA solution to adjust the pH as needed. Sonicating in a water bath can help resolubilize sample if needed.

7. Purify samples using ZipTips per manufacturer's protocol. In brief, rinse the tip with 50/50 ACN/water and then equilibrate with the resuspension solution. Bind the sample

and then wash with more resuspension solution to remove salts and other contaminants. Elute sequentially with the elution solutions listed above.

8. Pool the elution solutions and dry down under vacuum.

Note: After extracting the neuropeptides, it is important to purify them prior to labeling to ensure minimal interference from other contaminants. C_{18} desalting is an effective means of purification, and we recommend using resin-packed pipettes, such as Millipore ZipTips or Agilent Omix Tips.

3.2 Labeling and Clean-up Steps

3.2.1 Materials and Equipment

1. Labeling Buffer (50/50 ACN/0.5 M triethylammonium bicarbonate, TEAB)

2. Anhydrous N,N-dimethylformamide (DMF)

3. N-methylmorpholine (NMM)

4. 4-(4,6-dimethoxy- 1,3,5-triazin-2- yl)-4-methylmorpholinium tetrafluoroborate (DMTMM)

5. 5% hydroxylamine in water

6. DiLeu tags. The synthesis of these tags has been described in detail by Frost et al.[22] and will not be described here.

7. Pierce Peptide Assay Kit (or another means of quantifying peptide content)

8. Strong cation exchange (SCX) resin-packed tips (e.g., Millipore ZipTips or polyLC TopTips)

9. SCX loading buffer: 0.1% FA, 20% ACN

10. SCX elution buffer: 0.4 M ammonium formate, 20% ACN

11. C_{18} desalting pipette tips and buffers described in 3.1.1

11. Vacuum centrifuge

3.2.2 Procedure

1. Quantify peptide content of purified sample. We recommend using a simple and reliable method, such as a BCA assay or Pierce Peptide Assay kit and following the manufacturer's protocol.

2. Using information from the BCA or peptide assay, resuspend samples in a suitable solution dependent on your sample (e.g., water) and split into 25 µg aliquots. Dry down the aliquots via vacuum centrifugation and store at -80 °C until ready to proceed with labeling.

3. Create fresh activation solution with 495 µL anhydrous DMF, 15.5 mg DMTMM, and 5.18 µL NMM

4. Add 50 µL activation solution to 1 mg of dry DiLeu tag and vortex at room temperature for 30 min. This yields 700 µg of active DiLeu tag capable of labeling primary amines.

5. While the tag is activating, resuspend the dry 25 µg aliquots of purified neuropeptides from Step 2 in 53.57 µL labeling buffer.

6. Add 35.71 µL (500 µg) of the activated label to the resuspended neuropeptides and vortex at room temperature for 1 hour.

Note: The protocol described here is to label a set amount of neuropeptides at a 20:1 label:peptide ratio, but there is room for flexibility. The starting amount of neuropeptides is sample dependent and the rest can be scaled. Additionally, the label:peptide ratio and labeling time can be adjusted by the experimenter. It is important to keep the total organic content (coming from the ACN in the resuspension buffer and DMF in the activation solution) during the labeling reaction at approximately 70% to prevent hydrolysis of the tag and incomplete labeling.

6. Quench the reaction with 4.7 µL 5% hydroxylamine (0.25% final concentration)

7. Pool differentially labeled samples together at this time and dry down via vacuum centrifugation.

Note: After labeling, excess reagents need to be removed. SCX has proven useful for this and we recommend using pipette tips (e.g., Millipore SCX ZipTips), spin tips (e.g., polyLC SCX TopTips), or offline fractionation with a SCX column of choice. The protocol described here is for spin tips.

8. Remove excess labeling reagents using SCX spin tips per manufacturer's protocol. Briefly, resuspend the multiplexed samples in 100 µL SCX loading buffer. Equilibrate the resin with 100 µL loading buffer three times and apply the sample. It is helpful to reapply the sample after it has flown through the tip, up to three times, to ensure binding of sample. Wash the sample with 100 µL loading buffer five times. Elute with 100 µL SCX elution buffer three times. Pool the eluents together and dry down via vacuum centrifugation.

9. To remove the salt (ammonium formate) incorporated during SCX, desalting needs to be performed once again prior to LC-MS analysis. This is achieved using the same protocol as Step 7 of 3.1.2, but due to the increased sample size (from pooling multiple together) it is recommended to use a larger tip with greater binding capacity. Volumes should then be scaled accordingly. Additionally, it is important to use Optima-grade solvents and FA as this is the final purification step prior to LC-MS analysis.
10. Dry down the samples and store at -80 °C until ready for LC-MS analysis.

3.3 LC-MS Analysis

3.3.1 Materials and Equipment

1. C_{18}-packed nanoLC column, 75 µm internal diameter, 15 cm length, 300 Å pore size, either commercially available or self-packed
2. Thermo Q Exactive HF with Dionex UltiMate3000 nanoLC system
3. Mobile phase A: Optima-grade 0.1% FA in water
4. Mobile phase B: Optima-grade 0.1% FA in ACN

3.3.2 Procedure

1. Resuspend the samples in Mobile phase A so the concentration of neuropeptides is approximately 0.5-1 µg/µL.
2. Equilibrate the nanoLC column and set up the gradient for each sample injection: 0-120 min 3-35% B; 120-135 min 95% B; 135-150 min 3% B, all at a flow rate of 0.3 µL/min.

3. Set up a DDA-MS acquisition method with the following parameters: 30k resolving power for both MS^1 and MS^2; 2 kV spray voltage; 200-2000 m/z precursor scan range; 100 m/z fixed first mass for MS^2 scans; normalized collision energy of 27; AGC target of 5e5 and 1e5 for MS^1 and MS^2 respectively; maximum injection time of 150 ms and 250 ms for MS^1 and MS^2 respectively; isolation window width of 2.0 m/z; 39 MS^2 scan events; 35 s dynamic exclusion window.

4. Inject 1-2 µL of sample with up to three technical replicates and a blank run between samples.

Note: The values listed above were those found to be optimal or sufficient for 4-plex labeled neuropeptides.[10] The true optimal values are dependent on the sample, instrument, etc. Optimization techniques are described in section 4.

3.4 Data Analysis

There are different software packages that can be used to analyze multiplexed DiLeu data. There are commercially available options, such as Proteome Discoverer and PEAKS, that allow users to add custom isobaric tags to the search parameters. Open-source programs like MaxQuant can also be viable alternatives. In general, an analyst needs software that is compatible with the file type they collect (not all instruments produce the same data type) and that are reliable for quantitation in isobaric workflows. We chose to use Proteome Discoverer and detail a procedure below for the analysis of neuropeptide data.

3.4.1 Procedure

1. Import the data and database into Proteome Discoverer (we used version 2.1).

2. Create a data processing method for searching the data: Precursor min/max masses of 350/5000 Da; 25 ppm precursor mass tolerance; 0.2 Da fragment mass tolerance; 1% target false discovery rate (FDR); co-isolation threshold of 50%; static DiLeu modification of N-termini and Lys; C-terminal amidation for peptides known to be amidated endogenously; dynamic deamidation of Asn and Gln; dynamic dehydration of Ala, Asp, Glu, Ser, Thr, and Tyr; dynamic methylation of Asp, Glu, His, Arg, Ser, Thr; and three max modifications per peptide. A detailed overview of the Proteome Discoverer workflow used here can be found in the supplemental information.

3. Process the data to benchmark method performance (comparing LC-MS methods during optimization), or to quantify changes in a system (comparing experimental conditions to a control).

4. If performing statistical analyses, exporting the data to the proper software (e.g., Excel) is necessary. There the necessary statistical tests can be performed, such as t-tests, ANOVA, Dunnett's test, and other means of determining statistically significant changes between samples.

4. Optimization of MS Data Acquisition

Several instrument parameters influence the analytes selected by DDA analyses, and these can vary greatly depending on instrument. For our analyses, we utilize Orbitrap mass spectrometers, and our discussion will be focused on them. It is worth noting that

the overall methods and workflows presented here are transferrable to other instrument types. In a DDA workflow, the user defines the number of tandem MS scans acquired per precursor scan (MS^2 scan events), the minimum amount of time required to pass before acquiring an MS^2 scan of an *m/z* previously acquired (dynamic exclusion window), the isolation window, the targeted amount of ions to be injected (automatic gain control target, or AGC target), and the amount of time allowed to accumulate ions prior to injection (maximum injection time), among others. Additionally, other parameters, such as the resolving power, do not directly contribute to DDA, but influence the duty cycle and total number of spectra that can be acquired.

The goal for optimizing these various parameters is to increase the number of acquired MS^2 scans for low abundance neuropeptides, decrease oversampling of high abundance analytes, and minimize the number of low-quality spectra. Optimizing the parameters listed above can be beneficial but is not so straightforward. For example, increasing the maximum injection time to allow more time for ions to accumulate from low abundance analytes could allow more neuropeptides to be identified from the acquired spectra, but it would also increase the cycle time and decrease the total number of acquired spectra from which to identify neuropeptides. Similarly, reducing the AGC target may allow more low abundance analytes to be sampled, but could also result in decreased signal-to-noise ratio (S/N) and therefore decreased confidence in the results.

Further complicating optimization progress, there is interplay between parameters that is difficult to predict but needs to be considered. While some interplay can be more easily predicted, such as needing to increase the maximum injection time in order to reach a higher AGC target, others are less clear. Increasing the number of MS^2 scan events, for example, could result in sampling some neuropeptides too early (i.e., not at the highest peak intensity), and if the dynamic exclusion window is set too high, that neuropeptide may not be sampled again and not be identified/quantified due to poor signal. Due to the complex influence and co-dependence of various DDA parameters, thorough, simultaneous optimization of parameters is required to facilitate deeper neuropeptidomic coverage when using isobaric tags. In this section, we describe two different methods of optimization for DDA parameters.

4.1 Orthogonal Array Optimization

Optimization of parameters can be performed using complex modeling and statistical analysis, but developing these models is complex, requires many tests, and does not guarantee efficacy for experiments. Design of experiments (DoE) can be useful for efficiently evaluating different sets of conditions.[33,34] The simplest of these is the factorial DoE in which different levels (x) of each parameter (y) are tested in a combinatorial fashion, requiring y^x tests.[35] This is feasible for small numbers, but quickly becomes time and resource intensive to evaluate many conditions. Alternatively, using an orthogonal array optimization (OAO) or Taguchi array, greatly improves efficiency. Using this method, an array of values is generated that determine the level of each

factor tested for a given experiment.[36] The orthogonality of these arrays results in a table in which combinations of values from each column appear the same number of times across the array.[37] This facilitates estimation of the same sample space as the more exhaustive factorial DoE but with far fewer total experiments. Different orthogonal arrays depending on the number of factors and levels to be explored have already been created and published, so the OAO method is readily accessible for new users. These arrays have notation of L_n (x^y), where L is for Latin squares, n is the number of rows, y is the number of factors, and x is the number of levels of each factor.[37]

In the context of optimizing DDA parameters, the OAO method is useful because it allows many parameters to be analyzed simultaneously while keeping the total number of experiments low. As an example, if seven parameters (number of MS^2 scans, dynamic exclusion window, isolation window, AGC target, maximum injection time, MS^1 resolution, and MS^2 resolution) are to be evaluated at two levels (low/high), a full factorial DoE would require 7^2 or 49 total experiments. Alternatively, by using an L_8 (2^7) orthogonal array (**Table 1**), only 8 total experiments need to be performed. If performing technical replicates, the benefits of the OAO method are even greater. Reducing the number of experiments not only reduces the time required, but also reduces the total amount of sample needed and the run-to-run variability due to instrumental drift.

[Table 1 here]

When evaluating the different experiments, the performance metrics are determined by the outcome the experimenter is trying to achieve. In an isobarically labeled neuropeptide workflow, this could be an increase in the number of identifiable neuropeptides, the quantitative accuracy (determined from the observed reporter ion ratios compared to the known ratios based upon how samples were pooled together), etc. When optimizing for a specific outcome, the experimenter can use the information from the OAO to better understand the interplay between factors and which factors have a greater effect on the outcome of the experiments. These factors can then be the subject of more extensive optimization (demonstrated in section 4.2).

4.2 Systematic Simplex Optimization

Design of experiments, like OAO, can provide experimenters with sufficient optimization to analyze neuropeptides, but more extensive optimization can offer further improvements. Using the knowledge gained from a DoE, or sometimes literature searches, the most impactful parameters can be determined. Systematically optimizing these parameters can then yield greater improvement in neuropeptidomic workflows as demonstrated in a recent publication.[10] Similar to DoE, there are different options for systematically optimizing select parameters, but we will focus on the simplex optimization strategy in this section as it is simple and capable of simultaneous optimization.

In a simplex optimization strategy, an initial set of conditions (simplex) is assessed, and the optimization is visualized graphically. The conditions are then ranked by performance (determined by the desired outcome of optimization) and the next set of conditions is generated in the geometric opposition of the condition of worst performance.[38] As more simplexes are evaluated, the conditions move toward optimization, and optimization is achieved experimentally when additional simplexes provide no increase in performance. An overview is shown in **Figure 4a**. Reaching the optimum values for each parameter can be time consuming, so the simplex method can be modified to expedite the process. In a modified simplex algorithm, the geometric reflection (R) is evaluated along with the addition of an elongated reflection (E), contracted reflection (C_R), and a contraction toward the point of worst performance (C_W)[38] (**Figure 4b**). By testing additional points in each simplex, the total number of simplexes that need to be tested can be reduced.

[Figure 4 here]

For the application of the simplex method, the experimenter must first generate an initial simplex of three vertices to be tested. These points should be based upon prior knowledge or published research for reasonable values of the selected parameters. After evaluating the initial simplex, the vertices are ranked by performance as best (B), second-best (S), and worst (W). The next simplex is generated by reflecting W across the midpoint of BS. The equations for these reflections are summarized in **Table 2**.

After evaluating the new points, the top performing condition of R, E, C_R, and C_W is ranked along with the best and second-best conditions from the prior simplex to generate a new BSW simplex. Again, W is reflected across the midpoint of BS as dictated by the equations in **Table 2**, the new points are evaluated, and the process repeats itself until an optimum is reached. A recent application of this method can be found in a publication by Sauer and Li. Briefly, two parameters were selected for simultaneous optimization–the dynamic exclusion window and the number of MS^2 scan events. Keeping other factors constant, 3 paired sets of conditions were evaluated based upon the number of neuropeptides that could be identified from a constant sample. After the first three conditions were evaluated, a second set of conditions was selected in the geometrically opposed region of the worst performing point. These second conditions were evaluated, and a third set of conditions was selected, again moving away from low performing points. In the initial points, only 25-30 neuropeptides were able to be identified. By the end of the optimization (reached when additional points provide no further improvement), 88 neuropeptides were able to be identified. This approximate 3-fold increase in identifications allowed the method to be used for the study of neuropeptide expression changes resulting from copper toxicity.

[Table 2 here]

Although effective, the simplex optimization does have limitations. Compared to the OAO, one of the major disadvantages to the simplex method is the time required for

optimization. Data must be collected and analyzed between simplexes so the next simplex can be generated, instead of comparing all conditions at once. Additionally, although the method is amenable to simultaneous optimization of several factors, it becomes impossible to visualize graphically with more than three factors. Equations for determining the geometric reflections in extended dimensions exist, but these do not mitigate the number of experiments that need to be performed. As each additional factor for optimization increases the number of vertices in each simplex, it is less feasible to use the simplex method to optimize more than 2-3 parameters.

5. Applications of Isobaric Tagging in Neuropeptidomics

The methods described in this chapter can help facilitate the application of isobaric labeling to neuropeptidomic workflows. One of the first published works in this area compared neuropeptides in lobster brains at different growth stages using 4-plex DiLeu tags.[39] This work by Jiang et al. did not employ extensive optimization, but nonetheless showed the feasibility in using isobaric tags to study neuropeptide expression changes. Building on this work, Sauer and Li reported the benefits of the modified simplex optimization described in section 4.2 and increased the neuropeptidomic coverage by approximately 3-fold in a single LC-MS run using 4-plex DiLeu tags.[10] Using these methods, neuropeptide expression changes were able to be quantified over time during acute copper exposure. Furthermore, several statistically significant changes were observed, demonstrating the potential role of allatostatin neuropeptides and others in the stress response to heavy metals like copper.[10] In addition to using DiLeu to

measure neuropeptides, isobaric tagging can influence neuropeptidomic studies by studying the associated neuroproteome. Liu et al. demonstrated the benefits of extracting both proteins and neuropeptides from the mouse brain and quantifying them using DiLeu and LFQ respectively.[27] Although the isobaric tagging approach is not used for neuropeptides, this work highlights the use of using DiLeu in a multi-omic workflow to better understand the neuroendocrine system. Isobaric tagging of neuropeptides is still relatively new, but we expect increased application in the future as the need for high-throughput, quantitative neuropeptidomics continues to increase.

6. Summary

The investigation of neuropeptides and their roles in signaling pathways has great potential to improve understanding of many biological processes, disease, etc., but requires sensitive, high-throughput analyses. LC-MS analysis of isobarically tagged neuropeptides enables robust quantitation with higher orders of multiplexing than isotopic labeling and LFQ methods. As neuropeptides are of low abundance *in vivo*, they are often omitted from tandem MS analyses and go without identification or quantitation. Design of experiments and simplex optimization require initial time investment but can greatly improve the depth of coverage of the neuropeptidome, enabling future studies of the neuroendocrine system.

Acknowledgements

This work was supported by National Science Foundation (CHE-1710140 and CHE-2108223) and National Institutes of Health through grants (R01DK071801, RF1 AG052324, and P41GM108538). C.S.S. acknowledges a National Institute of Environmental Health Sciences fellowship as part of the National Ruth L. Kirschstein Research Service Award fellowship program (F31ES031859). L.L. acknowledges a Vilas Distinguished Achievement Professorship and Charles Melbourne Johnson Professorship with funding provided by the Wisconsin Alumni Research Foundation and University of Wisconsin-Madison School of Pharmacy.

References

1. Christie AE, Stemmler EA, Dickinson PS. Crustacean neuropeptides. *Cell Mol Life Sci*. 2010;67(24):4135-4169. doi:10.1007/s00018-010-0482-8

2. Hook V, Lietz CB, Podvin S, Cajka T, Fiehn O. Diversity of Neuropeptide Cell-Cell Signaling Molecules Generated by Proteolytic Processing Revealed by Neuropeptidomics Mass Spectrometry. *J Am Soc Mass Spectrom*. 2018;29(5):807-816. doi:10.1007/s13361-018-1914-1

3. Romanova E V, Sweedler J V. Peptidomics for the discovery and characterization of neuropeptides and hormones. *Trends Pharmacol Sci*. 2015;36(9):579-586. doi:10.1016/j.tips.2015.05.009

4. Li L, Sweedler J V. Peptides in the Brain: Mass Spectrometry–Based Measurement Approaches and Challenges. *Annu Rev Anal Chem*. 2008;1(1):451-483. doi:10.1146/annurev.anchem.1.031207.113053

5. Hu M, Helfenbein K, Buchberger AR, Delaney K, Liu Y, Li L. Exploring the Sexual Dimorphism of Crustacean Neuropeptide Expression Using Callinectes sapidus as a Model Organism. *J Proteome Res*. 2021;20:2739-2750. doi:10.1021/acs.jproteome.1c00023

6. Han B, Fang Y, Feng M, et al. Quantitative Neuropeptidome Analysis Reveals Neuropeptides Are Correlated with Social Behavior Regulation of the Honeybee Workers. *J Proteome Res*. 2015;14(10):4382-4393. doi:10.1021/acs.jproteome.5b00632

7. DeLaney K, Hu M, Hellenbrand T, Dickinson PS, Nusbaum MP, Li L. Mass spectrometry quantification, localization, and discovery of feeding-related neuropeptides in cancer borealis. *ACS Chem Neurosci*. 2021. doi:10.1021/acschemneuro.1c00007

8. Buchberger AR, Sauer CS, Vu NQ, DeLaney K, Li L. A Temporal Study of the Perturbation of Crustacean Neuropeptides Due to Severe Hypoxia Using 4-Plex Reductive Dimethylation. *J Proteome Res*. 2020;19:1548-1555. doi:10.1021/acs.jproteome.9b00787

9. Liu Y, Buchberger AR, Delaney K, Li Z, Li L. Multifaceted Mass Spectrometric Investigation of Neuropeptide Changes in Atlantic Blue Crab, Callinectes sapidus , in Response to Low pH Stress. *J Proteome Res*. 2019;18:2759-2770. doi:10.1021/acs.jproteome.9b00026

10. Sauer CS, Li L. Mass Spectrometric Profiling of Neuropeptides in Response to Copper Toxicity via Isobaric Tagging. *Chem Res Toxicol*. 2021. doi:10.1021/acs.chemrestox.0c00521

11. Li C, Wu X, Liu S, et al. Roles of Neuropeptide Y in Neurodegenerative and Neuroimmune Diseases. *Front Neurosci*. 2019;13:1-11. doi:10.3389/fnins.2019.00869

12. Hulme H, Fridjonsdottir E, Gunnarsdottir H, et al. Neurobiology of Disease Simultaneous mass spectrometry imaging of multiple neuropeptides in the brain and alterations induced by experimental parkinsonism and L-DOPA therapy. *Neurobiol Dis*. 2020;137(December 2019):104738. doi:10.1016/j.nbd.2020.104738

13. Hulme H, Fridjonsdottir E, Gunnarsdottir H, et al. Simultaneous mass spectrometry imaging of multiple neuropeptides in the brain and alterations induced by

experimental parkinsonism and L-DOPA therapy. *Neurobiol Dis*. 2020;137(December 2019):104738. doi:10.1016/j.nbd.2020.104738

14. Maes K, Van Liefferinge J, Viaene J, et al. Improved sensitivity of the nano ultra-high performance liquid chromatography-tandem mass spectrometric analysis of low-concentrated neuropeptides by reducing aspecific adsorption and optimizing the injection solvent. *J Chromatogr A*. 2014;1360:217-228. doi:10.1016/j.chroma.2014.07.086

15. Mast DH, Checco JW, Sweedler J V. Differential post-translational amino acid isomerization found among neuropeptides in aplysia californica. *ACS Chem Biol*. 2020;15(1):272-281. doi:10.1021/acschembio.9b00910

16. Cao L, Qu Y, Zhang Z, Wang Z, Prykova I, Wu S. Intact Glycopeptide Characterizatoin Using Mass Spectrometry. *Physiol Behav*. 2017;176(3):139-148. doi:10.1586/14789450.2016.1172965.Intact

17. Buchberger A, Yu Q, Li L. Advances in Mass Spectrometric Tools for Probing Neuropeptides. *Annu Rev Anal Chem*. 2015;8(1):485-509. doi:10.1146/annurev-anchem-071114-040210

18. Sauer CS, Phetsanthad A, Riusech OL, Li L. Developing Mass Spectrometry for the Quantitative Analysis of Neuropeptides. *Expert Rev Proteomics*. 2021. doi:10.1080/14789450.2021.1967146

19. DeLaney K, Buchberger AR, Li L. Chapter 17: Identification, Quantitation, and Imaging of the Crustacean Peptidome. In: *Methods in Molecular Biology*. Vol 1719. ; 2018:247-269. doi:10.1007/978-1-4939-7537-2_18

20. Tashima AK, Fricker LD. Quantitative Peptidomics with Five-plex Reductive Methylation labels. *J Am Soc Mass Spectrom*. 2017;29:866-878. doi:10.1007/s13361-017-1852-3

21. Boonen K, Haes W De, Houtven J Van, et al. Chapter 9 Quantitative Peptidomics with Isotopic and Isobaric Tags. In: *Peptidomics: Methods and Strategies, Methods in Molecular Biology*. Vol 1719. ; 2018:141-159.

22. Frost DC, Greer T, Li L. High-resolution enabled 12-plex DiLeu isobaric tags for quantitative proteomics. *Anal Chem*. 2015;87(3):1646-1654. doi:10.1021/ac503276z

23. Frost DC, Feng Y, Li L. 21-plex DiLeu Isobaric Tags for High-Throughput Quantitative Proteomics. *Anal Chem*. 2020;92(12):8228-8234. doi:10.1021/acs.analchem.0c00473

24. Li J, Vranken JG Van, Vaites LP, et al. TMTpro reagents: a set of isobaric labeling mass tags enables simultaneous proteome-wide measurements across 16 samples. *Nat Methods*. 2020;17(April). doi:10.1038/s41592-020-0781-4

25. Wiese S, Reidegeld KA, Meyer HE, Warscheid B. Protein labeling by iTRAQ: A new tool for quantitative mass spectrometry in proteome research. *Proteomics*. 2007;7(3):340-350. doi:10.1002/pmic.200600422

26. Xiang F, Ye H, Chen R, Fu Q, Li N. N,N-Dimethyl leucines as novel Isobaric tandem mass tags for quantitative proteomics and peptidomics. *Anal Chem*. 2010;82(7):2817-2825. doi:10.1021/ac902778d

27. Liu R, Wei P, Keller C, et al. Integrated Label-Free and 10-Plex DiLeu Isobaric Tag Quantitative Methods for Pro fi ling Changes in the Mouse Hypothalamic

Neuropeptidome and Proteome: Assessment of the Impact of the Gut Microbiome. *Anal Chem*. 2020;92:14021-14030. doi:10.1021/acs.analchem.0c02939

28. Yu Q, Zhong X, Chen B, et al. Isobaric Labeling Strategy Utilizing 4-Plex N, N-Dimethyl Leucine (DiLeu) Tags Reveals Proteomic Changes Induced by Chemotherapy in Cerebrospinal Fluid of Children with B-Cell Acute Lymphoblastic Leukemia. *J Proteome Res*. 2020;19(7):2606-2616. doi:10.1021/acs.jproteome.0c00291

29. Hao L, Thomas S, Greer T, et al. Quantitative proteomic analysis of a genetically induced prostate inflammation mouse model via custom 4-plex DiLeu isobaric labeling. *Am J Physiol - Ren Physiol*. 2019;316(6):F1236-F1243. doi:10.1152/ajprenal.00387.2018

30. Zhong X, Frost DC, Yu Q, Li M, Gu TJ, Li L. Mass Defect-Based DiLeu Tagging for Multiplexed Data-Independent Acquisition. *Anal Chem*. 2020;92(16):11119-11126. doi:10.1021/acs.analchem.0c01136

31. Delaney K, Li L. Data Independent Acquisition Mass Spectrometry Method for Improved Neuropeptidomic Coverage in Crustacean Neural Tissue Extracts. *Anal Chem*. 2019;91(8):5150-5158. doi:10.1021/acs.analchem.8b05734

32. Saidi M, Kamali S, Beaudry F. Neuropeptidomics: Comparison of parallel reaction monitoring and data-independent acquisition for the analysis of neuropeptides using high-resolution mass spectrometry. *Biomed Chromatogr*. 2019;33(7):1-11. doi:10.1002/bmc.4523

33. Hecht ES, McCord JP, Muddiman DC. Definitive Screening Design Optimization of Mass Spectrometry Parameters for Sensitive Comparison of Filter and Solid Phase

Extraction Purified, INLIGHT Plasma N-Glycans. *Anal Chem*. 2015;87(14):7305-7312. doi:10.1021/acs.analchem.5b01609

34. Randall SM, Cardasis HL, Muddiman DC. Factorial experimental designs elucidate significant variables affecting data acquisition on a quadrupole orbitrap mass spectrometer. *J Am Soc Mass Spectrom*. 2013;24(10):1501-1512. doi:10.1007/s13361-013-0693-y

35. Andrews GL, Dean RA, Hawkridge AM, Muddiman DC. Improving proteome coverage on a LTQ-orbitrap using design of experiments. *J Am Soc Mass Spectrom*. 2011;22(4):773-783. doi:10.1007/s13361-011-0075-2

36. Rao RS, Kumar CG, Prakasham RS, Hobbs PJ. The Taguchi methodology as a statistical tool for biotechnological applications: A critical appraisal. *Biotechnol J*. 2008;3(4):510-523. doi:10.1002/biot.200700201

37. Bolboacă SD, Jäntschi L. Design of experiments: Useful orthogonal arrays for number of experiments from 4 to 16. *Entropy*. 2007;9(4):198-232. doi:10.3390/e9040198

38. Bezerra MA, dos Santos QO, Santos AG, Novaes CG, Ferreira SLC, de Souza VS. Simplex optimization: A tutorial approach and recent applications in analytical chemistry. *Microchem J*. 2016;124:45-54. doi:10.1016/j.microc.2015.07.023

39. Jiang X, Xiang F, Jia C, Buchberger AR, Li L. Relative Quantitation of Neuropeptides at Multiple Developmental Stages of the American Lobster Using *N* , *N* -Dimethyl Leucine Isobaric Tandem Mass Tags. *ACS Chem Neurosci*. 2018:acschemneuro.7b00521. doi:10.1021/acschemneuro.7b00521

Figures/Tables

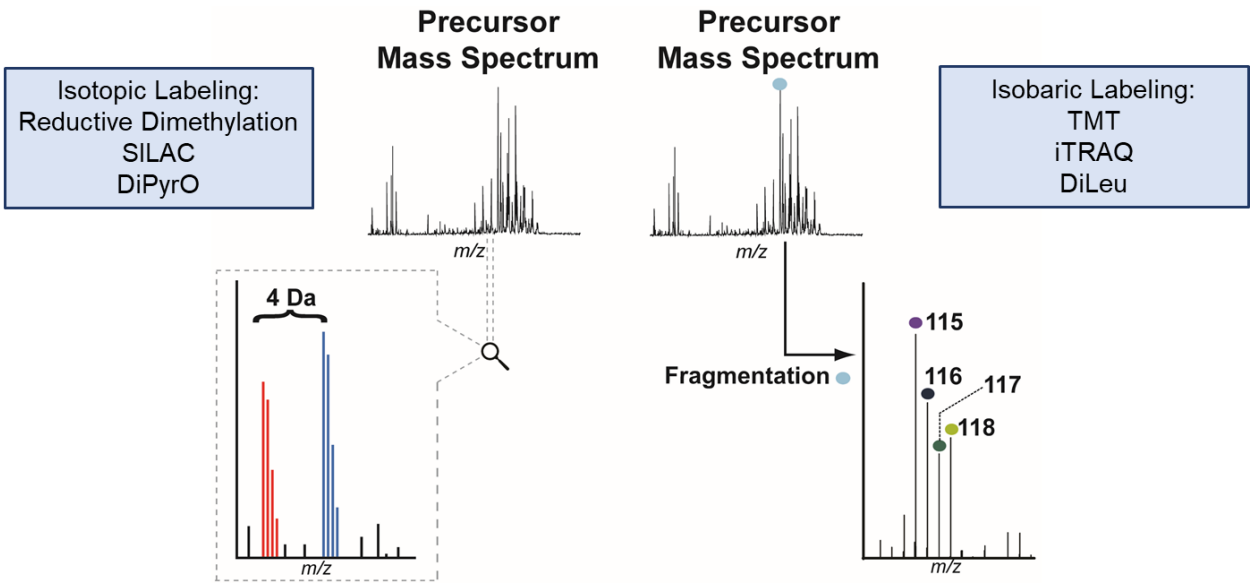

Figure 1: Isotopic *vs.* Isobaric Labeling. In an isotopic workflow, stable isotopes are incorporated to create a mass shift between differentially labeled samples (left). Isobaric tagging results in no mass shift between samples, but instead yields unique reporter ions at the MS^2 level that correlate to relative abundances from each sample (right).

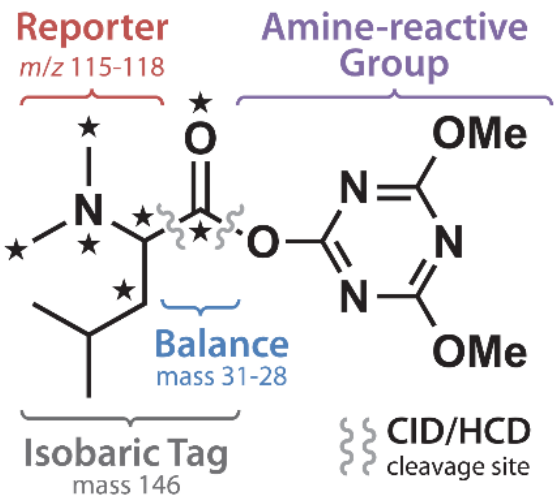

DiLeu Label	Stable Isotopes		Reporter Mass
	Reporter	Balance	
115a	●	●●	115.12476
115b	●	●●	115.13108
116a	●●	●	116.12812
116b	●●	●	116.13444
116c	●●	●	116.14028
117a	●●●	●	117.13147
117b	●●●	●	117.13731
117c	●●●	●	117.14363
118a	●●●●		118.13483
118b	●●●●		118.14067
118c	●●●●		118.14699
118d	●●●●		118.15283

● ^{13}C ● ^{2}H ● ^{15}N ● ^{18}O

Figure 2: DiLeu structure and masses. The chemical structure of the activated DiLeu tag is shown with stars denoting locations for stable isotope incorporation. The table beneath the structure shows the reporter ion masses for each of the 12-plex channels, along with the isotope placement for each tag. This figure was reprinted with permission from Frost et al.[22]

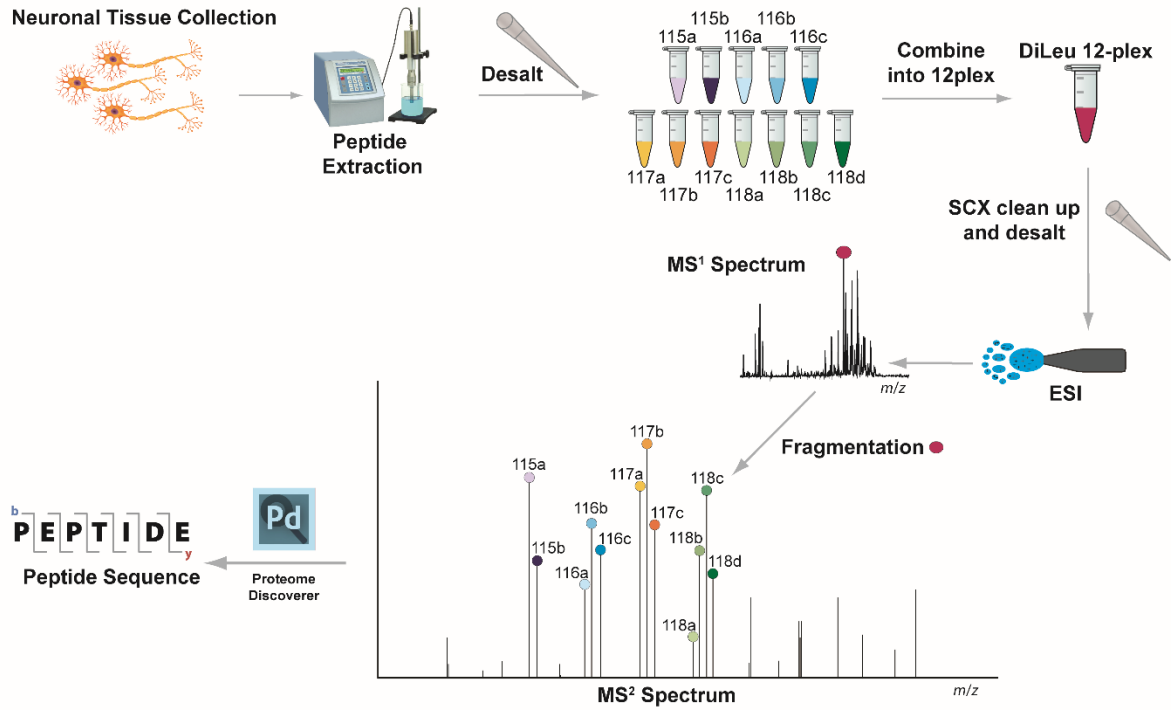

Figure 3: Overall neuropeptidomic workflow. In brief, neuropeptides are extracted from tissues, cells, or fluids via ultrasonication. These neuropeptides are then desalted and purified so they can be labeled with DiLeu tags. The differentially labeled samples are then pooled and cleaned up further using SCX and C_{18} desalting before being analyzed by LC-MS. Data is then analyzed by Proteome Discoverer 2.1 to identify and quantify neuropeptides in the sample.

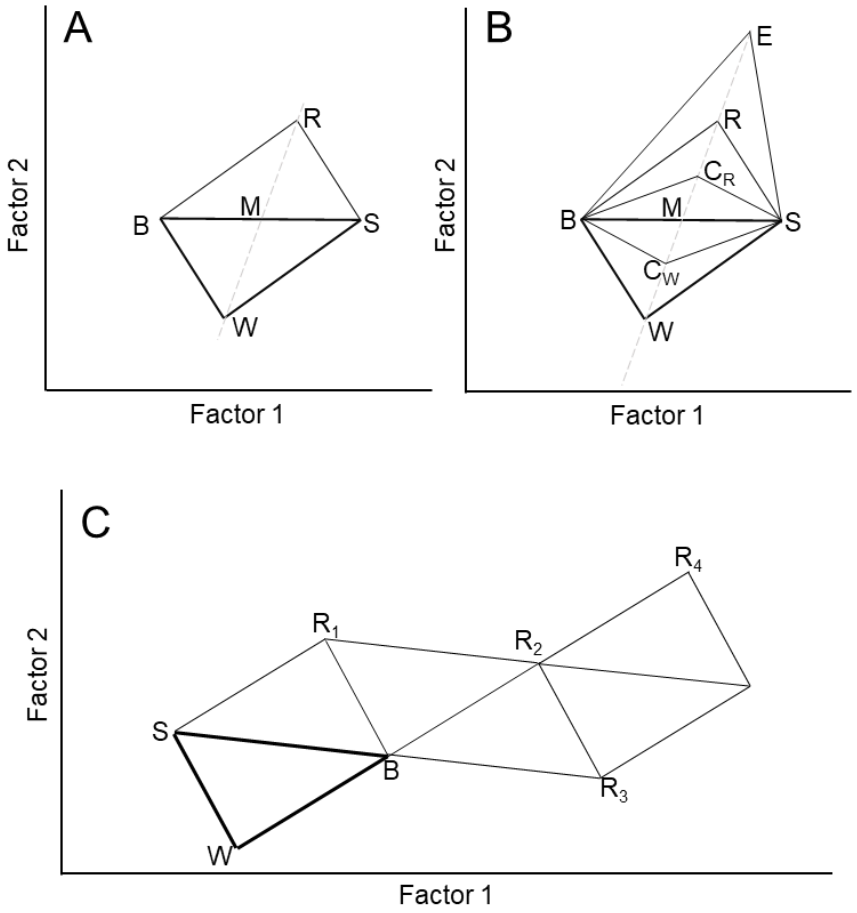

Figure 4: Simplex optimization overview. The basic simplex is given in A and shows the reflection (R) across the midpoint of the best (B) and second-best (S) vertices away from the worst vertex (W). Modifications to the workflow are given in B, where the next simplex also includes an elongated reflection (E), contracted reflection (C_R), and a contracted reflection towards W (C_W). The process of reflecting away from the worst performing points is repeated until an optimum is reached. This is shown in C where the reflected vertices are sequentially labeled R_1, R_2, etc.

Table 1: Orthogonal array optimization. In this L_8 (2^7) array, 7 parameters are evaluated at two levels each, high (H) and low (L).

Experiment	MS^2 scan events	Dynamic Exclusion Window	Isolation Window	AGC Target	Maximum Injection Time	MS^1 Resolution	MS^2 Resolution
1	H	H	H	H	H	H	H
2	H	H	H	L	L	L	L
3	H	L	L	H	H	L	L
4	H	L	L	L	L	H	H
5	L	H	L	H	L	H	L
6	L	H	L	L	H	L	H
7	L	L	H	H	L	L	H
8	L	L	H	L	H	H	L

Table 2: Simplex modification equations. These equations are used to determine the new vertices to test. A is the average of points B and S (best and second-best), and W is the worst performing point. These equations are to be used for each factor being tested–if two factors are being tested, there will be two values making each coordinate point, and the equations need to be used twice to generate a new coordinate in the x,y grid.

Vertex	Geometric Translation	Equation
R	Reflection	$2A - W$
E	Elongated Reflection	$3A - 2W$
C_R	Contracted Reflection	$1.5A - 0.5W$
C_W	Contracted Reflection towards W	$0.5A + 0.5W$

Chapter 7

Relative Quantitation of Intact Metallothionein Proteins via Isobaric DiLeu Tags

Abstract

Top-down mass spectrometry is capable of providing more detailed structural information and discernment between proteoforms but has room for growth in terms of quantitation. Isobaric tagging can provide relative quantitation of many samples without added precursor mass complexity, making it amenable to the analysis of intact proteins. Isobaric tagging is frequently demonstrated in the analysis of peptides but has had limited used in top-down analyses. Here, N,N-dimethyl leucine (DiLeu) isobaric tags are applied to the analysis of intact metallothionein proteins. Using a modified reduction and alkylation approach, all 20 cysteine residues of these proteins can be alkylated with high efficiency, enabling effective isobaric tagging without side reactions. Acetone precipitation is used to quickly isolate the metallothionein proteins from the excess tagging reagents to facilitate mass spectrometry analysis of the intact proteins. The modified isobaric tagging workflow resulted in high quantitative accuracy across a 20-fold dynamic range, demonstrating reliable performance for future biological applications.

Introduction

Copper is a growing environmental concern as aqueous copper concentrations are increasing due to agricultural runoff, industrial pollution, and poorly managed wastewater.[1] Additionally, the bioavailability of copper is increasing as atmospheric carbon dioxide causes acidification of ocean water.[2] Copper is a necessary nutrient with important roles in protein structure,[3] enzyme activity,[4] and signal modulation.[5] At

elevated levels, however, copper has toxic effects as it can disrupt ion channels and, more importantly, it can participate in redox reactions to cause oxidative stress.[6] As a result, maintaining metal homeostasis is critical to ensure normal physiological processes can continue without incurring harm.[7] Heavy metals like copper are tightly regulated by different chelating molecules, such as metallothionein proteins (MTs),[8,9] and antioxidants, like glutathione.[10] These molecules bind, chaperone, and transport metals so they can be metabolized or excreted. Dysregulation of metallothionein proteins has deleterious effects and has been implicated in genetic disorders (e.g., Wilson's disease and Menke's disease)[11] and neurological disorders (e.g., Alzheimer's disease).[12,13] Characterization of MTs is therefore critical not only for the study of environmental toxicity, but also related diseases.

MTs are a family of proteins that are well-conserved amongst organisms. These proteins are low molecular weight (6-7 kDa) and highly cysteine-rich (~30%).[9] The sulfhydryl groups of the cysteine residues coordinate metal ions. **Figure 1** depicts the 3D structure of a MT along with its sequence. Despite their conserved structure, different MTs are capable of binding different metals with high specificity, and as a result, they are involved in different biological processes. MTs are often studied using spectrophotometry assays or SDS-PAGE, but these methods do not always provide metal-binding information, post-translational modification status, and differentiation of structurally similar proteins.[14] Conversely, mass spectrometry (MS) is capable of providing this information with high sensitivity and can also enable quantitation of the proteins. Typically, this is achieved by bottom-up proteomics in which the MTs are

digested and detected by liquid chromatography (LC)-MS.[11,15–17] The peptide fragments have considerable overlap due to the structural similarities of the MTs, leading to potentially ambiguous identifications.

Alternatively, studying the intact proteins by top-down MS allows for the discernment of MTs and identification of different PTMs. Studying intact proteins is, however, more difficult as the larger mass requires a greater resolving power to accurately interpret spectra. Additionally, dynamic tertiary structure can lead to poor chromatographic separations and less efficient labeling. Smaller proteins, like MTs, are less susceptible to some of these issues, but the challenges are still present. Despite these challenges, developing methods to not only characterize MTs using top-down MS, but also quantify the different proteoforms present in a sample has potential impacts in the study of many diseases and biochemical processes.

Quantitative MS strategies have certainly matured but are less developed for the study of intact proteins. Label-free quantitation (LFQ) methods are routinely used in top-down MS.[18] Using these methods, samples are analyzed separately, and proteins are quantified by peak intensity or area under the curve.[19] The relative signal of a specific proteoform is compared to the total signal of the protein to quantify the presence of a given feature. LFQ methods are able to quantify many proteins and proteoforms but lack throughput as experimental conditions must be analyzed separately. Labeling strategies allow multiple samples to be differentially labeled and analyzed simultaneously to reduce overall sample needs, instrumental drift, and analysis times.[20] Isotopic labeling methods, including stable isotope labeling by amino acids in

cell culture (SILAC), have been reported.[21] These methods allow some degree of multiplexing, but the overlap in isotopic envelopes for differentially labeled samples makes deconvolution difficult and less reliable. Alternatively, isobaric tagging incorporates the same nominal mass for each channel, resulting in far less complicated mass spectra. Quantitation is performed at the MS^2 level by the relative intensities of unique reporter ions from each channel. Isobaric tagging has had limited applications to top-down MS due to the challenges with labeling intact proteins but has been successfully reported using tandem mass tags (TMT)[22] and the thiol-reactive version of TMT, iodoTMT.[23] These commercially available tags are robust, but costly for many academic labs. Conversely, the feasibility of using a cost-effective, custom synthesized isobaric tag, *N,N*-dimethyl leucine (DiLeu),[24] is demonstrated here.

In this study, a commercially available rabbit MT isolate containing different MT isoforms was used to develop a workflow for the analysis of DiLeu-labeled MTs to facilitate multiplex quantitation of intact proteins. DiLeu tags were initially developed as 4-plex isobaric tags for bottom-up proteomics experiments[24] and later expanded to 12-plex[25] and 21-plex versions.[26] The tags label primary amines, such as N-termini and Lys residues. Applying these tags to intact MTs can be difficult as acetylation of the N-terminus is a conserved PTM. Additionally, the many cysteine residues can react with tags to form unwanted byproducts that inhibit identification and quantitation. To prevent these reactions from occurring, the cysteine residues still need to be alkylated even though the protein will not be digested. Because there are approximately 20

cysteine residues for each MT, different alkylating reagents (iodoacetamide and acrylamide) were evaluated for efficiency and the formation of unwanted side products.

Alkylated MTs were differentially labeled with DiLeu and pooled in known ratios to evaluate quantitative accuracy. The removal of excess tagging reagents is a crucial step with many labeling protocols as the excess tagging reagents can form unwanted side products and inhibit ionization efficiency of analytes. Selectively removing these reagents is difficult due to similarities in hydrophobicity, so commonly used solid-phase extraction methods, like C18 ZipTips, are less useful. In this work, three different clean up methods are evaluated: strong cation exchange (SCX), molecular weight cut-off (MWCO) membrane filtration, and acetone precipitation. These methods all remove the tags by different mechanisms based on charge, size, and solubility respectively. Removal of the tagging reagents allows for the MS analysis of the labeled MTs and the evaluation of quantitative accuracy. An overview of the experimental workflow is given in **Figure 2**. The adaptation of established bottom-up proteomic workflows has led to the development of an isobaric labeling strategy amenable to top-down MS analysis of MTs with high labeling efficiency and quantitative accuracy. These methods can be applied to the study of metal toxicity and related diseases to better understand the roles MTs play in biochemical processes.

Methods

Materials

Acetone, acetonitrile (ACN), LC-MS solvents, formic acid (FA), urea, ethylenediaminetetraacetic acid (EDTA), and tris-base were purchased from Fisher Scientific (Pittsburgh, PA). Triethylammonium bicarbonate (TEAB), hydrochloric acid, N,N-dimethylformamide (DMF), ammonium formate, trifluoroacetic acid (TFA), dithiothreitol (DTT), iodoacetamide (IAA), acrylamide (AA), 2-nitrophloroglucinol (2-NPG), 4-(4,6-dimethoxy- 1,3,5-triazin-2-yl)-4-methylmorpholinium tetrafluoroborate (DMTMM), and isotopic leucine and formaldehyde were purchased from Sigma-Aldrich (St. Louis, MO). N-methylmorpholine (NMM) was purchased from TCI America, (Tokyo, Japan). Strong cation exchange (SCX) spin tips were purchased from PolyLC (Columbia, MD). C18 ZipTips and 3 kDa Amicon Ultra molecular weight cut-off filters were purchased from Millipore (Burlington, MA). The rabbit metallothionein isolate was purchased from Creative Biomart (Shirley, NY).

Reduction and Alkylation

The rabbit metallothionein isolate was split into 25 µg aliquots and dried down by vacuum centrifugation. These aliquots were resuspended in 100 µL of a reduction buffer containing 8 M urea, 100 mM Tris, 3.5 mM EDTA, and 10 mM DTT (adjusted to pH ~7.4 with HCl) and vortexed at 37 °C for 60 min to reduce any disulfide bonds and denature the protein. Immediately after reducing, 0.5 M alkylating agent (IAA or AA) was added to a final concentration of 56 mM. The alkylation reaction took place at room temperature in the dark and was quenched after 60 or 90 min by the addition of 2 µL 0.5 M DTT. The reduced and alkylated samples were then purified using C18 ZipTips

per manufacturer's protocol. Briefly, TFA was added to ensure pH <4 and the samples were bound to the equilibrated resin-packed pipette tips, washed with 0.1% TFA in H_2O, and eluted in 0.1% TFA in 50/50 ACN/H_2O. Purified samples were dried by vacuum centrifugation and stored at -80 °C.

DiLeu Labeling

The synthesis of the DiLeu tags has been described previously along with the labeling protocol.[25] Briefly, the reduced and alkylated samples containing ~25 µg protein were resuspended in 50:50 ACN:0.25 M TEAB. One mg aliquots of DiLeu tag were activated to their triazine ester form by the addition of 50 µL activation solution (14.08 mg DMTMM in 495 µL dry DMF with 4.72 µL NMM) and vortexed for 30 min at room temperature. Active DiLeu tag was added to the samples at a ratio of 20:1 label:protein by mass and vortexed at room temperature for 60 min. The reaction was quenched with 5% NH_2OH to a final concentration of 0.25% NH_2OH. Samples were pooled in known ratios (e.g., 1:1:1:1 or 1:5:10:20) before further processing.

Post-labeling purification

After labeling, excess tagging reagents were removed from the samples. Three different methods were evaluated, a chromatographic method (SCX), a size-based method (MWCO), and a protein precipitation method (acetone precipitation).

Strong Cation Exchange. Samples were dried down after labeling and purified using poly-LC SCX spin tips per manufacturer's protocol. Protein was loaded to the

column in and washed with 0.1% FA, 20% ACN. Protein was eluted with 0.4 M ammonium formate in 20% ACN and dried down by vacuum centrifugation. To remove the ammonium formate, the protein was purified by C18 ZipTips using the manufacturer's protocol. Protein was loaded and washed in 0.1% TFA and eluted in 0.1% TFA in 50% ACN. The proteins were dried down by vacuum centrifugation and stored at -80 °C.

Molecular Weight Cut-off. Samples were dried down after labeling and resuspended in H_2O. The resuspended samples were applied to an Amicon 3 kDa filter per manufacturer's protocol. The filter was initially rinsed with H_2O, then sample was applied and concentrated by centrifugation at 14,000 x g. An additional volume of H_2O was added, and the sample was further concentrated to improve the removal of excess tagging reagents. The concentrated protein was recovered from the filter and then dried down by vacuum centrifugation and stored at -80 °C.

Acetone Precipitation. Immediately after labeling, a 4x volume of chilled acetone (~ -20 °C) was added to each multiplexed sample and stored at -20 °C overnight. The samples were then centrifuged at 12,000 x g for 5 min and the supernatant was discarded. An equal volume of acetone was added, and after mixing briefly, the sample was again centrifuged for 5 min at 12,000 x g. The supernatant was discarded, and the sample was dried down (briefly) by vacuum centrifugation and stored at -80 °C.

Mass Spectrometry Analysis

To quickly evaluate different steps in the protocol (e.g., alkylation and labeling), matrix assisted laser desorption/ionization (MALDI)-MS was performed using a Bruker RapiFlex. Aliquots of the protein after alkylation, labeling, and each clean up step were spotted with 2-NPG matrix (12 mg/mL in 70% ACN, with 0.1% FA). Spectra were collected using a laser power of 80%. For the quantitation experiments, electrospray ionization (ESI) is required to generate fragmentable ions. Multiplexed samples were analyzed by LC-MS on a Thermo Orbitrap Elite coupled to a Waters nanoAcquity LC using a homemade 15 cm C18 column. Proteins were eluted over a gradient of 60 min from 5-35% solvent B (solvent A = 0.1% FA in H_2O; solvent B = 0.1% FA in ACN). Spectra were collected from m/z 500-2000 with 60k MS^1 resolving power and 30k MS^2 resolving power with HCD for fragmentation (NCE = 28).

Results and Discussion

The cysteine residues of MTs are capable of reacting with the DiLeu tags to form unwanted byproducts, so blocking these residues is critical for effective isobaric tagging. Alkylating the sulfhydryl groups is effective in preventing these reactions but ensuring full alkylation of a protein containing ~20 cysteine residues can be difficult. Many alkylating reagents exist and have known to have different efficiencies and side reactions;[27] here acrylamide (AA) and iodoacetamide (IAA) are compared in their alkylation of MTs. IAA was selected due to its ubiquitous use in proteomics experiments, and AA was selected due to reports of increased reaction efficiency.[27] To test their effectiveness in alkylating MTs, a modified protocol was used based upon the

work of Shabb, J.B., et al in which a greater concentration of DTT and reducing agent is used to ensure more complete alkylation of the many cysteine residues.[28] The reaction is quenched by the addition of additional DTT and immediate C18 solid phase extraction via ZipTips. LC-MS analysis of MTs after alkylation with either IAA or AA is shown in **Figures S1 and S2** respectively.

Using IAA resulted in incomplete labeling, but the major isoforms in the rabbit MT isolate, MT2A and MT2B, were able to be detected in their fully alkylated forms. Conversely, using AA resulted in detection of only MT2A, as well as both several unwanted side reactions and missed alkylation sites. The incomplete labeling caused by using IAA is more addressable than the combination of unwanted byproducts and incomplete alkylation from using AA, so it was decided that IAA would be used for future experiments. By increasing the reaction time to 90 min, more complete alkylation was achieved. This was verified using MALDI-MS. The alkylated MT was spotted with 2-NPG matrix to generate multiply charged ions and quickly analyze the product. Additionally, because there is no separation prior to MALDI-MS, the species with different alkylation efficiencies are still analyzed in the same spectra, minimizing quantitative differences that could arise when using LC-MS. The average of the collected spectra is given in **Figure 3**. Calculating the alkylation efficiency from the peak areas resulted in a reaction efficiency of 93.7%, demonstrating feasibility of the method. Furthermore, the extended reaction time did not increase the presence of unwanted side reactions, and there were no detected byproducts.

A major limitation of using DiLeu tags, or any labeling strategy, is the need to remove excess tagging reagents. The reaction used here is performed at a 20:1 label:protein ratio. The excess label helps ensure complete labeling but, if not removed, will inhibit ionization, and therefore, detection of the analyte. Removing the DiLeu tags from the protein cannot be accomplished by commonly used solid phase extraction methods, like C18 ZipTips, because the hydrophobicity of the tags and proteins are too similar. As a result, DiLeu labeled samples are typically cleaned up using SCX. The labeling of intact proteins also presents alternative purification methods, not typically available to tryptic peptides. Size-based methods like molecular weight cut-off filtration can be used to concentrate proteins and remove small molecules. Additionally, proteins can be precipitated by an organic solvent, centrifuged, and the tagging reagents remain in the organic supernatant. To better recover the labeled product, SCX, MWCO filtration, and acetone precipitation were all evaluated, with the results summarized in **Table 1**.

Unlike when used for the clean-up of labeled peptides,[29] SCX proved ineffective for the DiLeu-labeled MTs. No protein was detected in the eluted fractions, but the wash fractions contained MTs. The lack of retention to the SCX resin could be due to the lack of charged residues on the protein; the lysine residues are labeled with DiLeu, the N-terminus is acetylated, and there are few, if any, arginine, and histidine residues on MTs. The lack of binding makes SCX unsuitable for cleaning up the sample. Similar to SCX, MWCO filtration was also found to be ineffective for the clean up of labeled proteins. Using a 3 kDa filter, the protein should be retained, and the excess tagging

reagents can flow through the filter to be discarded. Although excess tagging reagents were not observed in the top portion of the filter, there was also minimal protein signal. The protein was also undetected in the flow through, so it is believed that the excess tagging reagents are causing membrane fouling, or that the DiLeu-labeled MTs are adhering to the filter and unable to be recovered. Conversely, acetone precipitation was effectively able to remove the proteins from the labeling reagents. Despite their low molecular weights, the proteins were still precipitated directly from the reaction buffer. Moreover, the excess tagging reagents remained soluble and were removed by simply discarding the supernatant. Acetone precipitation not only demonstrated high performance, but also requires the least amount of sample handling, potentially improving overall recovery of the target analytes.

Using the extended alkylation reaction and acetone precipitation allowed the DiLeu labeling of intact MTs to be assessed. **Figure 4** shows the averaged MS^1 spectra for an LC-MS analysis of the labeled MTs. Complete labeling of the protein was observed, denoted by the blue stars, with the +6 charge state being the most abundant. Incidents of under labeling (red stars) were also seen, along with evidence of over labeling (yellow star). Interestingly, differences in charge state preference were observed for different labeling efficiencies. The over labeled protein is observed only at a +7 charge state, and the under labeled protein is observed only at +5 and +6 charge states. The completely labeled protein is present at both +6 and +7 charge states. This could be because the increase in hydrophobicity from the DiLeu tag can affect ionization

efficiency and tertiary structure to make the protein more susceptible to protonation during electrospray ionization.[30]

The lack of complete labeling could inhibit accurate quantitation, but the most abundant peak is still the completely labeled protein. Additionally, the labeling efficiency was calculated to be 85.6% when comparing peak areas of the completely labeled protein to the total peak area for the protein. Moreover, the observed reporter ion ratios were 1:5.1:8.9:24. These ratios are within 20% of the theoretical 1:5:10:24 across a 20-fold dynamic range, demonstrating adequate quantitative accuracy. These ratios are depicted in **Figure 5**. The reporter ions are produced with high intensity, but the rest of the spectrum (unshown) is of low signal. The poor fragmentation efficiency of an intact protein is still a problem and results in ambiguous b-/y-ions upon higher energy collision dissociation (HCD). Alternative fragmentation patterns, like electron-based methods, can improve fragmentation,[31] but need to be evaluated with DiLeu. When working with purified proteins, identification of protein based upon intact mass may be sufficient, but reliable fragmentation is necessary to provide confident identifications of proteins from a complex sample.

Conclusions

Characterization of intact proteins can offer many advantages over bottom-up proteomics, including the maintenance of structural information and preservation of post-translational modifications. Quantitation of intact proteins has unfortunately lagged

behind peptide quantitation due to difficulties in deconvoluting isotopically labeled data, or issues with isobaric labeling reactions and solvent compatibility with proteins. Here, an isobaric workflow is developed for the analysis of intact metallothionein proteins. These proteins are small, but still present challenges due to their unique high cysteine content. Methods were developed to ensure full alkylation of these cysteine residues to minimize interference with labeling. Additionally, different post-labeling clean-up steps were evaluated, and acetone precipitation demonstrated high effectiveness in both removing tagging reagents and recovering protein. These improvements allowed for the MS analysis of isobarically tagged proteins, which demonstrated high quantitative accuracy spanning a 20-fold dynamic range. Work needs to be done to improve the fragmentation and peptide backbone analysis of the labeled proteins to enable future applications. Additionally, extracting proteins from tissues, fluid, etc., needs to be optimized before actual comparisons between experimental conditions can be performed. Overall, the methods developed here present new opportunities for quantifying intact proteins and proteoforms with greater throughput and reduced run-to-run variability.

References

1. Keller AA, Adeleye AS, Conway JR, et al. Comparative environmental fate and toxicity of copper nanomaterials. *NanoImpact*. 2017;7(May):28-40. doi:10.1016/j.impact.2017.05.003
2. Dietrich AM, Postlethwait N, Gallagher DL. Quantifying Bioavailability and Toxicity

of Copper to Americamysis bahia - Mysid Shrimp. *Int J Environ Sci Dev*. 2013;4(1):37-43. doi:10.7763/IJESD.2013.V4.299

3. Rainer J, Brouwer M. Hemocyanin synthesis in the blue crab Callinectes sapidus. *Comp Biochem Physiol B Biochem Mol Biol*. 1993;104(1):69-73. http://www.ncbi.nlm.nih.gov/entrez/query.fcgi?cmd=Retrieve&db=PubMed&dopt=Citation&list_uids=8448995.
4. Van Bael S, Watteyne J, Boonen K, et al. Mass spectrometric evidence for neuropeptide-amidating enzymes in Caenorhabditis elegans. *J Biol Chem*. 2018;293(16):6052-6063. doi:10.1074/jbc.RA117.000731
5. Kardos J, Héja L, Simon Á, Jablonkai I, Kovács R, Jemnitz K. Copper signalling : causes and consequences. 2018;3:1-22.
6. Jo HJ, Choi JW, Lee SH, Hong SW. Acute toxicity of Ag and CuO nanoparticle suspensions against Daphnia magna: The importance of their dissolved fraction varying with preparation methods. *J Hazard Mater*. 2012;227-228:301-308. doi:10.1016/j.jhazmat.2012.05.066
7. Brouwer M, Brouwer TH. Biochemical defense mechanisms against copper-induced oxidative damage in the blue crab, Callinectes sapidus. *Arch Biochem Biophys*. 1998;351(2):257-264. doi:10.1006/abbi.1997.0568
8. De Martinez Gaspar Martins C, Bianchini A. Metallothionein-like proteins in the blue crab Callinectes sapidus: Effect of water salinity and ions. *Comp Biochem Physiol - A Mol Integr Physiol*. 2009;152(3):366-371. doi:10.1016/j.cbpa.2008.11.005

9. Lavradas RT, Hauser-Davis RA, Lavandier RC, et al. Metal, metallothionein and glutathione levels in blue crab (Callinectes sp.) specimens from southeastern Brazil. *Ecotoxicol Environ Saf*. 2014;107:55-60. doi:10.1016/j.ecoenv.2014.04.013

10. Rossbach LM, Shaw BJ, Piegza D, Vevers WF, Atfield AJ, Handy RD. Sub-lethal effects of waterborne exposure to copper nanoparticles compared to copper sulphate on the shore crab (Carcinus maenas). *Aquat Toxicol*. 2017;191(April):245-255. doi:10.1016/j.aquatox.2017.08.006

11. Nakazato K, Tomioka S, Nakajima K, et al. Determination of the serum metallothionein (MT)1/2 concentration in patients with Wilson's disease and Menkes disease. *J Trace Elem Med Biol*. 2014;28(4):441-447. doi:10.1016/j.jtemb.2014.07.013

12. Juárez-Rebollar D, Rios C, Nava-Ruíz C, Méndez-Armenta M. Metallothionein in Brain Disorders. *Oxid Med Cell Longev*. 2017;2017(Figure 1). doi:10.1155/2017/5828056

13. Schlief ML. NMDA Receptor Activation Mediates Copper Homeostasis in Hippocampal Neurons. *J Neurosci*. 2005;25(1):239-246. doi:10.1523/jneurosci.3699-04.2005

14. Irvine GW, Stillman MJ. Residue modification and mass spectrometry for the investigation of structural and metalation properties of metallothionein and cysteine-rich proteins. *Int J Mol Sci*. 2017;18(5). doi:10.3390/ijms18050913

15. Gunn AP, McLean CA, Crouch PJ, Roberts BR. Quantification of metallothionein-III in brain tissues using liquid chromatography tandem mass spectrometry. *Anal*

Biochem. 2021;630(July):114326. doi:10.1016/j.ab.2021.114326

16. Rodríguez-Menéndez S, Fernández B, García M, et al. Quantitative study of zinc and metallothioneins in the human retina and RPE cells by mass spectrometry-based methodologies. *Talanta*. 2018;178(June 2017):222-230. doi:10.1016/j.talanta.2017.09.024
17. Mehus AA, Muhonen WW, Garrett SH, Somji S, Sens DA, Shabb JB. Quantitation of Human Metallothionein Isoforms: A Family of Small, Highly Conserved, Cysteine-rich Proteins. *Mol Cell Proteomics*. 2014;13(4):1020-1033. doi:10.1074/mcp.m113.033373
18. Catherman AD, Skinner OS, Kelleher NL. Top Down Proteomics: Facts and Perspectives. *Biochem Biophys Res Commun*. 2014;445(4):683-693. doi:10.1016/j.bbrc.2014.02.041.Top
19. Tucholski T, Cai W, Gregorich ZR, et al. Distinct hypertrophic cardiomyopathy genotypes result in convergent sarcomeric proteoform profiles revealed by top-down proteomics. *Proc Natl Acad Sci U S A*. 2020;117(40):24691-24700. doi:10.1073/pnas.2006764117
20. Anand S, Samuel M, Ang C, Keerthikumar S, Mathivanan S. Chapter 4 Label-Based and Label-Free Strategies for Protein Quantitation. In: *Proteome Bioinformatics, Methods in Molecular Biology*. Vol 1549. ; 2017:31-43. doi:10.1007/978-1-4939-6740-7
21. Hebert AS, Merrill AE, Bailey DJ, et al. Neutron-encoded mass signatures for multiplexed proteome quantification. *Nat Methods*. 2013;10(4):332-334.

doi:10.1038/nmeth.2378

22. Yu D, Wang Z, Cupp-Sutton KA, et al. Quantitative Top-Down Proteomics in Complex Samples Using Protein-Level Tandem Mass Tag Labeling. *J Am Soc Mass Spectrom*. 2021;32(6):1336-1344. doi:10.1021/jasms.0c00464
23. Winkels K, Koudelka T, Tholey A. Quantitative Top-Down Proteomics by Isobaric Labeling with Thiol-Directed Tandem Mass Tags. *J Proteome Res*. 2021;20(9):4495-4506. doi:10.1021/acs.jproteome.1c00460
24. Xiang F, Ye H, Chen R, Fu Q, Li N. N,N-Dimethyl leucines as novel Isobaric tandem mass tags for quantitative proteomics and peptidomics. *Anal Chem*. 2010;82(7):2817-2825. doi:10.1021/ac902778d
25. Frost DC, Greer T, Li L. High-resolution enabled 12-plex DiLeu isobaric tags for quantitative proteomics. *Anal Chem*. 2015;87(3):1646-1654. doi:10.1021/ac503276z
26. Frost DC, Feng Y, Li L. 21-plex DiLeu Isobaric Tags for High-Throughput Quantitative Proteomics. *Anal Chem*. 2020;92(12):8228-8234. doi:10.1021/acs.analchem.0c00473
27. Müller T, Winter D. Systematic evaluation of protein reduction and alkylation reveals massive unspecific side effects by iodine-containing reagents. *Mol Cell Proteomics*. 2017;16(7):1173-1187. doi:10.1074/mcp.M116.064048
28. Shabb JB, Muhonen WW, Mehus AA. *Quantitation of Human Metallothionein Isoforms in Cells, Tissues, and Cerebrospinal Fluid by Mass Spectrometry*. Vol 586. 1st ed. Elsevier Inc.; 2017. doi:10.1016/bs.mie.2016.11.004

29. Sauer, Christopher S., Li L. Multiplex Dimethylated Leucine (DiLeu) Isobaric Tags to Probe Neuropeptidomic Response to Copper Toxicity in the Blue Crab, Callinectes sapidus. In: Atlanta, GA: American Society for Mass Spectrometry; 2019.

30. Testa L, Brocca S, Santambrogio C, et al. Extracting structural information from charge-state distributions of intrinsically disordered proteins by non-denaturing electrospray-ionization mass spectrometry. *Intrinsically Disord Proteins*. 2013;1(1):e25068. doi:10.4161/idp.25068

31. Graca DC, Hartmer R, Jabs W, et al. Detection of Proteoforms Using Top-Down Mass Spectrometry and Diagnostic Ions. In: Brun V, Coute Y, eds. *Proteomics for Biomarker Discovery: Methods and Protocols*. Vol 1905. Springer Nature; 2019:173-183. doi:10.1007/978-1-4939-9164-8

Figures

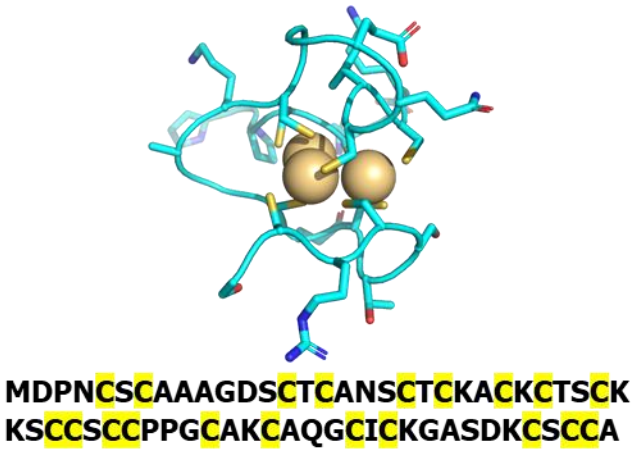

Figure 1: 3D structure and sequence of rabbit metallothionein MT2A. The structure shows the coordination of copper ions with the sulfhydryl groups of the many cysteine residues (highlighted in the sequence). The 3D structure was generated in Pymol using data from Uniprot.

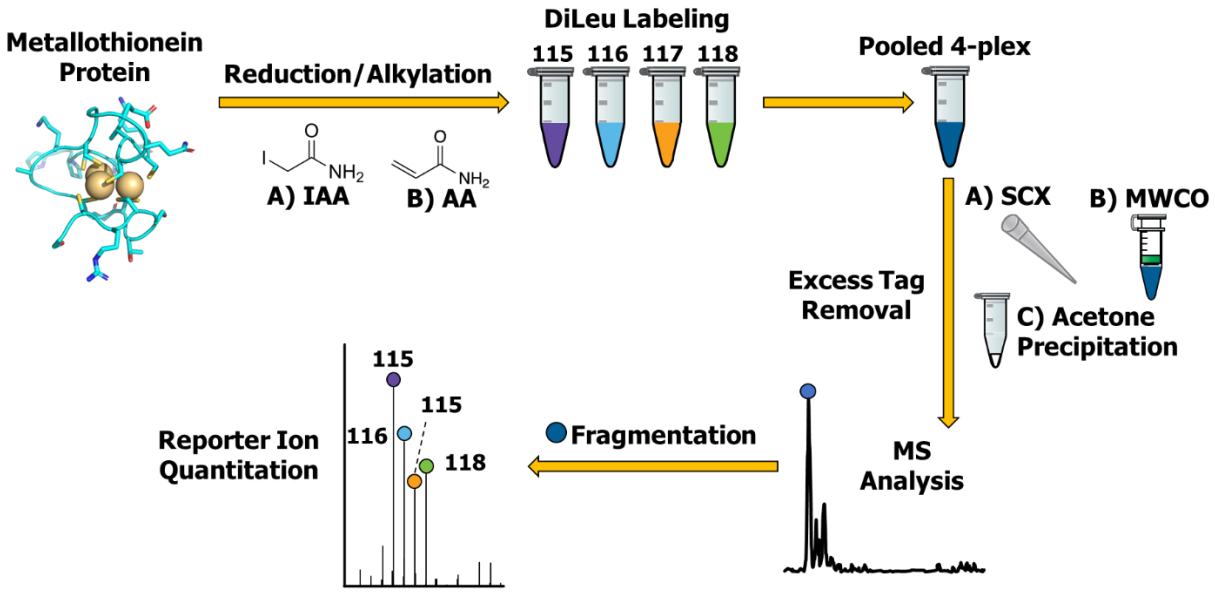

Figure 2: Overall workflow for the labeling and analysis of metallothionein proteins. Proteins are alkylated prior to labeling with 4-plex DiLeu. The multiplexed sample is then cleaned up to remove the excess tagging reagents before MS analysis. Different alkylating reagents were evaluated: iodoacetamide (IAA) and acrylamide (AA). Additionally, different clean up steps were compared: strong cation exchange (SCX), molecular weight cut-off (MWCO), and acetone precipitation.

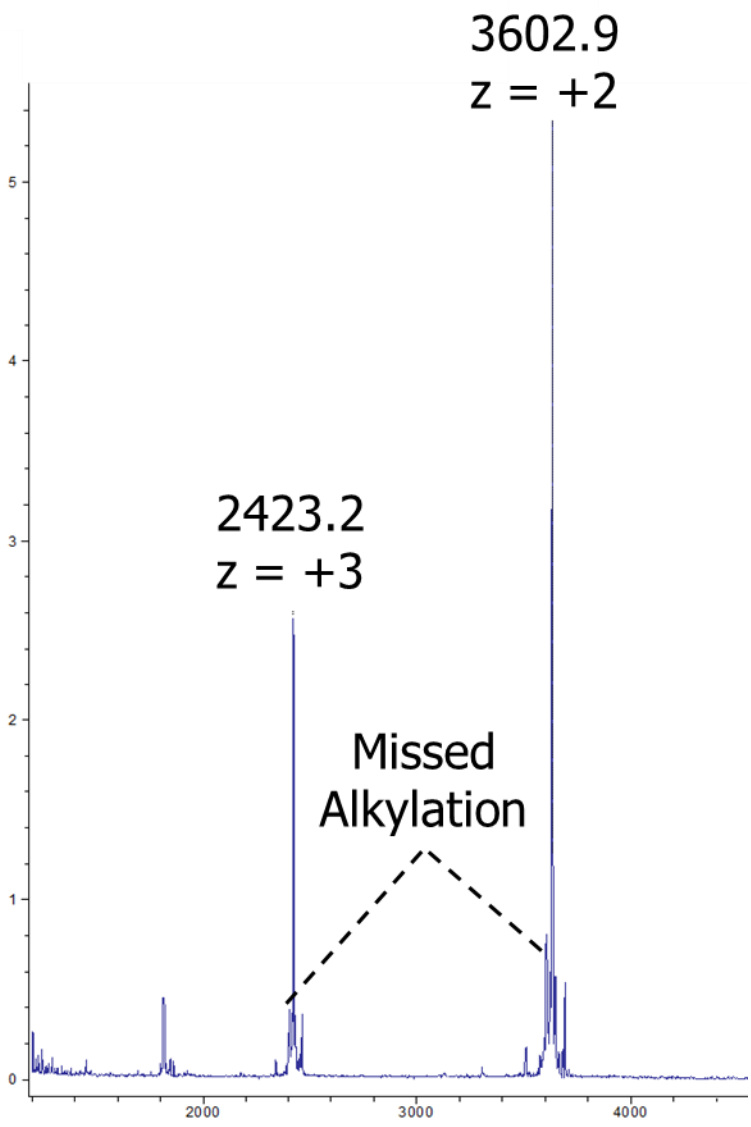

Figure 3: Alkylation efficiency with extended reaction time. The spectrum was collected using MALDI-MS with a 2-NPG matrix to generate multiply charged ions. The overall reaction efficiency, based on peak areas of the fully alkylated peaks and the peaks corresponding to missed alkylation, was 93.7%.

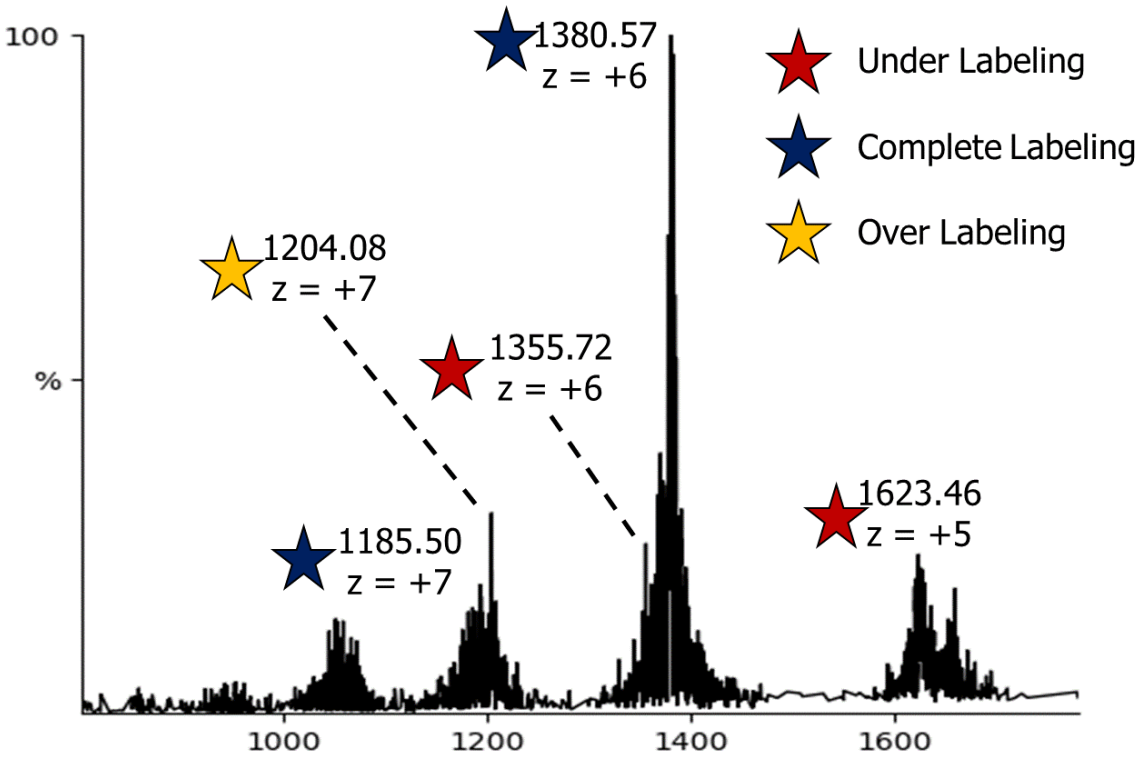

Figure 4: DiLeu labeling efficiency of alkylated metallothionein proteins. Instances of under and over labeling (red and yellow star respectively) were observed, but the completely labeled peak is the most abundant. Data was collected using a Thermo Orbitrap Elite mass spectrometer coupled to nanoLC.

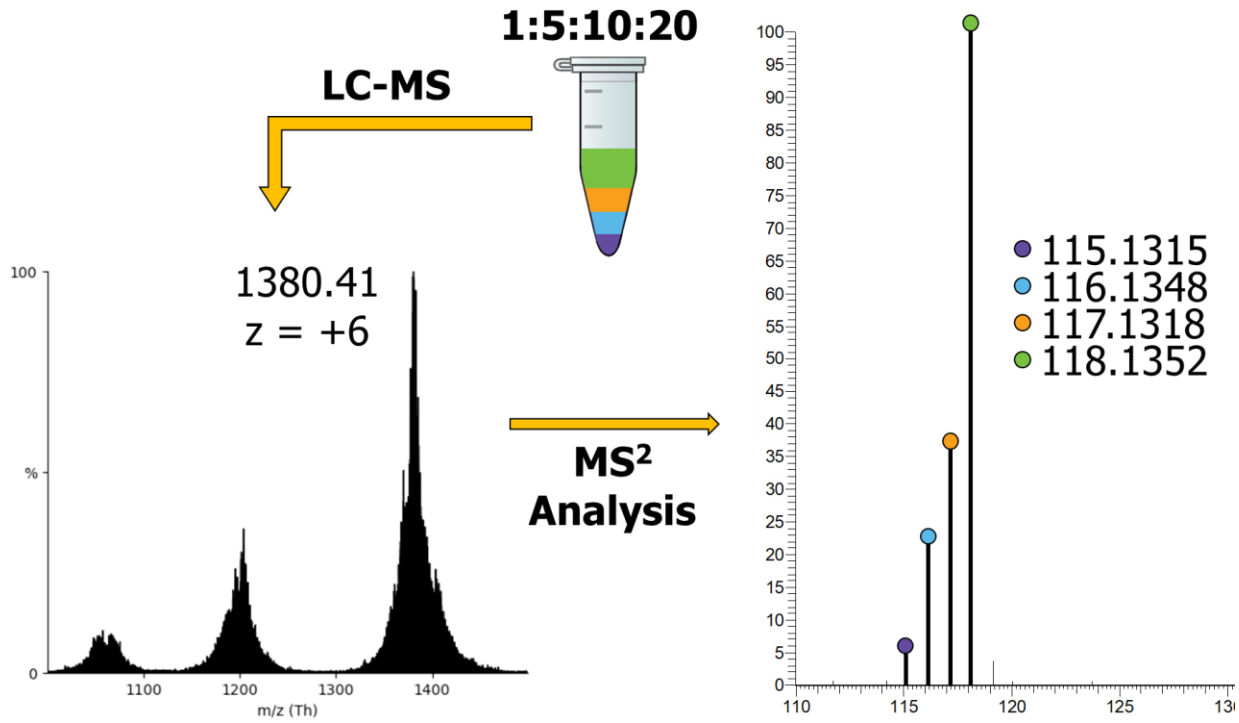

Figure 5: Quantitative performance of the isobaric tagging workflow. Differentially labeled proteins were pooled at a ratio of 1:5:10:20 and analyzed by LC-MS. The selected precursor ion (*m/z* 1380.41) reporter ions showed relative intensities of 1:5.1:8.9:24.

Table 1: Results from different methods to purify labeled metallothionein. SCX was performed using spin-tips, and molecular weight cut-off was performed using membrane filters. Of the three methods evaluated, only the acetone precipitation was effective for removing the excess labeling reagents from the analytes.

Clean-up Method	Results
Strong Cation Exchange	Metallothionein protein detected only in wash; resin does not effectively bind labeled metallothionein
Molecular Weight Cut-off	Adequate for concentrating protein but does not effectively remove labeling reagents.
Acetone Precipitation	Effective for both recovering protein and removing labeling reagents

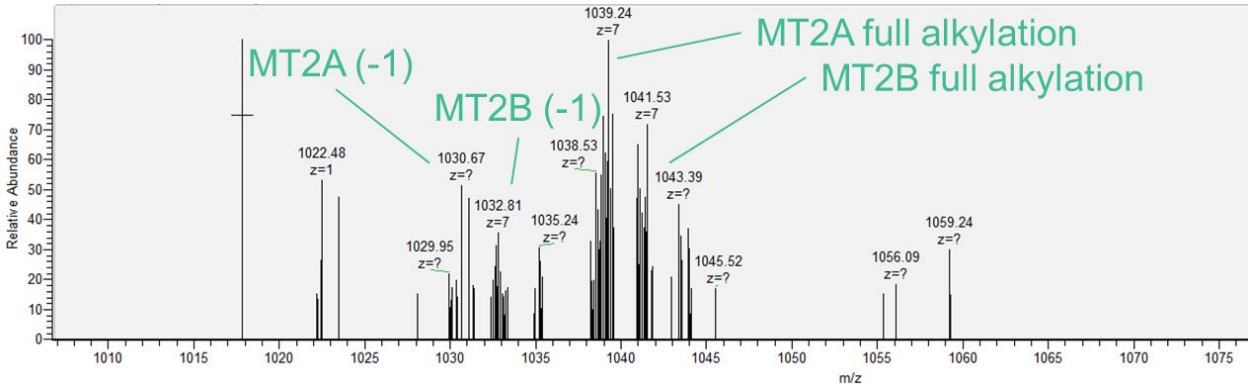

Figure S1: Example spectrum from MTs alkylated with iodoacetamide. The MT2A and MT2B forms were observable with full alkylation, but there were also missed alkylation, denoted by the (-1).

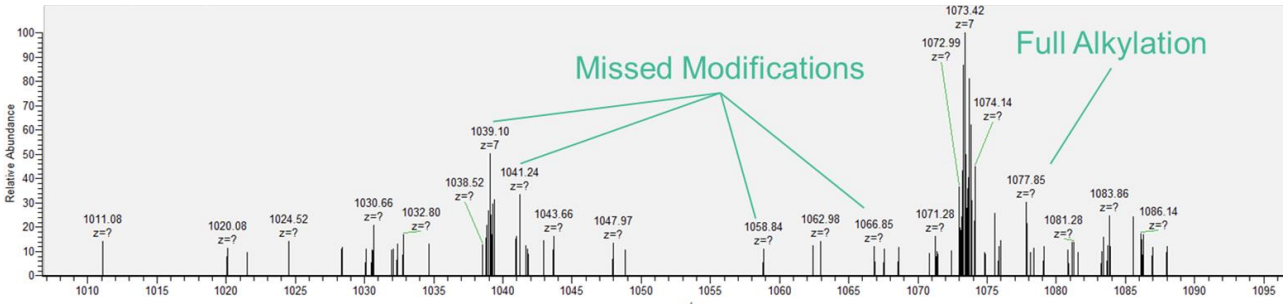

Figure S2: Example spectrum from MTs alkylated with acrylamide. Only the MT2A form is detectable with full alkylation. Several peaks corresponding to missed modifications were also observed. The peaks between *m/z* 1072-1074 are unidentified side reactions.

Chapter 8

WISL Chapter

Written for the Wisconsin Initiative for Scientific Literacy to describe this thesis work for a broader audience.

Over the last five years of graduate school, I have been asked "So what is it that you do?" more times than I can count. Although I find it easier to answer that question for people with a background in my field, it is arguably more important to answer the question for those unfamiliar with proteomics, analytical chemistry, etc. I wrote this chapter not only to prevent seeing the look of confusion on my parents' faces (the same one I have when my dad tries to explain what pass interference is), but also to learn to present my work more succinctly and successfully to broader audiences. As scientists, it is important to acknowledge the importance of communicating results and delivering a product to the people that supported our research (i.e., taxpayers). I am thankful for the help and feedback provided by the Wisconsin Initiative for Science Literacy, especially Elizabeth Reynolds, Cayce Osborne and Bassam Shakhashiri.

Crustacean Model Organisms

The human nervous system is incredibly complex and includes not just the brain, but also the spinal cord and nerves throughout the body. This system is comprised of specialized cells called neurons that allow the different parts of the body to communicate with one another. Communication between different parts of the body is an incredibly broad function, explaining the complexity of the nervous system and the reasons it is so challenging to study. Studying the nervous system is important, however, as it provides researchers with more information about many neurological disorders like dementia, Parkinson's disease, and depression.

To better understand the human nervous system researchers often start with a simpler model organism. Where some labs study mice, rats, etc., our lab studies crustaceans, specifically the blue crab, *Callinectes sapidus*. Blue crabs have well-defined nervous systems with far fewer neurons than humans, making it significantly easier to study them. Although it is simpler, the overall processes in the crustacean nervous system are similar to humans and other organisms, so researchers can apply the techniques used and developed in this work to more relevant biological problems in humans.

Understanding the Nervous System

There are many ways that neurons communicate with one another to send signals. This can be done with electrical signals, similar to circuits, or chemically. With chemical signaling, one can think of neurons as buildings and the connections between neurons as roads. In this analogy, the chemical signals are the cars and pedestrians traveling on the roads to different buildings. These chemical signals are released due to a stimulus, such as people leaving their homes to go to work because of the time of day. Trying to study how specific neurons communicate with each other in relation to the entire system is incredibly difficult as there are too many (up to billions depending on the organism) interactions to feasibly study. Instead, looking at the overall trends in signaling is not only easier, but can still provide information on how different biological states affect signaling. By comparing signaling in a healthy organism and one with a particular disease like Alzheimer's disease, we can start to uncover what is going wrong

at a molecular level. Using the traffic example, trying to observe differences between a few pedestrians in New York City is difficult, but if an entire subway line is closed, there will be changes in the overall traffic across the city that are observable. This information can provide researchers with new tools for understanding, diagnosing, and treating diseases.

There are many different types of chemical signals that are created in and released by neurons, but one of particular interest to our lab is neuropeptides. Neuropeptides are simply peptides that originate in the neuroendocrine system. They can exert their signaling effects locally at adjacent neurons, or they can be released into the circulating fluid and exert their effects at distant neurons throughout the body.[1] Neuropeptides have been shown to be involved in different diseases, stress response, wake-sleep cycles, and many more biological processes.[2–4] As a result, their dysregulation–when their concentration levels are out of balance–has been implicated in different neurological disorders.

Improving the Detection of Neuropeptides

As mentioned before, neuropeptides are peptides originating in the neuroendocrine system, and peptides are simply chains of amino acids. Amino acids are typically viewed as the building blocks of peptides and proteins; there are 20 different amino acids, and the exact number of them in a particular chain (peptide) and the order of them in that chain is critical to their structure and the role they play in the body. Amino acids are assigned letter codes, so peptides can be thought of as strings of

letters to make a word, except the alphabet only has 20 letters. Like letters in a word, the amino acids in a peptide and the order of them is important. Adding a letter to a word (e.g, RIDE to PRIDE) changes its meaning, as does rearranging the letters of a word (e.g., RIDE to DIRE).

Techniques to analyze neuropeptides must be capable of determining the neuropeptide sequence–its amino acid content and order of those amino acids–to discern different neuropeptides. Mass spectrometry (MS) is a technique that allows the researcher to determine the sequence of a neuropeptide based on its mass. These instruments act almost as molecular scales, allowing the mass of a peptide to be observed. The peptide is then broken apart and the pieces are "weighed" as well. By combining the information from the mass of the intact peptide as well as its fragments, an analytical instrument (i.e., mass spectrometer) and computer output a spectrum of masses corresponding to different fragments. Researchers, either manually or using data processing software, can determine the peptide sequence from the spectrum based on the unique combination of peaks in it. An overview of this is given in **Figure 1**. What makes MS such a powerful technique is that it can be used to determine the sequence (identity) and relative expression (quantity) of all neuropeptides in a single analysis. This allows researchers to not only see which neuropeptides are present, but also how they are changing between two or more samples, such as stressed vs unstressed or diseased vs healthy samples.

When analyzing neuropeptides, MS can provide quantitative information using different strategies.[5] By tagging the neuropeptides, the samples can be analyzed at the

same time and the relative peak intensities in the mass spectrum can be used to determine the amount of neuropeptide from each starting sample. This not only allows more samples to be analyzed in the same amount of time, but also reduces variation caused by the instrument, improving accuracy. One type of labeling is known as isotopic labeling. In these methods, a part of the neuropeptide is labeled with a chemical tag, like formaldehyde to cause a shift in the mass of the peptide. Different channels of the same tag have different isotopes of certain atoms; these isotopes are the same chemical element but differ in mass from one another due to differences in the number of neutrons they have. For example, ^{12}C and ^{13}C are both carbon atoms, but one has a mass of 12 and the other has a mass of 13 (from the mass of an additional neutron compared to ^{12}C). The different channels with different isotopes therefore increase the mass of the neuropeptides by a different amount. By labeling Sample A (e.g., diseased) with one tag and Sample B (e.g., healthy) with another tag, there will be a mass difference and two peaks will be observed. The relative signal of these peaks is then indicative of the concentrations of that neuropeptide in the biological samples (visually explained in **Figure 2**). We have applied isotopic labeling to study changes in neuropeptides across four samples.[2]

Another labeling method, known as isobaric tagging, is like isotopic labeling, but each channel of the tag incorporates the same mass. Neuropeptides from Sample A and Sample B will appear identical, but when they are analyzed by their fragments (also known as MS^2), reporter ions form for each channel. These reporter ions are unique to each tag and result in peaks that can be used for quantification. In other words, these

diagnostic ions report the relative signal from each sample and correlate to quantitative differences between the two samples.

To compare isotopic and isobaric labeling, it is important to remember that they have the same goal: quantify relative differences between samples in a single analysis. Isotopic labeling achieves this by adding tags of different masses to the sample, and isobaric tagging adds tags with the same mass, but the isobaric tags result in distinct fragments (reporter ions) for the different channels. This can be thought of like voting in an election. In Scenario A (analogous to isotopic labeling), each person that votes receives an "I voted" sticker, but the number of stickers they receive is indicative of the candidate they voted for. Votes are tabulated by counting the number of voters that have one sticker, two stickers, etc. Conversely, in Scenario B (isobaric labeling), everyone receives one sticker, but the color of the sticker is dependent on the selected candidate. Votes are then tabulated by comparing the number of people with blue stickers, red stickers, etc. The primary advantage of the isobaric label is that there are fewer peaks in the spectra (or stickers handed out), so data-interpretation is less complicated. By minimizing complexity, isobaric tagging allows for more samples to be analyzed at the same time to improve throughput. **Figure 3** shows the main differences between isotopic and isobaric tagging. While many isobaric tags exist, in the Li Lab, we use a custom isobaric tag known as DiLeu (*N,N*-dimethyl leucine).[6]

In most MS experiments, data is collected in a manner known as data-dependent acquisition (DDA). In a DDA experiment, an initial spectrum is collected without fragmentation, known as an MS^1 or precursor scan, and subsequent scans are collected

in which the top peaks of the precursor scan are fragmented and analyzed (MS^2 scans). The initial scan measures the mass of the intact peptides in the sample, and then the instrument (depending on the data it just acquired, hence data-dependent acquisition) selects the peptides with the greatest signal in that spectrum to be fragmented and analyzed further. DDA methods allow many samples to be quickly and easily analyzed and many neuropeptides can be identified from each sample. Not all neuropeptides, however, are going to be the peaks with the highest signal, so they can often be omitted from the MS^2 scans. By not selecting these neuropeptides for MS^2 scans, the instrument can only output information about the intact mass. If we again compare neuropeptides to words, the intact mass is incapable of distinguishing between RIDE and DIRE. Additionally, the reporter ions required for quantification rely on the instrument fragmenting the intact neuropeptides and generating MS^2 information–trying to quantify the neuropeptides without MS^2 information would be like having a person with colorblindness tabulate the votes in the earlier analogy. By omitting neuropeptides from the MS^2 scans, the mass spectrometer prohibits researchers from confidently identifying and quantifying neuropeptides. To address this, we have demonstrated how we can adjust the various DDA parameters to increase the number of relevant spectra collected. This work led to a 3-fold increase in the number of neuropeptides we could identify and quantify in a single analysis. **Figure 4** summarizes the results of the optimization by showing how each iteration increases the number of identified neuropeptides. We then applied these optimized methods to the study of copper toxicity to gain insights into how crabs survive influxes of copper in the ecosystem.[7]

Related Protein Studies

We have shown neuropeptides to be dysregulated in response to copper toxicity, but there are likely other molecules involved. One of particular interest are metallothionein proteins (MTs). Proteins are structurally similar to peptides, made up of the same amino acids, but they are much larger and have more dynamic structure and function. MTs are of interest because they bind metals, like copper, in the body so they can be transported.[8] Copper is a necessary nutrient in the body, but also toxic at high levels; MTs help keep the amount of copper in the body at a desirable range. Large influxes of copper are therefore likely to cause a change in the amount of MTs observed.

Using the same DiLeu isobaric tag that was used for the neuropeptide studies, we developed a method for quantifying MTs using MS. This presented some challenges as MTs are larger than most peptides and have more labeling sites that need to be taken into account. Additionally, the proteins are high in cysteine, a specific amino acid that gives the protein their metal-binding properties. These cysteine components are able to interfere with the DiLeu labeling process, so they need to be modified by chemical reaction to prevent side reactions during the labeling. The work presented in this thesis demonstrates the effectiveness of using a modified DiLeu labeling strategy to measure relative amounts of intact metallothionein proteins. Typically, because they are much larger than peptides, proteins are often split into smaller pieces before analyzing them, a process known as digestion. Digesting the proteins makes it easier for the

instrument to accurately analyze the proteins, simply because it is easier to measure differences between small molecules compared to large molecules. Although effective, this digestion process can lead to losses in information, such as differences between similar metallothionein proteins. By measuring the proteins intact (without digestion), researchers gain more information about the system. The labeling method developed here is one of the first to demonstrate the ability to use isobaric tags to quantify changes in intact proteins. Briefly, proteins are chemically labeled with four different channels (distinct tags) of DiLeu, similar to the neuropeptide experiments. In real biological samples, protein concentration can vary greatly. We created a sample to mimic this that had set amounts of labeled protein from each channel; channels 116, 117, and 118 were present in this sample at concentrations 5, 10, and 20 times greater than channel 115 respectively. each channel were pooled together to create a sample that would yield reporter ions of different, but known, relative intensities. Comparing the observed signal intensities to the theoretical intensities (1:5:10:20), the accuracy of the method could be determined (summarized in **Figure 5**). We observed accuracy >80%, demonstrating the method is suitable for future biological applications.

Research Impact and Future Goals

This research aims to develop the tools to better study neuropeptides and related biomolecules involved in different biological processes. Specifically, this work creates a framework for studying these important biomolecules with improved speed and accuracy by incorporating DiLeu isobaric tags. The developed methods are applied

to the study of crustacean neuropeptides to show relative changes after exposure to an environmental stressor like copper toxicity. These methods are transferable to other biological problems, however, and can have impact in clinical research to study neurological disorders like Alzheimer's disease and Parkinson's disease. By expanding the tags to other targets, like proteins and neurotransmitters, there are even greater possibilities for discovering new ways to diagnose and treat disease.

Acknowledgements

The research described here was supported by the Biotechnology Training Program through the National Institute of General Medical Sciences of the NIH under Award Number T32GM008349 and the National Institutes of Health-Environmental Health Sciences F31 National Research Service Award (F31ES031859). I also acknowledge the guidance and editorial support provided by the Wisconsin Initiative for Scientific Literacy.

References

1. Li L, Sweedler J V. Peptides in the Brain: Mass Spectrometry–Based Measurement Approaches and Challenges. *Annu Rev Anal Chem*. 2008;1(1):451-483. doi:10.1146/annurev.anchem.1.031207.113053

2. Buchberger AR, Sauer CS, Vu NQ, DeLaney K, Li L. A Temporal Study of the Perturbation of Crustacean Neuropeptides Due to Severe Hypoxia Using 4-Plex Reductive Dimethylation. *J Proteome Res*. 2020;19:1548-1555.

doi:10.1021/acs.jproteome.9b00787

3. Li C, Wu X, Liu S, et al. Roles of Neuropeptide Y in Neurodegenerative and Neuroimmune Diseases. *Front Neurosci*. 2019;13:1-11. doi:10.3389/fnins.2019.00869

4. DeLaney K, Hu M, Hellenbrand T, Dickinson PS, Nusbaum MP, Li L. Mass spectrometry quantification, localization, and discovery of feeding-related neuropeptides in cancer borealis. *ACS Chem Neurosci*. 2021. doi:10.1021/acschemneuro.1c00007

5. Sauer CS, Phetsanthad A, Riusech OL, Li L. Developing Mass Spectrometry for the Quantitative Analysis of Neuropeptides. *Expert Rev Proteomics*. 2021. doi:10.1080/14789450.2021.1967146

6. Xiang F, Ye H, Chen R, Fu Q, Li N. N,N-Dimethyl leucines as novel Isobaric tandem mass tags for quantitative proteomics and peptidomics. *Anal Chem*. 2010;82(7):2817-2825. doi:10.1021/ac902778d

7. Sauer CS, Li L. Mass Spectrometric Profiling of Neuropeptides in Response to Copper Toxicity via Isobaric Tagging. *Chem Res Toxicol*. 2021. doi:10.1021/acs.chemrestox.0c00521

8. Lavradas RT, Hauser-Davis RA, Lavandier RC, et al. Metal, metallothionein and glutathione levels in blue crab (Callinectes sp.) specimens from southeastern Brazil. *Ecotoxicol Environ Saf*. 2014;107:55-60. doi:10.1016/j.ecoenv.2014.04.013

Figures

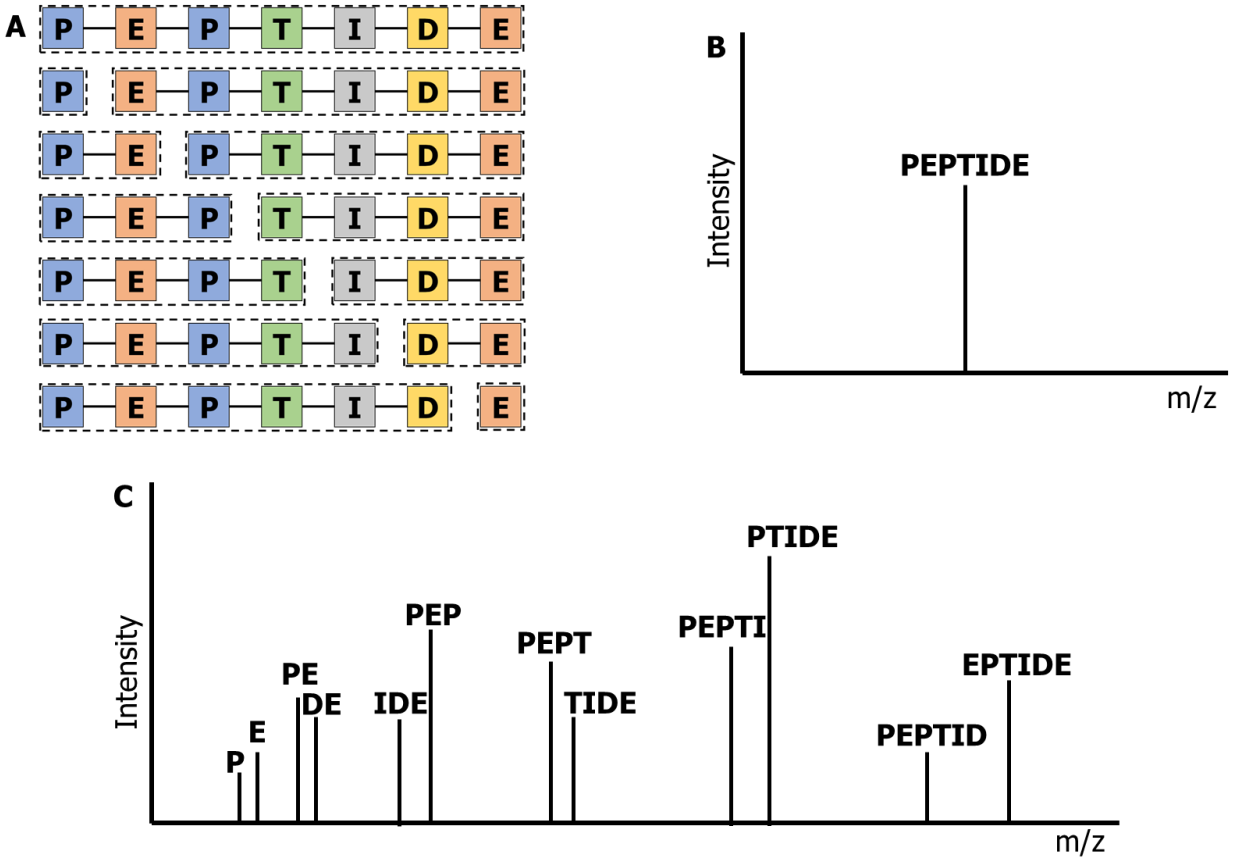

Figure 1: An example MS analysis of a peptide with sequence PEPTIDE. **A** shows the sequence of the peptide with dashed lines around the fragments that are shown in **B** and **C**. **B** is the MS^1 or precursor mass spectrum where the intact mass is observed. **C** is the MS^2 spectrum where the fragments from **A** are observed.

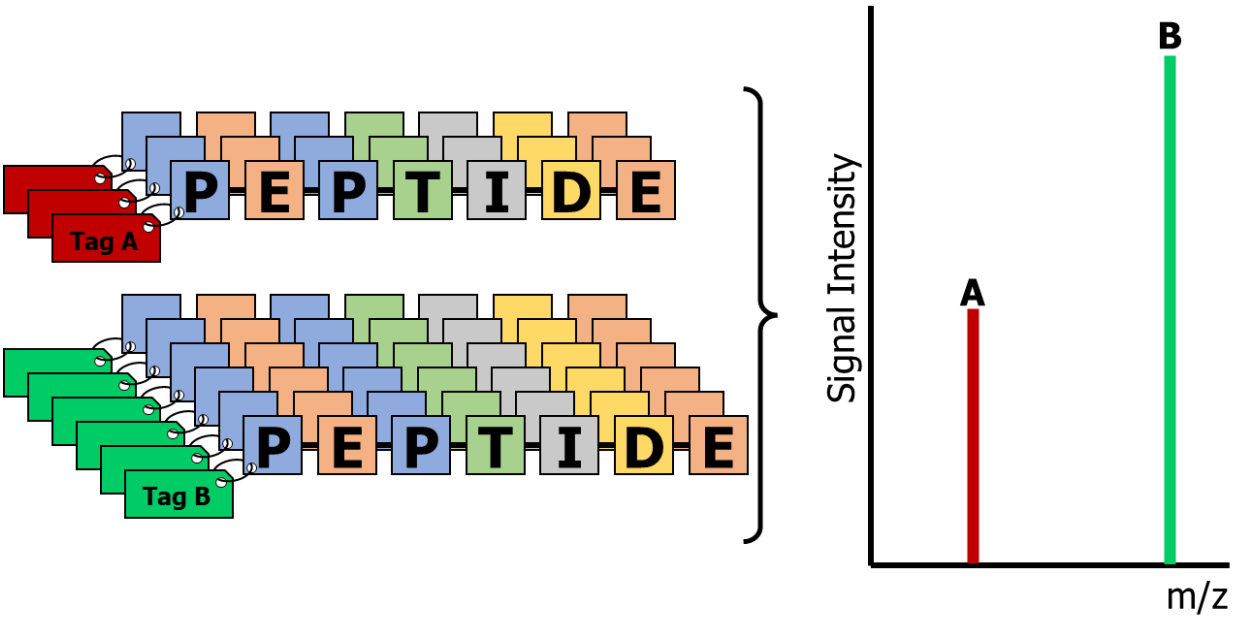

Figure 2: Quantification of labeled samples. The peptides are labeled with different tags depending on the samples they came from. Different tags yield different signals and can be distinguished by mass spectrometry. In this example, the signal from Sample B is twice this signal of Sample A as the amount of peptide is doubled from Sample A to B.

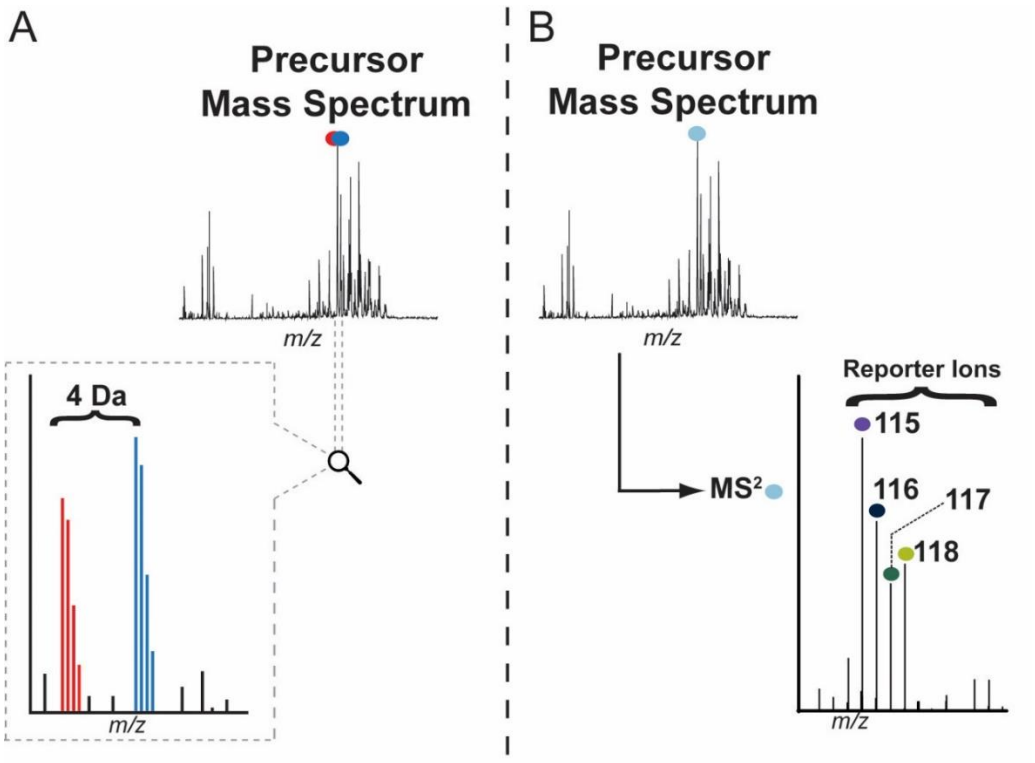

Figure 3: Comparison between isotopic and isobaric labeling. In isotopic labeling (**A**), samples have different masses added to them to create a mass shift between molecules of interest (analytes). In isobaric labeling (**B**), the same mass is added, but analytes are distinguishable at the MS^2 level where unique reporter ions form.

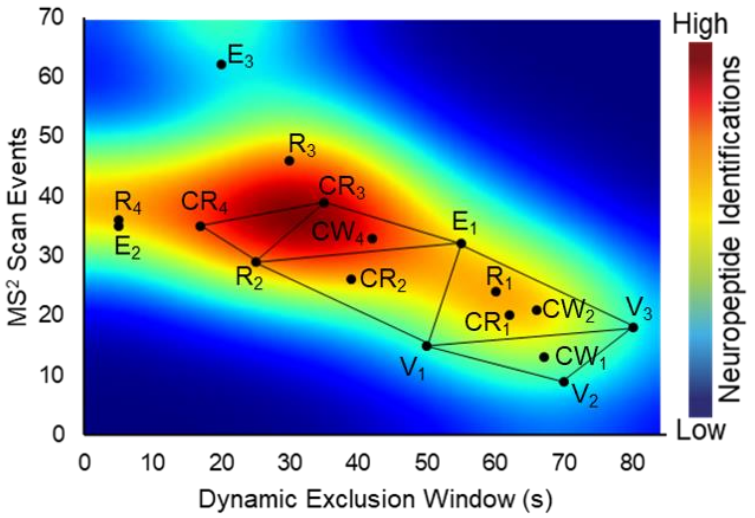

Simplex	Vertex	Dynamic Exclusion Window (s)	MS^2 Scan Events	Neuropeptides Identified
1	V1	50	15	29
	V2	70	9	25
	V3	80	18	27
2	R1	60	24	29
	E1	55	32	41
	CR1	62	20	35
	CW1	67	13	24
3	R2	25	29	88
	E2	5	35	81
	CR2	39	26	63
	CW2	66	21	54
4	R3	30	46	54
	E3	20	62	53
	CR3	35	39	72
5	R4	5	36	64
	CR4	42	33	55
	CW4	17	35	66

Figure 4: Optimization of DDA parameters. Two DDA parameters, the dynamic exclusion window and MS^2 scan events, were optimized stepwise. With each iteration, new conditions were tested, moving away from the conditions that had worse performance. The optimization of these parameters resulted in a 3-fold increase between the initial, unoptimized parameters, and the optimized parameters. The optimum region is shown on the heatmap in the red region (region with more identified

neuropeptides). The table below the heatmap shows the more specific numbers for each point.

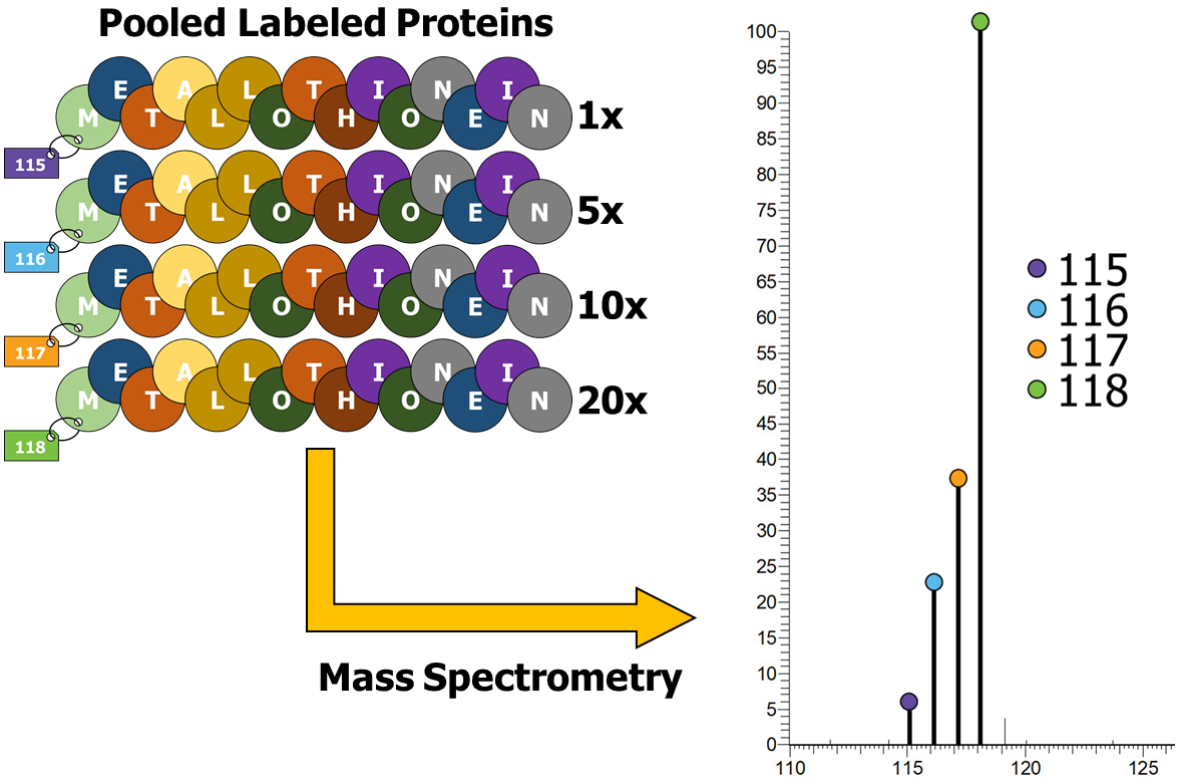

Figure 5: Example mass spectrometry of labeled metallothionein. Proteins labeled with different tags (115, 116, 117, or 118) were combined in different amounts (1:5:10:20) (shown left). MS analysis of the pooled sample showed reporter ion intensities that are within 80% of the expected values (shown right). The high accuracy of the method demonstrates feasibility for applications to future biological applications.

Chapter 9

Conclusions and Future Directions

Conclusions

Neuropeptides are involved in many signaling pathways, and their study is important because it can provide information into biochemical processes, potential therapeutic routes, and biomarker discovery.[1] Their functions are diverse and dependent on the presence of other co-modulating neuropeptides, emphasizing the need for global profiling of neuropeptides. This dissertation is focused on the development of quantitative mass spectrometry (MS) methods for the study of neuropeptides and related biomolecules. Many quantitative MS strategies exist and are routinely used in various -omic analyses, with work being performed to translate them to neuropeptidomics. These methods are explored in more detail in **Chapter 2** and further developed in the other chapters of this thesis.

A potential limitation of neuropeptide analyses by MS is the time requirements. Analysis times of 2 hours per sample are typical and can inhibit more detailed biological applications. Multiplexing allows samples from different experimental conditions to be analyzed simultaneously to greatly reduce the number of analyses, sample requirements, and run-to-run variation from instrumental drift. In **Chapter 3**, a 4-plex reductive dimethylation strategy is developed and applied to the time course study of neuropeptides in response to hypoxia. These methods enabled quantitation of changes between different exposure durations that would have previously been undetected due to the number of samples needed and/or instrument time required. Additionally, the use of both liquid chromatography (LC)-MS using electrospray ionization (ESI) and matrix-assisted laser desorption/ionization (MALDI)-MS were able to provide complimentary

coverage of the neuropeptidome to improve the number of significant changes observed.

The 4-plex reductive dimethylation scheme is effective at improving throughput but is limited in multiplexing capabilities as the precursor ion mass difference increases spectral complexity multiplicatively with each additional channel. This is addressed in **Chapter 4** in which N,N-dimethyl leucine (DiLeu) isobaric tags are used to quantify neuropeptides in response to copper toxicity. Analyzing neuropeptides via isobaric tagging can be difficult as the low abundance neuropeptides are often not selected for tandem MS (MS/MS or MS^2) analysis, and therefore are not able to be identified or quantified. Through extensive optimization of the MS acquisition settings, however, more unique neuropeptides were able to be detected in a single LC-MS run. The 3-fold increase in neuropeptides identified and quantified enabled the application of the method to study copper toxicity. Several significant changes were observed in neuropeptide expression over the course of 4 hours, including upregulation of inhibitory peptides and possible transport of a pigment dispersing hormone from the sinus glands to the brain. These methods were further developed in **Chapter 5** to expand the multiplexing capabilities using 12-plex DiLeu tags. These tags rely on mass defects that require higher resolution and subsequently, scan times are increased. To balance the increase in throughput with the potential decrease in identifiable neuropeptides, an orthogonal array strategy was used to optimize additional MS acquisition settings. This design of experiments allows for much faster optimization compared to factorial designs and resulted in a 2.75-fold increase in identifiable neuropeptides. Additionally, the

orthogonal array allowed the impact of the different parameters to be estimated, but it was observed that the sum effect of the different parameters was more important than any single parameter. Future work should optimize selected parameters simultaneously for improved results. The methods used in **Chapters 4 and 5** are detailed in a protocols chapter, **Chapter 6**.

To improve understanding of copper toxicity past neuropeptidomic changes, metal-binding proteins (i.e., metallothionein proteins) are also studied. These proteins are small and uniquely cysteine-rich with similar sequences. A method to quantify the proteins intact (i.e., without digestion), was developed in **Chapter 7**. This method addressed challenges in labeling and cleaning up the intact metallothionein proteins (MTs) using a combination of extended alkylation, DiLeu tagging, and acetone precipitation. Moreover, the method showed high quantitative accuracy over a 20-fold dynamic range. This study demonstrates the feasibility of applying isobaric tags, specifically DiLeu, to top-down proteomics. This is advantageous as multiplexing is able to be achieved without the isotopic interference that occurs with isotopic labeling methods like SILAC. Combining these methods with the quantitative methods for neuropeptidomics in previous chapters will facilitate a better understanding of the underlying signaling pathways and biochemical processes involved in environmental stress. Additionally, the methods developed here are translatable to other biological problems and can help inform other multi-omic studies.

Future Directions

The methods developed here have created improvements in neuropeptide detection, identification, and especially quantitation. There are of course still limitations in the field that, if addressed, could further improve our understanding of the complexities within the neuroendocrine system. Methods to improve sensitivity are critical to discovering new neuropeptides and analyzing those with low abundance. Additionally, improving multi-omic analyses by expanding the quantitative methods here to proteins and small molecules will lead to a more complete understanding of biological problems of interest, such as environmental stress. Assessing the functional roles of all these molecules can also open new possibilities for biomarker discover and treatments.

The enhanced detection of neuropeptides described in **Chapter 3** are easily adopted by many labs as they simply require isotopic formaldehyde and borane pyridine. In this work, the MS data is only acquired using data-dependent acquisition (DDA) parameters, but other work has shown data-independent acquisition (DIA) to be even more effective for the analysis of low abundance analytes like neuropeptides.[2] Isobaric labeling workflows are incompatible with these methods, but because the mass shift is at the precursor mass level, reductive dimethylation could be compatible with DIA. Similarly, the methods are compatible with both LC-MS and MALDI-MS; this could lead to the creation of workflows in which MALDI-MS is used to provide spatial information via MS imaging (MSI) and LC-MS provides confident identifications through tandem MS. These functional studies could in turn inform functional studies for specific neuropeptides.

Isobaric tagging has been demonstrated in **Chapters 4 and 5** to be effective in analyzing neuropeptides with greater throughput via DiLeu tags. Applying these methods to a biological study, especially using 12-plex DiLeu, would not only provide more confident proof of principal, but also allow a biological problem to be studied in more detail. By reducing the number of samples to be analyzed by a factor of 12, additional exposure durations, stress severities, drug doses, life stages, etc., can be examined. Additionally, the added throughput could be beneficial to studying the hemolymph (circulating fluid that functions as a mix of blood and lymph) in the crab model for neuropeptide changes. This could be accomplished by withdrawing hemolymph from crabs or performing microdialysis[3] and collecting samples over time.

Quantitative mass spectrometry has become one of the top means for global profiling of neuropeptides, but additional experiments are required to discern the impact of specific neuropeptides. Using a crustacean model, an ex vivo heart preparation can be performed in which the heart is removed from the crab and kept alive. A force transducer is then able to measure the rhythm and amplitude of heart contractions.[4] The global neuropeptidomic studies performed in **Chapters 3, 4, and 5** can then inform future experiments in which a synthesized neuropeptide is infused into the ex vivo heart and the changes in amplitude and rhythm are recorded to help determine the functional role of the neuropeptide. An example of this data is given in **Figure 1**.[4]

In this dissertation, an initial framework was developed for the study of intact MTs using both isobaric labeling and top-down MS, but this was performed using a high purity rabbit MT isolate from liver tissue. Work still needs to be performed to improve

the extraction of MTs from tissue, particularly in a crustacean model organism, so biological studies can be performed. This has been challenging as the hepatopancreas–a tissue with properties of both liver and pancreas that is a rich source of MTs–is a complex matrix of lipids, proteins, and metabolites. Both large proteins and small molecules can interfere with extraction and inhibit ionization efficiency to make detection of MTs difficult. Molecular weight cut-off filtration has been used to remove large proteins by having the low molecular weight MTs flow through the filter. Despite the molecular weight of MTs is <7 kDa, the protein does not flow through 10 kDa or 30 kDa filters, likely due to interactions with the filter, protein-protein aggregation, etc. Using 50 kDa MWCO filters has been effective in removing the MTs from large proteins, but as the filter pore size increases, more interfering proteins are also able to pass through as well. Determining the balance between MT recovery and the recovery of unwanted proteins is still a concern for this project.

Affinity-based strategies are a viable alternative to size-based separation methods (e.g., MWCO) for enriching MTs. For example, immobilized metal affinity chromatography (IMAC) has been reported successful in enriching metal-binding proteins like MTs.[5] In an IMAC enrichment, metal (e.g., copper) is immobilized to a chelating resin. Protein extracts are loaded to the column and metal-binding proteins bind to the immobilized metal and the non-binding proteins are washed away. A high concentration of imidazole then releases the MTs and other metal-binding proteins from the resin. A schematic is provided in **Figure 2**. An initial experiment was performed to see if the rabbit MT isolate could be enriched via IMAC. While some MT was detected in

the eluent, substantially higher signal was observed in the wash and loading flow through, demonstrating non-binding. This could be due to the protein being denatured and not able to bind as tightly, or perhaps conversely, the protein is able to bind the copper with greater affinity than the chelating resin and is simply stripping the column of the copper. Evaluating different buffers, elution mechanisms, flow rates, etc., could facilitate a more effective enrichment using IMAC. Alternatively, antibody-based enrichment methods could be feasible, but are more expensive to perform. Additionally, the antibody-MT interaction would have to be independent of MT structure which is known to be highly dynamic in solution. Despite the challenges with affinity-based enrichments, their development is of interest as it could result in a concentrated sample with minimal interfering compounds.

The quantitative analysis of peptides and proteins can provide insights into expression changes, signaling pathways, etc., but additional information can be gained from structural analyses. Ion mobility mass spectrometry (IM-MS) is a useful tool for studying confirmation changes in molecules. This is done by calculating the collisional cross-section of the molecule of interest based on its drift time.[6] Using IM-MS is capable of providing information on how specific neuropeptides and metallothionein proteins change in confirmation upon copper exposure and/or binding of copper. Where quantitative analyses may observe no changes in expression levels, IM-MS can still provide insights into the biological processes involved in responding to copper toxicity. An example of the collisional cross-section data from a recent publication in the Russel Lab is provided in **Figure 3**,[7] demonstrating the stabilities of different metalated MT

species. Similar experiments could reveal the mechanisms by which copper is bound to MTs and how stable this interaction is.

Neuropeptides and MTs are important targets for studying environmental stress, but incorporation of metabolomic data would provide a more comprehensive multi-omic study of the response to copper toxicity. Antioxidant molecules, like glutathione, are often the first line of defense in protecting against oxidative stress and have been shown to be involved in mediating heavy metal influxes.[8] Additionally, small molecule neurotransmitters could play important roles in signaling pathways that enable organisms to survive environmental metal fluctuations. Isotopic DiLeu (iDiLeu) can facilitate the absolute quantitation of these molecules. These 5-plex tags are used to label a standard at four different concentrations to generate a calibration curve. The fifth channel is reserved for the biological sample and all samples are analyzed simultaneously to perform absolute quantitation in a single LC-MS run. An overview is given in **Figure 4**.[9] These tags are similar to DiLeu but differ in mass additions at the MS^1 level to enable quantitation by area under the curve and have been found to be more reliable for absolute quantitation than their isobaric counterparts. Although the tags are only able to be incorporated into primary amine-containing analytes, many metabolomic targets can be detected, including neurotransmitters and glutathione. Adding metabolomic data into the workflow can help show how the alterations in signaling lead to different phenotypic responses.

Overall, the findings of this research are useful in determining the biochemical pathways that allow organisms to manage and survive environmental stress. This is

mainly studied from the perspective of neuropeptides, but by adding proteomic and metabolomic data, the downstream products of signaling pathways can be better understood. The methods described here are also able to be applied to the study of many other biological processes and are not limited to crustacean models. Ultimately, this dissertation provides a foundation for further research into understanding the complex, multi-omic processes of the neuroendocrine system.

References

1. Li L, Sweedler J V. Peptides in the Brain: Mass Spectrometry–Based Measurement Approaches and Challenges. *Annu Rev Anal Chem*. 2008;1(1):451-483. doi:10.1146/annurev.anchem.1.031207.113053

2. Delaney K, Li L. Data Independent Acquisition Mass Spectrometry Method for Improved Neuropeptidomic Coverage in Crustacean Neural Tissue Extracts. *Anal Chem*. 2019;91(8):5150-5158. doi:10.1021/acs.analchem.8b05734

3. Jiang S, Liang Z, Hao L, Li L. Investigation of signaling molecules and metabolites found in crustacean hemolymph via in vivo microdialysis using a multifaceted mass spectrometric platform. *Electrophoresis*. 2016;37(7-8):1031-1038. doi:10.1002/elps.201500497

4. Wiwatpanit T, Powers B, Dickinson PS. Inter-animal variability in the effects of C-type allatostatin on the cardiac neuromuscular system in the lobster Homarus americanus. *J Exp Biol*. 2012;215(13):2308-2318. doi:10.1242/jeb.069989

5. Honda RT, Araújo RM, Horta BB, Val AL, Demasi M. One-step purification of metallothionein extracted from two different sources. *J Chromatogr B Anal Technol Biomed Life Sci*. 2005;820(2):205-210. doi:10.1016/j.jchromb.2005.03.017

6. Li G, Delafield DG, Li L. Improved structural elucidation ofpeptide isomers and their receptors using advanced ion mobility-mass spectrometry. *Trends Anal Chem*. 2019. doi:10.1016/j.trac.2019.05.048

7. Dong S, Shirzadeh M, Fan L, Laganowsky A, Russell DH. Ag+Ion Binding to Human Metallothionein-2A Is Cooperative and Domain Specific. *Anal Chem*. 2020;92(13):8923-8932. doi:10.1021/acs.analchem.0c00829

8. Brouwer M, Brouwer TH. Biochemical defense mechanisms against copper-induced oxidative damage in the blue crab, Callinectes sapidus. *Arch Biochem Biophys*. 1998;351(2):257-264. doi:10.1006/abbi.1997.0568

9. Greer T, Lietz CB, Xiang F, Li L. Novel isotopic N,N-Dimethyl Leucine (iDiLeu) reagents enable absolute quantification of peptides and proteins using a standard curve approach. *J Am Soc Mass Spectrom*. 2014;26(1):107-119. doi:10.1007/s13361-014-1012-y

Figures

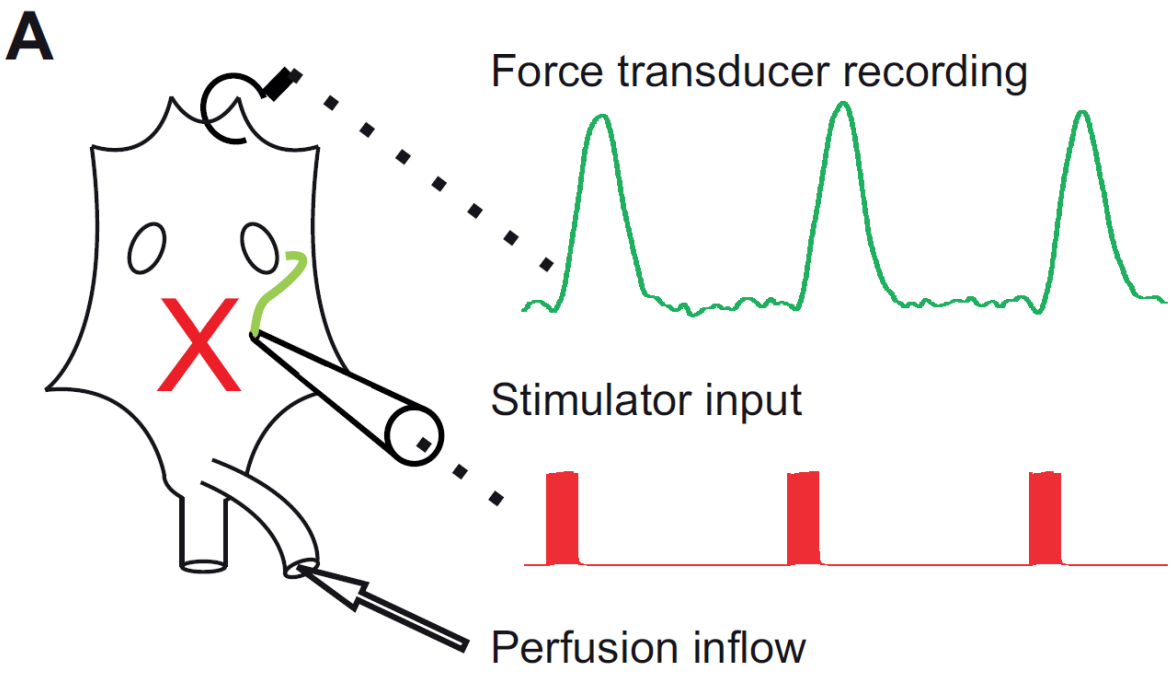

Figure 1: An overview of the ex vivo heart perfusion experiments. Peptides are perfused into the posterior artery and the force transducer records the contraction amplitude. Figure taken with permission from Wiwatpanit, T.; Powers, B.; Dickinson, P. J Exp Biol 2012, 215, 2308-2318.

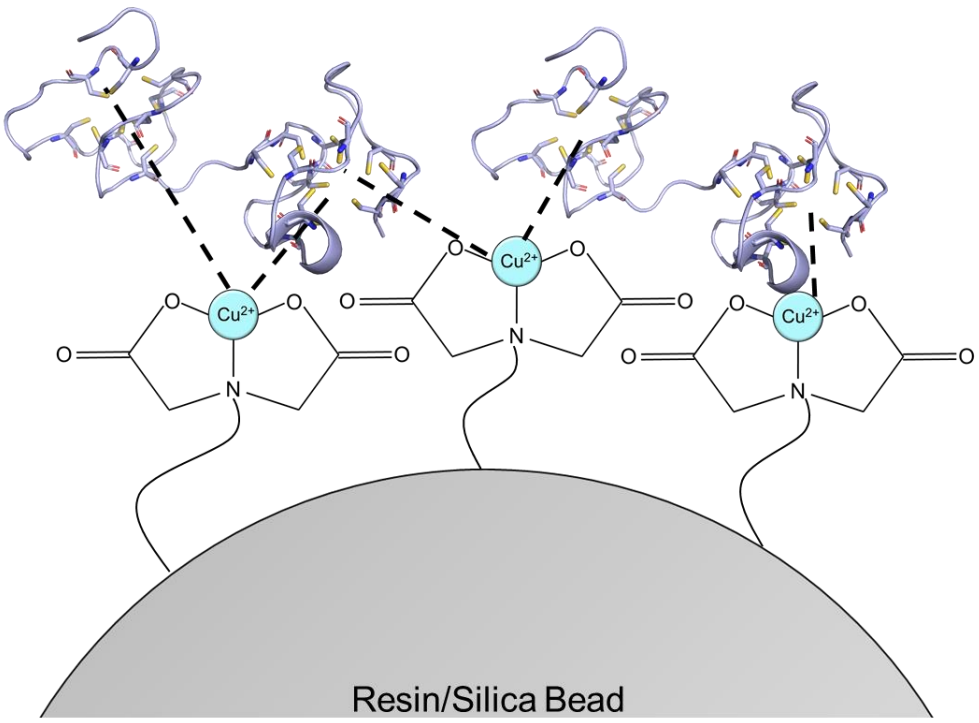

Figure 2: Copper-IMAC interaction. Copper (Cu^{2+}) is loaded to an iminodiacetic acid-containing resin. As the metallothionein flows past, it binds to the copper with its many cysteine residues (shown in yellow) and non-binding proteins are washed away.

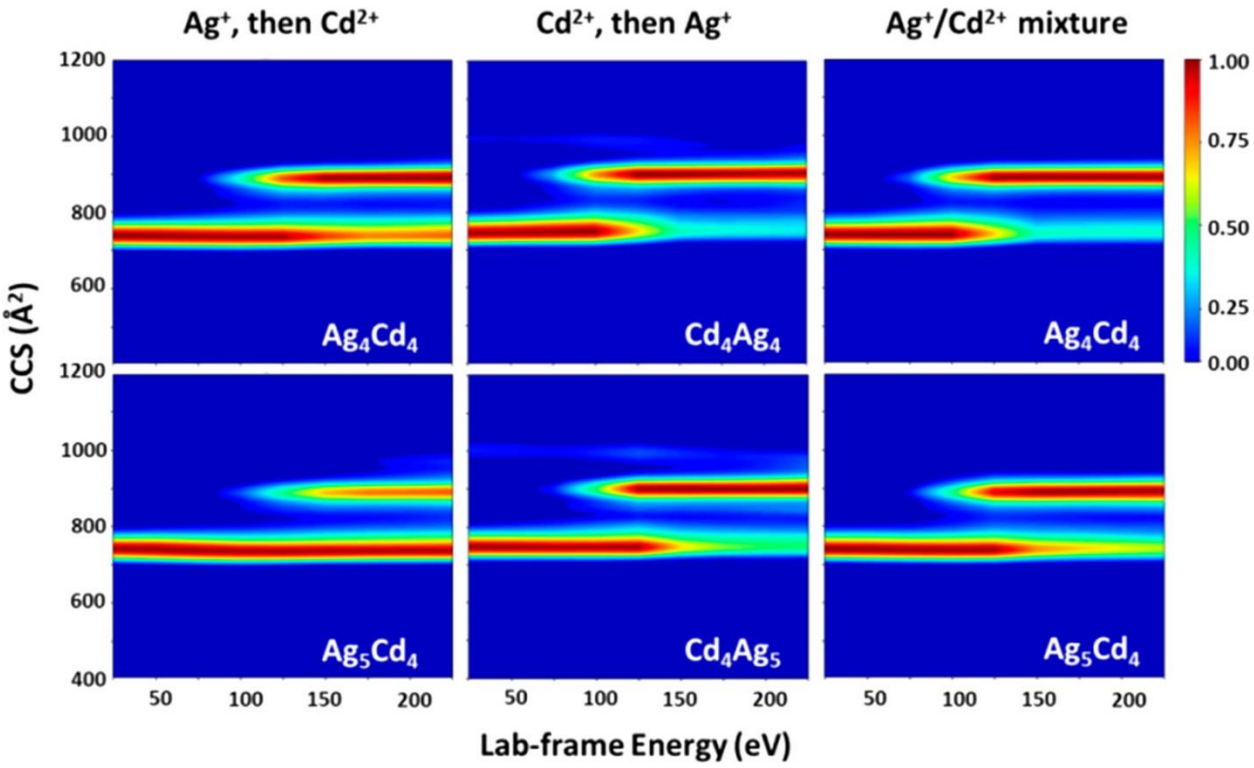

Figure 3: Collison-induce unfolding heat maps for metalated MT. Different rates of unfolding are observed from different combination of metalation and the order of metal incorporation. This figure is taken with permission from Dong, S., et al. **2020.** *Anal. Chem.* 2020, 92, 8923–8932.

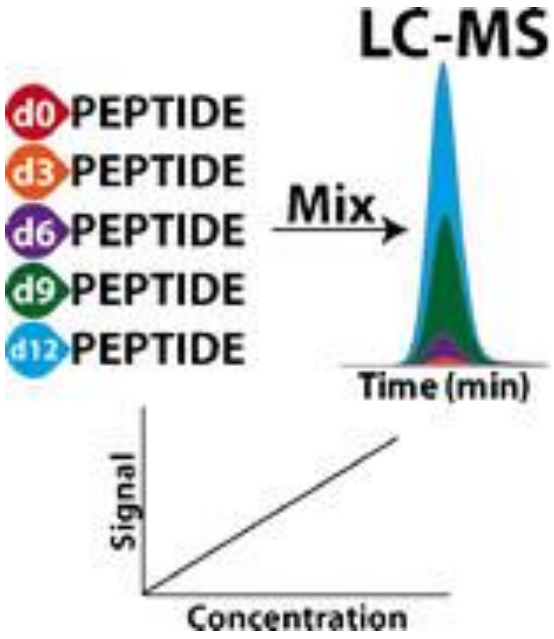

Figure 4: Overview of iDiLeu labeling. A synthetic standard is labeled with four different channels of iDiLeu and combined at different ratios to generate a calibration curve. The fifth channel corresponds to the experimental sample and the absolute concentration of that sample is determined from the calibration curve. Figure reprinted with permission from Greer, T., et al. *J. Am. Soc. Mass Spectrom*. (2015) 26:107-119.

Appendix I

List of Publications, Presentations, and Grants

Publications

1. Sauer, C.S., Vu, N.Q., Job, M.A., Li, L. Relative Quantitation of Intact Metallothionein Proteins via Isobaric DiLeu Tags. In preparation.

2. Sauer, C.S., Covaleski, J., Li, L. Enhancing Neuropeptidomics Throughput via 12-plex DiLeu Isobaric Tags. In preparation.

3. Sauer, C.S., Li, L. Multiplexed Quantitative Neuropeptidomics via DiLeu Isobaric Tagging. *Method in Enzymology*, Vol. 633. 2021. (Invited Book Chapter Accepted for Publication)

4. Sauer, C.S., Phetsanthad, A., Riusech, O.L., Li, L. Developing Mass Spectrometry for the Quantitative Analysis of Neuropeptides. *Expert Review of Proteomics.* 2021. https://doi.org/10.1080/14789450.2021.1967146

5. Sauer, C.S., Li, L. Mass Spectrometric Profiling of Neuropeptides in Response to Copper Toxicity via Isobaric Tagging. *Chem. Res. Toxicol.* 2021, 34, 1329-1336

6. Sauer, C.S.*, Buchberger, A.R.*, Vu, N.Q., DeLaney, K., Li, L. A Temporal Study of the Perturbation of Crustacean Neuropeptides Due to Severe Hypoxia Stress Using 4-Plex Reductive Dimethylation. *J. Proteome Res.* 2020, 19, 1548-1555. *Co-First Authors

7. DeLaney, K., Sauer, C.S., Vu, N.Q., Li, L. Recent Advances and New Perspectives in Capillary Electrophoresis-Mass Spectrometry for Single-Cell "Omics". *Molecules* 2019, 24(1), 42.

Presentations

1. Sauer, C., Job, M., Li, L. Quantitation of Intact Metallothionein Proteins via DiLeu Isobaric Tags to Probe Changes Resulting from Copper Exposure. 69th Annual ASMS Conference on Mass Spectrometry and Allied Topics. Philadelphia, PA. November 2021.

2. Sauer, C., Li, L. Multiplex Quantitation of Neuropeptides in Response to Copper Toxicity in the Blue Crab, Callinectes sapidus. Oral Presentation. Dynamic Neural Networks: STG Meeting 2020 (remote). October 2020.

3. Sauer, C., Li, L. Multiplex Quantitation Of Biomolecules Involved In Copper Toxicity Via Custom N,N-Dimethylated Leucine (DiLeu) 12-Plex Isobaric Tags. Poster. 68th Annual ASMS Conference on Mass Spectrometry and Allied Topics. Houston, TX (remote). June 2020.

4. Sauer, C., Li, L. Multiplex Quantification of Crustacean Neuropeptides via Custom Isobaric Tags (DiLeu). Oral Presentation. Pittcon Conference and Expo. Chicago, IL. February 2020.

5. Sauer, C., Li, L. Multiplex Dimethylated Leucine (DiLeu) Isobaric Tags to Probe Neuropeptidomic Response to Copper Toxicity in the Blue Crab, *Callinectes sapidus*. Poster. 67th Annual ASMS Conference on Mass Spectrometry and Allied Topics. Atlanta, GA. June 2019.

6. Sauer, C., Buchberger, A., Li, L. Improving Coverage and Quantification of the Crustacean Neuropeptidome via Custom 4-plex Dimethylated Leucine (DiLeu) Isobaric Tags. Poster. 66th Annual ASMS Conference on Mass Spectrometry and Allied Topics. San Diego, CA. June 2018.

7. Sauer, C., Buchberger, A., DeLaney, K., Li, L. Multiplex Quantitation of Crustacean Neuropeptides after Hypoxia Exposure Using Custom 4-plex Dimethylated Leucine (DiLeu) Isobaric Tags. Poster. 65th Annual ASMS Conference on Mass Spectrometry and Allied Topics. Indianapolis, IN. June 2017.

Grants

1. Development of Multiplex Multiomic Mass Spectrometry Methods for Probing the Response to Copper Toxicity in the Blue Crab, Callinectes sapidus.
   Funding Agency: NIH/NIEHS
   Type: NRSA F31 Predoctoral Fellowship
   Duration: June 2020-January 2022

2. Biotechnology Training Program Trainee
   Funding Agency: NIH/NIGMS
   Type: T32 Training Grant
   Duration: January 2017-December 2017, September 2018-August 2019